
Wayne State University Dissertations

1-1-2013

Use Of Focused Ultrasound For Transcranial Sonothrombolysis

Golnaz Ahadi

Wayne State University,

Follow this and additional works at: http://digitalcommons.wayne.edu/oa_dissertations

Recommended Citation

Ahadi, Golnaz, "Use Of Focused Ultrasound For Transcranial Sonothrombolysis" (2013). *Wayne State University Dissertations*. Paper 744.

This Open Access Dissertation is brought to you for free and open access by DigitalCommons@WayneState. It has been accepted for inclusion in Wayne State University Dissertations by an authorized administrator of DigitalCommons@WayneState.

USE OF FOCUSED ULTRASOUND FOR TRANSCRANIAL SONOTHROMBOLYSIS

by

GOLNAZ AHADI

DISSERTATION

Submitted to the Graduate School

of Wayne State University,

Detroit, Michigan

in partial fulfillment of the requirements

for the degree of

DOCTOR OF PHILOSOPHY

2013

MAJOR: BIOMEDICAL ENGINEERING

Approved by:

Advisor _____ Date _____

Co-Advisor _____ Date _____

© COPYRIGHT BY

GOLNAZ AHADI

2013

All Rights Reserved

DEDICATION

With love, I dedicate this work to my parents, for sacrificing their world to give my brother and I the chance to live freely and the opportunity to achieve our dreams.

ACKNOWLEDGMENTS

“The way to true knowledge does not go through soft grass covered with flowers.

To find it, a person must climb steep mountains.” –Josh Ruskin

It was only through the support and encouragement of many people that I have been able to complete this life goal. This journey has been an unconventional one, which at times seemed to be insurmountable. I would first like to thank my dear advisors Dr. Thilo Hoelscher and Dr. Michele Grimm for their unwavering support and energy.

I want to express deep gratitude to Dr. Thilo Hoelscher, who has continually been there when I needed him, and whose guidance always helped me gain clarity. I greatly value his mentorship, and for imparting in me his love of work and balance in life. There is some inherent risk in becoming a principal investigator’s first student; however, in this case, the rewards outweighed the risk many times over. I am honored to be his first PhD student, and truly appreciate all his help.

I am grateful for the privilege of having Dr. Michele Grimm as my advisor, as her efforts helped make this dream a reality for me. Throughout the arduous, sometimes seemingly impossible process, she has stood by my side and remained my greatest advocate. She has taught me so much about integrity and dedication, demonstrating to me through her actions that the impossible truly can become possible. She has invested a tremendous amount of time and energy into me, which has fueled my drive for academic success, and for which I will always be thankful.

Along with my advisors, I would like to thank other members of my Ph.D Committee: Dr. Cynthia Bir, Dr. Zhifeng Kou, and Dr. Jeffry Powers for their guidance, support, encouragement, and patience as they saw me through this journey. I would like to especially thank Dr. Bir for affording me this opportunity and for the confidence she has always maintained in my abilities. I would also like to express my appreciation to Dr. Svetlana Eremenko and Dr. Bir for being phenomenal teachers and role models.

I have been blessed with the opportunity to work with wonderful people who contribute a wide-range of expertise and encourage an amazing group atmosphere. The Brain Ultrasound Research Laboratory team at University of California, San Diego has provided me with invaluable education, friendships, and a strong support network. Similarly, I will always be appreciative to the Wayne State University staff and faculty who supported me through this innovative pathway. I am thankful to my closest friends and family, for all the love and patience that they have shown me. I have grown a great deal both personally and professionally over the past four years, and I owe this maturation in large part to the strong role models that have been present in my life.

My deepest gratitude goes to my family. To my parents, I cannot possibly express in words my appreciation and love for all that they have done for me. It will always be an honor and a privilege to be their daughter. Their endless love, support, encouragement, patience, and sacrifices never cease to amaze me—they are my inspiration. To my new family, Dr. Kentaro Suzuki, I am thankful to have him as my partner, as my accountabilibuddy, and best friend. He has been there through the toughest times of the

journey, continually easing my fears, and providing me with perspective on the process.

For all this and more I am grateful.

Without the enthusiastic support and dedication from so many of you I would not have been able to rise to this occasion. As I reflect back at the end of this long journey, I am appreciative of the lessons I have learned along the way, and will use them to guide my way in my future journeys. I hope to make you proud.

TABLE OF CONTENTS

Dedication.....	ii
Acknowledgments	iii
List of Tables	ix
List of Figures	xii
List of Abbreviations	xv
Chapter 1 BACKGROUND & SIGNIFICANCE.....	1
CLINICAL PROBLEM: STROKE.....	1
CURRENT THERAPEUTIC APPROACHES AND THEIR DEFICIENCIES.....	2
INTRODUCTION TO FOCUSED ULTRASOUND	5
Chapter 2 SPECIFIC OBJECTIVES.....	9
OBJECTIVE 1: TECHNIQUE FEASIBILITY.....	10
OBJECTIVE 2: PARAMETER OPTIMIZATION	10
OBJECTIVE 3: ACOUSTIC FIELD CHARACTERIZATION.....	11
OBJECTIVE 4: SONOTHROMBOLYSIS & FRAGMENTATION	12
Chapter 3 COMMON RESEARCH APPROACH	13
MATERIALS & METHODS.....	13
Chapter 4 FEASIBILITY OF FUS AS A THROMBOLYTIC THERAPY.....	22
OBJECTIVE 1: TECHNIQUE FEASIBILITY.....	22
MATERIALS & METHODS.....	22
RESULTS.....	25

DISCUSSION.....	34
SUMMARY.....	36
Chapter 5 PARAMETER OPTIMIZATION	37
OBJECTIVE 2: PARAMETER OPTIMIZATION	37
MATERIALS & METHODS.....	37
RESULTS.....	38
DISCUSSION.....	40
SUMMARY.....	42
Chapter 6 ACOUSTIC FIELD CHARACTARIZATION.....	43
OBJECTIVE 3: ACOUSTIC FIELD CHARACTERIZATION.....	43
MATERIALS & METHODS.....	43
RESULTS.....	53
DISCUSSION.....	61
SUMMARY.....	64
Chapter 7 SONOTHROMBOLYSIS & FRAGMENTATION	66
OBJECTIVE 4: SONOTHROMBOLYSIS & FRAGMENTATION	66
MATERIALS & METHODS.....	66
RESULTS.....	69
DISCUSSION.....	75
SUMMARY.....	79
Chapter 8 SUMMARY & FUTURE WORK	80
Appendix A: Objective 1: Technique Feasibility	84

Appendix B: Objective 2: Parameter Optimization	104
Appendix C: Objective 3: Acoustic Field Characterization	132
Appendix D: Objective 4: Sonothrombolysis & Fragmentation.....	138
References	213
Abstract.....	228
Autobiographical Statement.....	230

LIST OF TABLES

Table 1 Percent weight loss as a result of skull variations, N per study group	23
Table 2 Percent weight loss as a function of acoustic output power using Skull #1, N per study group.....	23
Table 3 Percent weight loss as a function of flow condition using Skull #1, N per study group	24
Table 4 Percent Clot Weight Loss by Skull Specimen Compared to Pre-Insonation Weights	27
Table 5 Pairwise Comparison of the Sonothrombolysis Efficacy as a Function of Skull Specimen	28
Table 6 Percent Clot Weight Loss by Intensity; P-values are from Wilcoxon Rank test to examine if median weight loss is different from 0.....	31
Table 7 Percent Clot Weight Loss by flow group and overall. P-Value is from Student's t-test comparing the groups.....	33
Table 8 Sample Size (N) for each combination of Duty Cycle (DC) and Pulse Width (PW) for the 16 study groups	38
Table 10 Anatomical parameters calculated from the CT data. Skull thickness and density were measured along vectors extending from the assorted transducer elements to the geometric focus. Incident angles were measured between the measurement vectors and the normal vector at the entry point on the skull surface. Calculations were performed in MATLAB	54
Table 11 Results of acoustic measurements for the 5 calvaria and the control.Acoustic power was calculated from the 2D scan (60mm x 60mm in X-Y plane) intensity and pressure measurements were calculated from the 3D scans (20mm x 20mm x 20mm in X-Y-Z)	56
Table 12 Acoustic Output Power and N per study group.....	67
Table 13 Percent Clot Weight Loss Lysis Efficacy as Related to Acoustic Output Power ...	70
Table 14 Clot Fragmentation (> 180 μm) as Indicated by Post-Pre Test Filter Weight. P-values reflect comparison to the 0 W group, adjusted for multiple comparison	72

Table 15 Clot Fragmentation (60 µm - 180 µm) as Indicated by Post-Pre Test Filter Weight. P-values reflect comparison to the 0 W group, adjusted for multiple comparison	73
Table 16 Clot Fragmentation (11 µm - 60 µm) as Indicated by Post-Pre Test Filter Weight. P-values reflect comparison to the 0 W group, adjusted for multiple comparison	74
Table 17 Acoustic parameters at the beam focus with tubing in place.....	74
Table A-1 Raw data on sonothrombolysis efficacy obtained using Skull #1	84
Table A-2 Raw data on sonothrombolysis efficacy obtained using Skull #2	86
Table A-3 Raw data on sonothrombolysis efficacy obtained using Skull #3	88
Table A-4 Raw data on sonothrombolysis efficacy obtained using acoustic output power of 100W (Skull #1)	90
Table A-5 Raw data on sonothrombolysis efficacy obtained using acoustic output power of 200W (Skull #1)	92
Table A-6 Raw data on sonothrombolysis efficacy obtained using acoustic output power of 235W (Skull #1)	94
Table A-7 Raw data on sonothrombolysis efficacy obtained using acoustic output power of 270W (Skull #1)	96
Table A-8 Raw data on sonothrombolysis efficacy obtained using acoustic output power of 400W (Skull #1)	97
Table A-9 Raw data on sonothrombolysis efficacy obtained with No-Flow (0ml/min) conditions (Skull #1)	99
Table A-10 Raw data on sonothrombolysis efficacy obtained with flow present at 10ml/min (Skull #1).....	101
Table B-1 Data acquired for 0.1ms, 1ms, 10ms, & 100ms PW at 5% DC, Groups 1-4.....	104
Table B-2 Data acquired for 0.1ms, 1ms, 10ms, & 100ms PW at 10% DC, Groups 5-8	111
Table B-3 Data acquired for 0.1ms, 1ms, 10ms, & 100ms PW at 20% DC, Groups 9-12 ..	118
Table B-4 Data acquired for 0.1ms, 1ms, 10ms, & 100ms PW at 50% DC, Groups 13-16	125

Table D-1 Raw data on sonothrombolysis efficacy obtained for 0W, used as the control group.....	138
Table D-2 Raw data on sonothrombolysis efficacy obtained using acoustic output power of 50W.....	141
Table D-3 Raw data on sonothrombolysis efficacy obtained using acoustic output power of 100W.....	144
Table D-4 Raw data on sonothrombolysis efficacy obtained using acoustic output power of 125W.....	147
Table D-5 Raw data on sonothrombolysis efficacy obtained using acoustic output power of 150W.....	150
Table D-6 Raw data on sonothrombolysis efficacy obtained using acoustic output power of 200W.....	153
Table D-7 Raw data on sonothrombolysis efficacy obtained using acoustic output power of 235W.....	156
Table D-8 Raw data on sonothrombolysis efficacy obtained using acoustic output power of 235W.....	159
Table D-9 Raw data on sonothrombolysis efficacy obtained using acoustic output power of 400W.....	162
Table D-10 Clot fragmentation data collected for 180 μ m sized mesh filters from all acoustic output groups tested.....	165
Table D-11 Clot fragmentation data collected for 60 μ m sized mesh filters from all acoustic output groups tested.....	181
Table D-12 Clot fragmentation data collected for 11 μ m sized mesh filters from all acoustic output groups tested.....	197

LIST OF FIGURES

Figure 1 Characteristics of the Focused Ultrasound System. Upper Left: Representation of the dimensions of the focused beam; Upper Center & Right: Representative sound field images; Bottom: The top view of the hemispheric FUS transducer.....	14
Figure 2 Blood clot organized around a silk thread, ready to be placed into PE tubing.....	16
Figure 3 Four different views of a sample cadaveric skull attached to fixture and placed in chamber. For the experiments, only the calvarium was mounted within the fixture.....	17
Figure 4 Left: An overturned view of a calvarium on an acrylic frame that is fixed to a plastic cover with hole in its to provide access to the skull cavity which is then attached to the cylindrical standoff. Once the skull is in position the entire device is placed upside down on top of the water filled hemispheric transducer. Right: Top view into the ExAblate 4000™ helmet showing a hydrophone and a calvarium attached to a fixture positioned in place. For acoustic measurements, the ExAblate™ is targeted at the geometric focus, and the hydrophone is scanned in 2D planes and 3D volumes about this point.....	18
Figure 5 Experimental set up with thrombus within the PE tubing inside the inverted calvarium, being connected to the flow system. The skull is positioned inside the FUS with a cylindrical standoff attached to the transducer so that deionized water is filled to a level of 220mm and degassed.....	20
Figure 6 Experimental setup, including filters used in Objective 4 to capture clot fragments.....	21
Figure 7 Top view of thrombus placed at FUS focus within human cadaveric calvaria. Left: Pre-FUS 30sec insonation, Right: Post-FUS 30sec insontation.....	25
Figure 8 Percent Clot Weight Loss: Boxplots by Skull ID #.....	27
Figure 9 Lysis Efficacy as a Function of Skull Characteristics: Scatter Plot by Skull ID #..	28
Figure 10 Representative CT images (Left) and radio density graphs (Right) for each of the three calvaria, please note the similarities in thickness and density between Skull #1 and Skull #2.....	29
Figure 11 Percent Clot Weight Loss: Boxplot by Intensity.	30

Figure 12 Lysis Efficacy as a Function of Acoustic Output Power: Scatter Plot by Intensity.....	31
Figure 13 Percent Clot Weight Loss: Boxplots by Flow Group.....	32
Figure 14 Lysis Efficacies as a Function of Flow Mechanics: Scatter Plot by Flow Group.....	33
Figure 15 Percent Clot Weight Loss: Boxplot by DC & PW combination Group.....	40
Figure 16 MATLAB reconstruction of CT images with thresholding set so that the stereotactic frame, fiducial holes and nylon securing screws are visible. Coordinates have been transformed into the AIMS/Exablate™ coordinate system, so that the calvarium appears in its orientation in the transducer. Top of the skull is toward the transducer, anterior aspect in the direction of the negative Y axis.....	44
Figure 17 Left: AIMS Scanning tank used in current experiments (pictures courtesy of ONDA Inc. [1]) Right: The overall measurement set-up, with a skull within the ExAblate™ FUS transducer placed inside the AIMS, with the hydrophones placed at the focus by the step motor.	46
Figure 18 3D reconstruction showing calvarium in stereotactic frame mounted in the FUS transducer, which is represented by the coordinates of its individual 973 elements. In the AIMS/ExAblate™ coordinate system, the origin is located near the lowest element, and the geometric focus is at 0,0,150 mm.	47
Figure 19 Plot of CT values along a representative measurement line that passes from a point in the skull interior to another external to the skull. The 2 points used to measure thickness are the first and last above half-maximum threshold. Points used for density calculations are within these boundaries, excluding the endpoints.	52
Figure 20 Calvaria thickness profiles mapped onto the skull outer surface at the points of measurement. Measurement vectors were created using the transducer element coordinates and the coordinates of the geometric focus as endpoints. As such, these measurements are influenced by the incident angle and may be more representative of the acoustic path length through the skull.	57
Figure 21 Average radiologic density in HU for each measurement profile as mapped onto the skull surfaces.....	58
Figure 22 Maps of insonation incident angles on the five calvaria used in this study. These maps show that the incident angles near the tops of the calvaria are	

consistently low, however the distribution over the remainder of the skulls shows considerable variation between specimens.....	59
Figure 23 Contour plots of normalized peak negative pressure measured at the Z=150mm plane for the control (lower right) and with interposing calvaria. In general, the location of the maximum value changes only slightly for calvaria A-D, but significant distortion and displacement is seen for calvarium E	60
Figure 24 3D scans of normalized peak negative pressure for the control (lower right) and interposing calvaria, measured in a 20mm cube centered about the focal target. Fields are thresholded at half-maximum value (-6dB).....	61
Figure 25 Percent clot weight loss for each acoustic output power group.....	71
Figure 26 Clot Fragmentation ($> 180 \mu\text{m}$) as Indicated by Post-Pre Test Filter Weight: Boxplot by Acoustic Output Power Group.....	73
Figure C-1 Acoustic intensity measurements within the focal region made with 1mm spacing.....	133
Figure C-2 Acoustic intensity measurements within the focal region made with 1mm spacing interpolated to 0.25mm spacing.....	134
Figure C-3 Acoustic intensity measurements within the focal region made with the exact function, actual 0.25mm measurement spacing.....	135
Figure C-4. Skull density values in HU were interpolated onto the measurement vector to create radiological density profiles, as is represented here for the measurement line for the 100 th FUS transducer element.....	136
Figure C-5 This is a zoomed-in representation of Figure C-5 where the point position for the density values have been included for the measurement line of the 100 th FUS transducer element.....	137

LIST OF ABBREVIATIONS

Acoustic Intensity Measurement System (AIMS)

Acoustic output power (AP)

Blood-Brain Barrier (BBB)

Computed Tomography (CT)

Continuous Wave (CW)

Decibel (dB)

Duty Cycle (DC)

Focused Ultrasound (FUS)

Food and Drug Administration (FDA)

High-Intensity Focused Ultrasound (HIFU)

Hounsfield Units (HU)

Insonation Duration (ID)

Magnetic Resonance Guided Focused Ultrasound (MRgFUS)

Magnetic Resonance Imaging (MRI)

Mechanical Embolism Removal Cerebral Ischemia (MERCI)

Peak Negative (or Rarefaction) Pressure (P_{NEG})

Peak Positive Pressure (P_{POS})

Polyethylene (PE)

Pulse Width (PW)

Sample Size (N)

Spatial Peak Temporal Average Intensity (I_{SPTA})

Three Dimensional (3D)

Tissue Plasminogen Activator (tPA)

Two Dimensional (2D)

Ultrasound (US)

University of California San Diego (UCSD)

Watts (W)

Chapter 1 BACKGROUND & SIGNIFICANCE

CLINICAL PROBLEM: STROKE

Worldwide, stroke is the second most common cause of death. Stroke claims 5.7 million lives each year, and it is projected that this current number of stroke deaths will increase by upwards of 30% within the next two decades. Ischemic stroke remains accountable for the majority of the 20 million devastating stroke events occurring globally each year [2]. In the United States stroke is the number one cause of serious chronic disability, with 800,000 U.S. citizens suffering from stroke every year [3]. Future-forecasting has predicted that in the next 20 years, there will be an increase in the aging population and a decline of socioeconomic standings, which will undoubtedly result in higher incidence of stroke and stroke related morbidity and mortality as these populations globally face greater risk factors and are most affected in terms of incidence and unfavorable outcomes of stroke [2]. As it stands today, the standards for stroke diagnosis and treatment are limited despite significant measures taken in stroke research. Tissue Plasminogen Activator (tPA) is the current gold standard of care worldwide, and in the United States it is the only drug approved by the Food and Drug Administration (FDA) for stroke treatment [4]. Stroke is one of the most devastating diseases, and, as current therapy is not deemed to be effective for the population at large, innovative prevention strategies are required, along with effective measures to promote access to effective stroke interventions worldwide.

CURRENT THERAPEUTIC APPROACHES AND THEIR DEFICIENCIES

Due to the restricted time window and various exclusion criteria, less than 3% of all stroke victims are eligible to receive tPA therapy, the standard of care in ischemic stroke. Only about 30% of stroke patients treated with tPA demonstrate good clinical recovery on the long term [5]. Innovative recanalization strategies or options to improve tPA efficacy are of high interest. Mechanical (ie, Mechanical Embolism Removal Cerebral Ischemia, MERCI) and chemical (ie, tPA or urokinase) methods to achieve successful thrombolysis continue to be evaluated with regard to therapeutic efficacy and clinical safety [6-18].

The currently available mechanical neurointerventional techniques to retrieve the vessel occluding blood clot are very promising [19-22], but are limited to highly specialized medical centers. Despite the unquestionable benefit of current treatment options for certain subgroups of stroke patients, the majority of these therapies are rather costly and/or restricted to comprehensive stroke centers. Eighty five percent of all deadly strokes, however, occur in low to middle income countries where 85% of the world's population resides [3] and where those therapeutic options are either not available, not commonly accessible, or simply too expensive.

Ultrasound techniques for sonothrombolysis are not yet an accepted treatment for stroke and, at this point in time, are purely investigational. There are convincing data related to the use of transcranial ultrasound (US) in combination with tPA administration for improved thrombolysis and early recanalization [6, 12, 23-30]. US energy is believed to enhance clot lysis partly by mechanical disaggregation of fibrin fibers—a reversible process that allows for improved distribution of plasminogen and tPA within a blood clot



[16, 23, 24, 31, 32]. However, due to the vast exclusion criteria for tPA, the patient population that could potentially benefit from this combined US and tPA therapy is still less than 3% of all stroke victims [5].

There has been a recent refocus on research into noninvasive, more widely applicable therapeutic stroke approaches, and first clinical studies on transcranial sonothrombolysis in stroke patients using diagnostic US parameters are promising [6, 11, 28, 30]. These early stage results of transcranial application of US indicate that it might provide the opportunity to induce clot lysis noninvasively and in the absence of tPA. Though much of transcranial sonothrombolysis research has been mainly directed toward feasibility [7, 14, 33-35], the limiting factors were noted as early as the 1950's and 1960's [36-38].

To date, the vast majority of US applications for therapy of the human body have been based on thermo-ablative effects [39]. Although accepted as a mechanism of treatment in other regions of the body, thermal effects remain a concern in brain application of US [39-42]. Due to its enclosed arrangement within the skull and the inherent sensitive nature of the brain, special consideration to insonation precision and thermal control must be put into effect to minimize adverse side effects of US therapy within the brain.

A further major limitation of transcranial US techniques results from the acoustic signal absorption and beam distortion via the skull. Ultrasound beams are widely and irregularly scattered by the inhomogeneous bone and brain tissue [40-45]. Successful sonothrombolysis could potentially demonstrate additional harmful effects caused by insonation-induced clot fragments. Clot fragments may lead to secondary vessel occlusion



farther downstream in the supply area of the affected vessel. This is a safety concern, because of the potential risk of secondary strokes [46].

NEED FOR IMPROVEMENT

The majority of strokes are ischemic, caused by intracranial thromboembolic arterial occlusion [47]. Vessel recanalization is the primary goal of all acute stroke treatment approaches. Achieving vessel recanalization quickly and without causing further damage is a key objective in effective treatment. Time is of the essence in stroke treatment, as about 2 million neurons die every minute in an ischemic brain [48]. In both diagnostic and therapeutic stroke care, the limiting and determining factor of a successful outcome is a patient's access to appropriate medical facilities, both in terms of time and the level of care available.

Optimum widespread care would effectively achieve thrombolysis mechanically without the administration of tPA therapy, to do away with the potential drug-related side effects, availability issues, and time restrictions. The current sonothrombolysis trials using diagnostic US are achieving efficacious clot lysis following an hour or more of insonation durations and with the aid of tPA [11, 12, 30, 49, 50]. Achievement of sonothrombolysis in seconds versus the standard hours would not simply reduce the total time of therapy, but it could potentially minimize the US exposure-related tissue damage. The standard in current sonothrombolysis trials is the use of conventional or customized [51] transcranial ultrasound systems that are not well focused, impacting significant regions of the brain tissue that are not the intended target site. As opposed to thermal ablation, controlled

cavitation produced by ultrasound at target sites could alternatively have desirable thrombolytic mechanical effects without damaging or heating the surrounding tissue [52].

Transcranial high-intensity Focused Ultrasound (FUS or HIFU) for stroke therapy is an innovative mechanical approach to achieving fast and efficacious sonothrombolysis. FUS provides the ability to transcranially deliver desired energy to a set, targeted region of the brain with precision and effectiveness, minimally affecting the brain tissue outside of the region of interest. Transcranial FUS for stroke therapy might be able to overcome the major concerns expressed in the field, especially with regard to US beam distortion and phase aberration, unwanted cavitation, thermal effects, and clot fragmentation.

INTRODUCTION TO FOCUSED ULTRASOUND

HISTORY OF FOCUSED ULTRASOUND IN THE BRAIN

In the 1940's, the use of FUS for noninvasive brain applications was initiated [53]. These initial, animal studies used FUS for its true purpose of delivering US energy to a small, predefined volume. The pioneer researches were able to lay the foundation for the application of FUS energy to generate localized brain tissue damage [54]. Their research provided important information on the ability to treat brain tissue while identifying quantitative thresholds that result in permanent changes at the target site [55]. This resulted in the desired outcome for the majority of brain FUS applications at the time, achieving FUS-induced thermal ablation leading to brain lesions at the target site [56, 57]. The Fry brothers at the University of Illinois were also able to transiently open the blood-brain barrier (BBB) via noninvasive FUS energy [58]. In 1957, the first clinical trials were initiated, using FUS for Parkinson's Disease therapy [59]. Due to difficulties in focusing the

US beam while passing through the skull, trepanation windows and craniotomies were performed commonly for treatment. A primary concern with transcranial FUS application was the occurrence of beam distortion and phase aberration, caused by passing the US wave through the skull. With the research dedication of the Fry brothers, in 1980 transcranial FUS delivery was possible at the desired target site, but beam distortions could not be alleviated [60]. In the 1990's, the current leading researchers Hynynen and Jolesz were able to create a beam distortion solution and phase aberration corrections to allow transcranial focused ultrasound delivery at targeted brain tissue [61].

In 1994, the first commercial, high intensity, focused ultrasound device was made available in Europe, but it was not approved for use in the brain. In 1999, focused ultrasound transducers that were made to be compatible with magnetic resonance imaging (MRI) were first developed [62]. Magnetic Resonance Guided Focused Ultrasound (MRgFUS) technology (InSightec Inc. Tirat Carmel, Israel) became the leading tool for monitoring therapeutic effects of FUS, with navigation of the applied FUS energy and the produced thermal changes in the tissue based on MRI derived thermometry, [45, 63, 64]. The ExAblate™ 3000 (InSightec Inc.) was the first MRgFUS system for clinical brain use, introduced in 2002 [65]. The present-day system, the ExAblate™ 4000, is the FUS system (not MR guided) used for all transcranial sonothrombolysis work performed for this research at the Brain Ultrasound Research Laboratory, University of California, San Diego.

FOCUSED ULTRASOUND THROMBOLYSIS

Until now, FUS sonothrombolysis research in the brain has been mostly done non-transcranially (using extracranial vessels or in an isolated system) and with the aid of tPA.

In 2006, Frenkel *et al.* [66] experimented with FUS thrombolysis in an *in vitro* model

using artificially made, human blood clots. After comparing clot lysis between four experimental groups (control, FUS, tPA, and FUS + tPA), the researcher found insignificant clot lysis in relation to the control when FUS treatment was used alone. However, when FUS was used in combination with tPA, clot lysis was significantly greater than when treated with tPA alone. They were also able to show that with pulse repetition frequency, as well as increasing acoustic power, greater clot lysis could be achieved. For this *in vitro* study, it could be concluded that use of FUS enhanced tPA-mediated clot lysis.

Stone *et al.* [67] studied thrombolysis in an *in vivo* clot model using the rabbit marginal ear vein. They compared clot lysis between four groups: control, FUS, tPA, and pulsed FUS in combination with administration of tPA boluses. The control and standalone FUS therapy groups did not achieve significant clot lysis. Clots treated with tPA alone were lysed, although incompletely, leading to partial vessel recanalization. Whereas, the combined FUS and tPA treatment method led to total vessel recanalization. Post treatment, no histological damage was assessed within the endothelial or extravascular tissues. The authors concluded that for their *in vivo* model, noninvasive, pulsed-FUS treatment could enhance tPA-mediated thrombolysis significantly.

Unlike the above mentioned research, Rosenschein et al. [68], achieved efficient clot lysis using FUS alone and in the absence of tPA. In this study, a therapeutic transducer was constructed using an acoustic lens and which had an integrated ultrasound imaging transducer. *In vitro* clots were created and inserted into bovine arterial segments that were then insonated with guidance from real-time imaging techniques. The combined FUS / imaging technology made it possible to visualize cavitation clouds during insonation, which led Rosenschein et al. to believe FUS-induced cavitation could play an effective role

in sonothrombolysis. The authors were able to show that thrombolysis efficacy using pulsed FUS depended on total insonation duration and the optimal FUS parameter selection. In this study, in addition to sonothrombolysis efficacy, the authors investigated vascular safety and clot fragmentation. The researchers found that, in their model, 93% of FUS-induced clot fragments were subcapillary in size. However, arterial damage was found in the bovine artery segments exposed to a sonication intensity (I_{spta}) of 45 W/cm² for ≥ 300 seconds of duration.

The goal of the current work was to investigate the potential use of FUS for noninvasive, transcranial clot lysis in the absence of tPA. The overall objective of this *in vitro* research was to investigate the use of our FUS headsystem, which has been designed for human applications, as a noninvasive, standalone method of achieving sonothrombolysis. Using FUS transcranially in the absence of tPA would have a major clinical impact, enabling treatment for millions of stroke victims worldwide who are presently not eligible for the current standard of care.

Chapter 2 SPECIFIC OBJECTIVES

Although others have described some of the basic mechanisms of sonothrombolysis, translating this knowledge into practice regarding feasibility and efficacy in order to treat stroke patients has not been established. Investigating the acoustic effects at the clot site with the use of various *ex vivo* skulls during insonation in a flow model should help us understand and determine the acoustic properties that are optimal for efficacious transcranial FUS insonation, both with respect to sonothrombolysis and potential clot fragmentation. The current investigation has been segmented and approached as four progressively building, specific objectives:

- (1) Determine the experimental feasibility of a FUS system for transcranial sonothrombolysis
- (2) Perform a parameter optimization for the FUS system for effective sonothrombolysis by varying duty cycle and pulse width settings
- (3) Characterize the acoustic field produced by the transcranial FUS and determine how it is affected by the skull
- (4) Determine how sonothrombolysis efficacy and potential clot fragmentation are impacted by varying the FUS intensity

This stepwise approach allows us to acquire knowledge and build on that knowledge in a systematic manner. This scientific method allows for experimental parameters and considerations to be isolated from the system and tested as independent variables. This is accomplished through specific objectives that will be developed to

collectively answer the investigational question: is focused ultrasound effective for transcranial sonothrombolysis in stroke? The expected outcome of this investigation will build on current knowledge and provide significant new insights to foster the potential, future use of focused ultrasound for transcranial sonothrombolysis for stroke treatment.

OBJECTIVE 1: TECHNIQUE FEASIBILITY

Question: Can FUS without the use of tPA induce sonothrombolysis and how does this depend on acoustic power, skull morphology, and vascular flow mechanics?

Rationale: The use of transcranial ultrasound in combination with tPA for sonothrombolysis has been demonstrated to be promising in initial investigations [6, 12, 23-30]. However, absorption and defocusing of the ultrasound beam occur during trans-skull insonation, limiting the efficiency of this approach to a high extent. The purpose of this research segment was to investigate the feasibility of using FUS for transcranial sonothrombolysis without the use of tPA in an *in vitro* flow model, concentrating on the effects of variations in acoustic power, skull anatomy, and blood flow through the cerebral vasculature on clot lysis.

OBJECTIVE 2: PARAMETER OPTIMIZATION

Question: What is the impact of varying duty cycle (DC) and pulse width (PW) on clot lysis and how can these FUS operating parameters be selected to optimize lysis efficacy?

Rationale: Based on knowledge gained in regard to feasibility (Objective 1), we now know that FUS for transcranial sonothrombolysis in the absence of tPA demonstrates



potential as a noninvasive, non drug-dependent therapeutic option for stroke. Yet, data describing the transcranial application of FUS as a potential treatment option for stroke patients is sparse on certain key details, including which operating parameter combinations might be preferable over others. The optimized parameter combinations for using FUS system are key in regard to the efficacy and safety of transcranial sonothrombolysis. In consideration of the previously mentioned concerns, thermal as well as cavitational effects are most feared. Consequently, the next objective after confirming feasibility of FUS for transcranial sonothrombolysis is parameter optimization. This was done by a parametric investigation, defining the most efficacious combinations of ultrasound operating parameters for sonothrombolysis.

OBJECTIVE 3: ACOUSTIC FIELD CHARACTERIZATION

Question: What is the effect of the skull on the acoustic field produced by transcranial FUS and how does this effect depend on skull bone thickness, density, and incident angle?

Rationale: The ExAblate™ 4000 headsysteem transducer is considered to be a low frequency FUS system due to its frequency preset at 220kHz. The therapeutic mechanism for low frequency FUS is controlled by the selected acoustic parameters, such as pulse width, duty cycle, and applied acoustic power. As examined for a maintained acoustic power, the optimized parameters for DC and PW were determined in Objective 2 for effective sonothrombolysis. The shape and location of the focus is well known for the ExAblate™ 4000 FUS system; however, the effect of varying skull specimens must also be established in regard to the location, shape, and intensity of the acoustic focal zone. MR can



locate the acoustic focus by thermal imaging, guiding the operator in the ultrasound beam path and therapy, but the spatial resolution is quite low. Before using MR to locate the focal spot, there exists considerable uncertainty as to its actual location. The current investigation was aimed at reducing this uncertainty by characterizing the effects of the skull on the applied acoustic field so that there is a basis of predictability for locating the acoustic focus in future studies.

OBJECTIVE 4: SONOTHROMBOLYSIS & FRAGMENTATION

Question: What is the impact of varying intensities on clot lysis efficacy and how does this correlate to potential clot fragmentation?

Rationale: Basic principles of using ultrasound to enhance thrombolysis have been described [23-27, 69], and first clinical studies on transcranial sonothrombolysis in stroke patients using diagnostic US devices are promising [6, 12, 28, 30]. Current research in thrombolysis has been mainly focused on clot lysis feasibility [7, 14, 33-35], but only to a limited extent on clot fragmentation. Only a few publications describe the interplay between both [68, 70-72]. This phase of the study investigated the impact of acoustic output power on transcranial thrombolysis efficacy and evaluated potential clot fragmentation using FUS, aiming to find a potential correlation linking increasing intensity, clot lysis, and fragmentation.

Chapter 3 COMMON RESEARCH APPROACH

MATERIALS & METHODS

ULTRASOUND SYSTEM AND PARAMETERS

An ExAblate™ 4000 Focused Ultrasound headsystem (InSightec Inc.), equipped with a transcranial transducer, was used for all experiments. This FUS system has been developed for brain applications. A key component of this system is a hemispherical phased array transducer with 973 single-piezo elements that operate individually and independently of one another. Along with this desirable feature, the geometry and symmetry of the ExAblate™ 4000 FUS allow the headsystem to insonate through the entire skull with 973 individual beams, a function that is unique to this FUS system. Other conventional ultrasound systems produce a single beam that must pass through a specific location on the skull in order to travel through the brain tissue and hit the target from a single direction. Each of the 973 individual beams of the ExAblate™ 4000 FUS system thus insonate at drastically lower intensity levels compared to the intensity of the single beam produced by a conventional ultrasound system. The 973 individual beams in the ExAblate™ 4000 FUS system come together in the center of the transducer to form a sharp, three dimensional (3D) beam focus, with a radius of 2.0mm in the X/Y-axes and 3.0mm in the Z-axis (Figure 1). The focus can be electronically steered in any direction without losing its shape, as long it is moved within a 3.0 cm radius from the center of the transducer. The three dimensional beam focus and its central location enables insonation of a target structure, such as a blood clot, from all directions of the hemispheric

headsystem [65]. The ExAblate™ 4000 FUS headsystem's preset transmit frequency is 220 KHz.

For the purpose of appropriate neuronavigation prior to and during a therapeutic procedure, the ExAblate™ 4000 FUS is designed to work in conjunction with MRI, using MR-Thermometry to visualize the focus beam. The current research was done purely *in vitro* with the use of the ExAblate™ 4000 FUS alone, but future clinical studies would have the added advantage of being used as a combined MRgFUS headsystem.

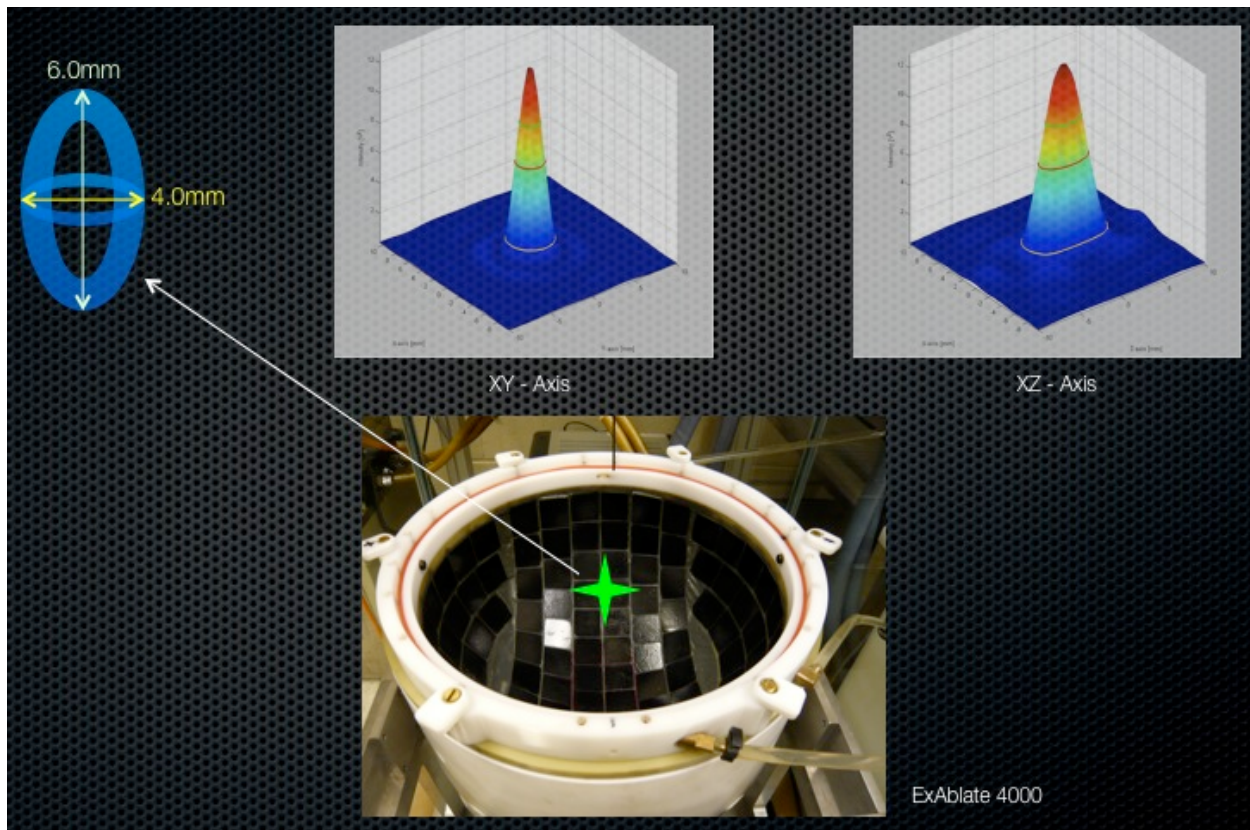


Figure 1 Characteristics of the Focused Ultrasound System. Upper Left: Representation of the dimensions of the focused beam; Upper Center & Right: Representative sound field images; Bottom: The top view of the hemispheric FUS transducer.

CLOT PREPARATION

Blood samples collected from healthy, un-medicated human volunteers were collected and used for research, as per a University of California San Diego (UCSD) Institutional Review Board approved protocol. Fresh, human, venous whole blood was drawn directly into citrate Vacutainer® tubes (Becton Dickinson, Franklin Lakes, NJ). Then a mixture of 0.5ml citrate blood with 40 μ l CaCl₂ (210mmol/l) was transferred into a boro-silicated glass tube, which had suspended within the center of its length a 2-0 silk thread. Thrombi were organized around the silk thread after incubating for 3.0 hours in a water bath preheated to 37 °C, allowing the clot to be freely positioned within the focus of the transducer. The formed thrombi had an average weight of 0.2519g ± 7%, and an approximate length of 2.5 cm (Figure 2). Formed clots along the silk thread were transferred into a polyethylene (PE) tube (Advanced Polymers, Inc., Salem, NH) having an inner diameter of 4.3 mm, a wall thickness of 25.4 μ m, and possessing preferred acoustic properties for ultrasound use. The loose end of the silk thread was fixed upstream inside the flow system within the transducer range, such that the location of the thrombus within the PE tubing was fixed within the natural FUS focus.

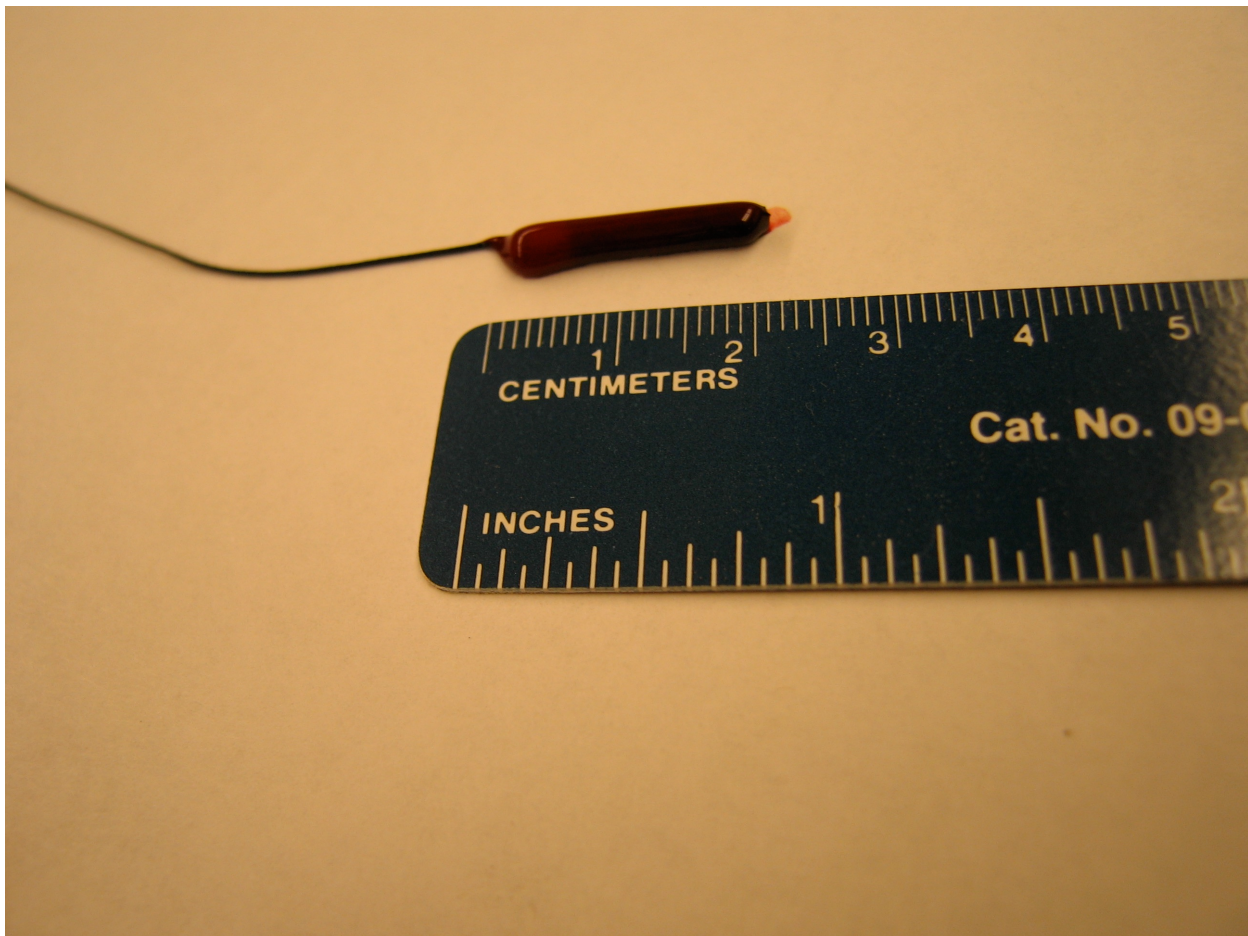


Figure 2 Blood clot organized around a silk thread, ready to be placed into PE tubing.

SKULL SPECIMENS

Human cadaver skull specimens were obtained from the UCSD Division of Anatomy. Only a numerical identifier identified the calvaria and no additional information was known about the donors.

FIXTURE

The calvaria specimens were attached to a custom-designed, acrylic frame fixture (Figure 3). This fixture enabled consistent specimen positioning within both the ultrasound transducer system and the Computed Tomography (CT) scanner, which also

allowed for the establishment of fiducial markers for coordinate system registration. The skull specimen remained attached to its specific fixture throughout the study, which allowed it to be placed back in the ultrasound system for additional measurements when desired, without loss of spatial registration (Figure 4).

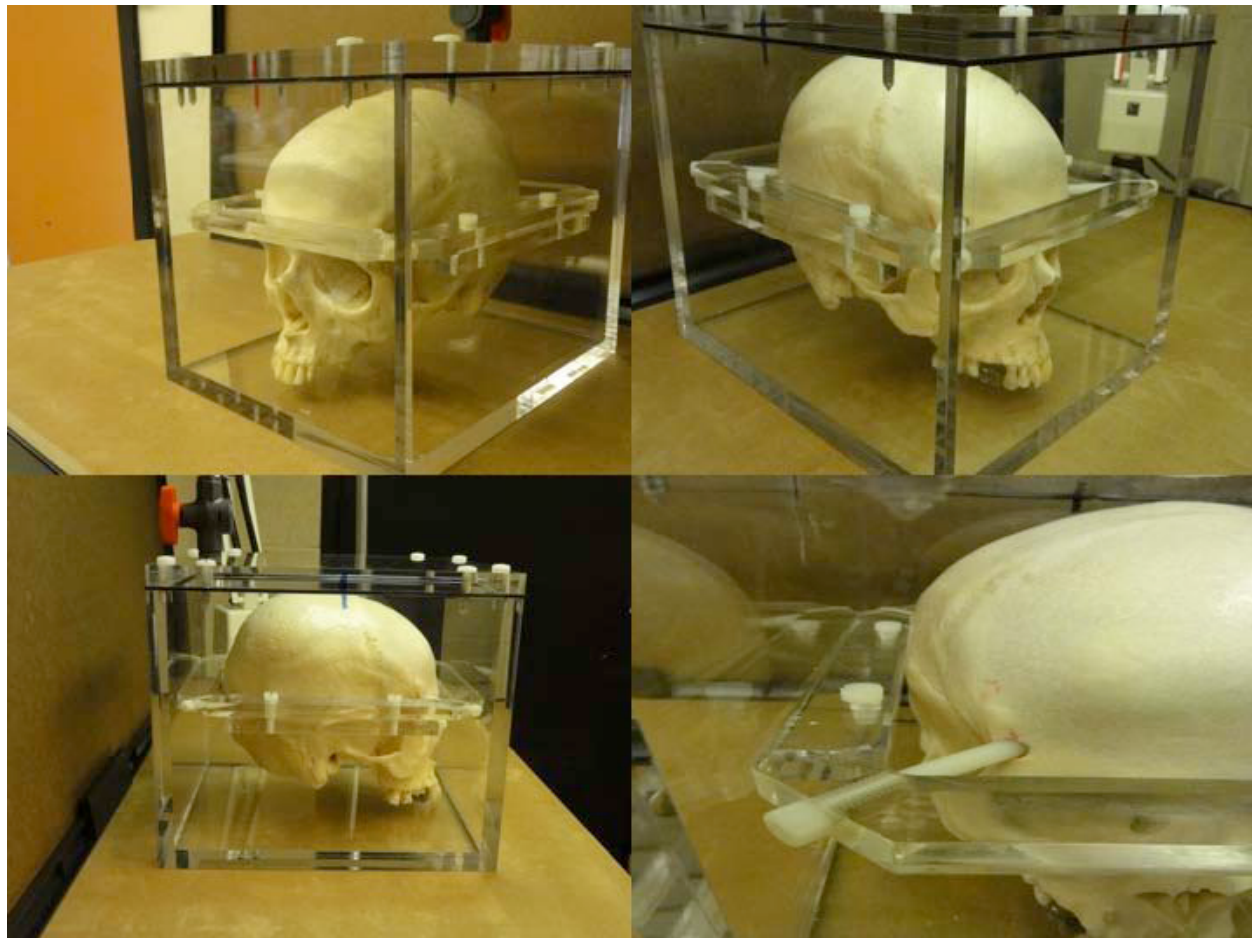


Figure 3 Four different views of a sample cadaveric skull attached to fixture and placed in chamber. For the experiments, only the calvarium was mounted within the fixture.

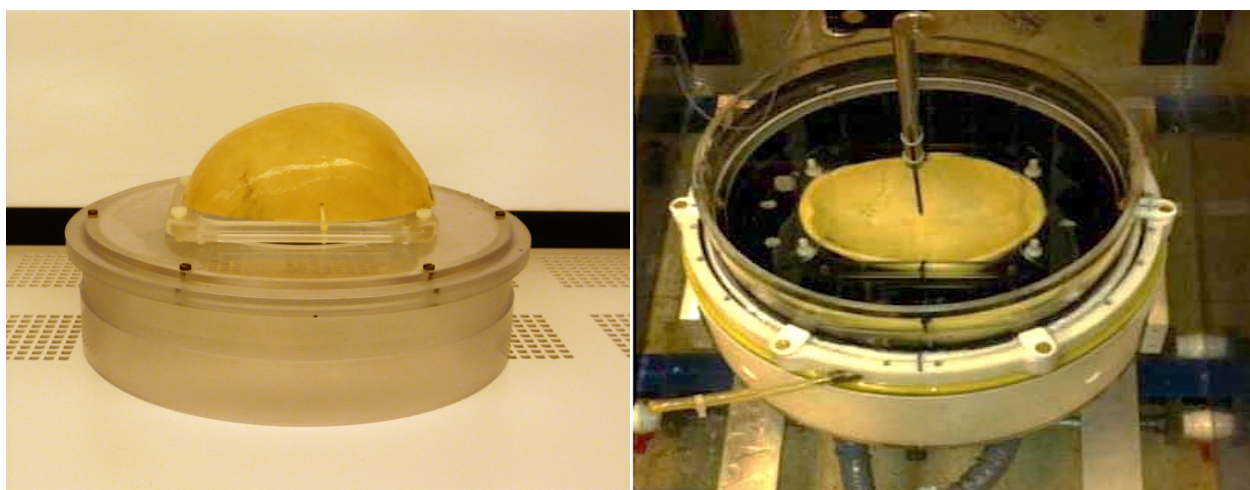


Figure 4 Left: An overturned view of a calvarium on an acrylic frame that is fixed to a plastic cover with hole in its center to provide access to the skull cavity which is then attached to the cylindrical standoff. Once the skull is in position the entire device is placed upside down on top of the water filled hemispheric transducer. Right: Top view into the ExAblate 4000™ helmet showing a hydrophone and a calvarium attached to a fixture positioned in place. For acoustic measurements, the ExAblate™ is targeted at the geometric focus, and the hydrophone is scanned in 2D planes and 3D volumes about this point.

SPECIMEN CHAMBER

Prior to CT scanning, each skull specimen – attached to its fixture – was placed and secured in a custom vacuum chamber filled with deionized molecular grade water. The chamber was then sealed and degassed by vacuum, at -300mm Hg for 72 to 96 hours.

3D COMPUTER TOMOGRAPHY DATA ACQUISITION

Each degassed calvarium specimen, on its fixture and in its chamber, then underwent computer tomography scanning (Discovery CT750 HD, 64 slice CT scanner, GE Healthcare). The skull orientation of the specimens was matched to a living human patient, producing axial image slices. Each CT image was comprised of 512 x 512 pixels, covering a 320mm x 320mm area, for pixel dimensions of 0.625mm. The slice thickness was

0.625mm, resulting in voxels measuring 0.625mm x 0.625mm x 0.625mm. Scanning was done in spiral mode using the high peak voltage of 120 kVp, which is ideal for skull imaging due to the increased bone penetration. Bone Plus kernel, an image reconstruction filter/algorithm, was used for CT imaging [73]. DICOM data of each calvarium specimen were saved and processed.

FUS EXPERIMENTAL SET UP

For consistent positioning and proper suspension of the skull within the transducer field, each of the cadaveric skull specimens was mounted on its custom-designed acrylic frame, as described above. The rim of the fixture was secured in a designated position with respect to the transducer. Once in position, the hemispheric transducer with an inverted cadaveric skull specimen was filled with degassed water, and fitted with a standoff to allow water to be filled an additional 50mm above the rim. The standoff was used to help avoid reflections from the air-water interface interfering with the signal at the focal zone (Figure 5). To physically locate the focal zone within the ExAblate™ 4000 FUS, a 3D step motor system navigated a pointer to indicate the focus in the center of the hemispheric transducer. Thus, this marking was used to manually align the center of the thrombus within the PE tubing at the natural FUS focus, within the cavity of the skull in the transducer. The PE tube was connected to a peristaltic pump to make possible a non-circulating, unidirectional flow system.

Experiments using the flow system were exposed to a pulse-perfusion system either with flow (10ml/min) or with no flow (0ml/min). The flow pump was turned off for no flow conditions to mimic flow stasis. The fluid medium within the transducer heads system

and the tubing was degassed, deionized molecular grade water and the temperature was kept at 24°C. A FUS insonation duration of 30 seconds was set for all sonothrombolysis experiments. The overall schematic of the experimental setup is shown in Figure 6.

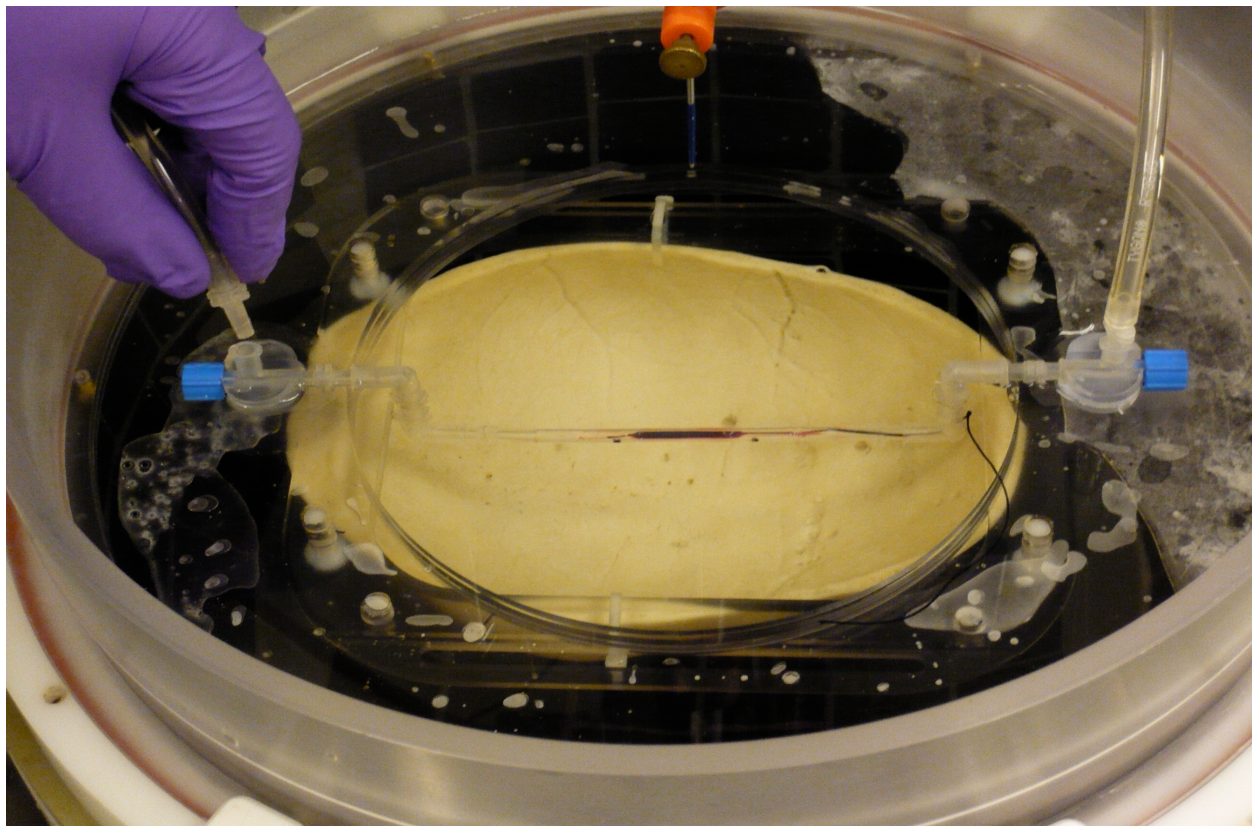


Figure 5 Experimental set up with thrombus within the PE tubing inside the inverted calvarium, being connected to the flow system. The skull is positioned inside the FUS with a cylindrical standoff attached to the transducer so that deionized water is filled to a level of 220mm and degassed.

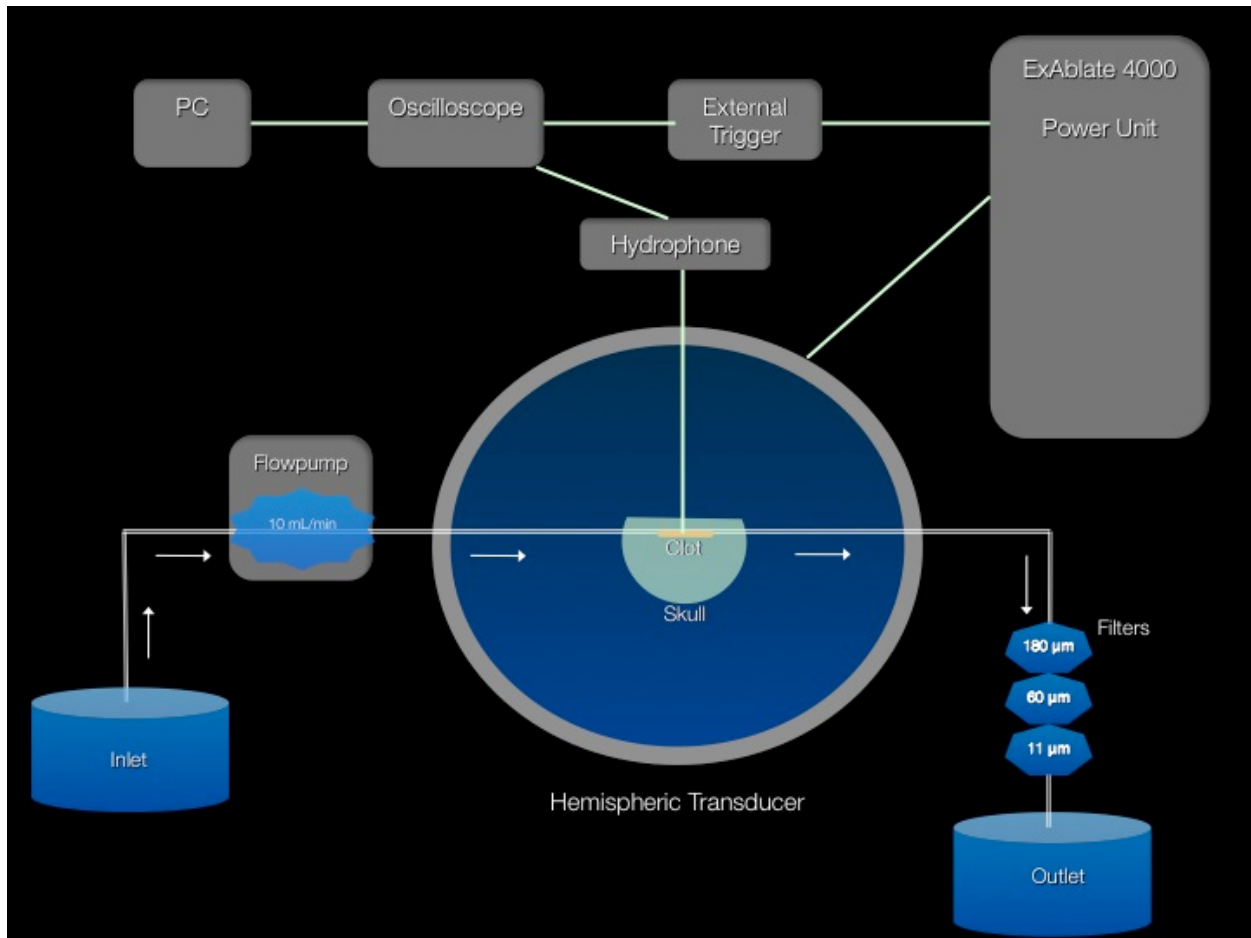


Figure 6 Experimental setup, including filters used in Objective 4 to capture clot fragments.

Chapter 4 FEASIBILITY OF FUS AS A THROMBOLYTIC THERAPY

OBJECTIVE 1: TECHNIQUE FEASIBILITY

Can FUS without the use of tPA induce sonothrombolysis, and how does this depend on acoustic power, skull morphology, and vascular flow mechanics?

MATERIALS & METHODS

PARAMETERS MEASURED

A total of 420 experiments were done in an effort to address transcranial sonothrombolysis feasibility as it relates to varying acoustic output powers, changing flow conditions, and different skull specimens. The sonothrombolysis efficacy was measured as clot weight loss. Lysis efficacy was tested for each research parameter variation, and results were presented as both percent and grams of post-experiment clot weight reduction. Tables 1 through 3 list the number of specimens for each parametric test.

Is FUS sonothrombolysis efficacy dependent on skull characteristics?

To test for the impact of skull characteristics on sonothrombolysis efficacy, 126 experiments were run using 3 human cadaver calvarias. The skull specimens identified as #1, #2, and #3, were the variables, while flow was present at 10ml/min and the FUS operating parameter were constant, set at:

Acoustic output power (AP) = 270W
 Duty cycle (DC) = 50%
 Pulse width (PW) = 200ms
 FUS duration (ID) = 30sec



Table 1 Percent weight loss as a result of skull variations, N per study group

	N
Skull #1	44
Skull #2	41
Skull #3	41
Overall	126

Is FUS sonothrombolysis dependent on acoustic output power?

To study the effect of acoustic output power on sonothrombolysis efficacy, all other experimental variables were held constant. Accordingly, the experimental variable, acoustic output power, was gradually increased while for all experiments Skull #1 was used, flow was present at 10ml/min, and the FUS operating parameters were held constant at:

Duty cycle (DC) = 50%
 Pulse width (PW) = 200ms
 FUS duration (ID) = 30sec

Table 2 Percent weight loss as a function of acoustic output power using Skull #1, N per study group

	N
100W	46
200W	41
235W	40
270W	40
400W	41
Overall	208

Is FUS sonothrombolysis dependent on flow mechanics?

A total of 86 experiments were performed, testing the impact of flow mechanics on clot lysis efficacy. For Group 1 studies, there was no flow during FUS insonation, while a

low velocity flow of 10ml/min was present during Group 2 experiments. Skull #1 was used for all of the experiments in the two groups, while the FUS operating parameters were held constant at:

Acoustic output power (AP) = 270W
 Duty cycle (DC) = 50%
 Pulse width (PW) = 200ms
 FUS duration (ID) = 30sec

Table 3 Percent weight loss as a function of flow condition using Skull #1, N per study group

	N
Flow	44
No Flow	42
Overall	86

STATISTICAL ANALYSIS

Student's t-tests was used to assess pre/post weight loss, and to test the relationship of various skulls' to clot weight loss, pair-wise comparisons were performed. The Bonferroni method was used to adjust for multiple comparisons. A Kruskal-Wallis test was used to examine if there is a difference in clot weight among varying intensity groups. Pairwise comparisons were performed using a Wilcoxon Rank Sum test, followed by Holm's adjustment for multiple comparison. A two sample Student's t-test was used to examine if there is a difference in clot weight loss between group with no flow and flow, using skull #1 and the same intensity.

RESULTS

Summary results are provided in the following chapter. Detailed results for all conducted experiments can be found in Appendix A.

In total, 420 *in vitro* sonothrombolysis experiments were conducted. Different parameter variations were examined to answer each of the following research questions.

Does FUS produce transcranial sonothrombolysis?

Transcranial sonothrombolysis was conceived feasible by FUS as all clots were significantly lysed after 30 seconds of insonation duration, without the use of any lytic agent (Figure 7). The amount of measured clot weight loss was dependent on the tested variables of the experimental groups. The lysis efficacy ranged from as low as 6.21% to as high as 77.26%, dependent on the skull characteristics, acoustic output power, and flow mechanics.

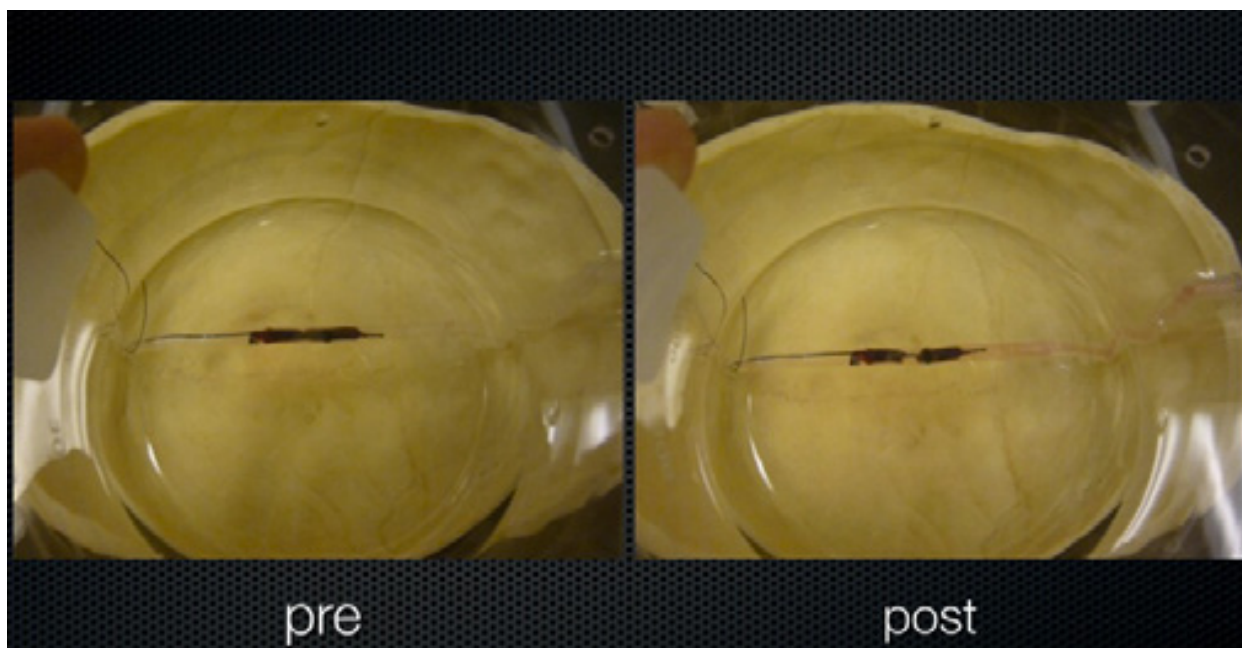


Figure 7 Top view of thrombus placed at FUS focus within human cadaveric calvaria. Left: Pre-FUS 30sec insonation, Right: Post-FUS 30sec insontation.

Is FUS sonothrombolysis efficacy dependent on skull characteristics?

The average percent clot weight loss by skull used is depicted in Figure 8, Table 4, and as scatter plot in Figure 9. For each of the three calvaria specimens, the average weight loss was statistically significant ($p<0.001$) for all of the sonothrombolysis experiments. A smaller percent weight loss was found in Skull #3 compared to Skull #1 and Skull #2 (both $p<0.001$). Likewise, there was a smaller percent clot weight loss in Skull #2 compared to Skull #1 (Table 5). However, when adjusted for multiple comparisons, the clot weight loss when using Skull #1 versus Skull #2 was not found to be statistically significant ($p=0.051$).

Analyses of measurement of bone thickness and density, expressed in Hounsfield Units (HU), based on 3D CT data acquisition of all three skulls are represented in Figure 10. Skull #1 and Skull #2 were found to have similar mean bone thickness (6.50mm vs. 6.00mm), respectively, and had the exact same mean radio density of 1883HU. Analysis of the CT data for Skull #3 confirmed the visual observation of greater average bone thickness, 9.30mm, and radio density, 2235HU, compared to the other skulls specimens.

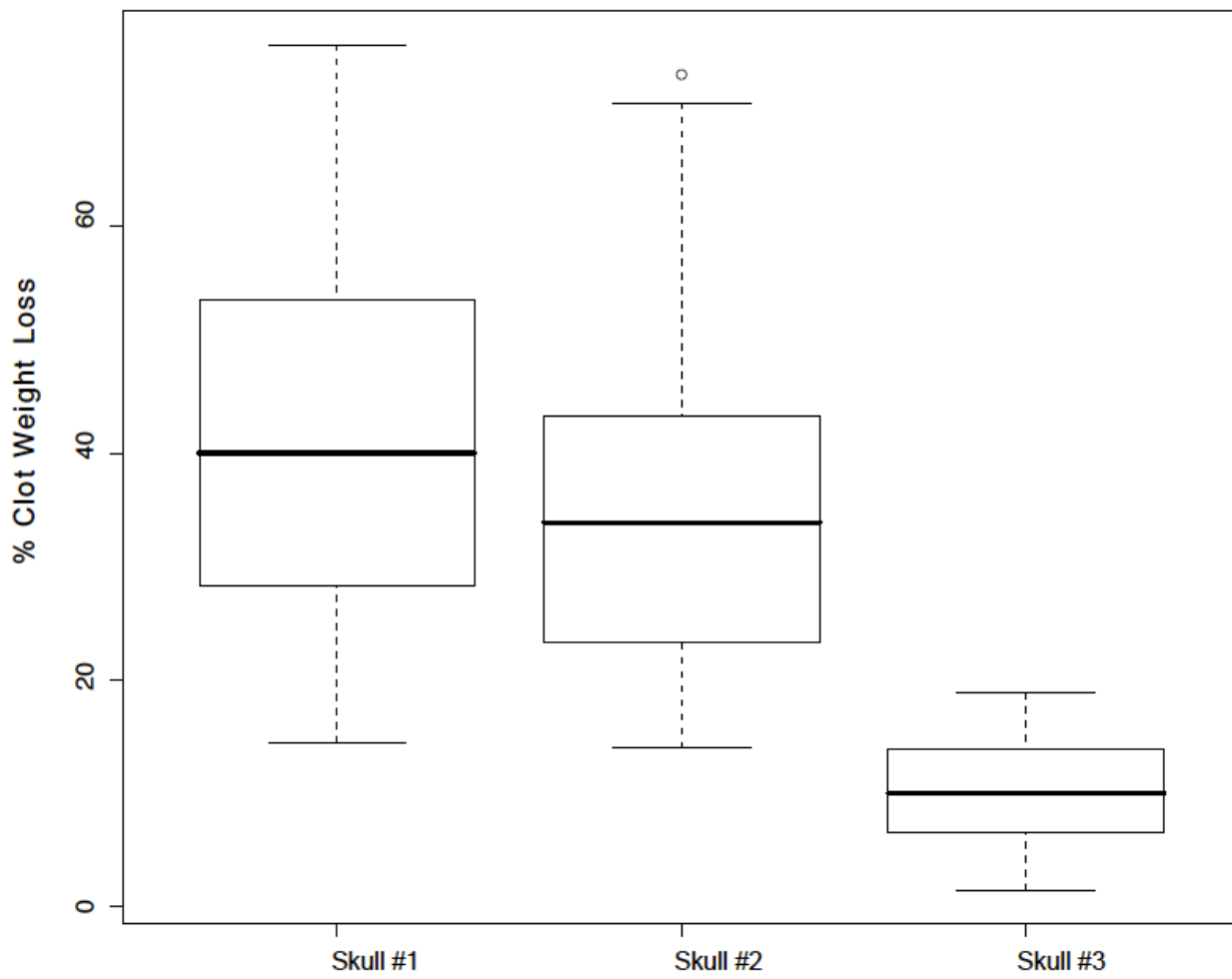


Figure 8 Percent Clot Weight Loss: Boxplots by Skull ID #.

Table 4 Percent Clot Weight Loss by Skull Specimen Compared to Pre-Insonation Weights

Groups	Number of Experiments	Mean	Standard Deviation	Minimum	Median	Maximum	P-value
Skull #1	44	42.12	16.15	14.50	40.04	76.01	<0.001
Skull #2	41	35.59	14.23	14.02	33.90	73.39	<0.001
Skull #3	41	10.32	4.35	1.47	10.02	18.86	<0.001
Overall	126	29.65	18.69	1.47	26.52	76.01	<0.001

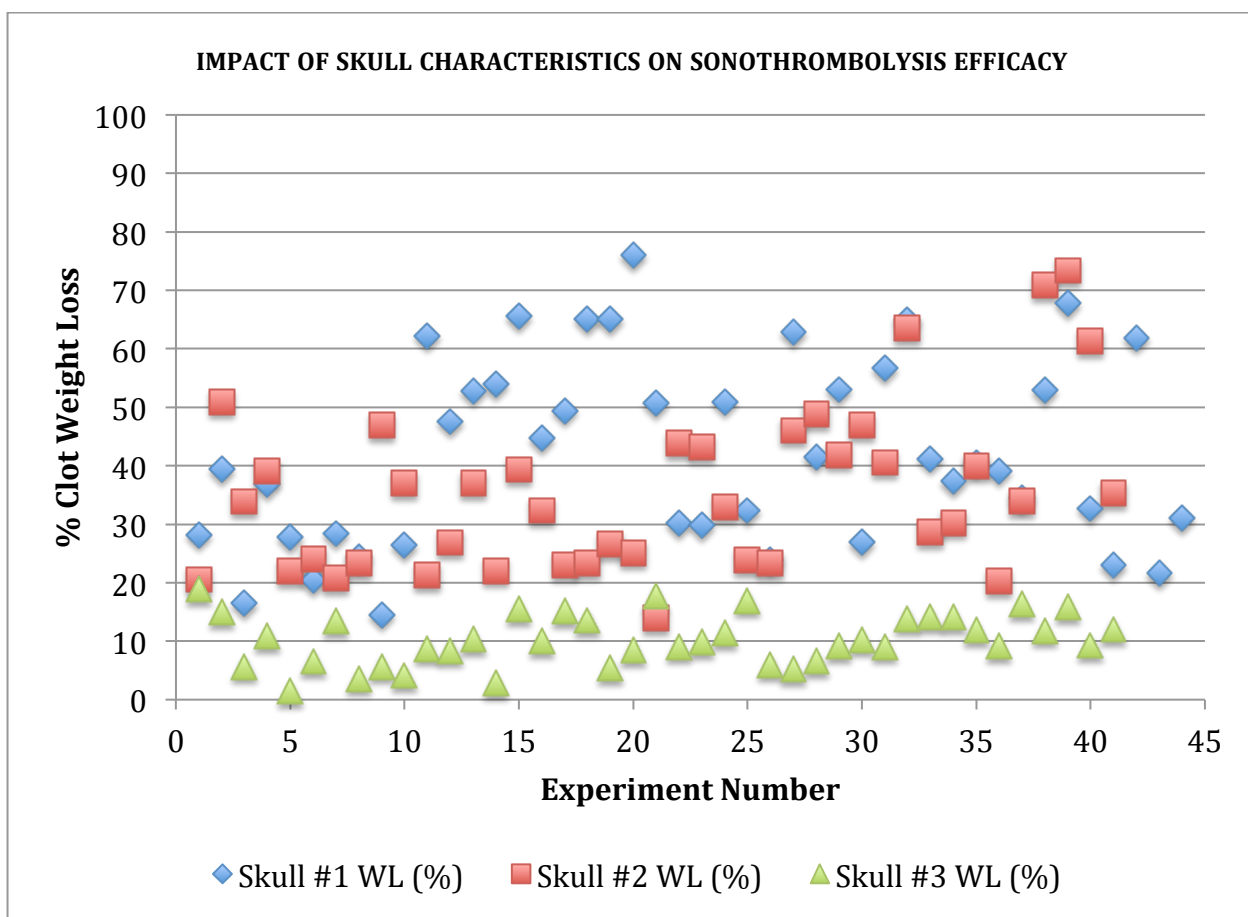


Figure 9 Lysis Efficacy as a Function of Skull Characteristics: Scatter Plot by Skull ID #.

Table 5 Pairwise Comparison of the Sonothrombolysis Efficacy as a Function of Skull Specimen

	P-values
Skull #1 vs. Skull #2	0.051
Skull #1 vs. Skull #3	<0.001
Skull #2 vs. Skull #3	<0.001

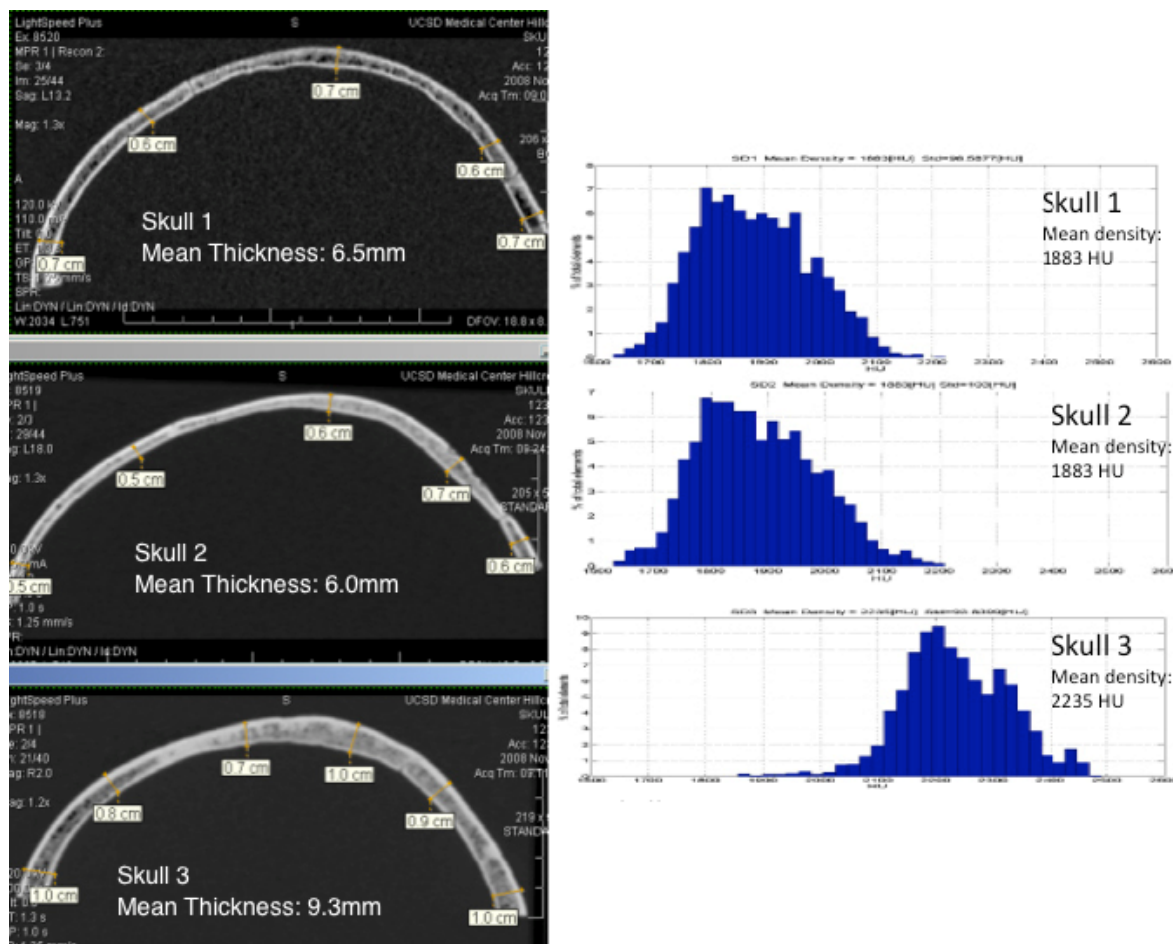


Figure 10 Representative CT images (Left) and radio density graphs (Right) for each of the three calvaria, please note the similarities in thickness and density between Skull #1 and Skull #2.

Is FUS sonothrombolysis dependent on acoustic output power?

Intensity was found to affect clot weight loss, with higher intensity resulting in a larger weight percent loss, these results are illustrated in Figures 11 and 12. Clot weight percent loss was found to be statistically different, with a p-value <0.0001, from 0 for all intensity groups (Table 6). Also, each step increase in intensity was found to positively affect clot weight percent loss overall (p-value from Kruskal-Wallis test < 0.001). All pairwise comparisons were found to be statistically significant when adjusted for multiple comparisons using Holm's method.

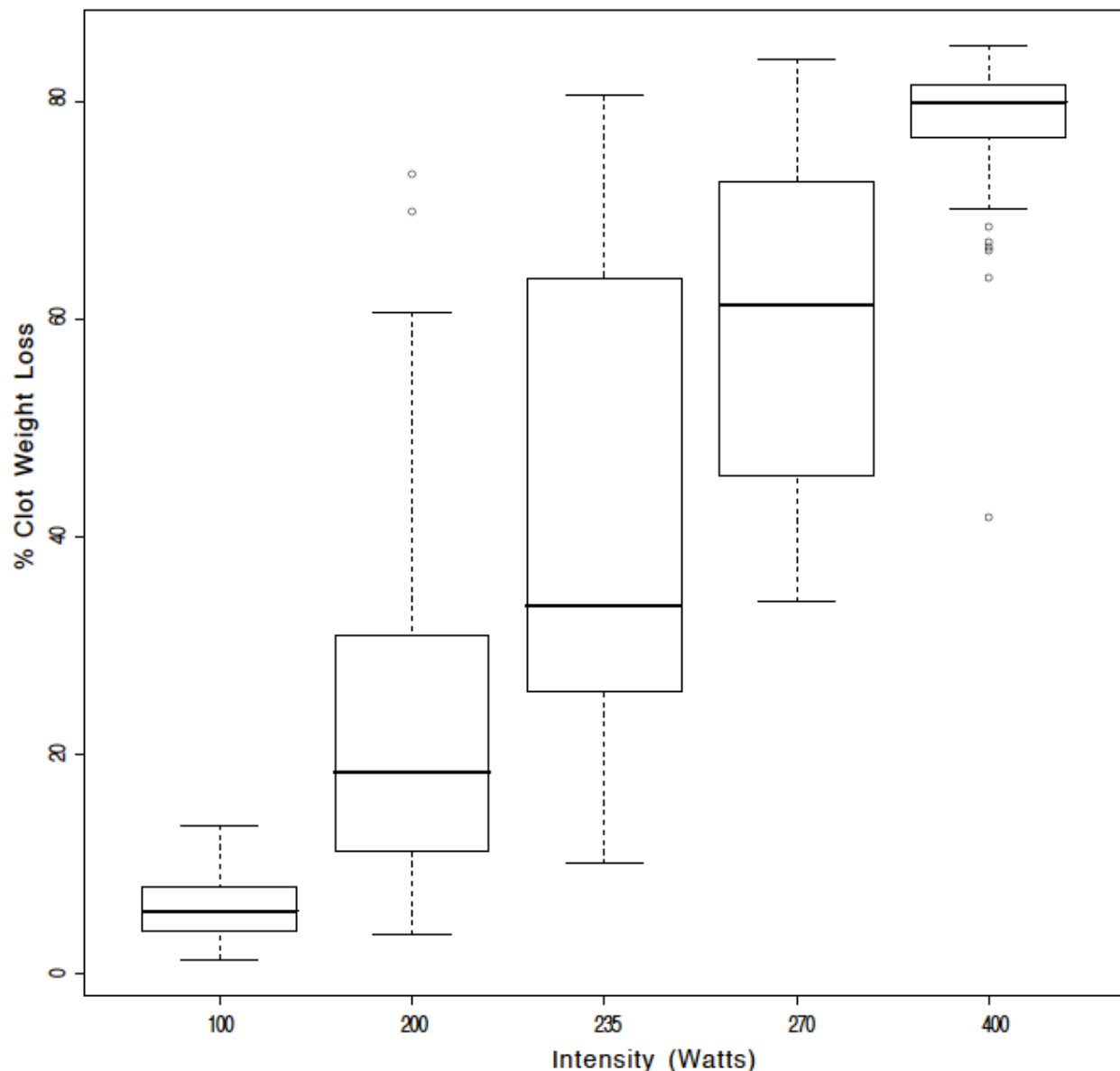


Figure 11 Percent Clot Weight Loss: Boxplot by Intensity.

Table 6 Percent Clot Weight Loss by Intensity; P-values are from Wilcoxon Rank test to examine if median weight loss is different from 0.

Groups	Number of Experiments	Mean	Standard Deviation	Minimum	Median	Maximum	P-values
100W	46	6.21	2.82	1.25	5.68	13.52	<0.0001
200W	41	23.59	17.63	3.52	18.47	73.29	<0.0001
235W	40	42.78	21.34	10.04	33.72	80.55	<0.0001
270W	40	60.03	14.07	34.15	61.32	83.91	<0.0001
400W	41	77.26	8.05	41.74	79.98	85.11	<0.0001
Overall	208	41.97	12.78	18.14	39.83	67.28	<0.0001

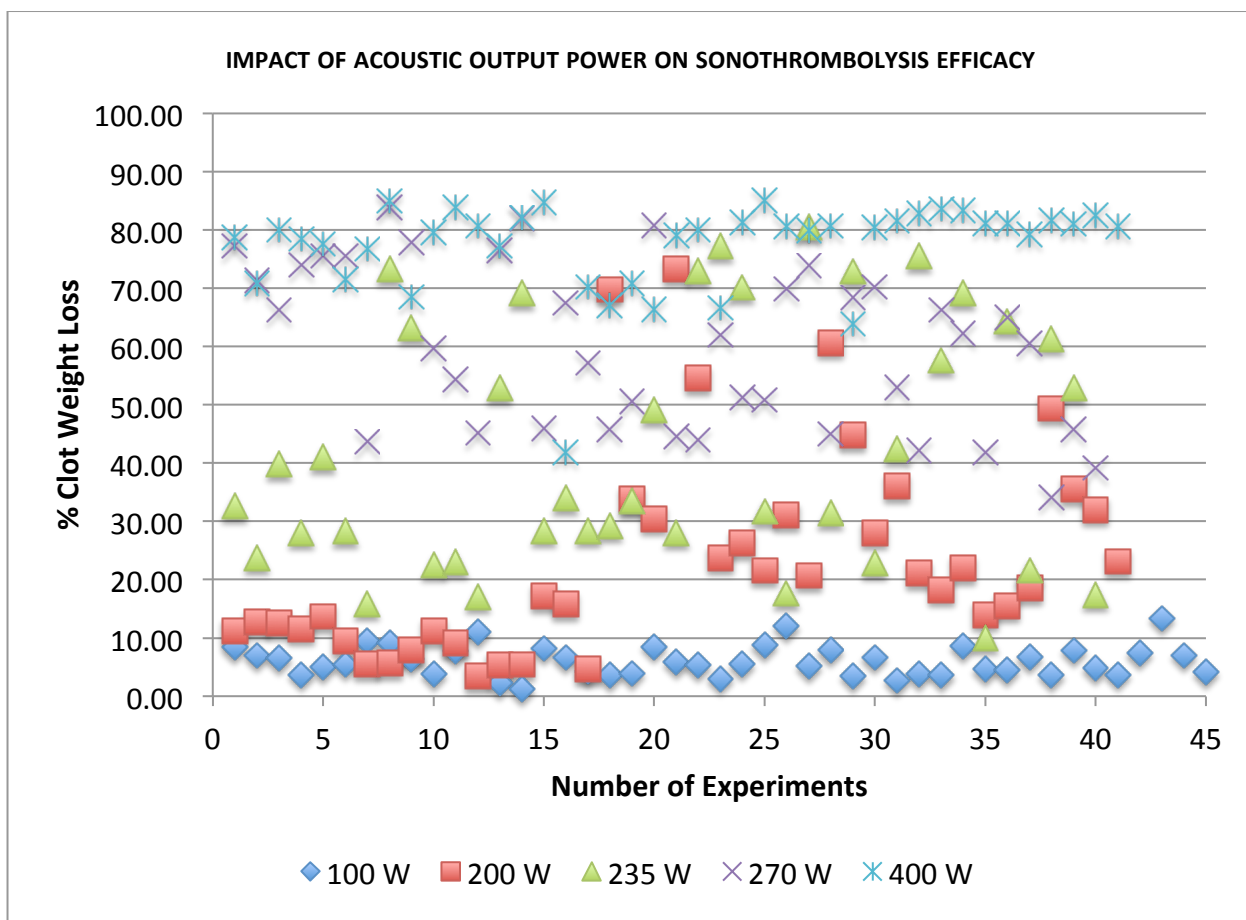


Figure 12 Lysis Efficacy as a Function of Acoustic Output Power: Scatter Plot by Intensity.

Is FUS sonothrombolysis dependent on flow mechanics?

As visualized in Figures 13 and 14, flow was found to affect clot weight loss. Clots exposed to flow were found to have a significantly larger percent weight loss than clots not exposed to flow ($p<0.001$). The mean weight loss was only 18.14% in Group 1, during no flow conditions. While an average weight loss of 42.12% could be achieved in Group 2, with flow present at 10ml/min during the insonation duration (Table 7).

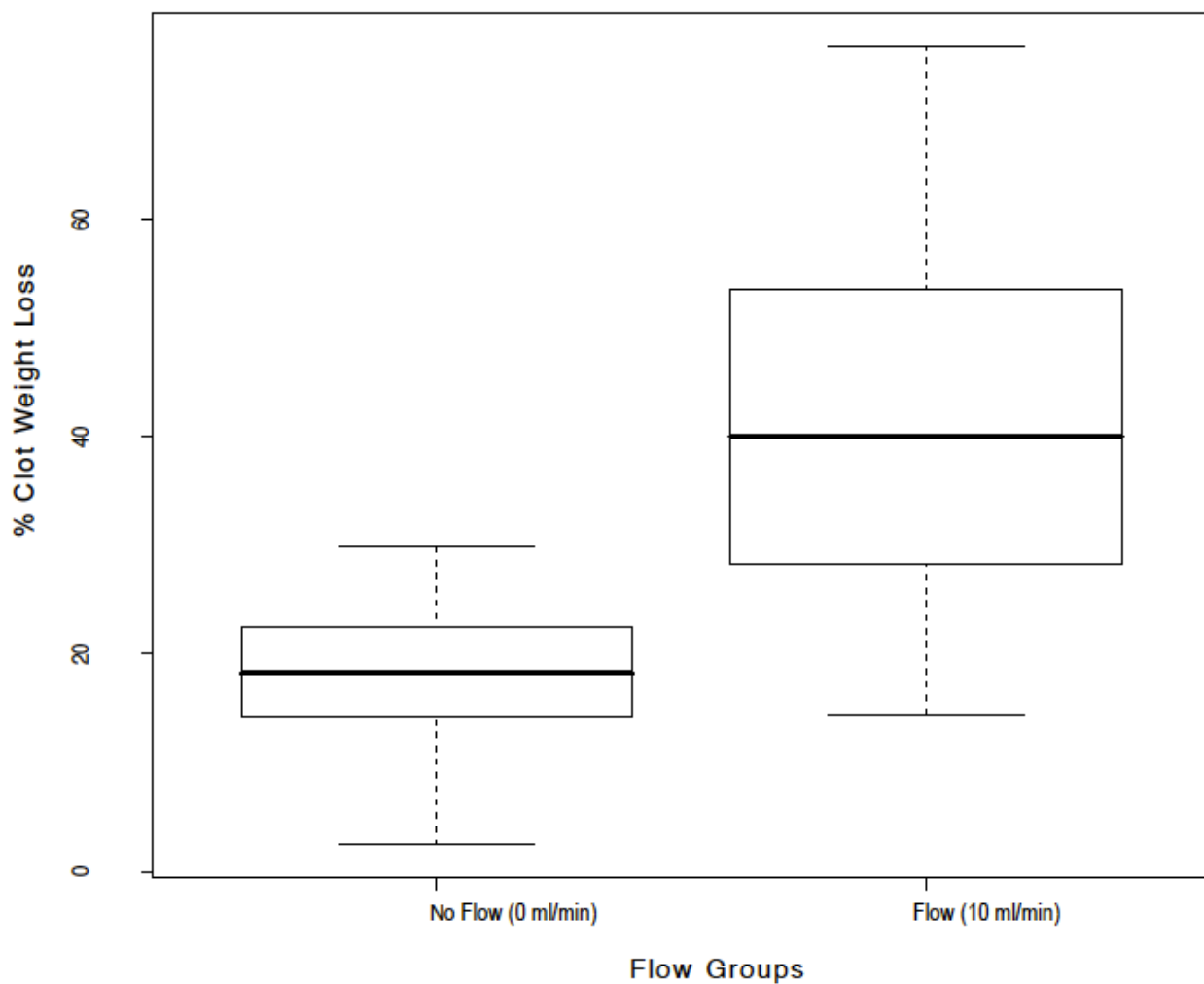


Figure 13 Percent Clot Weight Loss: Boxplots by Flow Group.

Table 7 Percent Clot Weight Loss by flow group and overall. P-Value is from Student's t-test comparing the groups

Groups	Number of Experiments	Mean	Standard Deviation	Minimum	Median	Maximum	P-values
No Flow	42	18.14	5.87	2.44	18.23	2989	<0.001
Flow	44	42.12	16.15	14.50	40.04	76.01	
Overall	86	30.41	17.14	2.44	24.52	76.01	

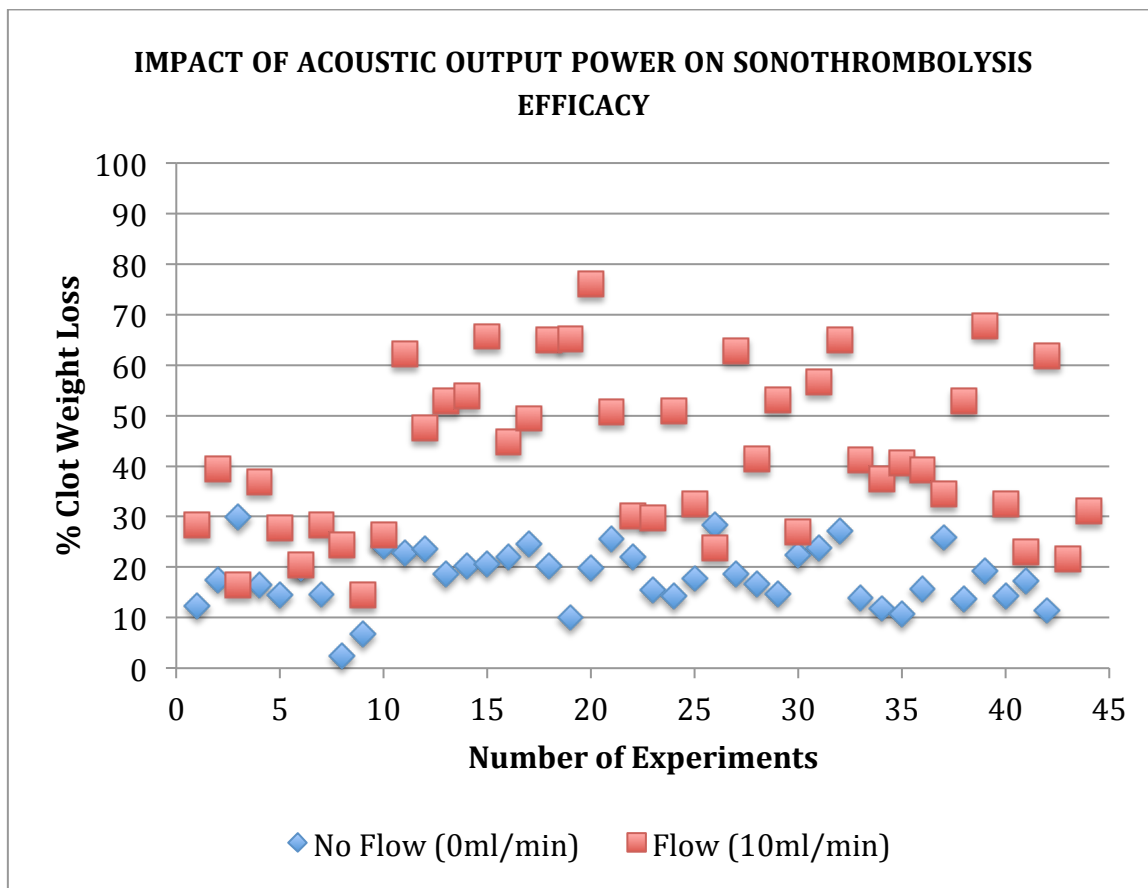


Figure 14 Lysis Efficacies as a Function of Flow Mechanics: Scatter Plot by Flow Group.

DISCUSSION

Does FUS cause transcranial sonothrombolysis?

At the focus of the FUS transducer, significant clot weight loss was achieved for all 420 *in vitro* experiments after only 30 seconds of insonation. From the findings, it can be expected that clot lysis can be successfully achieved within seconds with the use of FUS transcranial insonation, but the lysis efficacy is dependent on an individual's physical skull characteristics, the applied FUS acoustic power, and intracranial flow mechanics.

Is FUS sonothrombolysis efficacy dependent on skull characteristics?

The results suggest that sonothrombolysis efficacy can vary from person to person simply by the physical properties of an individual's skull. Based on our observation, such differences as bone thickness or density can be assumed to play a role in transcranial sonothrombolysis. The human skull is constructed of a trabecular bone layer in the middle, surrounded by cortical layers on the outer and inner layers [74]. CT analysis confirmed the visual observation in the physical differences in the three skull specimens. CT data for bone thickness and density demonstrated skull characteristic variations that corresponded with the clot lysis efficacy for the three skulls.

The attributes of the human skull need to be further characterized to fully identify their impact on transcranial sonothrombolysis. Acoustic measurements taken at the focus with varying skulls could provide more insight into the impact of skulls on FUS acoustic field. This matter is investigated further in Objective 3.

Is FUS sonothrombolysis dependent on acoustic output power?

It can be confirmed by our results that the applied FUS acoustic output power, the insonation intensity at the focus on the clot, impacts lysis efficacy. With an increase in the

tested wave intensities, the achieved clot weight loss was greater. While it is known that sonothrombolysis efficacy is dependent on the acoustic energy, it can be expected that the relationship between insonation power used on a clot and the resulting clot weight loss will have both minimum and maximum limits. There should be low acoustic output power values where sonothrombolysis efficacy is not significantly different from 0W, indicative of a minimum threshold. Conversely, at a value of power that produces maximum lysis efficacy, more significant clot lysis cannot be achieved with further increased energies. We know these thresholds to be true based on our preliminary studies, as no significant lysis at 27W was achieved and the efficacy rate of 100% lysis was not seen for various acoustic output powers above 400W, indicating possibly a maximum efficacy. At lower acoustic output power FUS may not affect thrombolysis, and at higher energy levels there are worries with regard to produced thermal effects. It has been reported that US-induced thermal elevations take part in augmenting clot lysis efficacy [75-77], yet thermal elevations *in vivo* could pose possible safety concerns. Measurements of increasing acoustic energies and the resulting effects on thermal elevation for efficacious transcranial sonothrombolysis would be helpful in better understanding the potential safety limits of transcranial FUS. The same holds true for investigation of clot fragmentation, which may also pose a safety concern with regard to thrombolysis, possibly produced as a result of increasing FUS insonation powers. These noted experimental weaknesses are accordingly proposed as studies for later research.

Is FUS sonothrombolysis dependent on flow mechanics?

Flow conditions proved to significantly affect sonothrombolysis efficacy. To mimic the event of flow stasis as it occurs *in vivo* during acute thrombotic vessel occlusion, we

simply turned off the flow pump for the duration of FUS insonation. During *in vivo* conditions of subtotal vessel occlusion or when partial recanalization has been achieved, low velocity transcranial flow may be present. In order to simulate this state, flow was present at 10ml/min for the duration of insonation. In the absence of flow, clot weight loss was significantly less than when there was low velocity flow. The clot lysis efficacy is enhanced by the presence of flow, and it can be assumed that with efficacious sonothrombolysis, greater flow would be achieved which would in turn aid in increased thrombolysis.

SUMMARY

Based on our *in vitro* setup, we can conclude that noninvasive FUS induced transcranial sonothrombolysis is feasible. We now know that 30 seconds of FUS application can effectively lyse thrombi without the aid of tPA, as we have also learned that the FUS operating parameters have a key role in sonothrombolysis. Using our *in vitro* experimental set-up, we aim to better understand the components of FUS affecting sonothrombolysis and the effect that the involved variables have on the lysis efficacy and potential *in vivo* safety.

Chapter 5 PARAMETER OPTIMIZATION

OBJECTIVE 2: PARAMETER OPTIMIZATION

What is the impact of varying DC and PW on clot lysis?

MATERIALS & METHODS

ULTRASOUND SYSTEM AND OPERATING PARAMETERS

To test the impact of various duty cycles (DC) and pulse widths (PW) on sonothrombolysis efficacy, the variability in other testing parameters was intentionally limited. To determine optimized parameters for FUS transcranial sonothrombolysis, four varying DC were tested in combination with four varying PW, for a total of 16 duty cycle/pulse width combinations. The ExAblate was externally triggered using a function generator (Agilent 3320A, Agilent Technologies, Loveland, CO) to control the generated DC and PW. Many of the constant parameters for Objective 2 experiments were derived and elected based on the findings from Objective 1 experiments that showed transcranial thrombolysis could be efficaciously achieved. Accordingly, for all of Objective 2 acoustic parameter optimization studies, Skull #1 was used and flow was present at a speed of 10ml/min. The other FUS parameters remained unchanged at:

Acoustic output power (AP) = 235W
FUS duration (ID) = 30sec

A total of 658 experiments were performed to ascertain the optimized parameter combination of DC and PW, for 16 groups, with regard to lysis efficacy (Table 8).

Table 8 Sample Size (N) for each combination of Duty Cycle (DC) and Pulse Width (PW) for the 16 study groups

Duty Cycle	Pulse Width							
	0.1ms		1ms		10ms		100ms	
5%	Group 1	N=40	Group 2	N=40	Group 3	N=40	Group 4	N=40
10%	Group 5	N=40	Group 6	N=44	Group 7	N=40	Group 8	N=40
20%	Group 9	N=41	Group 10	N=40	Group 11	N=41	Group 12	N=43
50%	Group 13	N=43	Group 14	N=40	Group 15	N=42	Group 16	N=44

STATISTICAL ANALYSIS

A Wilcoxon Signed Rank Test was used to compare the percent clot weight loss between each of the 16 duty cycle/pulse width combinations. A Kruskal-Wallis test was used to determine the difference in clot weight loss between the four PW settings within each DC group. Where the overall difference in clot weight is shown to be statistically significant, pair-wise comparisons were performed by a Wilcoxon Rank Sum test, adjusting for p-values using a Bonferroni-Holm correction for multiple comparisons.

RESULTS

Summary results are provided in the following chapter. Detailed results for all conducted experiments can be found in Appendix B.

For each of the specimens in the 16 study groups of parameter optimization experiments, as shown in Table 9, the percent clot weight loss was found to be statistically

different ($p<0.001$) from 0. For the tested parameters, clot lysis efficacy increased with increasing DC and increasing PW settings (Figure 15). Increasing the PW, however, did not lead to greater clot weight loss, when the DC was set at 50%.

Table 9 Percent Clot Weight Loss by DC & PW combination Group. P-values are from Wilcoxon Rank test to examine if median is different from 0.

Group	DC	PW	N	Mean	SD	Min.	Median	Max.	Pvalue
1	5%	0.1ms	40	10.28	11.95	0	5	51	<0.0001
2	5%	1ms	40	17.55	7.08	4	17.5	37	<0.0001
3	5%	10ms	40	23.62	11.97	3	23.5	64	<0.0001
4	5%	100ms	40	27.15	20.75	0	25	82	<0.0001
5	10%	0.1ms	40	17.12	9.1	0	16.5	41	<0.0001
6	10%	1ms	44	24.32	15.88	0	21.5	80	<0.0001
7	10%	10ms	40	29.08	17.33	0	28.5	73	<0.0001
8	10%	100ms	40	42.92	24.67	2	34.5	83	<0.0001
9	20%	0.1ms	41	30.02	20.12	0	27	71	<0.0001
10	20%	1ms	40	37.7	21.83	0	32.5	83	<0.0001
11	20%	10ms	41	39.9	21.5	1	40	83	<0.0001
12	20%	100ms	43	59.6	19.16	9	66	85	<0.0001
13	50%	0.1ms	43	48.67	23.7	0	55	85	<0.0001
14	50%	1ms	40	53.58	20.85	5	56.5	82	<0.0001
15	50%	10ms	42	51.43	21.85	0	50	85	<0.0001
16	50%	100ms	44	59.23	17.1	21	63	85	<0.0001
Overall			658	36.05	23.84	0	30	85	<0.0001

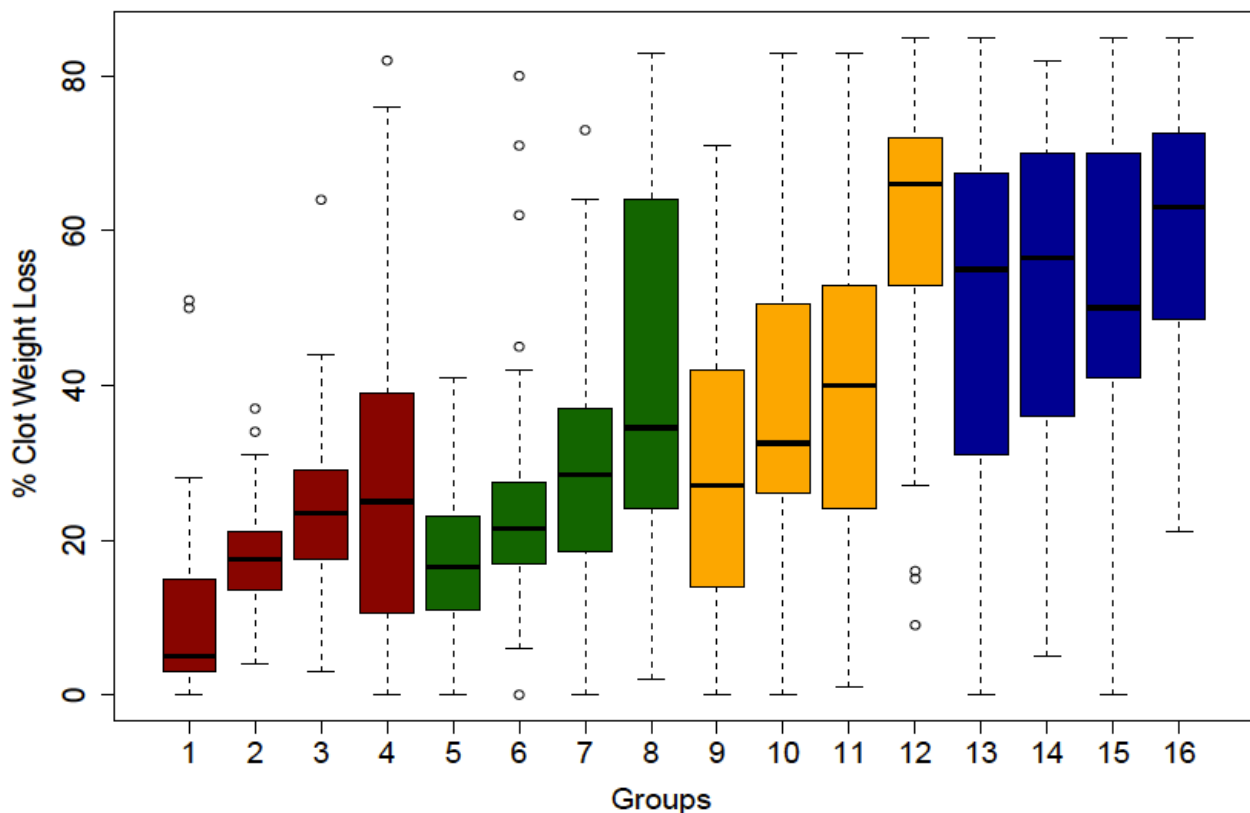


Figure 15 Percent Clot Weight Loss: Boxplot by DC & PW combination Group.

DISCUSSION

We were able to show that sonothrombolysis efficacy is affected by the combination of duty cycle and pulse width. It was found that for the 16 parameter combinations tested, greater clot weight loss was observed with increasing DC and PW. Similar to findings reported by Schafer *et al* [78] for their *in vitro* investigation of US parameters on sonothrombolysis, we were able to demonstrate that clot lysis increased as the acoustic output power was kept constant at the focus with increasing PW for a given DC. As the PW increases, the total number of pulses per insonation duration is decreased, while the energy in these longer pulses is considered to be greater, resulting in more

efficacious clot lysis [78]. The clot weight loss was more pronounced when the PW was increased for short duty cycles. For a longer DC (as in 50%), the impact of increasing PW on clot lysis was dampened.

In this study, acoustic measurements were not taken at the focus when the parameters for duty cycle and pulse length were changed, and the acoustic output power and insonation duration remained unchanged. While the same acoustic output power was used in all experiments, the intensities generated at the focus varied, as they were dependent on the DC and PW parameter combination used [26, 68, 78]. In an *in vitro* FUS sonothrombolysis study by Rosenschein *et al* [68], the acoustic output power was adjusted, working to keep the acoustic intensity at the focus constant, so as to investigate the potential impact of DC and PW parameters on lysis efficacy. The researchers were able to achieve efficacious clot lysis by using short DC's. They reported an optimized parameter combination of 4% DC and 200 μ s PW. The parameters and insonation duration tested by Rosenschein *et al* were different (pulse widths much shorter and the insonation duration much longer) than those tested in the current study, but one could make the assumption that clot lysis efficacy would be enhanced with increasing acoustic intensities at the focus.

The acoustic measurements at the focus and the impact of the skull on the produced field needs to be established in order to gain understanding into achieving efficacious sonothrombolysis transcranially. We will next, in Objective 3, address this experimental limitation by characterizing the sound field produced by the FUS system, and examine how varying *ex vivo* skulls impact the FUS acoustic field at the focus.

SUMMARY

With a constant acoustic power, we concluded that higher DC and longer PW resulted in a preferred parameter combination for FUS induced sonothrombolysis efficacy. Significant thrombolysis could be achieved within seconds and without the use of lytic drugs in vitro for all 16 study groups.

Chapter 6 ACOUSTIC FIELD CHARACTERIZATION

OBJECTIVE 3: ACOUSTIC FIELD CHARACTERIZATION

What is the effect of the skull on the acoustic field produced by transcranial FUS?

MATERIALS & METHODS

The aim of this project was to add to the body of work that seeks to address focusing uncertainties [79-83] by characterizing the effects of the skull on the applied acoustic field with comprehensive acoustic measurements and CT scans. FUS operating parameters were held constant at:

Acoustic output power (AP) = 10W
 Duty cycle (DC) = 1%
 Pulse width (PW) = 0.1ms
 FUS duration (ID) = 5sec

SKULL CHARACTERIZATION

Five new calvaria specimens identified by letters (A, B, C, D, and E) were obtained and their effect on applied acoustic field were examined. For each skull, a hydrophone was used to make acoustic measurements and CT scans were made and imported into MATLAB (Figure 16) for measurements and visualization, in 2D and 3D. At the natural focus of the ExAblate™ 4000 headsystem, we examined the effects of the skull on the location, shape, and intensity of the acoustic field.

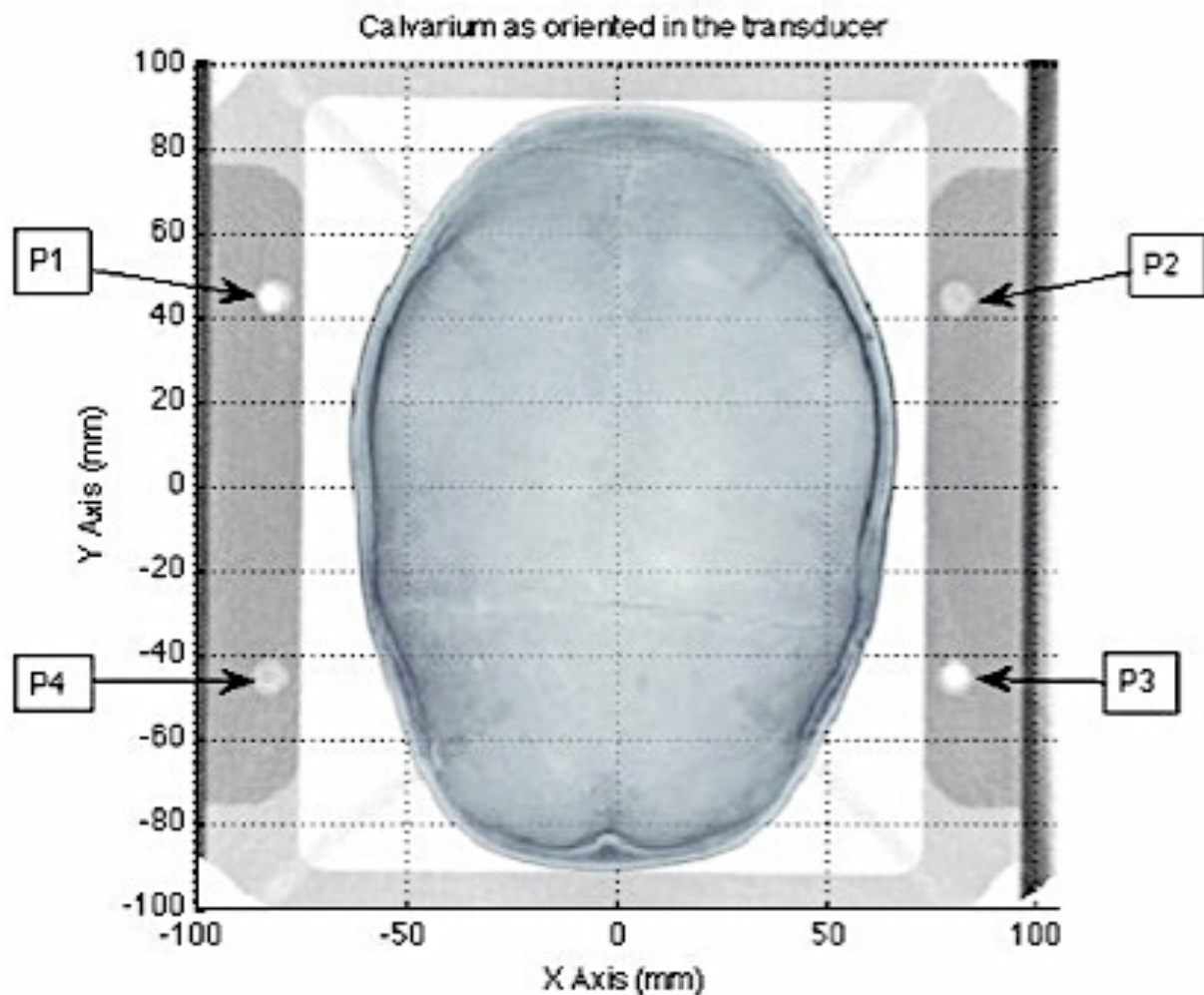


Figure 16 MATLAB reconstruction of CT images with thresholding set so that the stereotactic frame, fiducial holes and nylon securing screws are visible. Coordinates have been transformed into the AIMS/Exablate™ coordinate system, so that the calvarium appears in its orientation in the transducer. Top of the skull is toward the transducer, anterior aspect in the direction of the negative Y axis.

ACOUSTIC FIELD MEASUREMENTS

An Acoustic Intensity Measurement System (AIMS) (ONDA Inc., Sunnyvale, CA), a sound field scanning system, as shown in Figure 17 was mounted on a wet tank in order to acquire the desired measurements and to map the acoustic field in the fluid environment.

The hemispheric FUS system was then placed in the wet tank of the measurement system under the stepper motor positioning system. This precise scanning system is suitable for use with a wide range of medical imaging devices, including both therapeutic and industrial ultrasounds using pulsed and Continuous Wave (CW) Doppler [1]. The 3D stepper motor system was used to navigate a hydrophone used for acoustic measurements (Model Y-120S Sonic Concepts, Bothell, WA), which was placed in the acoustic field to perform the specified scans for each skull specimen. At all measurement points, the acoustic data acquired at the focus of each skull were the spatial peak temporal average intensity (I_{STPA}), peak negative (or sometimes rarefraction) pressure (P_{NEG}), peak positive pressure (P_{POS}), and the -3 decibel (dB) focus area. The -3dB area, was measured by the summation of the pixels of the intensity that were above the half maximum value of intensity. The I_{STPA} , P_{POS} , and P_{NEG} volumes were the summation of voxels for which the associated measurements were above the half maximum.

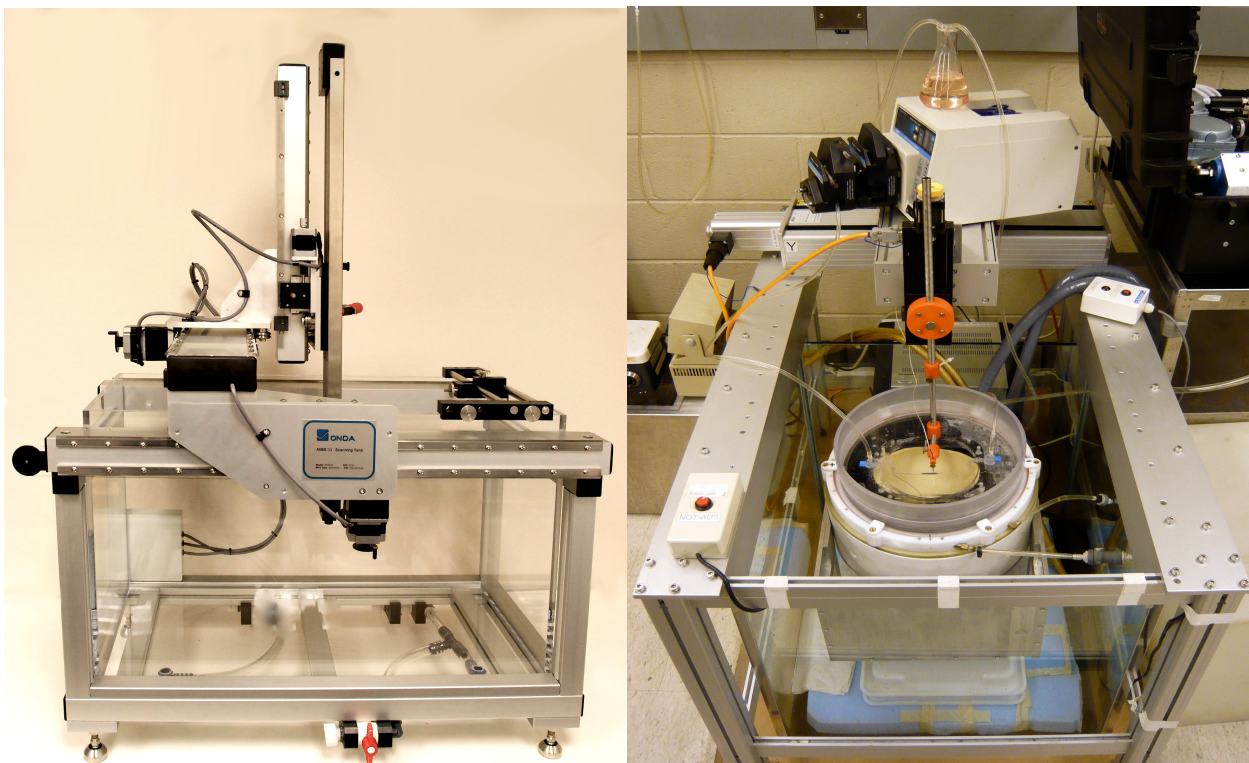


Figure 17 Left: AIMS Scanning tank used in current experiments (pictures courtesy of ONDA Inc. [1]) Right: The overall measurement set-up, with a skull within the ExAblate™ FUS transducer placed inside the AIMS, with the hydrophones placed at the focus by the step motor.

ALIGNMENT

To allow for a correlation between acoustic measurements and the assessment of skull geometry, the AIMS and the FUS coordinates were co-registered and aligned in the same 3D coordinate system (Figure 18). The axes alignment and co-registration of the AIMS and ExAblate™ coordinates were confirmed by direct measurement.

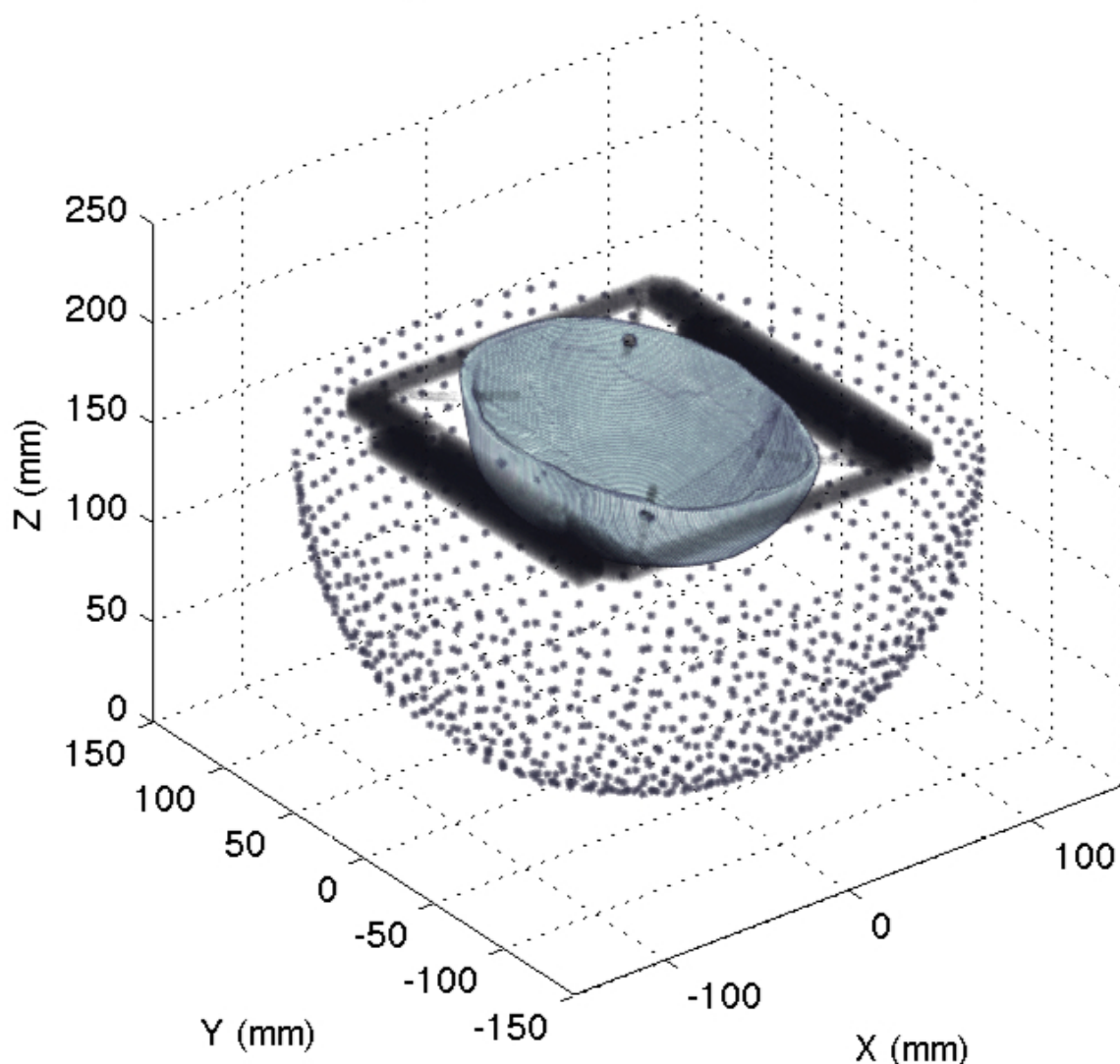


Figure 18 3D reconstruction showing calvarium in stereotactic frame mounted in the FUS transducer, which is represented by the coordinates of its individual 973 elements. In the AIMS/ExAblate™ coordinate system, the origin is located near the lowest element, and the geometric focus is at 0,0,150 mm.

ACOUSTIC SIGNAL

As in Objective 2, an external trigger (Agilent 3320A, Agilent Technologies, Loveland, CO) was used to control the generated DC and PW. The FUS parameters were selected to produce an energy level sufficient for the purpose of acoustic data acquisition

inside the skull. However, they were not comparable to the settings chosen to achieve sonothrombolysis. An experimental concern was that the hydrophone, once introduced in the water filled transducer, might act as a cavitation nucleation site [84]. This phenomenon must be avoided to protect the functionality of the very delicate and costly hydrophone and to avoid signal degradation. The selected parameters led to a peak rarefactional pressure of 1.6MPa at the transducer focus, which, in combination to the low DC value selected, prevented the spontaneous occurrence of cavitation-induced microbubbles at the hydrophone tip.

HYDROPHONE

The Y-120S hydrophone (Sonic Concepts, Bothell, WA) used for acoustic measurements had a frequency bandwidth of 50kHz to 1.9MHz. The hydrophone was comprised of a 6-inch stainless steel shaft with a 0.8mm diameter active element located at its detecting tip. The active element is circumscribed by a protective ceramic layer that makes the hydrophone ideal for use in a high-pressure field.

DATA ACQUISITION

AIMS-denoted scan dimensions and point spacing along with the transmit time of the ExAblate™ were set to accommodate the data acquisition time. The acoustic signal captured by the hydrophone was then acquired in the form of a voltage signal and digitized by a digital storage oscilloscope (Agilent DSO5012A, Colorado Springs, CO). These captured waveforms were then sent to the AIMS computer, where the acoustic field measurements of I_{SPTA} , P_{NEG} , P_{POS} , and -3 dB focus area were processed and stored.

For the control (no skull) and all calvaria specimens, three 2D scans and one 3D



scan were made. The 2D scans were: 1) a 60mm x 60mm grid, sampled at 1mm spacing, 2) a 20mm x 20mm grid sampled at 0.5mm spacing, and 3) a 10mm x 10mm grid sampled at 0.25mm spacing. All scans were in the Z = 150mm plane, centered at X,Y = 0mm. The 3D scan was constructed from a stack of 2D scans from Z=140mm to Z=160mm. The scan volume was a cube with 20mm sides, a 1mm measurement lattice, and a total of 9261 measurement points. As with the 2D scans, acoustic field measurements were acquired at all measurement points.

COORDINATE TRANSFORMATION MATRICES AND CT DATA ANALYSIS

In order to visualize and analyze the relationship between the transmitted acoustic field and skull geometry, all of the CT images, the acoustic measurements, and the coordinates of the transducer elements were imported into MATLAB (MathWorks, Natick, MA). CT images of the skull specimen fixtures were made compatible for OsiriX (OsiriX Foundation, Geneva, Switzerland) DICOM viewer to locate the fiducial holes and to establish their coordinates with respect to the CT coordinate system. The fiducial points were aligned with the X and Y-axes, the coordinate vectors of the AIMS. The cosine of the angle between the vectors of both systems were calculated and used in forming directional cosine transformation matrices [85, 86]. The coordinated transformation matrices made it possible to express a set of vector coordinates of one system on the basis of another [86]. CT values of the DICOM images were constructed into 3D CT image stacks by MATLAB, along with the voxel coordinates. The CT data was filtered by selecting a threshold value such that lower-valued materials (ie. air, water, plastic) were set below threshold (set to zero), leaving only the much higher bone values. The CT data imported into MATLAB were used to characterize the apparent density of the skull following a previously described

method [83]. Using the “rescale slope” and “rescale intercept” obtained from the CT meta-files, raw CT data imported into MATLAB were converted to Hounsfield units (HU) in order to maintain consistency with the pixel values of the DICOM viewer.

SPLINE INTERPOLATION AND ACOUSTIC DATA ANALYSIS

Similar to the CT data analysis, the AIMS Acoustic data files were imported into MATLAB for the creation of data arrays and matrices, along with the associated 3D coordinate values. The CT scans were spline interpolated to obtain more complete image information, so that the interpolated scans provided the same image quality and information as the actual scans [87]. The spline interpolation of the 60mm 2D scans increased the resolution from 1mm to 0.25mm, thus improving the visualization of the acoustic field. When the resolution was compared to that of the exact function, the actual high resolution scans presented no notable difference (Appendix C). In view of this result, the analysis of the 2D and 3D scans was applied to spline-interpolated scans to increase their resolution.

A MATLAB routine was developed by an expert programmer to threshold the data in order to identify the half-maximum boundaries and the spatial coordinates of the maximum values. Acoustic data for the calvaria specimens within the transducer were compared to the control, baseline measurements taken with just degassed deionized water within the transducer. Calculations were then done to measure the attenuation, determine the change in focus position, and evaluate the changes in the shape of the acoustic field at the focus due to the presence of each skull. For the 2D scans, total power was calculated along with the 3dB dimensions. For the 3D scans, half-maximum boundaries as well as the

associated volumes (by voxel summation) were calculated and were compared to the control to assess field dilation.

SKULL THICKNESS AND DENSITY ASSESSMENT

To calculate the skull thickness and density, the 3D coordinates of the individual transducer elements were used, with each of these coordinates defined as an endpoint of a vector that originated at the geometric focus of the array, at the center of the hemispheric transducer. Based on the unique geometry of the FUS system, transducer elements are relatively evenly distributed in a hemisphere around the skull. The vector travels a path in space beginning at the focus and ending at any given element. Along its path, each vector virtually pierces the skull data volume. This information was used to measure thickness and density at 973 element locations. The coordinates of the transducer elements and the geometric focus were transformed from the AIMS coordinate space to that of the CT images. A MATLAB routine was developed by an expert programmer to create measurement lines, with the length of 150 mm divided into 300 increments of 0.5mm. Once the coordinates of the measurement line increments were identified, then we were able to use a spline-interpolation of the CT values in Hounsfield Units in the data volume to create radiological density profiles. A typical measurement profile is illustrated in Figure 19. From left to right, the measurement line passes through the interior of the skull, the interior cortical layer, the diploe, the exterior cortical layer and onwards. This allowed us to measure the thickness and density of the skull by using a MATLAB routine that located appropriate points along the measurement line [88, 89] (Appendix C).

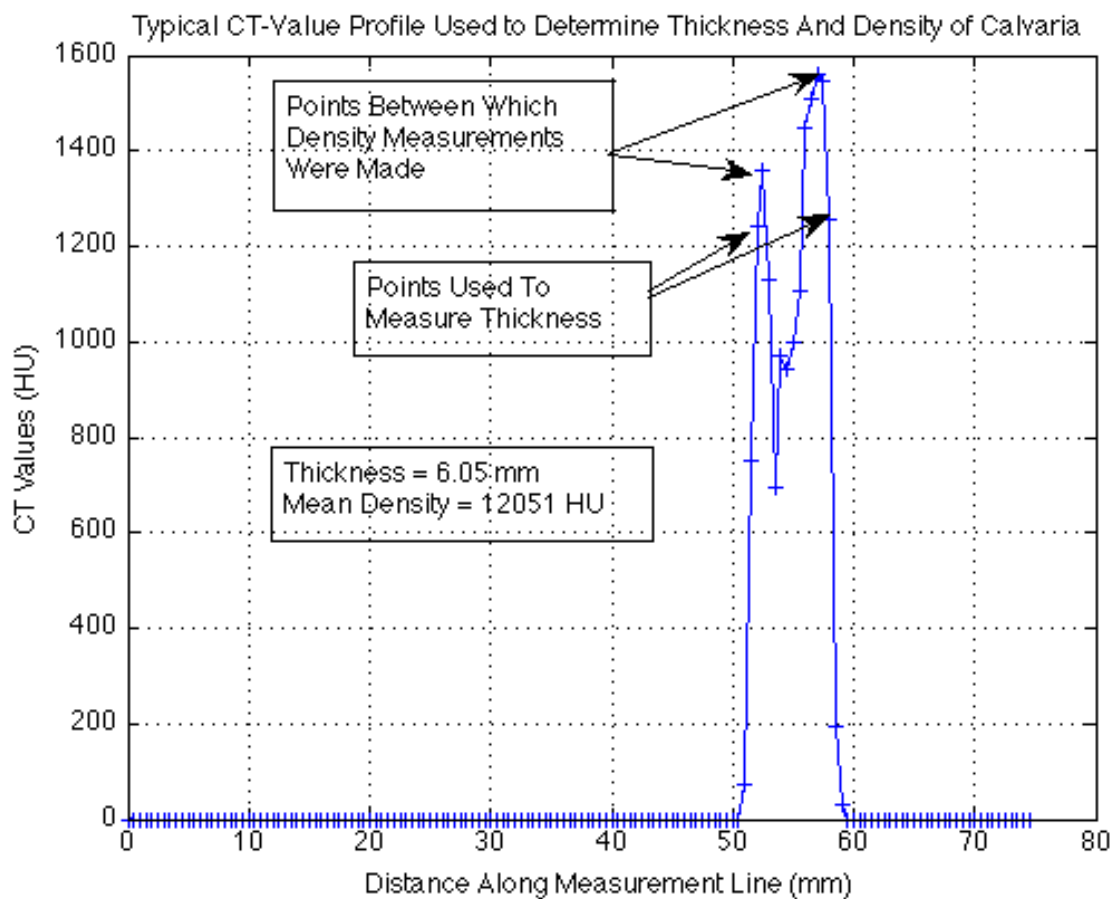


Figure 19 Plot of CT values along a representative measurement line that passes from a point in the skull interior to another external to the skull. The 2 points used to measure thickness are the first and last above half-maximum threshold. Points used for density calculations are within these boundaries, excluding the endpoints.

INCIDENT ANGLE ASSESSMENT

A MATLAB code developed especially per our request was used to calculate the incident angle of each measurement line at the outer surface of the skull for each specimen. The MATLAB routine identifies a point on the outer surface of the skull in addition to its two neighboring points, also located on the outer surface, to determine a tangent plane. The cross product of the two vectors will produce the normal vector at the measurement

point, and the dot product with the measurement vector will produce the cosine of the incident angle. The incident angles were then determined, and could be displayed parametrically on the skull surface, in the same manner as the thickness and density.

All programming routines, (ie. MATLAB codes) were written and defined by program developers, based on parameters developed and at the request of our team of investigators.

RESULTS

Summary results are provided in the following chapter. Detailed results for all conducted experiments can be found in Appendix C.

We found that the attenuation of the transmitted power varied from 4.98dB to -13.01 dB (mean 8.37dB) over the five calvaria. The focus shifted on average by 1.9 mm from the control (no-skull) focal spot. After passing through the skulls, the 3dB dimensions of the FUS focal volume increased on average by 33%. Sources of attenuation include reflection at each of the skull-water interfaces and absorption resulting from the skull thickness, density, and shape. The distribution of thickness, density and incident angle was quantified and mapped for each skull and compared to the associated acoustic measurements.

Results of the analysis of the CT anatomical data are shown in Table 10. This includes the measurements of mean thickness and mean density for each skull, and also the associated standard deviations. Also tabulated is the total number of FUS transducer elements for which the incident angle at the skull outer surface was less than 20°, greater

than 30°, and greater than 45°. Figures 20, 21, & 22 allow for a visual comparison (the voxels in these projections have been enlarged to aid visualization) of these data as they are mapped parametrically onto the individual skull surfaces. Across all skulls, bilateral symmetry could be seen with regard to thickness, density, and insonation incident angles. As shown in Figure 22, the incident angles near the top of the calvaria are consistently low across all five skulls, while there is variation in the rest of the regions between the skulls. In terms of variability in skull thickness versus density, the coefficient of variation (SD/mean) for skull thickness was found to be greater, at 21%, than the 14% coefficient of variation for density among the specimens.

Table 10 Anatomical parameters calculated from the CT data. Skull thickness and density were measured along vectors extending from the assorted transducer elements to the geometric focus. Incident angles were measured between the measurement vectors and the normal vector at the entry point on the skull surface. Calculations were performed in MATLAB

		Skull A	Skull B	Skull C	Skull D	Skull E	Overall
Thickness	Mean (mm)	4.59	7.48	5.57	7.59	5.64	6.174
	Standard Deviation	0.91	1.27	1.39	1.49	1.33	1.278
Density	Mean (HU)	1197	1213	982	804	1172	1073.6
	Standard Deviation	95	123	182	171	172	148.6
Incident Angles	Mean (degrees)	25.5	27.7	22.6	28.1	31.8	27.14
	Standard Deviation	8.1	9	7.5	9.6	11.8	9.2
	# elements <20°	194	196	344	183	184	220.2
	# elements >30°	277	427	182	462	582	386
	# elements >45°	5	6	0	11	130	30.4

Table 11 lists the results of the acoustic measurements, from both the 2D and 3D scans. The data show how the skull specimens affect the measured acoustic parameters by changing attenuation, distorting the shape and shifting the beam's location from the original focus. The measurement of acoustic power is relatively independent of the Z-distance, as the 60mm x 60mm scan area was large enough to accommodate any field-spread due to skull-induced aberrations.

Along with Table 11, Figures 23 and 24 illustrate acoustic field spread and displacement. Figure 23's contour plots and Figure 24's 3D plots depict the peak negative pressure (P_{NEG}) for the control (no skull) and for each of the skulls. Similarly, any of the measured acoustic parameters could have been plotted to show the impact of the acoustic wave distortions. For skulls A-D, the peak displacement was rather small, with an average of $1.4\text{mm} \pm 0.65\text{mm}$. For these skulls, no particular direction was favored for displacement in the X, Y, and Z coordinates. Skull E, however, had a mean peak displacement of over 4mm, primarily along the Z-axis. Skull E also had a considerably larger 3dB area, and the 3D shape of the field was quite distorted compared to the other skulls. Looking to Table 10 for some clues to explain this behavior, no particularly remarkable data for the thickness and density values of Skull E were found. However, many more elements with incident angles greater than 45° were counted for Skull E than for the other skulls.

Table 11 Results of acoustic measurements for the 5 calvaria and the control. Acoustic power was calculated from the 2D scan (60x60mm in X-Y plane) intensity and pressure measurements were calculated from the 3D scans (20x20mmx20mm in X-Y-Z)

		Control	Skull A	Skull B	Skull C	Skull D	Skull E	Overall Skull Mean	Overall Skull SD
Acoustic Measurements	Acoustic Power (mW)	105.4	33.5	18.8	15.8	5.3	16.2	17.92	10.13
	3dB Area (mm ²)	8.2	11.8	9.4	11.2	10.4	30.9	14.74	9.08
	Attenuation (dB)		5	7.5	8.2	13	8.1	8.36	2.90
Intensity	Peak Value (mW/cm ²)	658.2	125.1	72.3	50.2	22.4	31	60.2	41.05
	3dB Volume (mm ³)	34.5	76.5	39.5	41.5	47.1	36	48.12	16.37
	Attenuation (dB)		7.2	9.6	11.2	14.7	13.3	11.2	2.97
	Peak Displacement (mm)		0.9	2.06	1.54	0.61	4.32	1.89	1.47
Peak Positive Pressure	Peak Value (MPa)	1.42	0.65	0.5	0.41	0.27	0.32	0.43	0.15
	6dB Volume (mm ³)	95.7	211.2	134.2	175.8	249.1	321.1	218.28	71.50
	Attenuation (dB)		6.8	9.1	10.8	14.3	12.9	10.78	2.98
	Peak Displacement (mm)		1.48	1.58	1.75	0.9	3.86	1.914	1.13
Peak Negative Pressure	Peak Value (MPa)	1.54	0.66	0.51	0.42	0.28	0.33	0.44	0.15
	6dB Volume (mm ³)	94.2	205.3	130.2	175.9	255.5	321.2	217.62	73.65
	Attenuation (dB)		7.3	9.6	11.3	14.8	13.5	11.3	3.00
	Peak Displacement (mm)		1.12	2.51	1.87	0.5	4.32	2.064	1.47

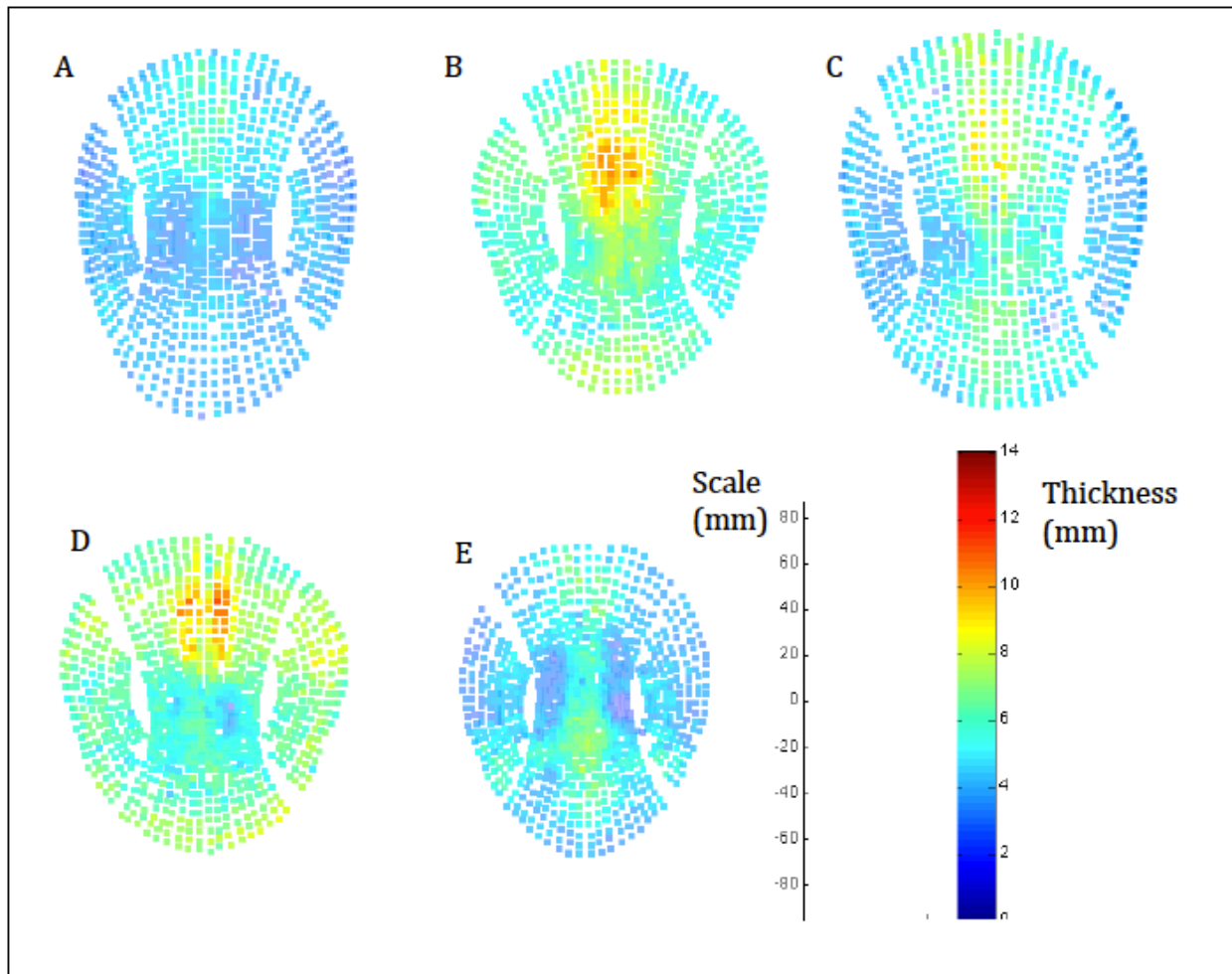


Figure 20 Calvaria thickness profiles mapped onto the skull outer surface at the points of measurement. Measurement vectors were created using the transducer element coordinates and the coordinates of the geometric focus as endpoints. As such, these measurements are influenced by the incident angle and may be more representative of the acoustic path length through the skull.

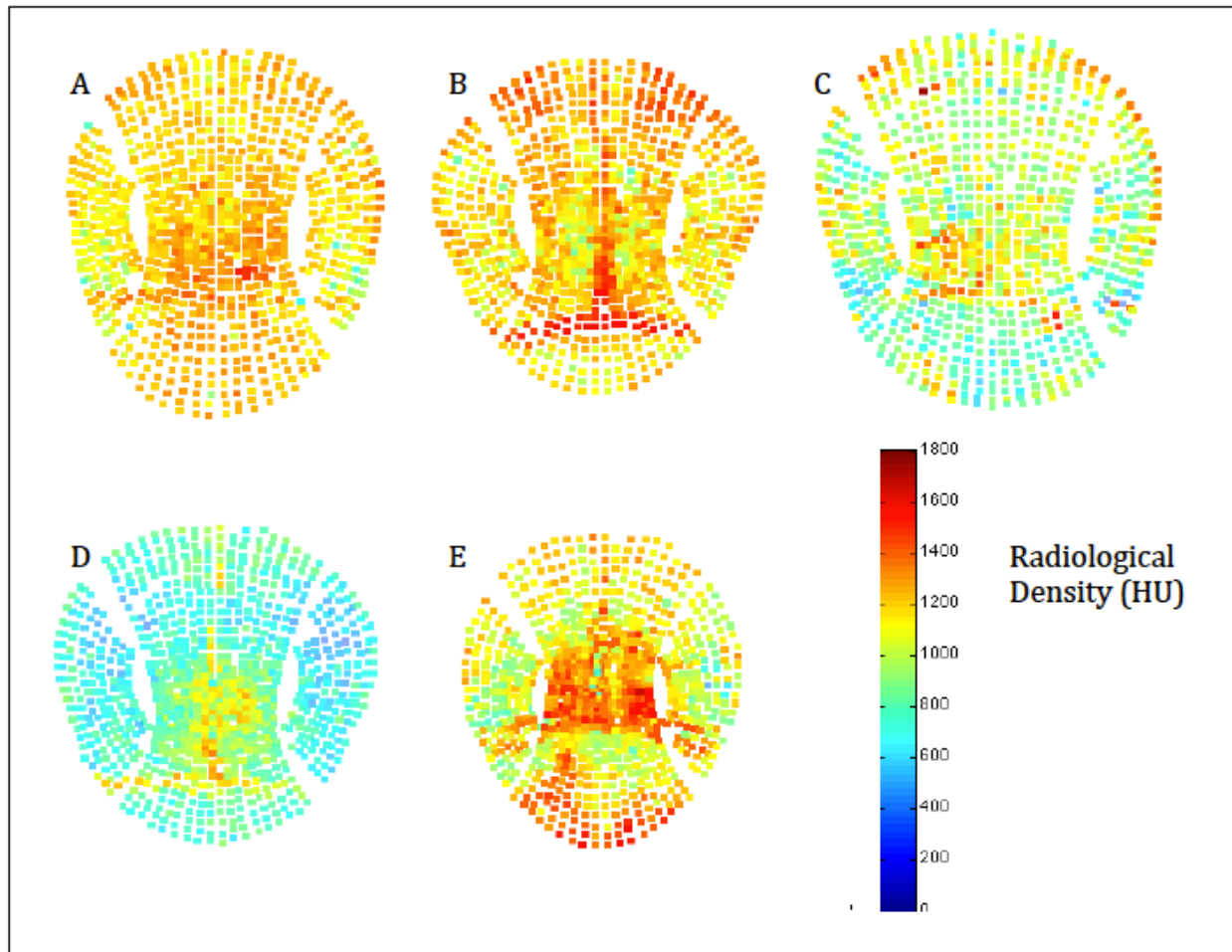


Figure 21 Average radiologic density in HU for each measurement profile as mapped onto the skull surfaces.

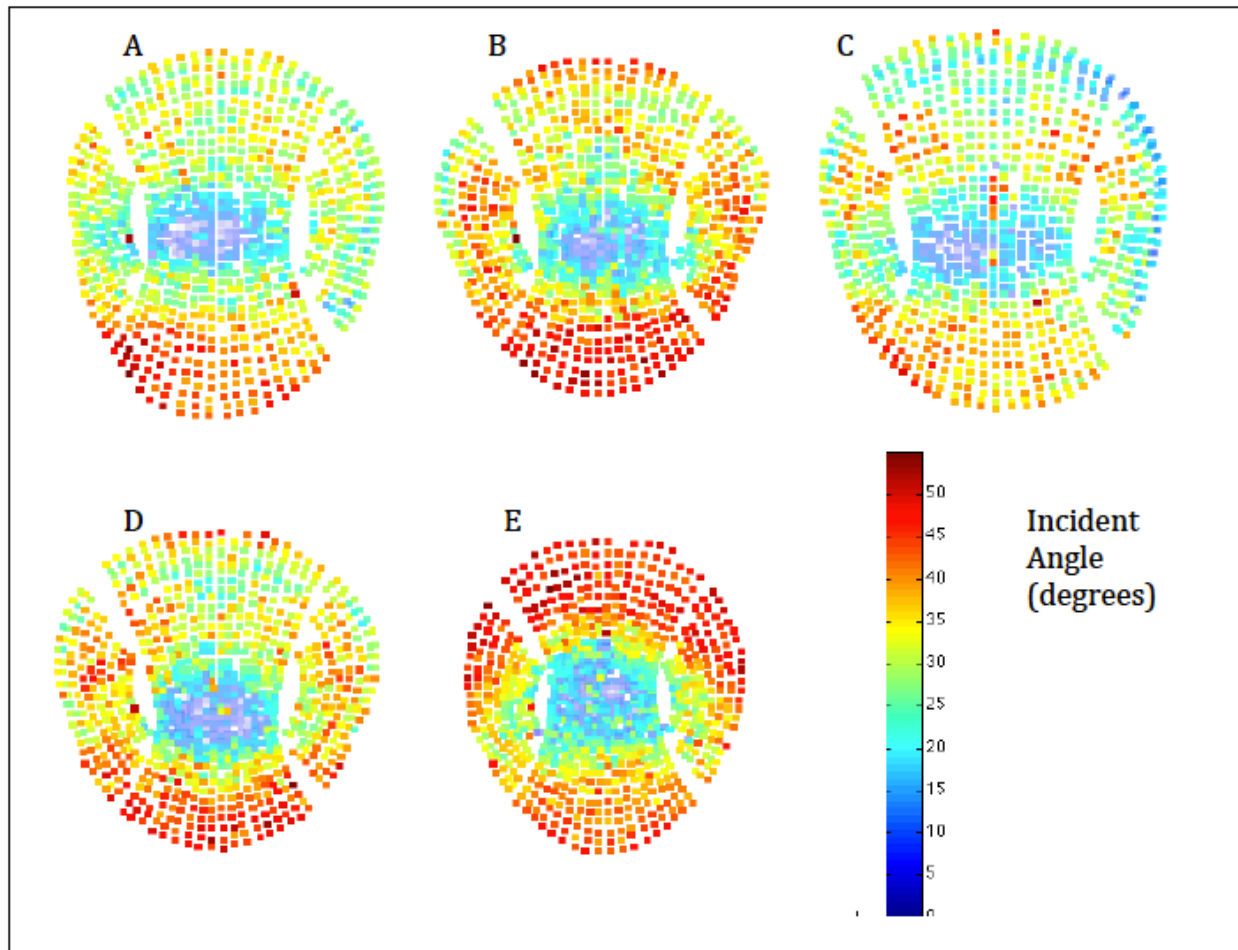


Figure 22 Maps of insonation incident angles on the five calvaria used in this study. These maps show that the incident angles near the tops of the calvaria are consistently low, however the distribution over the remainder of the skulls shows considerable variation between specimens.

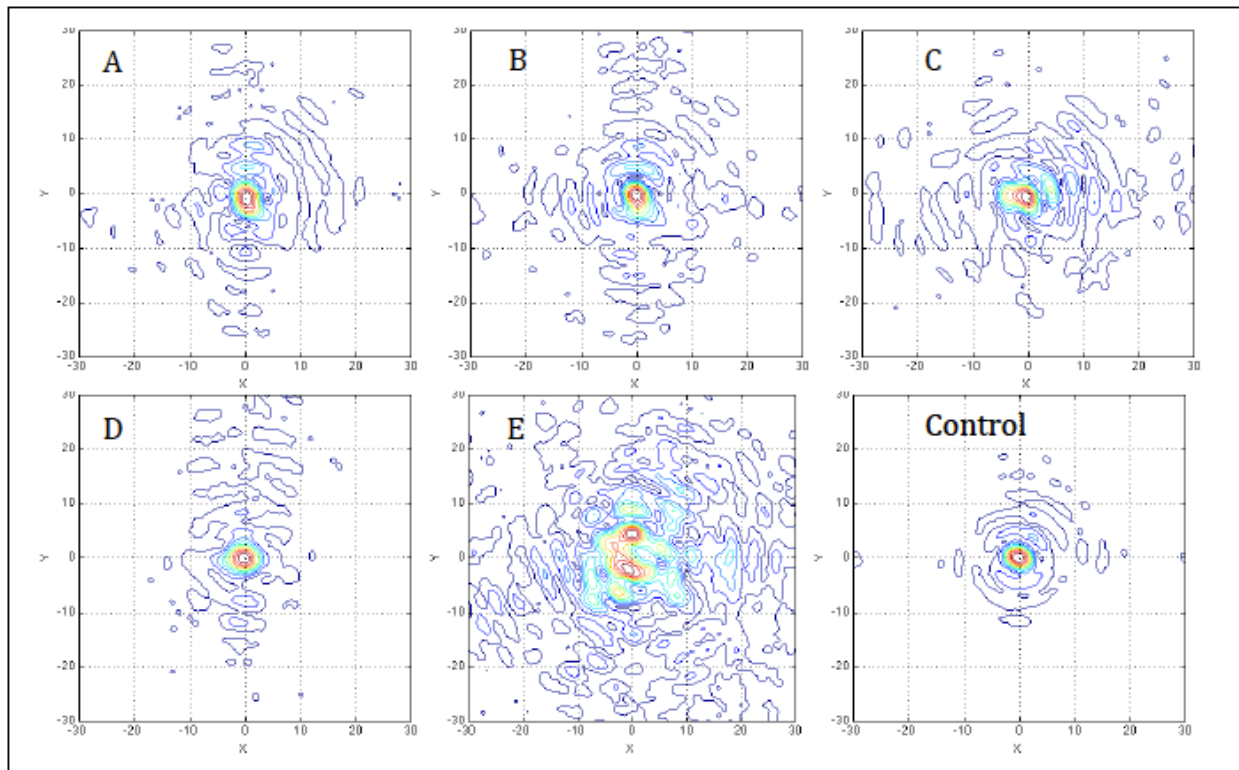


Figure 23 Contour plots of normalized peak negative pressure measured at the Z=150mm plane for the control (lower right) and with interposing calvaria. In general, the location of the maximum value changes only slightly for calvaria A-D, but significant distortion and displacement is seen for calvarium E.

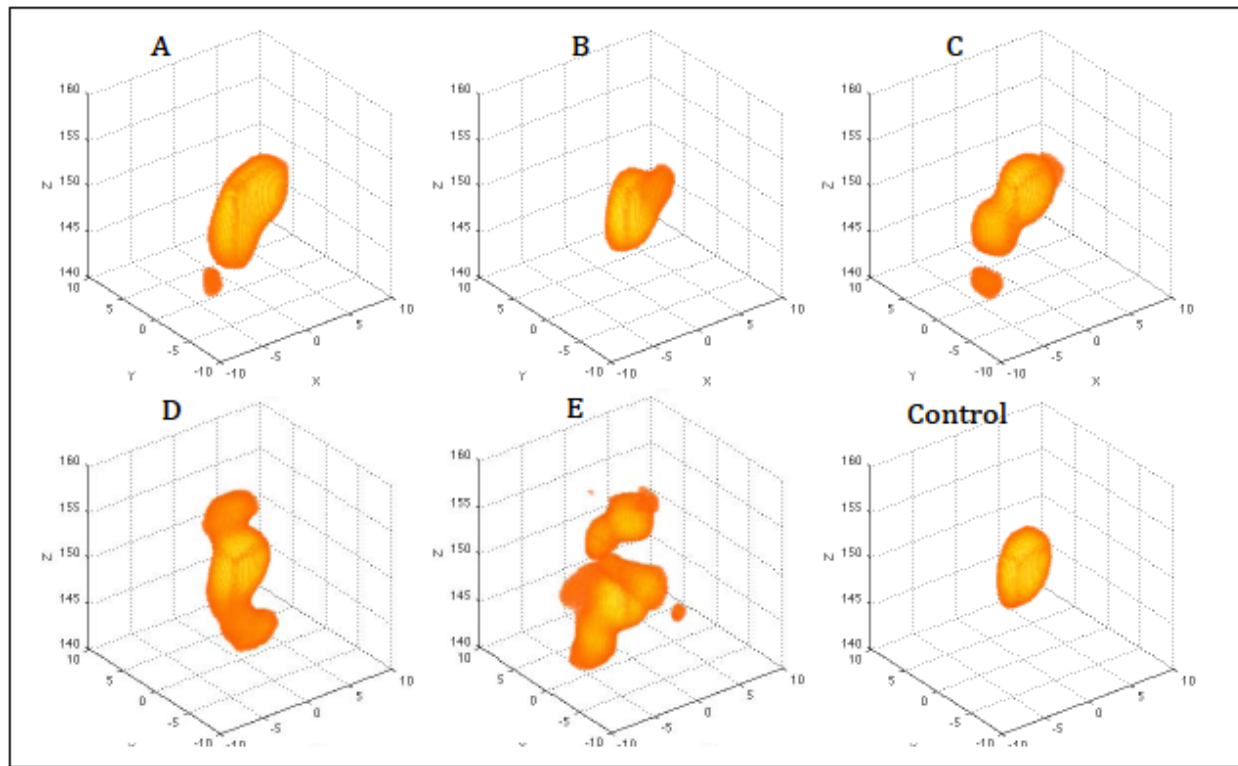


Figure 24 3D scans of normalized peak negative pressure for the control (lower right) and interposing calvaria, measured in a 20mm cube centered about the focal target. Fields are thresholded at half-maximum value (-6dB).

DISCUSSION

Table 10 and Figures 20-24 demonstrate that there are considerable differences across the five calvaria included in this study, in terms of thickness, density and shape. There are also differences in the effect of the skulls on the acoustic field generated by the FUS transducer, which were examined.

Table 11 shows that the attenuation of the acoustic wave is quite high. The mean attenuation of acoustic power is 8.37dB. The literature on current working systems with higher frequencies [90-92] would lead us to expect much lower values of attenuation for a transmission frequency as low as 220kHz. Most previous studies differed from this one, in

that the transducers used were typically smaller, with approximately normal angle of insonation. The regions of skull that were involved in the ultrasound transmission were also relatively small, compared with the present study. Also, in studies that examined the effect of varying incident angle, it was assumed that the transducer and skull were oriented at a single angle [83, 93-95], as opposed to an assortment of angles as shown in Figure 22.

We may also expect the incident angles associated with the various transducer elements to play a significant role in the attenuation and diffusion of the ultrasound field. The overall mean incident angle for the five skulls was 27°. Previous studies have shown that ultrasound transmission due to longitudinal waves drops off sharply beyond incident angles of 20°, however at higher angles shear wave propagation makes a contribution to the acoustic field [98]. It is difficult to estimate the effect of the incident angles on the overall ultrasound transmission; however, we did assume that waves with an incident angle greater than 45° were completely reflected and did not contribute to the measured field [90, 99, 100]. Table 10 lists the number of elements with incident angles less than 20°, greater than 30° and greater than 45°.

Table 11 summarizes the acoustic measurements and calculations for the control and the five calvaria from both 2D and 3D scans. Looking at the attenuation numbers, it is seen that the power attenuation is less than the attenuation of acoustic parameters in the focal zone (I_{stpa} , P_{pos} , and P_{neg}) for each skull. This is because acoustic power is calculated as a summation of intensity over the 2D scan area. As such, it is not as affected by the dispersion of the field due to the skull to the same extent as the focal parameters. For the latter, attenuation is calculated by comparing peak values to those of the control, and these

values are affected by both the field diffusion and the scattering/absorption due to the skull. It is conceivable that phasing algorithms to refocus the field may restore the beam shape. The difference between the power and the intensity attenuation should indicate how much the focal parameters can be increased should this be accomplished.

In regard to the cause of the field distortion seen in skull E, Figures 20 and 22 yield some clues that this may be due to the differences in thickness and incident angle distribution for this skull. We see that the lower-valued incident angles are concentrated near the top of the calvarium to a greater degree than the other skulls. From the thickness profiles, we see that there are thin areas on each side of the sagittal suture for skull E, which are not as pronounced for the other specimens. This may lead to defocusing and distortion of the field at the focus due to refraction at the inner surface of this portion of the skull. The fact that incident angles describe something of an acoustic aperture at the top of the calvarium may be why the focal zone displacement was primarily along the Z-axis.

Interestingly, skull E did not have the highest attenuation, despite the factors listed above. That distinction goes to skull D, which had a power attenuation of over 13dB, with the other skulls in the range of 5 to 8 dB. A clue to this high attenuation may be obtained by comparison to skull B in Table 10. Here, it is seen that these skulls have similar profiles in terms of thickness and incident angles. However skull B has a power attenuation of 7.49 dB, considerably less than skull D. In Table 10, the major difference between these skulls is the radiological density, the mean value being 1213 HU for skull B and 804 HU for skull D. This makes intuitive sense because the lower density indicates either a thicker diploe layer, or larger, more numerous inclusions in the diploe, or both. The diploe layer of the skull has

long been identified as a major factor for trans-skull attenuation [101-103]. These reports also described a minimum or inflection point, beyond which the attenuation increases as density increases.

If skull density was the primary predictor of attenuation, one might expect a relatively high value for skull C, with a mean density of 982 HU, the second lowest value of the five skulls. The power attenuation for skull C was 8.23 dB, which is also the second highest after skull D, however this value cannot be said to be remarkably different from skulls A, B and E. Possibly offsetting the effect of density may be the relatively low thickness (5.57mm), and the high number of incident angles less than 20° (344), with no elements having incident angles above 45°.

Skull thickness as we have described it is more accurately a measure of the acoustic path length through the skull, provided the effects of refraction are minimal. In this way the incident angles come into play, increasing the acoustic path length through the skull with increasing angle values. Skull thickness describes the distance through an attenuating layer and will also correlate negatively with ultrasound transmission.

SUMMARY

As a general trend, we found that: a) the sound transmission was inversely proportional to the skull thickness, b) the number of elements with incident angles greater than 45°, and c) the standard deviation of the density. The sound transmission seemed to be proportional to the mean density. The overall attenuation was found to be a bit higher than expected compared to historical results from transcranial ultrasound studies conducted within a standard diagnostic parameter range. This higher attenuation is

attributed to reflection and the effect of insonation angles over the surfaces of the calvaria. For one skull specimen, the observed field distortion and focal displacement was believed to be a result of the relatively high number of elements with incident angles greater than 45° (130 of 973) and unusual thickness variations of that specimen. The majority of the skull specimens, the remaining four calvaria, exhibited relatively minor field distortion and focal displacement, and the most significant effect was the overall attenuation.

Chapter 7 SONOTHROMBOLYSIS & FRAGMENTATION

OBJECTIVE 4: SONOTHROMBOLYSIS & FRAGMENTATION

What is the impact of varying intensities on clot lysis efficacy and how does this correlate to potential clot fragmentation?

MATERIALS & METHODS

ULTRASOUND SYSTEM AND OPERATING PARAMETERS

In total, 561 sonothrombolysis studies were done. Studies were divided into 9 groups with exposure to increasing acoustic output power levels ranging from 0 to 400 Watts (Table 12). Clot lysis and clot fragmentation in each group (50W, 100W, 125W, 150W, 200W, 235W, 270W, 400W) were compared to the 0W group, for its respective difference.

The effects of increasing acoustic output powers were studied with regard to lysis efficacy and clot fragmentation. For all Objective 4 experiments Skull #1 was used and flow was present (10ml/min), while FUS operating parameters were held constantly at:

Duty cycle (DC) = 50%
 Pulse width (PW) = 100ms
 FUS duration (ID) = 30sec

As in the previous objectives, the sonothrombolysis efficacy was determined by the clot weight loss, and in these studies the differentiation of clot lysis between the experimental groups was also noted. To assess clot fragmentation, three filters of different

mesh pore sizes were used to establish if clot fragmentation (post-/pre-filter weight) were different between groups for each separate filter size (11, 60 and 180 microns).

Table 12 Acoustic Output Power and N per study group

Groups	Acoustic Output Power (W)	Number of Experiments
GP 1	0	60
GP 2	50	62
GP 3	100	66
GP 4	125	63
GP 5	150	65
GP 6	200	61
GP 7	235	61
GP 8	270	62
GP 9	400	61

ASSESSMENT OF CLOT LYSIS AND FRAGMENTATION

After the 30 seconds of insonation, uni-directional flow of degassed, deionized water was continued for an additional 2 minutes through the tubing and was collected in a beaker. Before entering the beaker, the solution passed through three differently sized mesh filters (Millipore, Ireland) with a mesh pore size of 180µm, 60µm and 11µm, respectively, to capture clot fragments of varying size. The serial filtration with descending mesh-sized filters as selected to represent small arteries, arterioles, and capillaries, respectively. Thrombi were weighed pre and post insonation. The percent weight loss for each individual insonation and the average percent weight loss for insonation groups was

calculated and recorded. The distribution of fragments from lysed clots were assessed in a fashion similar to the work published in 2000 by Rosenschein *et al.* [68] The amount of clot fragmentation per filter size was calculated by subtracting the pre-insonation wet filter weights from the post-insonation wet filter weights, with the difference documented in percent clot weight. The percent weight difference for a filter size indicates the clot fragment weight and is presented as a percentage value, representative of clot fragmentation present downstream, resulting from FUS-induced thrombolysis.

ACOUSTIC MEASUREMENTS

For all experimental groups, and first without the test tubing in place the acoustic parameters I_{SPTA} , P_{NEG} , and P_{POS} were measured using a FUS hydrophone (Model Y120, Sonic Concepts, Seattle, WA), calibrated for the frequency of 220 kHz. To account for the interference of the PE tubing itself the acoustic measurements were repeated by placing the hydrophone at focus inside the tubing, which showed no notable differences compared to measurements without the tubing. This confirmed that the tubing used in our sonothrombolysis experimental setup possesses appropriate acoustic properties for US, as mainly defined by its minimal sound absorption and beam distortion due to the thin walls and the polyethylene material itself.

STATISTICAL ANALYSIS

Efficacy

For efficacy, the aim was to establish if weight loss (in percent and grams) was different among groups. A linear regression model was used to examine if there was a difference in mean weight loss among groups (primarily, is each group different from the 0

W group).

Fragmentation

For fragmentation, the aim was to establish if clot fragmentation (post-/pre- filter weight) was different among groups for each separate filter size (11, 60 and 180 microns). Wilcoxon-rank sum tests were used to examine if clot fragmentation in each group (50W, 100W, 150W, 200W, 235W, 270W, 400W) was different from the clot fragmentation in the 0 W group. The p-values were adjusted using the Holm's procedure to correct for multiple comparisons. Descriptive statistics and boxplots for clot fragmentation overall and by group were developed.

RESULTS

Summary results are provided in the following chapter. Detailed results for all conducted experiments can be found in Appendix D.

Efficacy

A total of 561 clots were studied, divided into 9 groups of increasing acoustic output powers. For Groups 4-9, tested acoustic output powers greater than 125W, a statistically significant ($p < 0.001$) weight loss was achieved (Table 13). For Groups 1-3, no significant ($p > 0.05$) weight loss could be seen. A visual presentation of the efficacy results is given in Figure 25.

Table 13 Percent Clot Weight Loss Lysis Efficacy as Related to Acoustic Output Power

Groups	Acoustic output power (W)	Number	Mean weight loss (g)	STDV	Mean weight loss (%)	STDV	p-value
GP 1	0	60	0.000	0.0096	1.75	4.01	> 0.05
GP 2	50	62	0.010	0.011	4.55	4.62	> 0.05
GP 3	100	66	0.010	0.0085	5.63	3.21	> 0.05
GP 4	125	63	0.020	0.015	8.97	6.30	< 0.001
GP 5	150	65	0.030	0.024	12.9	9.75	< 0.001
GP 6	200	61	0.070	0.046	28.2	18.7	< 0.001
GP 7	235	61	0.10	0.054	41.4	20.3	< 0.001
GP 8	270	62	0.15	0.039	61.0	14.6	< 0.001
GP 9	400	61	0.18	0.031	74.8	10.1	< 0.001

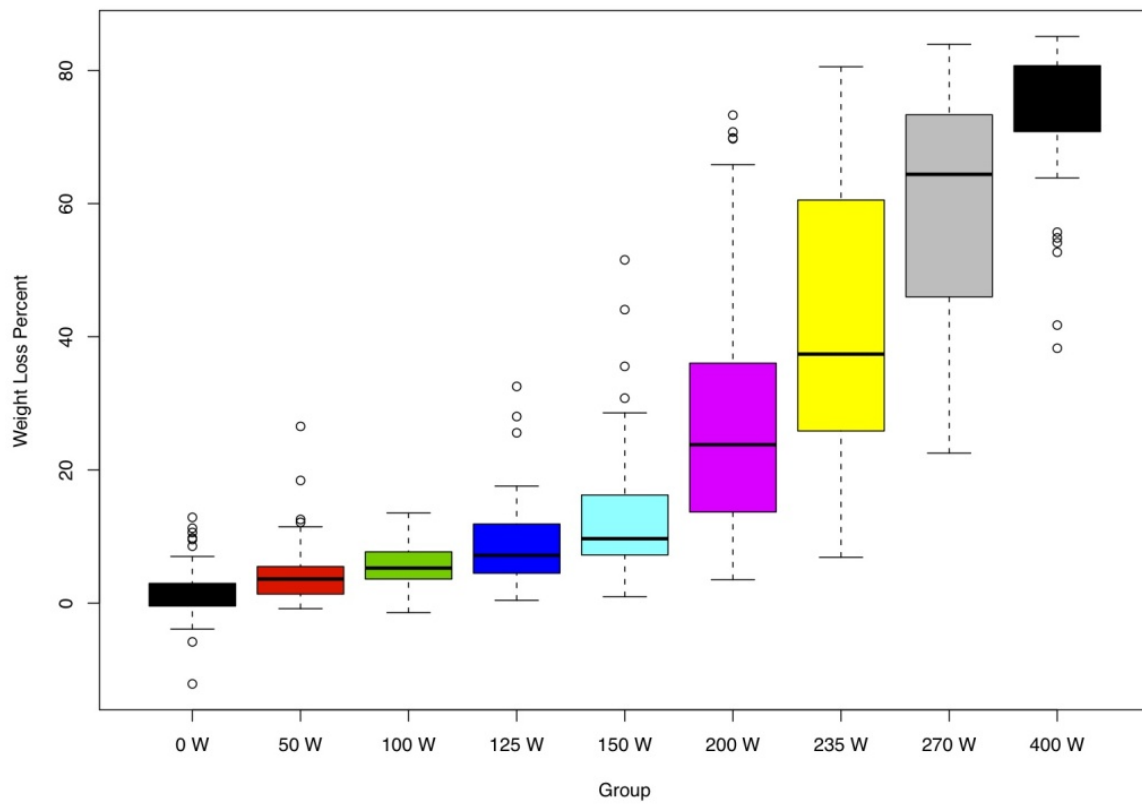


Figure 25 Percent clot weight loss for each acoustic output power group.

Fragmentation

Overall, 352 experiments were performed to test for clot fragmentation, three different filter sizes were used. For the 400W as well as for the 150W acoustic output power groups, significant clot fragmentation could be observed for the 180 μm filter size. For the 60 μm and 11 μm filters in these two groups, as well as for all other study groups and filter sizes, no statistically different clot fragmentation was observed when compared to the control group (0W). For the mean weight difference, negative changes were considered to be a value of 0, as a result of the poor measurement precision. For all

acoustic power groups, detailed findings of clot fragmentation for all filter sizes are given in Tables 14-16. Figure 26 illustrates clot fragmentation weight per acoustic power group for the 180 μm filters, the observed weight difference were very small, for all three filters, with the exception of the two groups for the 180 μm sized filters mentioned above

Table 14 Clot Fragmentation ($> 180 \mu\text{m}$) as Indicated by Post-Pre Test Filter Weight. P-values reflect comparison to the 0 W group, adjusted for multiple comparison

Groups	Acoustic output power (W)	N	Mean weight difference (g)	STDV	Min. (g)	Median	Max. (g)	p-value
GP 1	0	60	-0.0042	0.006	-0.0185	-0.0055	0.0085	—
GP 2	50	62	-0.0026	0.0068	-0.0135	-0.003	0.0155	0.6666
GP 3	100	20	-0.001	0.0048	-0.0105	0	0.0075	0.1285
GP 4	125	63	-0.0017	0.0061	-0.0155	-0.0015	0.0145	0.1134
GP 5	150	65	-0.0012	0.0053	-0.0125	-0.0015	0.0105	0.0266
GP 6	200	20	0.0183	0.098	-0.0175	-0.003	0.4335	0.6666
GP 7	235	20	-0.0028	0.0045	-0.0105	-0.0035	0.0065	0.6666
GP 8	270	22	-0.0013	0.0068	-0.0125	-0.0015	0.0155	0.2868
GP 9	400	20	0.002	0.0068	-0.0175	5e-04	0.0185	0.0048
Overall	—	352	0	0.024	-0.02	0	0.43	—

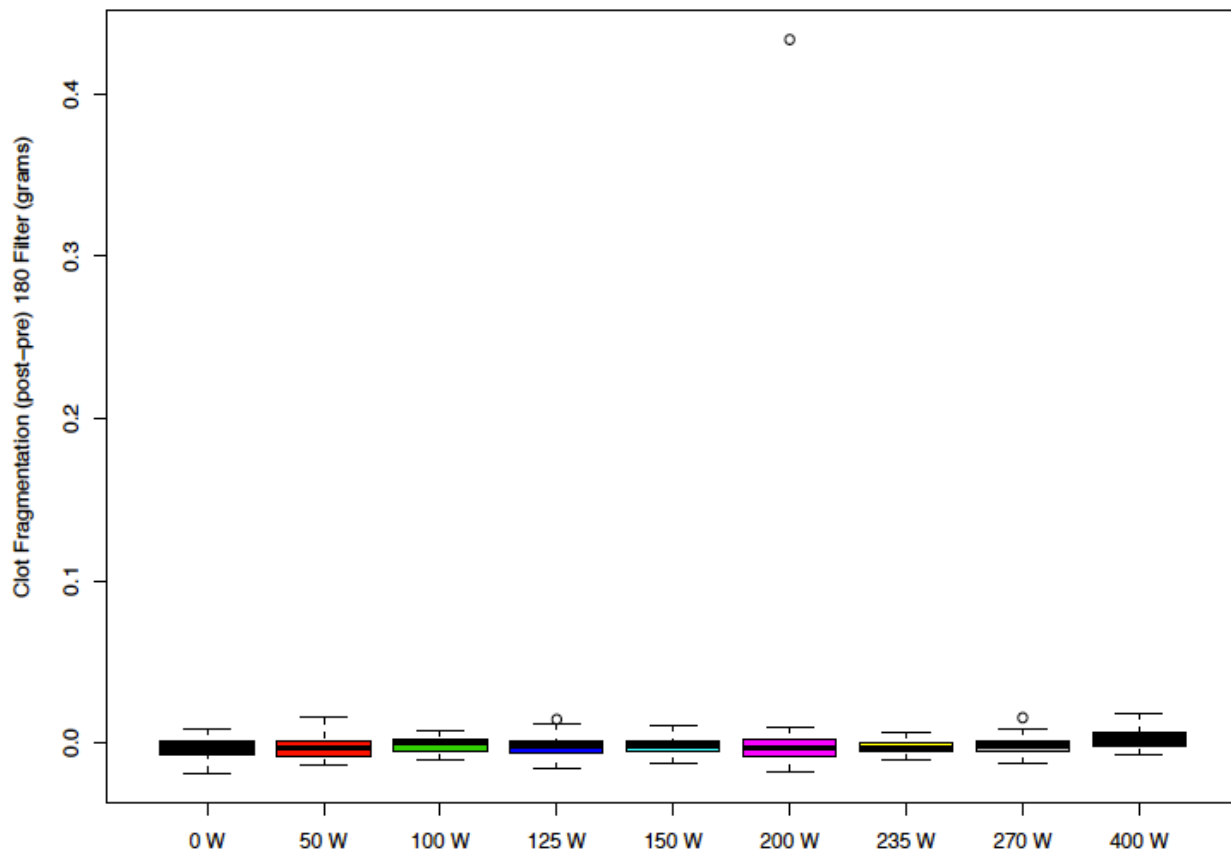


Figure 26 Clot Fragmentation ($> 180 \mu\text{m}$) as Indicated by Post-Pre Test Filter Weight: Boxplot by Acoustic Output Power Group.

Table 15 Clot Fragmentation ($60 \mu\text{m} - 180 \mu\text{m}$) as Indicated by Post-Pre Test Filter Weight. P-values reflect comparison to the 0 W group, adjusted for multiple comparison.

Groups	Acoustic output power (W)	Number	Mean weight difference (g)	STDV	Min. (g)	Median	Max. (g)	p-value
GP 1	0	60	0.0037	0.0034	-0.0011	0.0029	0.0219	—
GP 2	50	62	0.0035	0.0031	-0.0011	0.0024	0.0109	>0.9999
GP 3	100	20	0.013	0.0396	0.0019	0.0039	0.1809	>0.9999
GP 4	125	63	0.0033	0.0028	-0.0041	0.0029	0.0119	>0.9999
GP 5	150	65	0.0032	0.0036	-0.0121	0.0029	0.0159	>0.9999
GP 6	200	20	0.0212	0.0564	-0.0021	0.0034	0.1909	>0.9999
GP 7	235	20	0.0026	0.0028	-0.0021	0.0019	0.0069	>0.9999
GP 8	270	22	0.0106	0.0382	-0.0061	0.0034	0.1809	>0.9999
GP 9	400	20	0.0134	0.0418	-0.0011	0.0039	0.1909	>0.9999
Overall	—	352	0.01	0.0217	-0.01	0	0.19	—

Table 16 Clot Fragmentation (11 µm - 60 µm) as Indicated by Post-Pre Test Filter Weight.
P-values reflect comparison to the 0 W group, adjusted for multiple comparison

Groups	Acoustic output power (W)	Number	Mean weight difference (g)	STDV	Min. (g)	Median	Max. (g)	p-value
GP 1	0	60	0.0024	0.0038	-0.0082	0.0018	0.0118	—
GP 2	50	62	0.0033	0.0042	-0.0082	0.0028	0.0198	>0.9999
GP 3	100	20	0.0185	0.0689	-0.0022	0.0033	0.3108	>0.9999
GP 4	125	63	0.0027	0.0038	-0.0062	0.0028	0.0138	>0.9999
GP 5	150	65	0.0042	0.0074	-0.0062	0.0028	0.0508	>0.9999
GP 6	200	20	0.003	0.0034	-0.0032	0.0028	0.0128	>0.9999
GP 7	235	20	0.0022	0.0023	-0.0022	0.0018	0.0058	>0.9999
GP 8	270	22	0.0022	0.0033	-0.0032	0.0023	0.0098	>0.9999
GP 9	400	20	0.0027	0.0026	-0.0012	0.0018	0.0098	>0.9999
Overall	—	352	0.0039	0.017	-0.0082	0.0028	0.3108	—

Ultrasound Parameters & Acoustic Properties

For each acoustic output power value, the I_{SPTA} , P_{POS} , P_{NEG} were measured at the beam focus with the tubing in place. The acoustic measurements at focus with the tubing in place are shown in Table 17.

Table 17 Acoustic parameters at the beam focus with tubing in place

AC Power (W)	I_{SPTA} (W/cm ²)	P_{NEG} (MPa)	P_{POS} (MPa)
0	0.00	0.00	0.00
50	29.71	1.45	1.32
100	59.27	2.07	1.93
125	75.57	2.34	2.11
150	92.05	2.55	2.34
200	121.05	2.95	2.73
235	144.22	3.27	2.91
270	130.43	3.81	3.09
400	193.24	4.32	3.76

DISCUSSION

Efficacy

A research aim was to study thrombolysis efficacy with increasing acoustic output power. Current literature suggests that FUS has the ability to induce clot lysis [66-68, 104]. To demonstrate efficacy for their *in vitro* thrombolysis experiments Rosenschein *et al.* sonicated clots via an external FUS system [68]. One of their key findings was that thrombolysis, as defined by percent clot weight loss, was found to correlate to the total sonication time. For their experimental setup, clots were placed in *ex vivo* bovine arteries and were insonated at three different points along their longitudinal axis for various durations ranging between 6 and 1800 s. The US parameters used were set to a sonication transmit frequency of 500 kHz, using an acoustic output power to achieve an I_{SPTA} of 35 ± 5 W/cm² at the target clot site. The pulse length was 200 μ s and the duty cycle was 4%. With these US parameters, they could achieve a thrombolysis rate of 91% within 4 minutes of insonation duration.

Similar to Rosenschein *et al.* [68], it could be demonstrated in the present study that thrombolysis can be accomplished by multi-site insonation without using fibrinolytic agents, yielding statistically significant clot lysis. Whereas no significant weight loss was seen in the lower power groups with a measured I_{SPTA} of 0 to 60 W/cm², statistically significant clot lysis was documented for all intensity values of 75 W/cm² or above. The highest amount of weight loss (74.83%) was seen at an I_{SPTA} of 193 W/cm². Different from Rosenschein's work, we did not see efficient clot lysis in the lower intensity groups. Potential reasons for the different outcomes might be explained, for example, by the choice

of experimental parameters and the difference in insonation duration. In the present study the duration of clot insonation was much shorter and kept to 30 seconds, whereas Rosenschein *et al.* found an insonation duration of 120 seconds or above to be efficacious. The pulse width and the duty cycle parameters used in this study were set to 100ms and 50%, respectively, which are greater than those used by Rosenschein *et al.* The transmission frequency used was less than half of what Rosenschein's team used for its *in vitro* study. Lastly, there was a difference in clot preparation between the two studies. Whereas Rosenschein used bovine blood for clot preparation, human citrate blood was used in the present study.

Fragmentation

The two main safety concerns with regard to focused ultrasound thrombolysis are potential thermal effects and clot fragmentation. To test for the latter in relation to increasing acoustic energies was a second, main aim of the present study. The goal was to collect data on clot fragments produced subsequent to thrombolysis and quantitatively evaluate the resultant fragment size distribution. An undesirable side effect of sonothrombolysis has been the potential harmful effects caused by clot fragments. These fragments may lead to secondary vessel occlusion. If the fragments produced from successful US-induced recanalization are large in size they may limit the blood flow farther downstream, causing secondary embolic strokes and leading to secondary ischemic tissue damage. Current literature addresses clot fragmentation as it relates to vessel size. During their *in vitro* sonothrombolysis experiments Rosenschein *et al.* examined clot fragmentation by performing a unidirectional saline flush post insonation through a segment of an *ex vivo* bovine artery with three different pore-sized filters [68]. Mesh filters

serially placed downstream of the sonication focus site captured clot fragments. Using mesh filter pore sizes of 400 μm , 50 μm and 8 μm , differences in their pre- and post-experimental weights were used to assess debris size profiles. The results demonstrated that independent of the I_{SPTA} delivered by their FUS system, 93% of the fragment material was subcapillary in size. Subcapillary was defined to be material smaller than 8 μm in size (not captured even by the 8 μm filter).

A similar, serial filtration setup was used in the present *in vitro* study to examine clot fragmentation as a result of FUS induced sonothrombolysis. The three pore sized mesh filters (180 μm , 60 μm and 11 μm) were weighed before and after insonation for all groups. In this study, continuous flow was present during insonation and for a few minutes thereafter, to provide a chance for potential clot fragments to be transported and captured by the filters.

Clot fragmentation was analyzed by comparing the median values for filter weight between the 0 W control group and each experimental group for each filter size. In none of the experimental groups did the clot fragmentation that was captured by the 11 μm or 60 μm sized filters differ significantly from the 0 W control group. For the 180 μm filter size only, a statistically significant difference ($p < 0.05$) from the control was found in filter weight change for the 150W and the 400W experimental groups, suggesting that production of clot fragments with a size greater than 180 μm was significantly greater than the control for these insonation powers. For the 150W group, the median value for the 180 μm filter size was negative (post wet filter weight – pre wet filter weight). Negative median values were seen in all other experimental groups which did not have a statistically

significant p-value, including the control group. The variations in pre/post filter weight can be explained by the relatively low sensitivity of the method itself. We are aware that the technique used for measuring filter weight differences is one with significant limitations, but for which there is currently no viable substitute.

Different from this, the median filter weight for the 400 W group was found to be significantly greater for the 180 μm filter size in comparison to the median filter weight of either the control or any other experimental group. Therefore, this finding was found to be significant and most likely clinically relevant. The fact that clot fragmentation was seen only in the highest intensity group and with the largest filter size suggests that larger pieces of the clot were torn apart, most likely due to the visible and vigorous displacement of the clot inside the tubeing during insonation. Similar observations regarding pulsed focused ultrasound displacements of in vitro blood clots were recently described by Wright *et al.* [105].

For the two smaller mesh filter sizes, no statistically significant differences in pre/post filter weights could be seen, independent from the acoustic output power or thrombolytic efficacy. This finding suggests that if clot fragmentation occurred at all, fragments were smaller than 11 μm . A possible reason for the small amount of detectable clot fragmentation with regard to FUS thrombolysis was given by Maxwell *et al.* [52]. The group suggested that the creation of cavitation clouds at the focus could trap clot fragments that might then be further fractionated even in the presence of directional flow.

The potential of using FUS for transcranial sonothrombolysis without causing adverse side effects due to clot fragmentation would suggest a rather safe vessel

recanalizing method, when insonating with an acoustic output powers that is less than 400W. It is common understanding, however, that the present results have to be interpreted with care until they can be reproduced *in vivo*.

SUMMARY

Using a first clinical transcranial FUS headsystem, it has been demonstrated *in vitro* that transcranial sonothrombolysis using FUS can be achieved within seconds in the absence of tPA and without significant clot fragmentation, except for high acoustic output powers beyond 400 Watts. Future research in this field would have to demonstrate the translation of this potential new therapeutic approach and the reproducibility of transcranial FUS sonothrombolysis *in vivo*. More importantly, safety of FUS has to be shown with the optimized parameters in an appropriate *in vivo* model.

Chapter 8 SUMMARY & FUTURE WORK

Focused ultrasound for transcranial sonothrombolysis is a novel approach that could lead to significant clinical impact in future stroke care. The first *in vitro* experiences using this new technology are very encouraging. From the four specific objectives of transcranial FUS sonothrombolysis experiments we have learned

1. FUS sonothrombolysis is feasible in an *in vitro* transcranial flow model
 - a. Skull characteristics impact sonothrombolysis
 - Skull thickness and density resulted in varying clot lysis efficacy
 - b. Acoustic output power, the insonation intensity at the focus on the clot, impacts sonothrombolysis
 - Increased acoustic powers tested resulted in greater clot lysis efficacy
 - c. Flow mechanics impact sonothrombolysis
 - Presence of flow resulted in greater clot lysis efficacy
2. FUS operating parameters such as duty cycle and pulse width can be varied for optimized clot lysis efficacy
 - a. Combination of duty cycle and pulse width impact sonothrombolysis
 - Increased DC and increased PW parameters resulted in greater clot lysis efficacy
3. Transcranial sonothrombolysis efficacy is also dependent on individual skull bone characteristics
 - a. Skull characteristics (thickness, density, and shape (incident angles)) impact the FUS-applied acoustic field location, shape, and sound transmission

- As a general trend, we found that the sound transmission was inversely proportional to the a) skull thickness, b) the number of elements with incident angles greater than 45°, and c) the standard deviation of the density. The sound transmission was proportional to the mean density.
4. Clot lysis depends on the acoustic output power of the FUS system as it relates to effective clot breakdown and potential clot fragments
- a. Acoustic output power impacts sonothrombolysis
 - Increased acoustic output powers resulted in increased clot lysis efficacy
 - Increased acoustic output powers less than 400W resulted in no significant clot fragmentation

As a next step, a more thorough study investigating the acoustic effects at the clot site with a larger sample size of *ex vivo* skulls during insonation in a flow model should help us understand and determine the acoustic properties that are optimal for efficacious transcranial FUS insonation in regard to sonothrombolysis and clot fragmentation.

Further investigations on FUS-induced sonothrombolysis should focus on whether the knowledge gained *in vitro* can be translated into *in vivo* stroke models, with special consideration to be given to potential undesirable effects with regard to safety concerns consequential to sonothrombolysis. The current investigation could subsequently be translated from future *in vivo* work into pre-clinical settings for an MRgFUS system that will effectively induce thrombolysis within seconds and without the aid of lytic agents.

A primary limitation of the present studies is the missing translation into an appropriate *in vivo* model. Second, temperature assessments are missing in the present

work. Although there is a common belief that the underlying mechanism of clot/fibrin disaggregation is of a mechanical nature, thermal effects cannot be excluded until appropriate measurements or appropriate calculations are available. This is extremely relevant to clinical application, since temperature elevation during sonothrombolysis would be a serious safety issue.

The experimental setup represents an *in vitro* sonothrombolysis model of efficacy assessment and resultant clot fragmentation. Thus, future sonothrombolysis efficacy studies will have to be performed in an appropriate *in vivo* model. The current *in vivo* model, which has been development in our lab, is a rabbit carotid artery model. This model has been chosen because it is a bifurcational model and therefore anatomically comparable to the intracranial internal carotid artery bifurcation into the middle and anterior cerebral artery or the bifurcation of the middle cerebral artery itself (M1 – M2 segments). With regard to clot fragmentation, the brain of the animal subjects will be studied post-mortem and quantitative analysis of the fragments will be performed.

The blood clots used in this study were artificially made using blood from healthy human volunteers. Accordingly, these blood clots are a limiting element for adequate demonstration of results for thrombolysis efficiency and clot fragmentation. Future experiments should incorporate the use of *ex vivo* thrombi taken from sufferers of an occluded vessel (harvested during neurointerventional procedures in actual stroke patients) [46]. Furthermore, besides fragmentation, cavitation and thermal effects have to be studied in depth due to the safety concerns. It has been shown that cavitation may lead to microvessel disruption, causing potential intracranial hemorrhages [106]. Thermal

effects are of concern with regard to heat-related tissue damage. Future safety experiments will have to focus on the effects of stable and inertial cavitation both inside and outside the vessel as well as thermal effects of transcranial sonothrombolysis. To address these concerns, currently passive cavitation detection and thermal calculations of the transcranial FUS heads system with various ultrasound parameters should be conducted and advanced measurement tools, such as fiber optic hydrophones, should be introduced.

The ultimate goal is to move the *in vitro* and animal model studies to the clinical application in humans. In order to do so, the FUS system will have to be combined with an MRI system for neuronavigation. Since the FUS brain system does not provide imaging capabilities it is – in the clinical setup – integrated with an MRI scanner to navigate the focus beam towards the target structure. The time to preparation of the patient and the high cost to use these two devices on stroke sufferers might be a limiting factors for therapeutic clinical use of this technology on a broader scale, except in very specialized comprehensive stroke centers. However, the potential impact of MRI-guided FUS in clinical use for treatment of ischemic stroke in the absence of therapeutic lytic agents is significant. Not using lytic agents in combination with US will result in avoidance of the side effects of these therapeutics, such as tPA-induced hemorrhages. Of great importance as well is the fact that a much larger stroke population that might benefit from sonothrombolytic treatment using transcranial FUS that are not eligible for tPA therapy.

APPENDIX A

OBJECTIVE 1: TECHNIQUE FEASIBILITY

This appendix includes additional data supporting Chapter 4.

Is FUS sonothrombolysis efficacy dependent on skull characteristics?

Three skull specimens were used to run 126 sonothrombolysis experiments, testing for the impact of skull characteristics on clot weight loss. The data recorded for each of the three human cadaver calvarias, Skull #1 (N=44), Skull #2 (N=41), and Skull #3 (N=41), can be seen in Tables A-1 through A-3, respectively.

Table A-1 Raw data on sonothrombolysis efficacy obtained using Skull #1

Exp #	Skull ID	AP (W)	DC (%)	PW (ms)	ID (sec)	Flow (ml/min)	PreFUS Wt (g)	PostFUS Wt (g)	Wt Loss (g)
1	Skull #1	270	50	200	30	10	0.18	0.13	0.05
2	Skull #1	270	50	200	30	10	0.21	0.13	0.08
3	Skull #1	270	50	200	30	10	0.21	0.18	0.04
4	Skull #1	270	50	200	30	10	0.19	0.12	0.07
5	Skull #1	270	50	200	30	10	0.19	0.14	0.05
6	Skull #1	270	50	200	30	10	0.25	0.20	0.05
7	Skull #1	270	50	200	30	10	0.24	0.17	0.07
8	Skull #1	270	50	200	30	10	0.25	0.19	0.06
9	Skull #1	270	50	200	30	10	0.24	0.21	0.04
10	Skull #1	270	50	200	30	10	0.25	0.19	0.07
11	Skull #1	270	50	200	30	10	0.23	0.09	0.14
12	Skull #1	270	50	200	30	10	0.24	0.13	0.11

13	Skull #1	270	50	200	30	10	0.25	0.12	0.13
14	Skull #1	270	50	200	30	10	0.23	0.11	0.13
15	Skull #1	270	50	200	30	10	0.28	0.10	0.18
16	Skull #1	270	50	200	30	10	0.24	0.13	0.11
17	Skull #1	270	50	200	30	10	0.23	0.12	0.11
18	Skull #1	270	50	200	30	10	0.23	0.08	0.15
19	Skull #1	270	50	200	30	10	0.24	0.08	0.16
20	Skull #1	270	50	200	30	10	0.23	0.06	0.18
21	Skull #1	270	50	200	30	10	0.25	0.12	0.13
22	Skull #1	270	50	200	30	10	0.23	0.16	0.07
23	Skull #1	270	50	200	30	10	0.24	0.17	0.07
24	Skull #1	270	50	200	30	10	0.25	0.12	0.13
25	Skull #1	270	50	200	30	10	0.26	0.17	0.08
26	Skull #1	270	50	200	30	10	0.23	0.18	0.06
27	Skull #1	270	50	200	30	10	0.25	0.09	0.16
28	Skull #1	270	50	200	30	10	0.27	0.16	0.11
29	Skull #1	270	50	200	30	10	0.23	0.11	0.12
30	Skull #1	270	50	200	30	10	0.23	0.17	0.06
31	Skull #1	270	50	200	30	10	0.23	0.10	0.13
32	Skull #1	270	50	200	30	10	0.28	0.10	0.18
33	Skull #1	270	50	200	30	10	0.25	0.15	0.10
34	Skull #1	270	50	200	30	10	0.25	0.16	0.09
35	Skull #1	270	50	200	30	10	0.23	0.14	0.10
36	Skull #1	270	50	200	30	10	0.26	0.16	0.10
37	Skull	270	50	200	30	10	0.28	0.18	0.10

	#1								
38	Skull #1	270	50	200	30	10	0.24	0.11	0.13
39	Skull #1	270	50	200	30	10	0.27	0.09	0.18
40	Skull #1	270	50	200	30	10	0.24	0.16	0.08
41	Skull #1	270	50	200	30	10	0.26	0.20	0.06
42	Skull #1	270	50	200	30	10	0.22	0.09	0.14
43	Skull #1	270	50	200	30	10	0.23	0.18	0.05
44	Skull #1	270	50	200	30	10	0.27	0.19	0.08

Table A-2 Raw data on sonothrombolysis efficacy obtained using Skull #2

Exp #	Skull ID	AP (W)	DC (%)	PW (ms)	ID (sec)	Flow (ml/min)	PreFUS Wt (g)	PostFUS Wt (g)	Wt Loss (g)
1	Skull #2	270	50	200	30	10	0.26	0.20	0.05
2	Skull #2	270	50	200	30	10	0.29	0.14	0.15
3	Skull #2	270	50	200	30	10	0.25	0.16	0.08
4	Skull #2	270	50	200	30	10	0.25	0.15	0.10
5	Skull #2	270	50	200	30	10	0.25	0.19	0.05
6	Skull #2	270	50	200	30	10	0.27	0.21	0.07
7	Skull #2	270	50	200	30	10	0.24	0.19	0.05
8	Skull #2	270	50	200	30	10	0.24	0.18	0.05
9	Skull #2	270	50	200	30	10	0.23	0.12	0.11
10	Skull #2	270	50	200	30	10	0.26	0.16	0.10
11	Skull #2	270	50	200	30	10	0.23	0.18	0.05
12	Skull #2	270	50	200	30	10	0.25	0.18	0.07
13	Skull #2	270	50	200	30	10	0.25	0.16	0.09
14	Skull	270	50	200	30	10	0.22	0.17	0.05

	#2								
15	Skull #2	270	50	200	30	10	0.27	0.16	0.11
16	Skull #2	270	50	200	30	10	0.23	0.15	0.07
17	Skull #2	270	50	200	30	10	0.25	0.20	0.06
18	Skull #2	270	50	200	30	10	0.22	0.17	0.05
19	Skull #2	270	50	200	30	10	0.26	0.19	0.07
20	Skull #2	270	50	200	30	10	0.23	0.17	0.06
21	Skull #2	270	50	200	30	10	0.22	0.19	0.03
22	Skull #2	270	50	200	30	10	0.27	0.15	0.12
23	Skull #2	270	50	200	30	10	0.28	0.16	0.12
24	Skull #2	270	50	200	30	10	0.26	0.18	0.09
25	Skull #2	270	50	200	30	10	0.25	0.19	0.06
26	Skull #2	270	50	200	30	10	0.27	0.21	0.06
27	Skull #2	270	50	200	30	10	0.28	0.15	0.13
28	Skull #2	270	50	200	30	10	0.28	0.15	0.14
29	Skull #2	270	50	200	30	10	0.24	0.14	0.10
30	Skull #2	270	50	200	30	10	0.28	0.15	0.13
31	Skull #2	270	50	200	30	10	0.26	0.15	0.10
32	Skull #2	270	50	200	30	10	0.25	0.09	0.16
33	Skull #2	270	50	200	30	10	0.27	0.19	0.08
34	Skull #2	270	50	200	30	10	0.25	0.18	0.08
35	Skull #2	270	50	200	30	10	0.25	0.15	0.10
36	Skull #2	270	50	200	30	10	0.28	0.22	0.06
37	Skull #2	270	50	200	30	10	0.28	0.19	0.10
38	Skull #2	270	50	200	30	10	0.23	0.07	0.16

39	Skull #2	270	50	200	30	10	0.28	0.07	0.20
40	Skull #2	270	50	200	30	10	0.28	0.11	0.17
41	Skull #2	270	50	200	30	10	0.29	0.18	0.10

Table A-3 Raw data on sonothrombolysis efficacy obtained using Skull #3

Exp #	Skull ID	AP (W)	DC (%)	PW (ms)	ID (sec)	Flow (ml/min)	PreFUS Wt (g)	PostFUS Wt (g)	Wt Loss (g)
1	Skull #3	270	50	200	30	10	0.26	0.21	0.05
2	Skull #3	270	50	200	30	10	0.25	0.21	0.04
3	Skull #3	270	50	200	30	10	0.26	0.25	0.01
4	Skull #3	270	50	200	30	10	0.28	0.25	0.03
5	Skull #3	270	50	200	30	10	0.26	0.26	0.00
6	Skull #3	270	50	200	30	10	0.27	0.25	0.02
7	Skull #3	270	50	200	30	10	0.29	0.25	0.04
8	Skull #3	270	50	200	30	10	0.24	0.23	0.01
9	Skull #3	270	50	200	30	10	0.27	0.26	0.02
10	Skull #3	270	50	200	30	10	0.26	0.25	0.01
11	Skull #3	270	50	200	30	10	0.23	0.21	0.02
12	Skull #3	270	50	200	30	10	0.23	0.21	0.02
13	Skull #3	270	50	200	30	10	0.28	0.25	0.03
14	Skull #3	270	50	200	30	10	0.24	0.23	0.01
15	Skull #3	270	50	200	30	10	0.23	0.20	0.04
16	Skull #3	270	50	200	30	10	0.24	0.22	0.02
17	Skull #3	270	50	200	30	10	0.26	0.22	0.04
18	Skull #3	270	50	200	30	10	0.25	0.22	0.03

19	Skull #3	270	50	200	30	10	0.24	0.23	0.01
20	Skull #3	270	50	200	30	10	0.24	0.22	0.02
21	Skull #3	270	50	200	30	10	0.28	0.23	0.05
22	Skull #3	270	50	200	30	10	0.26	0.23	0.02
23	Skull #3	270	50	200	30	10	0.23	0.20	0.02
24	Skull #3	270	50	200	30	10	0.25	0.22	0.03
25	Skull #3	270	50	200	30	10	0.29	0.24	0.05
26	Skull #3	270	50	200	30	10	0.23	0.22	0.01
27	Skull #3	270	50	200	30	10	0.26	0.25	0.01
28	Skull #3	270	50	200	30	10	0.22	0.21	0.01
29	Skull #3	270	50	200	30	10	0.23	0.21	0.02
30	Skull #3	270	50	200	30	10	0.24	0.22	0.02
31	Skull #3	270	50	200	30	10	0.23	0.21	0.02
32	Skull #3	270	50	200	30	10	0.27	0.23	0.04
33	Skull #3	270	50	200	30	10	0.26	0.23	0.04
34	Skull #3	270	50	200	30	10	0.26	0.22	0.04
35	Skull #3	270	50	200	30	10	0.24	0.22	0.03
36	Skull #3	270	50	200	30	10	0.23	0.21	0.02
37	Skull #3	270	50	200	30	10	0.28	0.23	0.05
38	Skull #3	270	50	200	30	10	0.23	0.21	0.03
39	Skull #3	270	50	200	30	10	0.26	0.22	0.04
40	Skull #3	270	50	200	30	10	0.25	0.22	0.02
41	Skull #3	270	50	200	30	10	0.25	0.22	0.03

Is FUS sonothrombolysis dependent on acoustic output power?

A total of 208 experiments were performed to test the impact of acoustic output power on clot lysis efficacy. The acoustic output power was gradually increased and the data recorded at 100W (N=46), 200W (N=41), 235W (N=40), 270W (N=40), and 400W (N=41) can be seen in Tables A-4 - A-8, respectively.

Table A-4 Raw data on sonothrombolysis efficacy obtained using acoustic output power of 100W (Skull #1)

Exp #	Skull ID	AP (W)	DC (%)	PW (ms)	ID (sec)	Flow (ml/min)	PreFUS Wt (g)	PostFUS Wt (g)	Wt Loss (g)
1	Skull #1	100	50	200	30	10	0.25	0.23	0.02
2	Skull #1	100	50	200	30	10	0.23	0.22	0.02
3	Skull #1	100	50	200	30	10	0.24	0.23	0.02
4	Skull #1	100	50	200	30	10	0.25	0.24	0.01
5	Skull #1	100	50	200	30	10	0.27	0.25	0.01
6	Skull #1	100	50	200	30	10	0.24	0.23	0.01
7	Skull #1	100	50	200	30	10	0.23	0.20	0.02
8	Skull #1	100	50	200	30	10	0.27	0.24	0.02
9	Skull #1	100	50	200	30	10	0.24	0.22	0.02
10	Skull #1	100	50	200	30	10	0.22	0.22	0.01
11	Skull #1	100	50	200	30	10	0.25	0.23	0.02
12	Skull #1	100	50	200	30	10	0.28	0.25	0.03
13	Skull #1	100	50	200	30	10	0.25	0.25	0.01
14	Skull #1	100	50	200	30	10	0.23	0.23	0.00
15	Skull #1	100	50	200	30	10	0.27	0.24	0.02
16	Skull #1	100	50	200	30	10	0.26	0.24	0.02

17	Skull #1	100	50	200	30	10	0.25	0.24	0.01
18	Skull #1	100	50	200	30	10	0.25	0.24	0.01
19	Skull #1	100	50	200	30	10	0.25	0.24	0.01
20	Skull #1	100	50	200	30	10	0.25	0.23	0.02
21	Skull #1	100	50	200	30	10	0.26	0.24	0.02
22	Skull #1	100	50	200	30	10	0.26	0.24	0.01
23	Skull #1	100	50	200	30	10	0.23	0.22	0.01
24	Skull #1	100	50	200	30	10	0.25	0.24	0.01
25	Skull #1	100	50	200	30	10	0.26	0.24	0.02
26	Skull #1	100	50	200	30	10	0.27	0.23	0.03
27	Skull #1	100	50	200	30	10	0.25	0.23	0.01
28	Skull #1	100	50	200	30	10	0.27	0.25	0.02
29	Skull #1	100	50	200	30	10	0.24	0.23	0.01
30	Skull #1	100	50	200	30	10	0.25	0.23	0.02
31	Skull #1	100	50	200	30	10	0.24	0.23	0.01
32	Skull #1	100	50	200	30	10	0.24	0.23	0.01
33	Skull #1	100	50	200	30	10	0.25	0.24	0.01
34	Skull #1	100	50	200	30	10	0.25	0.23	0.02
35	Skull #1	100	50	200	30	10	0.24	0.23	0.01
36	Skull #1	100	50	200	30	10	0.24	0.23	0.01
37	Skull #1	100	50	200	30	10	0.26	0.25	0.02
38	Skull #1	100	50	200	30	10	0.24	0.23	0.01
39	Skull #1	100	50	200	30	10	0.28	0.26	0.02
40	Skull #1	100	50	200	30	10	0.26	0.25	0.01
41	Skull	100	50	200	30	10	0.23	0.23	0.01

	#1								
42	Skull #1	100	50	200	30	10	0.27	0.25	0.02
43	Skull #1	100	50	200	30	10	0.27	0.23	0.04
44	Skull #1	100	50	200	30	10	0.24	0.23	0.02
45	Skull #1	100	50	200	30	10	0.23	0.22	0.01
46	Skull #1	100	50	200	30	10	0.25	0.22	0.03

Table A-5 Raw data on sonothrombolysis efficacy obtained using acoustic output power of 200W (Skull #1)

Exp #	Skull ID	AP (W)	DC (%)	PW (ms)	ID (sec)	Flow (ml/min)	PreFUS Wt (g)	PostFUS Wt (g)	Wt Loss (g)
1	Skull #1	200	50	200	30	10	0.24	0.22	0.03
2	Skull #1	200	50	200	30	10	0.28	0.24	0.04
3	Skull #1	200	50	200	30	10	0.24	0.21	0.03
4	Skull #1	200	50	200	30	10	0.24	0.21	0.03
5	Skull #1	200	50	200	30	10	0.26	0.22	0.03
6	Skull #1	200	50	200	30	10	0.24	0.21	0.02
7	Skull #1	200	50	200	30	10	0.27	0.26	0.02
8	Skull #1	200	50	200	30	10	0.23	0.22	0.01
9	Skull #1	200	50	200	30	10	0.27	0.25	0.02
10	Skull #1	200	50	200	30	10	0.26	0.23	0.03
11	Skull #1	200	50	200	30	10	0.25	0.23	0.02
12	Skull #1	200	50	200	30	10	0.22	0.21	0.01
13	Skull #1	200	50	200	30	10	0.27	0.25	0.01
14	Skull #1	200	50	200	30	10	0.22	0.21	0.01
15	Skull #1	200	50	200	30	10	0.27	0.22	0.05
16	Skull	200	50	200	30	10	0.26	0.22	0.04

	#1								
17	Skull #1	200	50	200	30	10	0.23	0.22	0.01
18	Skull #1	200	50	200	30	10	0.29	0.09	0.20
19	Skull #1	200	50	200	30	10	0.25	0.17	0.09
20	Skull #1	200	50	200	30	10	0.29	0.20	0.09
21	Skull #1	200	50	200	30	10	0.24	0.06	0.18
22	Skull #1	200	50	200	30	10	0.25	0.11	0.14
23	Skull #1	200	50	200	30	10	0.27	0.21	0.07
24	Skull #1	200	50	200	30	10	0.25	0.19	0.07
25	Skull #1	200	50	200	30	10	0.24	0.19	0.05
26	Skull #1	200	50	200	30	10	0.27	0.19	0.08
27	Skull #1	200	50	200	30	10	0.27	0.22	0.06
28	Skull #1	200	50	200	30	10	0.25	0.10	0.15
29	Skull #1	200	50	200	30	10	0.28	0.16	0.13
30	Skull #1	200	50	200	30	10	0.26	0.19	0.07
31	Skull #1	200	50	200	30	10	0.26	0.17	0.09
32	Skull #1	200	50	200	30	10	0.23	0.18	0.05
33	Skull #1	200	50	200	30	10	0.24	0.19	0.04
34	Skull #1	200	50	200	30	10	0.23	0.18	0.05
35	Skull #1	200	50	200	30	10	0.23	0.20	0.03
36	Skull #1	200	50	200	30	10	0.23	0.20	0.04
37	Skull #1	200	50	200	30	10	0.24	0.20	0.04
38	Skull #1	200	50	200	30	10	0.25	0.13	0.12
39	Skull #1	200	50	200	30	10	0.24	0.15	0.08
40	Skull #1	200	50	200	30	10	0.25	0.17	0.08

41	Skull #1	200	50	200	30	10	0.24	0.18	0.05
----	----------	-----	----	-----	----	----	------	------	------

Table A-6 Raw data on sonothrombolysis efficacy obtained using acoustic output power of 235W (Skull #1)

Exp #	Skull ID	AP (W)	DC (%)	PW (ms)	ID (sec)	Flow (ml/min)	PreFUS Wt (g)	PostFUS Wt (g)	Wt Loss (g)
1	Skull #1	235	50	200	30	10	0.26	0.18	0.09
2	Skull #1	235	50	200	30	10	0.24	0.18	0.06
3	Skull #1	235	50	200	30	10	0.25	0.15	0.10
4	Skull #1	235	50	200	30	10	0.25	0.18	0.07
5	Skull #1	235	50	200	30	10	0.27	0.16	0.11
6	Skull #1	235	50	200	30	10	0.26	0.19	0.07
7	Skull #1	235	50	200	30	10	0.25	0.21	0.04
8	Skull #1	235	50	200	30	10	0.25	0.07	0.18
9	Skull #1	235	50	200	30	10	0.27	0.10	0.17
10	Skull #1	235	50	200	30	10	0.22	0.17	0.05
11	Skull #1	235	50	200	30	10	0.25	0.19	0.06
12	Skull #1	235	50	200	30	10	0.26	0.22	0.04
13	Skull #1	235	50	200	30	10	0.26	0.12	0.14
14	Skull #1	235	50	200	30	10	0.25	0.08	0.17
15	Skull #1	235	50	200	30	10	0.24	0.17	0.07
16	Skull #1	235	50	200	30	10	0.27	0.18	0.09
17	Skull #1	235	50	200	30	10	0.26	0.19	0.07
18	Skull #1	235	50	200	30	10	0.26	0.18	0.08
19	Skull #1	235	50	200	30	10	0.27	0.18	0.09
20	Skull	235	50	200	30	10	0.26	0.13	0.13

	#1								
21	Skull #1	235	50	200	30	10	0.27	0.20	0.08
22	Skull #1	235	50	200	30	10	0.25	0.07	0.18
23	Skull #1	235	50	200	30	10	0.27	0.06	0.21
24	Skull #1	235	50	200	30	10	0.25	0.07	0.17
25	Skull #1	235	50	200	30	10	0.26	0.18	0.08
26	Skull #1	235	50	200	30	10	0.27	0.22	0.05
27	Skull #1	235	50	200	30	10	0.27	0.05	0.22
28	Skull #1	235	50	200	30	10	0.25	0.17	0.08
29	Skull #1	235	50	200	30	10	0.26	0.07	0.19
30	Skull #1	235	50	200	30	10	0.23	0.18	0.05
31	Skull #1	235	50	200	30	10	0.24	0.14	0.10
32	Skull #1	235	50	200	30	10	0.27	0.07	0.20
33	Skull #1	235	50	200	30	10	0.26	0.11	0.15
34	Skull #1	235	50	200	30	10	0.25	0.08	0.17
35	Skull #1	235	50	200	30	10	0.25	0.22	0.03
36	Skull #1	235	50	200	30	10	0.27	0.10	0.17
37	Skull #1	235	50	200	30	10	0.25	0.20	0.05
38	Skull #1	235	50	200	30	10	0.24	0.09	0.15
39	Skull #1	235	50	200	30	10	0.23	0.11	0.12
40	Skull #1	235	50	200	30	10	0.25	0.21	0.04

Table A-7 Raw data on sonothrombolysis efficacy obtained using acoustic output power of 270W (Skull #1)

Exp #	Skull ID	AP (W)	DC (%)	PW (ms)	ID (sec)	Flow (ml/min)	PreFUS Wt (g)	PostFUS Wt (g)	Wt Loss (g)
1	Skull #1	270	50	200	30	10	0.24	0.05	0.18
2	Skull #1	270	50	200	30	10	0.23	0.07	0.16
3	Skull #1	270	50	200	30	10	0.24	0.08	0.16
4	Skull #1	270	50	200	30	10	0.25	0.07	0.19
5	Skull #1	270	50	200	30	10	0.26	0.06	0.20
6	Skull #1	270	50	200	30	10	0.27	0.07	0.21
7	Skull #1	270	50	200	30	10	0.23	0.13	0.10
8	Skull #1	270	50	200	30	10	0.28	0.05	0.24
9	Skull #1	270	50	200	30	10	0.25	0.06	0.19
10	Skull #1	270	50	200	30	10	0.23	0.09	0.14
11	Skull #1	270	50	200	30	10	0.27	0.12	0.15
12	Skull #1	270	50	200	30	10	0.25	0.14	0.11
13	Skull #1	270	50	200	30	10	0.29	0.07	0.22
14	Skull #1	270	50	200	30	10	0.24	0.04	0.20
15	Skull #1	270	50	200	30	10	0.23	0.13	0.11
16	Skull #1	270	50	200	30	10	0.28	0.09	0.19
17	Skull #1	270	50	200	30	10	0.27	0.12	0.15
18	Skull #1	270	50	200	30	10	0.27	0.15	0.12
19	Skull #1	270	50	200	30	10	0.26	0.13	0.13
20	Skull #1	270	50	200	30	10	0.29	0.06	0.23
21	Skull #1	270	50	200	30	10	0.27	0.15	0.12
22	Skull #1	270	50	200	30	10	0.26	0.14	0.11

23	Skull #1	270	50	200	30	10	0.26	0.10	0.16
24	Skull #1	270	50	200	30	10	0.25	0.12	0.13
25	Skull #1	270	50	200	30	10	0.25	0.12	0.13
26	Skull #1	270	50	200	30	10	0.24	0.07	0.17
27	Skull #1	270	50	200	30	10	0.26	0.07	0.19
28	Skull #1	270	50	200	30	10	0.28	0.16	0.13
29	Skull #1	270	50	200	30	10	0.24	0.08	0.17
30	Skull #1	270	50	200	30	10	0.24	0.07	0.17
31	Skull #1	270	50	200	30	10	0.27	0.13	0.15
32	Skull #1	270	50	200	30	10	0.25	0.15	0.11
33	Skull #1	270	50	200	30	10	0.24	0.08	0.16
34	Skull #1	270	50	200	30	10	0.27	0.10	0.17
35	Skull #1	270	50	200	30	10	0.25	0.14	0.10
36	Skull #1	270	50	200	30	10	0.24	0.09	0.16
37	Skull #1	270	50	200	30	10	0.25	0.10	0.15
38	Skull #1	270	50	200	30	10	0.24	0.16	0.08
39	Skull #1	270	50	200	30	10	0.25	0.14	0.11
40	Skull #1	270	50	200	30	10	0.25	0.15	0.10

Table A-8 Raw data on sonothrombolysis efficacy obtained using acoustic output power of 400W (Skull #1)

Exp #	Skull ID	AP (W)	DC (%)	PW (ms)	ID (sec)	Flow (ml/min)	PreFUS Wt (g)	PostFUS Wt (g)	Wt Loss (g)
1	Skull #1	400	50	200	30	10	0.25	0.05	0.20
2	Skull #1	400	50	200	30	10	0.25	0.07	0.17
3	Skull	400	50	200	30	10	0.26	0.05	0.20

	#1								
4	Skull #1	400	50	200	30	10	0.25	0.05	0.20
5	Skull #1	400	50	200	30	10	0.25	0.06	0.19
6	Skull #1	400	50	200	30	10	0.26	0.08	0.19
7	Skull #1	400	50	200	30	10	0.26	0.06	0.20
8	Skull #1	400	50	200	30	10	0.27	0.04	0.23
9	Skull #1	400	50	200	30	10	0.24	0.08	0.17
10	Skull #1	400	50	200	30	10	0.24	0.05	0.19
11	Skull #1	400	50	200	30	10	0.25	0.04	0.21
12	Skull #1	400	50	200	30	10	0.26	0.05	0.21
13	Skull #1	400	50	200	30	10	0.26	0.06	0.20
14	Skull #1	400	50	200	30	10	0.26	0.05	0.22
15	Skull #1	400	50	200	30	10	0.26	0.04	0.22
16	Skull #1	400	50	200	30	10	0.25	0.14	0.10
17	Skull #1	400	50	200	30	10	0.25	0.08	0.18
18	Skull #1	400	50	200	30	10	0.25	0.08	0.17
19	Skull #1	400	50	200	30	10	0.25	0.07	0.18
20	Skull #1	400	50	200	30	10	0.22	0.07	0.15
21	Skull #1	400	50	200	30	10	0.26	0.05	0.20
22	Skull #1	400	50	200	30	10	0.26	0.05	0.21
23	Skull #1	400	50	200	30	10	0.26	0.09	0.17
24	Skull #1	400	50	200	30	10	0.26	0.05	0.21
25	Skull #1	400	50	200	30	10	0.26	0.04	0.22
26	Skull #1	400	50	200	30	10	0.26	0.05	0.21
27	Skull #1	400	50	200	30	10	0.23	0.05	0.19

28	Skull #1	400	50	200	30	10	0.24	0.05	0.20
29	Skull #1	400	50	200	30	10	0.22	0.08	0.14
30	Skull #1	400	50	200	30	10	0.21	0.04	0.17
31	Skull #1	400	50	200	30	10	0.23	0.04	0.19
32	Skull #1	400	50	200	30	10	0.26	0.04	0.22
33	Skull #1	400	50	200	30	10	0.24	0.04	0.20
34	Skull #1	400	50	200	30	10	0.25	0.04	0.21
35	Skull #1	400	50	200	30	10	0.24	0.04	0.19
36	Skull #1	400	50	200	30	10	0.23	0.04	0.19
37	Skull #1	400	50	200	30	10	0.23	0.05	0.18
38	Skull #1	400	50	200	30	10	0.25	0.05	0.20
39	Skull #1	400	50	200	30	10	0.25	0.05	0.20
40	Skull #1	400	50	200	30	10	0.24	0.04	0.20
41	Skull #1	400	50	200	30	10	0.23	0.05	0.19

Is FUS sonothrombolysis dependent on flow mechanics?

Overall 86 experiments were performed to test the impact of flow mechanics on clot lysis efficacy. Table A-9 contains the raw data (N=42) obtained for studies when there was no flow during FUS insonation, while Table A-10 has the data points collected during experiments (N=44) that had a low velocity flow of 10ml/min present.

Table A-9 Raw data on sonothrombolysis efficacy obtained with No-Flow (0ml/min) conditions (Skull #1)

Exp #	Skull ID	AP (W)	DC (%)	PW (ms)	ID (sec)	Flow (ml/min)	PreFUS Wt (g)	PostFUS Wt (g)	Wt Loss (g)
1	Skull #1	270	50	200	30	0	0.27	0.24	0.03

100										
2	Skull #1	270	50	200	30	0	0.26	0.21	0.04	
3	Skull #1	270	50	200	30	0	0.26	0.18	0.08	
4	Skull #1	270	50	200	30	0	0.27	0.23	0.05	
5	Skull #1	270	50	200	30	0	0.25	0.21	0.04	
6	Skull #1	270	50	200	30	0	0.27	0.22	0.05	
7	Skull #1	270	50	200	30	0	0.26	0.22	0.04	
8	Skull #1	270	50	200	30	0	0.22	0.22	0.01	
9	Skull #1	270	50	200	30	0	0.25	0.23	0.02	
10	Skull #1	270	50	200	30	0	0.27	0.20	0.06	
11	Skull #1	270	50	200	30	0	0.27	0.21	0.06	
12	Skull #1	270	50	200	30	0	0.25	0.19	0.06	
13	Skull #1	270	50	200	30	0	0.25	0.20	0.05	
14	Skull #1	270	50	200	30	0	0.27	0.21	0.05	
15	Skull #1	270	50	200	30	0	0.27	0.21	0.06	
16	Skull #1	270	50	200	30	0	0.27	0.21	0.06	
17	Skull #1	270	50	200	30	0	0.24	0.18	0.06	
18	Skull #1	270	50	200	30	0	0.25	0.20	0.05	
19	Skull #1	270	50	200	30	0	0.25	0.23	0.03	
20	Skull #1	270	50	200	30	0	0.28	0.22	0.06	
21	Skull #1	270	50	200	30	0	0.28	0.21	0.07	
22	Skull #1	270	50	200	30	0	0.26	0.21	0.06	
23	Skull #1	270	50	200	30	0	0.26	0.22	0.04	
24	Skull #1	270	50	200	30	0	0.25	0.22	0.04	
25	Skull #1	270	50	200	30	0	0.26	0.22	0.05	
26	Skull	270	50	200	30	0	0.26	0.18	0.07	

	#1								
27	Skull #1	270	50	200	30	0	0.25	0.20	0.05
28	Skull #1	270	50	200	30	0	0.27	0.22	0.04
29	Skull #1	270	50	200	30	0	0.23	0.19	0.03
30	Skull #1	270	50	200	30	0	0.23	0.18	0.05
31	Skull #1	270	50	200	30	0	0.27	0.21	0.07
32	Skull #1	270	50	200	30	0	0.22	0.16	0.06
33	Skull #1	270	50	200	30	0	0.28	0.24	0.04
34	Skull #1	270	50	200	30	0	0.24	0.21	0.03
35	Skull #1	270	50	200	30	0	0.23	0.20	0.02
36	Skull #1	270	50	200	30	0	0.29	0.24	0.05
37	Skull #1	270	50	200	30	0	0.28	0.21	0.07
38	Skull #1	270	50	200	30	0	0.23	0.19	0.03
39	Skull #1	270	50	200	30	0	0.25	0.21	0.05
40	Skull #1	270	50	200	30	0	0.28	0.24	0.04
41	Skull #1	270	50	200	30	0	0.28	0.23	0.05
42	Skull #1	270	50	200	30	0	0.23	0.21	0.03

Table A-10 Raw data on sonothrombolysis efficacy obtained with flow present at 10ml/min (Skull #1)

Exp #	Skull ID	AP (W)	DC (%)	PW (ms)	ID (sec)	Flow (ml/min)	PreFUS Wt (g)	PostFUS Wt (g)	Wt Loss (g)
1	Skull #1	270	50	200	30	10	0.18	0.13	0.05
2	Skull #1	270	50	200	30	10	0.21	0.13	0.08
3	Skull #1	270	50	200	30	10	0.21	0.18	0.04
4	Skull #1	270	50	200	30	10	0.19	0.12	0.07

5	Skull #1	270	50	200	30	10	0.19	0.14	0.05
6	Skull #1	270	50	200	30	10	0.25	0.20	0.05
7	Skull #1	270	50	200	30	10	0.24	0.17	0.07
8	Skull #1	270	50	200	30	10	0.25	0.19	0.06
9	Skull #1	270	50	200	30	10	0.24	0.21	0.04
10	Skull #1	270	50	200	30	10	0.25	0.19	0.07
11	Skull #1	270	50	200	30	10	0.23	0.09	0.14
12	Skull #1	270	50	200	30	10	0.24	0.13	0.11
13	Skull #1	270	50	200	30	10	0.25	0.12	0.13
14	Skull #1	270	50	200	30	10	0.23	0.11	0.13
15	Skull #1	270	50	200	30	10	0.28	0.10	0.18
16	Skull #1	270	50	200	30	10	0.24	0.13	0.11
17	Skull #1	270	50	200	30	10	0.23	0.12	0.11
18	Skull #1	270	50	200	30	10	0.23	0.08	0.15
19	Skull #1	270	50	200	30	10	0.24	0.08	0.16
20	Skull #1	270	50	200	30	10	0.23	0.06	0.18
21	Skull #1	270	50	200	30	10	0.25	0.12	0.13
22	Skull #1	270	50	200	30	10	0.23	0.16	0.07
23	Skull #1	270	50	200	30	10	0.24	0.17	0.07
24	Skull #1	270	50	200	30	10	0.25	0.12	0.13
25	Skull #1	270	50	200	30	10	0.26	0.17	0.08
26	Skull #1	270	50	200	30	10	0.23	0.18	0.06
27	Skull #1	270	50	200	30	10	0.25	0.09	0.16
28	Skull #1	270	50	200	30	10	0.27	0.16	0.11
29	Skull	270	50	200	30	10	0.23	0.11	0.12

	#1								
30	Skull #1	270	50	200	30	10	0.23	0.17	0.06
31	Skull #1	270	50	200	30	10	0.23	0.10	0.13
32	Skull #1	270	50	200	30	10	0.28	0.10	0.18
33	Skull #1	270	50	200	30	10	0.25	0.15	0.10
34	Skull #1	270	50	200	30	10	0.25	0.16	0.09
35	Skull #1	270	50	200	30	10	0.23	0.14	0.10
36	Skull #1	270	50	200	30	10	0.26	0.16	0.10
37	Skull #1	270	50	200	30	10	0.28	0.18	0.10
38	Skull #1	270	50	200	30	10	0.24	0.11	0.13
39	Skull #1	270	50	200	30	10	0.27	0.09	0.18
40	Skull #1	270	50	200	30	10	0.24	0.16	0.08
41	Skull #1	270	50	200	30	10	0.26	0.20	0.06
42	Skull #1	270	50	200	30	10	0.22	0.09	0.14
43	Skull #1	270	50	200	30	10	0.23	0.18	0.05
44	Skull #1	270	50	200	30	10	0.27	0.19	0.08

APPENDIX B

OBJECTIVE 2: PARAMETER OPTIMIZATION

This appendix includes additional data supporting Chapter 5.

Overall, a total of 658 parameter optimization experiments were performed. The effect of 16 groups of varying DC and PW combinations of FUS parameters were studied with regard to lysis efficacy. Tables B-1—B-4 illustrate the complete collection of data points, partitioned by DC, 5%, 10%, 20%, and 50%, respectively.

Table B-1 Data acquired for 0.1ms, 1ms, 10ms, & 100ms PW at 5% DC, Groups 1-4

Exp #	Grp #	Skull ID	AP (W)	DC (%)	PW (ms)	ID (sec)	Flow (ml/min)	PreFUS Wt (g)	PostFUS Wt (g)	Wt Loss (g)
1	1	Skull #1	235	5	0.1	30	10	0.23	0.22	0.01
2	1	Skull #1	235	5	0.1	30	10	0.27	0.19	0.08
3	1	Skull #1	235	5	0.1	30	10	0.24	0.24	0.00
4	1	Skull #1	235	5	0.1	30	10	0.26	0.24	0.02
5	1	Skull #1	235	5	0.1	30	10	0.24	0.23	0.01
6	1	Skull #1	235	5	0.1	30	10	0.26	0.25	0.01
7	1	Skull #1	235	5	0.1	30	10	0.26	0.23	0.02
8	1	Skull #1	235	5	0.1	30	10	0.27	0.25	0.02
9	1	Skull #1	235	5	0.1	30	10	0.20	0.19	0.02
10	1	Skull #1	235	5	0.1	30	10	0.25	0.24	0.01
11	1	Skull #1	235	5	0.1	30	10	0.21	0.21	0.00
12	1	Skull #1	235	5	0.1	30	10	0.21	0.22	-0.01
13	1	Skull	235	5	0.1	30	10	0.22	0.21	0.01

		#1								
14	1	Skull #1	235	5	0.1	30	10	0.21	0.21	0.00
15	1	Skull #1	235	5	0.1	30	10	0.22	0.22	0.00
16	1	Skull #1	235	5	0.1	30	10	0.21	0.20	0.01
17	1	Skull #1	235	5	0.1	30	10	0.24	0.23	0.01
18	1	Skull #1	235	5	0.1	30	10	0.23	0.22	0.01
19	1	Skull #1	235	5	0.1	30	10	0.22	0.19	0.03
20	1	Skull #1	235	5	0.1	30	10	0.21	0.21	0.00
21	1	Skull #1	235	5	0.1	30	10	0.21	0.20	0.01
22	1	Skull #1	235	5	0.1	30	10	0.23	0.22	0.01
23	1	Skull #1	235	5	0.1	30	10	0.23	0.22	0.01
24	1	Skull #1	235	5	0.1	30	10	0.23	0.17	0.06
25	1	Skull #1	235	5	0.1	30	10	0.23	0.22	0.01
26	1	Skull #1	235	5	0.1	30	10	0.25	0.25	0.00
27	1	Skull #1	235	5	0.1	30	10	0.24	0.22	0.02
28	1	Skull #1	235	5	0.1	30	10	0.26	0.25	0.01
29	1	Skull #1	235	5	0.1	30	10	0.21	0.18	0.03
30	1	Skull #1	235	5	0.1	30	10	0.21	0.18	0.04
31	1	Skull #1	235	5	0.1	30	10	0.21	0.17	0.04
32	1	Skull #1	235	5	0.1	30	10	0.24	0.20	0.04
33	1	Skull #1	235	5	0.1	30	10	0.25	0.20	0.05
34	1	Skull #1	235	5	0.1	30	10	0.24	0.12	0.12
35	1	Skull #1	235	5	0.1	30	10	0.24	0.21	0.03
36	1	Skull #1	235	5	0.1	30	10	0.25	0.22	0.04
37	1	Skull #1	235	5	0.1	30	10	0.25	0.21	0.04

38	1	Skull #1	235	5	0.1	30	10	0.25	0.12	0.13
39	1	Skull #1	235	5	0.1	30	10	0.24	0.23	0.01
40	1	Skull #1	235	5	0.1	30	10	0.21	0.18	0.03
1	2	Skull #1	235	5	1	30	10	0.31	0.25	0.06
2	2	Skull #1	235	5	1	30	10	0.23	0.18	0.05
3	2	Skull #1	235	5	1	30	10	0.24	0.20	0.04
4	2	Skull #1	235	5	1	30	10	0.27	0.21	0.06
5	2	Skull #1	235	5	1	30	10	0.22	0.17	0.05
6	2	Skull #1	235	5	1	30	10	0.29	0.23	0.07
7	2	Skull #1	235	5	1	30	10	0.29	0.24	0.05
8	2	Skull #1	235	5	1	30	10	0.20	0.18	0.02
9	2	Skull #1	235	5	1	30	10	0.22	0.18	0.04
10	2	Skull #1	235	5	1	30	10	0.24	0.19	0.05
11	2	Skull #1	235	5	1	30	10	0.26	0.21	0.05
12	2	Skull #1	235	5	1	30	10	0.22	0.21	0.01
13	2	Skull #1	235	5	1	30	10	0.22	0.19	0.03
14	2	Skull #1	235	5	1	30	10	0.22	0.21	0.01
15	2	Skull #1	235	5	1	30	10	0.24	0.19	0.05
16	2	Skull #1	235	5	1	30	10	0.23	0.22	0.01
17	2	Skull #1	235	5	1	30	10	0.23	0.22	0.02
18	2	Skull #1	235	5	1	30	10	0.23	0.21	0.03
19	2	Skull #1	235	5	1	30	10	0.21	0.18	0.03
20	2	Skull #1	235	5	1	30	10	0.22	0.18	0.03
21	2	Skull #1	235	5	1	30	10	0.25	0.22	0.03
22	2	Skull	235	5	1	30	10	0.26	0.21	0.05

		#1								
23	2	Skull #1	235	5	1	30	10	0.28	0.24	0.05
24	2	Skull #1	235	5	1	30	10	0.23	0.19	0.04
25	2	Skull #1	235	5	1	30	10	0.23	0.19	0.04
26	2	Skull #1	235	5	1	30	10	0.24	0.21	0.03
27	2	Skull #1	235	5	1	30	10	0.25	0.22	0.02
28	2	Skull #1	235	5	1	30	10	0.27	0.19	0.09
29	2	Skull #1	235	5	1	30	10	0.24	0.19	0.05
30	2	Skull #1	235	5	1	30	10	0.22	0.18	0.04
31	2	Skull #1	235	5	1	30	10	0.21	0.16	0.04
32	2	Skull #1	235	5	1	30	10	0.21	0.18	0.03
33	2	Skull #1	235	5	1	30	10	0.28	0.18	0.10
34	2	Skull #1	235	5	1	30	10	0.27	0.19	0.07
35	2	Skull #1	235	5	1	30	10	0.24	0.21	0.03
36	2	Skull #1	235	5	1	30	10	0.25	0.19	0.06
37	2	Skull #1	235	5	1	30	10	0.26	0.20	0.05
38	2	Skull #1	235	5	1	30	10	0.26	0.17	0.09
39	2	Skull #1	235	5	1	30	10	0.26	0.23	0.04
40	2	Skull #1	235	5	1	30	10	0.25	0.19	0.05
1	3	Skull #1	235	5	10	30	10	0.23	0.21	0.02
2	3	Skull #1	235	5	10	30	10	0.24	0.20	0.05
3	3	Skull #1	235	5	10	30	10	0.24	0.15	0.10
4	3	Skull #1	235	5	10	30	10	0.26	0.18	0.08
5	3	Skull #1	235	5	10	30	10	0.25	0.22	0.03
6	3	Skull #1	235	5	10	30	10	0.28	0.21	0.07

7	3	Skull #1	235	5	10	30	10	0.27	0.25	0.02
8	3	Skull #1	235	5	10	30	10	0.28	0.23	0.05
9	3	Skull #1	235	5	10	30	10	0.32	0.24	0.09
10	3	Skull #1	235	5	10	30	10	0.28	0.20	0.08
11	3	Skull #1	235	5	10	30	10	0.24	0.19	0.05
12	3	Skull #1	235	5	10	30	10	0.20	0.15	0.05
13	3	Skull #1	235	5	10	30	10	0.23	0.19	0.05
14	3	Skull #1	235	5	10	30	10	0.21	0.07	0.13
15	3	Skull #1	235	5	10	30	10	0.22	0.17	0.05
16	3	Skull #1	235	5	10	30	10	0.24	0.19	0.06
17	3	Skull #1	235	5	10	30	10	0.25	0.14	0.11
18	3	Skull #1	235	5	10	30	10	0.24	0.16	0.08
19	3	Skull #1	235	5	10	30	10	0.24	0.17	0.07
20	3	Skull #1	235	5	10	30	10	0.22	0.18	0.04
21	3	Skull #1	235	5	10	30	10	0.23	0.22	0.01
22	3	Skull #1	235	5	10	30	10	0.21	0.19	0.02
23	3	Skull #1	235	5	10	30	10	0.29	0.28	0.01
24	3	Skull #1	235	5	10	30	10	0.22	0.18	0.04
25	3	Skull #1	235	5	10	30	10	0.23	0.18	0.05
26	3	Skull #1	235	5	10	30	10	0.27	0.24	0.03
27	3	Skull #1	235	5	10	30	10	0.27	0.20	0.07
28	3	Skull #1	235	5	10	30	10	0.23	0.20	0.03
29	3	Skull #1	235	5	10	30	10	0.22	0.17	0.05
30	3	Skull #1	235	5	10	30	10	0.22	0.18	0.04
31	3	Skull	235	5	10	30	10	0.22	0.17	0.05

		#1								
32	3	Skull #1	235	5	10	30	10	0.26	0.19	0.07
33	3	Skull #1	235	5	10	30	10	0.23	0.13	0.10
34	3	Skull #1	235	5	10	30	10	0.25	0.17	0.08
35	3	Skull #1	235	5	10	30	10	0.23	0.16	0.07
36	3	Skull #1	235	5	10	30	10	0.24	0.14	0.10
37	3	Skull #1	235	5	10	30	10	0.23	0.17	0.05
38	3	Skull #1	235	5	10	30	10	0.28	0.21	0.07
39	3	Skull #1	235	5	10	30	10	0.24	0.18	0.06
40	3	Skull #1	235	5	10	30	10	0.24	0.20	0.04
1	4	Skull #1	235	5	100	30	10	0.21	0.21	0.00
2	4	Skull #1	235	5	100	30	10	0.24	0.25	-0.01
3	4	Skull #1	235	5	100	30	10	0.24	0.22	0.02
4	4	Skull #1	235	5	100	30	10	0.31	0.14	0.17
5	4	Skull #1	235	5	100	30	10	0.21	0.20	0.01
6	4	Skull #1	235	5	100	30	10	0.25	0.14	0.11
7	4	Skull #1	235	5	100	30	10	0.23	0.21	0.02
8	4	Skull #1	235	5	100	30	10	0.24	0.14	0.09
9	4	Skull #1	235	5	100	30	10	0.24	0.15	0.09
10	4	Skull #1	235	5	100	30	10	0.26	0.19	0.07
11	4	Skull #1	235	5	100	30	10	0.20	0.20	0.00
12	4	Skull #1	235	5	100	30	10	0.29	0.22	0.08
13	4	Skull #1	235	5	100	30	10	0.24	0.04	0.20
14	4	Skull #1	235	5	100	30	10	0.26	0.12	0.14
15	4	Skull #1	235	5	100	30	10	0.23	0.19	0.04

16	4	Skull #1	235	5	100	30	10	0.23	0.16	0.07
17	4	Skull #1	235	5	100	30	10	0.24	0.20	0.04
18	4	Skull #1	235	5	100	30	10	0.21	0.16	0.05
19	4	Skull #1	235	5	100	30	10	0.21	0.05	0.16
20	4	Skull #1	235	5	100	30	10	0.22	0.17	0.05
21	4	Skull #1	235	5	100	30	10	0.26	0.20	0.06
22	4	Skull #1	235	5	100	30	10	0.24	0.17	0.06
23	4	Skull #1	235	5	100	30	10	0.22	0.16	0.06
24	4	Skull #1	235	5	100	30	10	0.21	0.22	-0.01
25	4	Skull #1	235	5	100	30	10	0.22	0.21	0.01
26	4	Skull #1	235	5	100	30	10	0.24	0.23	0.01
27	4	Skull #1	235	5	100	30	10	0.26	0.21	0.05
28	4	Skull #1	235	5	100	30	10	0.23	0.22	0.01
29	4	Skull #1	235	5	100	30	10	0.21	0.19	0.02
30	4	Skull #1	235	5	100	30	10	0.24	0.19	0.05
31	4	Skull #1	235	5	100	30	10	0.21	0.16	0.05
32	4	Skull #1	235	5	100	30	10	0.22	0.18	0.04
33	4	Skull #1	235	5	100	30	10	0.23	0.16	0.07
34	4	Skull #1	235	5	100	30	10	0.24	0.17	0.07
35	4	Skull #1	235	5	100	30	10	0.24	0.13	0.11
36	4	Skull #1	235	5	100	30	10	0.22	0.17	0.06
37	4	Skull #1	235	5	100	30	10	0.26	0.10	0.16
38	4	Skull #1	235	5	100	30	10	0.25	0.14	0.10
39	4	Skull #1	235	5	100	30	10	0.22	0.09	0.13
40	4	Skull	235	5	100	30	10	0.26	0.18	0.09

		#1							
--	--	----	--	--	--	--	--	--	--

Table B-2 Data acquired for 0.1ms, 1ms, 10ms, & 100ms PW at 10% DC, Groups 5-8

Exp #	Grp #	Skull ID	AP (W)	DC (%)	PW (ms)	ID (sec)	Flow (ml/min)	PreFUS Wt (g)	PostFUS Wt (g)	Wt Loss (g)
1	5	Skull #1	235	10	0.1	30	10	0.24	0.23	0.01
2	5	Skull #1	235	10	0.1	30	10	0.24	0.21	0.03
3	5	Skull #1	235	10	0.1	30	10	0.24	0.23	0.01
4	5	Skull #1	235	10	0.1	30	10	0.26	0.22	0.04
5	5	Skull #1	235	10	0.1	30	10	0.23	0.21	0.02
6	5	Skull #1	235	10	0.1	30	10	0.27	0.21	0.07
7	5	Skull #1	235	10	0.1	30	10	0.26	0.23	0.03
8	5	Skull #1	235	10	0.1	30	10	0.30	0.26	0.04
9	5	Skull #1	235	10	0.1	30	10	0.24	0.18	0.06
10	5	Skull #1	235	10	0.1	30	10	0.19	0.19	0.00
11	5	Skull #1	235	10	0.1	30	10	0.20	0.16	0.05
12	5	Skull #1	235	10	0.1	30	10	0.25	0.19	0.06
13	5	Skull #1	235	10	0.1	30	10	0.24	0.16	0.08
14	5	Skull #1	235	10	0.1	30	10	0.23	0.18	0.05
15	5	Skull #1	235	10	0.1	30	10	0.25	0.20	0.05
16	5	Skull #1	235	10	0.1	30	10	0.21	0.16	0.05
17	5	Skull #1	235	10	0.1	30	10	0.23	0.18	0.04
18	5	Skull #1	235	10	0.1	30	10	0.23	0.23	0.00
19	5	Skull #1	235	10	0.1	30	10	0.21	0.19	0.01
20	5	Skull #1	235	10	0.1	30	10	0.23	0.22	0.01

21	5	Skull #1	235	10	0.1	30	10	0.22	0.18	0.03
22	5	Skull #1	235	10	0.1	30	10	0.21	0.17	0.04
23	5	Skull #1	235	10	0.1	30	10	0.23	0.16	0.07
24	5	Skull #1	235	10	0.1	30	10	0.28	0.21	0.07
25	5	Skull #1	235	10	0.1	30	10	0.23	0.21	0.02
26	5	Skull #1	235	10	0.1	30	10	0.22	0.17	0.05
27	5	Skull #1	235	10	0.1	30	10	0.21	0.19	0.03
28	5	Skull #1	235	10	0.1	30	10	0.21	0.18	0.04
29	5	Skull #1	235	10	0.1	30	10	0.26	0.20	0.05
30	5	Skull #1	235	10	0.1	30	10	0.22	0.20	0.02
31	5	Skull #1	235	10	0.1	30	10	0.25	0.17	0.08
32	5	Skull #1	235	10	0.1	30	10	0.25	0.21	0.05
33	5	Skull #1	235	10	0.1	30	10	0.23	0.19	0.04
34	5	Skull #1	235	10	0.1	30	10	0.25	0.22	0.03
35	5	Skull #1	235	10	0.1	30	10	0.24	0.14	0.10
36	5	Skull #1	235	10	0.1	30	10	0.25	0.17	0.08
37	5	Skull #1	235	10	0.1	30	10	0.21	0.19	0.02
38	5	Skull #1	235	10	0.1	30	10	0.24	0.20	0.04
39	5	Skull #1	235	10	0.1	30	10	0.25	0.21	0.04
40	5	Skull #1	235	10	0.1	30	10	0.25	0.21	0.04
1	6	Skull #1	235	10	1	30	10	0.26	0.21	0.06
2	6	Skull #1	235	10	1	30	10	0.24	0.19	0.06
3	6	Skull #1	235	10	1	30	10	0.23	0.18	0.05
4	6	Skull #1	235	10	1	30	10	0.25	0.20	0.05
5	6	Skull	235	10	1	30	10	0.20	0.16	0.04

		#1								
6	6	Skull #1	235	10	1	30	10	0.24	0.17	0.06
7	6	Skull #1	235	10	1	30	10	0.24	0.19	0.05
8	6	Skull #1	235	10	1	30	10	0.28	0.22	0.06
9	6	Skull #1	235	10	1	30	10	0.21	0.19	0.01
10	6	Skull #1	235	10	1	30	10	0.24	0.19	0.06
11	6	Skull #1	235	10	1	30	10	0.23	0.19	0.04
12	6	Skull #1	235	10	1	30	10	0.22	0.16	0.05
13	6	Skull #1	235	10	1	30	10	0.22	0.17	0.05
14	6	Skull #1	235	10	1	30	10	0.23	0.18	0.04
15	6	Skull #1	235	10	1	30	10	0.22	0.22	0.00
16	6	Skull #1	235	10	1	30	10	0.21	0.18	0.03
17	6	Skull #1	235	10	1	30	10	0.23	0.18	0.04
18	6	Skull #1	235	10	1	30	10	0.25	0.18	0.07
19	6	Skull #1	235	10	1	30	10	0.22	0.16	0.06
20	6	Skull #1	235	10	1	30	10	0.21	0.17	0.04
21	6	Skull #1	235	10	1	30	10	0.24	0.16	0.09
22	6	Skull #1	235	10	1	30	10	0.21	0.06	0.15
23	6	Skull #1	235	10	1	30	10	0.22	0.20	0.02
24	6	Skull #1	235	10	1	30	10	0.23	0.21	0.02
25	6	Skull #1	235	10	1	30	10	0.22	0.20	0.02
26	6	Skull #1	235	10	1	30	10	0.23	0.22	0.01
27	6	Skull #1	235	10	1	30	10	0.23	0.16	0.07
28	6	Skull #1	235	10	1	30	10	0.22	0.18	0.03
29	6	Skull #1	235	10	1	30	10	0.24	0.19	0.05

30	6	Skull #1	235	10	1	30	10	0.25	0.17	0.08
31	6	Skull #1	235	10	1	30	10	0.27	0.10	0.16
32	6	Skull #1	235	10	1	30	10	0.26	0.15	0.11
33	6	Skull #1	235	10	1	30	10	0.22	0.17	0.05
34	6	Skull #1	235	10	1	30	10	0.21	0.11	0.09
35	6	Skull #1	235	10	1	30	10	0.22	0.16	0.06
36	6	Skull #1	235	10	1	30	10	0.21	0.19	0.02
37	6	Skull #1	235	10	1	30	10	0.22	0.14	0.08
38	6	Skull #1	235	10	1	30	10	0.23	0.05	0.19
39	6	Skull #1	235	10	1	30	10	0.21	0.16	0.05
40	6	Skull #1	235	10	1	30	10	0.24	0.18	0.05
41	6	Skull #1	235	10	1	30	10	0.23	0.19	0.04
42	6	Skull #1	235	10	1	30	10	0.26	0.24	0.02
43	6	Skull #1	235	10	1	30	10	0.25	0.17	0.08
44	6	Skull #1	235	10	1	30	10	0.22	0.18	0.04
1	7	Skull #1	235	10	10	30	10	0.34	0.25	0.09
2	7	Skull #1	235	10	10	30	10	0.26	0.19	0.08
3	7	Skull #1	235	10	10	30	10	0.26	0.19	0.08
4	7	Skull #1	235	10	10	30	10	0.21	0.14	0.08
5	7	Skull #1	235	10	10	30	10	0.22	0.13	0.08
6	7	Skull #1	235	10	10	30	10	0.25	0.17	0.09
7	7	Skull #1	235	10	10	30	10	0.26	0.18	0.07
8	7	Skull #1	235	10	10	30	10	0.24	0.09	0.15
9	7	Skull #1	235	10	10	30	10	0.24	0.17	0.07
10	7	Skull	235	10	10	30	10	0.28	0.14	0.14

		#1								
11	7	Skull #1	235	10	10	30	10	0.23	0.16	0.07
12	7	Skull #1	235	10	10	30	10	0.22	0.16	0.06
13	7	Skull #1	235	10	10	30	10	0.21	0.14	0.08
14	7	Skull #1	235	10	10	30	10	0.23	0.22	0.00
15	7	Skull #1	235	10	10	30	10	0.24	0.20	0.04
16	7	Skull #1	235	10	10	30	10	0.24	0.19	0.05
17	7	Skull #1	235	10	10	30	10	0.20	0.10	0.11
18	7	Skull #1	235	10	10	30	10	0.27	0.18	0.09
19	7	Skull #1	235	10	10	30	10	0.21	0.19	0.02
20	7	Skull #1	235	10	10	30	10	0.22	0.21	0.01
21	7	Skull #1	235	10	10	30	10	0.23	0.19	0.05
22	7	Skull #1	235	10	10	30	10	0.22	0.15	0.07
23	7	Skull #1	235	10	10	30	10	0.25	0.26	-0.01
24	7	Skull #1	235	10	10	30	10	0.21	0.16	0.05
25	7	Skull #1	235	10	10	30	10	0.23	0.22	0.01
26	7	Skull #1	235	10	10	30	10	0.23	0.12	0.11
27	7	Skull #1	235	10	10	30	10	0.23	0.17	0.06
28	7	Skull #1	235	10	10	30	10	0.24	0.20	0.05
29	7	Skull #1	235	10	10	30	10	0.21	0.17	0.05
30	7	Skull #1	235	10	10	30	10	0.27	0.23	0.04
31	7	Skull #1	235	10	10	30	10	0.27	0.16	0.12
32	7	Skull #1	235	10	10	30	10	0.28	0.26	0.02
33	7	Skull #1	235	10	10	30	10	0.28	0.17	0.11
34	7	Skull #1	235	10	10	30	10	0.23	0.06	0.17

35	7	Skull #1	235	10	10	30	10	0.25	0.09	0.16
36	7	Skull #1	235	10	10	30	10	0.27	0.12	0.15
37	7	Skull #1	235	10	10	30	10	0.22	0.18	0.04
38	7	Skull #1	235	10	10	30	10	0.26	0.20	0.05
39	7	Skull #1	235	10	10	30	10	0.26	0.20	0.06
40	7	Skull #1	235	10	10	30	10	0.24	0.21	0.03
1	8	Skull #1	235	10	100	30	10	0.27	0.13	0.14
2	8	Skull #1	235	10	100	30	10	0.26	0.17	0.09
3	8	Skull #1	235	10	100	30	10	0.25	0.11	0.15
4	8	Skull #1	235	10	100	30	10	0.26	0.05	0.21
5	8	Skull #1	235	10	100	30	10	0.24	0.11	0.13
6	8	Skull #1	235	10	100	30	10	0.26	0.07	0.19
7	8	Skull #1	235	10	100	30	10	0.27	0.08	0.19
8	8	Skull #1	235	10	100	30	10	0.28	0.07	0.20
9	8	Skull #1	235	10	100	30	10	0.26	0.05	0.21
10	8	Skull #1	235	10	100	30	10	0.25	0.07	0.18
11	8	Skull #1	235	10	100	30	10	0.22	0.15	0.07
12	8	Skull #1	235	10	100	30	10	0.26	0.09	0.17
13	8	Skull #1	235	10	100	30	10	0.24	0.05	0.20
14	8	Skull #1	235	10	100	30	10	0.26	0.05	0.22
15	8	Skull #1	235	10	100	30	10	0.22	0.15	0.06
16	8	Skull #1	235	10	100	30	10	0.21	0.11	0.11
17	8	Skull #1	235	10	100	30	10	0.22	0.20	0.03
18	8	Skull #1	235	10	100	30	10	0.22	0.19	0.03
19	8	Skull	235	10	100	30	10	0.24	0.12	0.12

		#1								
20	8	Skull #1	235	10	100	30	10	0.24	0.04	0.20
21	8	Skull #1	235	10	100	30	10	0.25	0.22	0.03
22	8	Skull #1	235	10	100	30	10	0.24	0.19	0.06
23	8	Skull #1	235	10	100	30	10	0.21	0.21	0.01
24	8	Skull #1	235	10	100	30	10	0.23	0.15	0.07
25	8	Skull #1	235	10	100	30	10	0.22	0.19	0.02
26	8	Skull #1	235	10	100	30	10	0.23	0.18	0.05
27	8	Skull #1	235	10	100	30	10	0.26	0.17	0.09
28	8	Skull #1	235	10	100	30	10	0.23	0.17	0.06
29	8	Skull #1	235	10	100	30	10	0.21	0.19	0.02
30	8	Skull #1	235	10	100	30	10	0.27	0.12	0.15
31	8	Skull #1	235	10	100	30	10	0.22	0.16	0.06
32	8	Skull #1	235	10	100	30	10	0.23	0.12	0.12
33	8	Skull #1	235	10	100	30	10	0.24	0.09	0.15
34	8	Skull #1	235	10	100	30	10	0.24	0.17	0.07
35	8	Skull #1	235	10	100	30	10	0.21	0.19	0.02
36	8	Skull #1	235	10	100	30	10	0.22	0.17	0.05
37	8	Skull #1	235	10	100	30	10	0.26	0.12	0.14
38	8	Skull #1	235	10	100	30	10	0.24	0.18	0.06
39	8	Skull #1	235	10	100	30	10	0.25	0.18	0.06
40	8	Skull #1	235	10	100	30	10	0.26	0.17	0.09

Table B-3 Data acquired for 0.1ms, 1ms, 10ms, & 100ms PW at 20% DC, Groups 9-12

Exp #	Grp #	Skull ID	AP (W)	DC (%)	PW (ms)	ID (sec)	Flow (ml/min)	PreFUS Wt (g)	PostFUS Wt (g)	Wt Loss (g)
1	9	Skull #1	235	20	0.1	30	10	0.24	0.21	0.03
2	9	Skull #1	235	20	0.1	30	10	0.23	0.22	0.02
3	9	Skull #1	235	20	0.1	30	10	0.24	0.22	0.02
4	9	Skull #1	235	20	0.1	30	10	0.23	0.16	0.07
5	9	Skull #1	235	20	0.1	30	10	0.23	0.16	0.06
6	9	Skull #1	235	20	0.1	30	10	0.27	0.16	0.12
7	9	Skull #1	235	20	0.1	30	10	0.23	0.11	0.11
8	9	Skull #1	235	20	0.1	30	10	0.26	0.09	0.18
9	9	Skull #1	235	20	0.1	30	10	0.26	0.08	0.19
10	9	Skull #1	235	20	0.1	30	10	0.25	0.17	0.08
11	9	Skull #1	235	20	0.1	30	10	0.28	0.18	0.10
12	9	Skull #1	235	20	0.1	30	10	0.23	0.17	0.05
13	9	Skull #1	235	20	0.1	30	10	0.25	0.16	0.09
14	9	Skull #1	235	20	0.1	30	10	0.21	0.20	0.02
15	9	Skull #1	235	20	0.1	30	10	0.22	0.19	0.03
16	9	Skull #1	235	20	0.1	30	10	0.24	0.23	0.01
17	9	Skull #1	235	20	0.1	30	10	0.22	0.13	0.09
18	9	Skull #1	235	20	0.1	30	10	0.25	0.17	0.08
19	9	Skull #1	235	20	0.1	30	10	0.21	0.17	0.04
20	9	Skull #1	235	20	0.1	30	10	0.23	0.16	0.07
21	9	Skull #1	235	20	0.1	30	10	0.21	0.21	0.00
22	9	Skull #1	235	20	0.1	30	10	0.27	0.25	0.02

23	9	Skull #1	235	20	0.1	30	10	0.22	0.13	0.09
24	9	Skull #1	235	20	0.1	30	10	0.23	0.11	0.13
25	9	Skull #1	235	20	0.1	30	10	0.22	0.21	0.01
26	9	Skull #1	235	20	0.1	30	10	0.23	0.23	0.01
27	9	Skull #1	235	20	0.1	30	10	0.25	0.22	0.04
28	9	Skull #1	235	20	0.1	30	10	0.21	0.16	0.05
29	9	Skull #1	235	20	0.1	30	10	0.22	0.16	0.05
30	9	Skull #1	235	20	0.1	30	10	0.21	0.19	0.03
31	9	Skull #1	235	20	0.1	30	10	0.21	0.16	0.06
32	9	Skull #1	235	20	0.1	30	10	0.23	0.08	0.15
33	9	Skull #1	235	20	0.1	30	10	0.24	0.13	0.12
34	9	Skull #1	235	20	0.1	30	10	0.27	0.12	0.15
35	9	Skull #1	235	20	0.1	30	10	0.26	0.15	0.11
36	9	Skull #1	235	20	0.1	30	10	0.25	0.10	0.15
37	9	Skull #1	235	20	0.1	30	10	0.25	0.09	0.16
38	9	Skull #1	235	20	0.1	30	10	0.27	0.14	0.13
39	9	Skull #1	235	20	0.1	30	10	0.22	0.19	0.03
40	9	Skull #1	235	20	0.1	30	10	0.23	0.20	0.04
41	9	Skull #1	235	20	0.1	30	10	0.22	0.17	0.05
1	10	Skull #1	235	20	1	30	10	0.26	0.18	0.08
2	10	Skull #1	235	20	1	30	10	0.25	0.16	0.09
3	10	Skull #1	235	20	1	30	10	0.19	0.18	0.01
4	10	Skull #1	235	20	1	30	10	0.20	0.13	0.08
5	10	Skull #1	235	20	1	30	10	0.22	0.15	0.07
6	10	Skull	235	20	1	30	10	0.21	0.13	0.07

		#1								
7	10	Skull #1	235	20	1	30	10	0.26	0.19	0.07
8	10	Skull #1	235	20	1	30	10	0.23	0.14	0.09
9	10	Skull #1	235	20	1	30	10	0.22	0.17	0.05
10	10	Skull #1	235	20	1	30	10	0.24	0.16	0.07
11	10	Skull #1	235	20	1	30	10	0.25	0.11	0.14
12	10	Skull #1	235	20	1	30	10	0.24	0.14	0.10
13	10	Skull #1	235	20	1	30	10	0.23	0.17	0.06
14	10	Skull #1	235	20	1	30	10	0.25	0.18	0.07
15	10	Skull #1	235	20	1	30	10	0.24	0.17	0.07
16	10	Skull #1	235	20	1	30	10	0.21	0.11	0.10
17	10	Skull #1	235	20	1	30	10	0.22	0.18	0.04
18	10	Skull #1	235	20	1	30	10	0.20	0.15	0.05
19	10	Skull #1	235	20	1	30	10	0.20	0.14	0.07
20	10	Skull #1	235	20	1	30	10	0.21	0.19	0.01
21	10	Skull #1	235	20	1	30	10	0.21	0.20	0.01
22	10	Skull #1	235	20	1	30	10	0.24	0.06	0.18
23	10	Skull #1	235	20	1	30	10	0.22	0.14	0.08
24	10	Skull #1	235	20	1	30	10	0.23	0.24	0.00
25	10	Skull #1	235	20	1	30	10	0.22	0.20	0.02
26	10	Skull #1	235	20	1	30	10	0.25	0.10	0.15
27	10	Skull #1	235	20	1	30	10	0.21	0.16	0.04
28	10	Skull #1	235	20	1	30	10	0.21	0.14	0.06
29	10	Skull #1	235	20	1	30	10	0.21	0.15	0.07
30	10	Skull #1	235	20	1	30	10	0.21	0.18	0.03

31	10	Skull #1	235	20	1	30	10	0.27	0.08	0.19
32	10	Skull #1	235	20	1	30	10	0.21	0.12	0.09
33	10	Skull #1	235	20	1	30	10	0.27	0.06	0.21
34	10	Skull #1	235	20	1	30	10	0.23	0.14	0.09
35	10	Skull #1	235	20	1	30	10	0.24	0.16	0.08
36	10	Skull #1	235	20	1	30	10	0.25	0.06	0.19
37	10	Skull #1	235	20	1	30	10	0.23	0.11	0.12
38	10	Skull #1	235	20	1	30	10	0.25	0.04	0.21
39	10	Skull #1	235	20	1	30	10	0.23	0.06	0.17
40	10	Skull #1	235	20	1	30	10	0.24	0.08	0.16
1	11	Skull #1	235	20	10	30	10	0.24	0.13	0.11
2	11	Skull #1	235	20	10	30	10	0.24	0.15	0.08
3	11	Skull #1	235	20	10	30	10	0.25	0.14	0.11
4	11	Skull #1	235	20	10	30	10	0.21	0.08	0.12
5	11	Skull #1	235	20	10	30	10	0.28	0.16	0.12
6	11	Skull #1	235	20	10	30	10	0.29	0.06	0.23
7	11	Skull #1	235	20	10	30	10	0.28	0.23	0.05
8	11	Skull #1	235	20	10	30	10	0.25	0.17	0.08
9	11	Skull #1	235	20	10	30	10	0.28	0.19	0.09
10	11	Skull #1	235	20	10	30	10	0.26	0.26	0.00
11	11	Skull #1	235	20	10	30	10	0.24	0.17	0.07
12	11	Skull #1	235	20	10	30	10	0.26	0.04	0.21
13	11	Skull #1	235	20	10	30	10	0.22	0.19	0.03
14	11	Skull #1	235	20	10	30	10	0.23	0.16	0.07
15	11	Skull	235	20	10	30	10	0.21	0.17	0.04

		#1								
16	11	Skull #1	235	20	10	30	10	0.21	0.17	0.04
17	11	Skull #1	235	20	10	30	10	0.22	0.17	0.05
18	11	Skull #1	235	20	10	30	10	0.22	0.16	0.06
19	11	Skull #1	235	20	10	30	10	0.21	0.14	0.07
20	11	Skull #1	235	20	10	30	10	0.21	0.10	0.11
21	11	Skull #1	235	20	10	30	10	0.21	0.17	0.04
22	11	Skull #1	235	20	10	30	10	0.24	0.19	0.05
23	11	Skull #1	235	20	10	30	10	0.22	0.13	0.09
24	11	Skull #1	235	20	10	30	10	0.22	0.21	0.01
25	11	Skull #1	235	20	10	30	10	0.20	0.18	0.03
26	11	Skull #1	235	20	10	30	10	0.25	0.15	0.10
27	11	Skull #1	235	20	10	30	10	0.23	0.14	0.10
28	11	Skull #1	235	20	10	30	10	0.21	0.09	0.12
29	11	Skull #1	235	20	10	30	10	0.22	0.13	0.09
30	11	Skull #1	235	20	10	30	10	0.21	0.12	0.09
31	11	Skull #1	235	20	10	30	10	0.22	0.15	0.07
32	11	Skull #1	235	20	10	30	10	0.24	0.14	0.10
33	11	Skull #1	235	20	10	30	10	0.27	0.05	0.22
34	11	Skull #1	235	20	10	30	10	0.26	0.05	0.21
35	11	Skull #1	235	20	10	30	10	0.22	0.08	0.13
36	11	Skull #1	235	20	10	30	10	0.27	0.07	0.19
37	11	Skull #1	235	20	10	30	10	0.24	0.10	0.15
38	11	Skull #1	235	20	10	30	10	0.21	0.10	0.11
39	11	Skull #1	235	20	10	30	10	0.26	0.10	0.16

40	11	Skull #1	235	20	10	30	10	0.22	0.17	0.06
41	11	Skull #1	235	20	10	30	10	0.23	0.19	0.04
1	12	Skull #1	235	20	100	30	10	0.24	0.04	0.20
2	12	Skull #1	235	20	100	30	10	0.27	0.05	0.22
3	12	Skull #1	235	20	100	30	10	0.24	0.08	0.16
4	12	Skull #1	235	20	100	30	10	0.22	0.14	0.08
5	12	Skull #1	235	20	100	30	10	0.25	0.09	0.16
6	12	Skull #1	235	20	100	30	10	0.23	0.07	0.16
7	12	Skull #1	235	20	100	30	10	0.25	0.12	0.14
8	12	Skull #1	235	20	100	30	10	0.28	0.04	0.23
9	12	Skull #1	235	20	100	30	10	0.24	0.08	0.16
10	12	Skull #1	235	20	100	30	10	0.23	0.09	0.15
11	12	Skull #1	235	20	100	30	10	0.26	0.04	0.21
12	12	Skull #1	235	20	100	30	10	0.22	0.11	0.12
13	12	Skull #1	235	20	100	30	10	0.21	0.13	0.08
14	12	Skull #1	235	20	100	30	10	0.22	0.05	0.17
15	12	Skull #1	235	20	100	30	10	0.21	0.09	0.12
16	12	Skull #1	235	20	100	30	10	0.20	0.09	0.12
17	12	Skull #1	235	20	100	30	10	0.20	0.07	0.13
18	12	Skull #1	235	20	100	30	10	0.25	0.07	0.18
19	12	Skull #1	235	20	100	30	10	0.22	0.05	0.17
20	12	Skull #1	235	20	100	30	10	0.22	0.06	0.17
21	12	Skull #1	235	20	100	30	10	0.26	0.22	0.04
22	12	Skull #1	235	20	100	30	10	0.23	0.17	0.06
23	12	Skull	235	20	100	30	10	0.23	0.19	0.04

		#1								
24	12	Skull #1	235	20	100	30	10	0.23	0.15	0.08
25	12	Skull #1	235	20	100	30	10	0.21	0.09	0.12
26	12	Skull #1	235	20	100	30	10	0.23	0.08	0.15
27	12	Skull #1	235	20	100	30	10	0.21	0.08	0.13
28	12	Skull #1	235	20	100	30	10	0.21	0.19	0.02
29	12	Skull #1	235	20	100	30	10	0.21	0.07	0.14
30	12	Skull #1	235	20	100	30	10	0.22	0.14	0.08
31	12	Skull #1	235	20	100	30	10	0.24	0.08	0.16
32	12	Skull #1	235	20	100	30	10	0.25	0.15	0.10
33	12	Skull #1	235	20	100	30	10	0.28	0.09	0.19
34	12	Skull #1	235	20	100	30	10	0.23	0.08	0.15
35	12	Skull #1	235	20	100	30	10	0.25	0.09	0.16
36	12	Skull #1	235	20	100	30	10	0.26	0.09	0.17
37	12	Skull #1	235	20	100	30	10	0.22	0.04	0.18
38	12	Skull #1	235	20	100	30	10	0.25	0.12	0.13
39	12	Skull #1	235	20	100	30	10	0.25	0.07	0.18
40	12	Skull #1	235	20	100	30	10	0.26	0.08	0.18
41	12	Skull #1	235	20	100	30	10	0.27	0.07	0.20
42	12	Skull #1	235	20	100	30	10	0.23	0.13	0.11
43	12	Skull #1	235	20	100	30	10	0.23	0.06	0.17

Table B-4 Data acquired for 0.1ms, 1ms, 10ms, & 100ms PW at 50% DC, Groups 13-16

Exp #	Grp #	Skull ID	AP (W)	DC (%)	PW (ms)	ID (sec)	Flow (ml/min)	PreFUS Wt (g)	PostFUS Wt (g)	Wt Loss (g)
1	13	Skull #1	235	50	0.1	30	10	0.24	0.17	0.07
2	13	Skull #1	235	50	0.1	30	10	0.25	0.09	0.17
3	13	Skull #1	235	50	0.1	30	10	0.26	0.07	0.19
4	13	Skull #1	235	50	0.1	30	10	0.25	0.08	0.17
5	13	Skull #1	235	50	0.1	30	10	0.25	0.09	0.16
6	13	Skull #1	235	50	0.1	30	10	0.20	0.07	0.13
7	13	Skull #1	235	50	0.1	30	10	0.26	0.16	0.11
8	13	Skull #1	235	50	0.1	30	10	0.28	0.08	0.20
9	13	Skull #1	235	50	0.1	30	10	0.28	0.04	0.24
10	13	Skull #1	235	50	0.1	30	10	0.28	0.10	0.17
11	13	Skull #1	235	50	0.1	30	10	0.35	0.13	0.22
12	13	Skull #1	235	50	0.1	30	10	0.22	0.18	0.04
13	13	Skull #1	235	50	0.1	30	10	0.24	0.10	0.14
14	13	Skull #1	235	50	0.1	30	10	0.24	0.11	0.13
15	13	Skull #1	235	50	0.1	30	10	0.23	0.15	0.07
16	13	Skull #1	235	50	0.1	30	10	0.21	0.08	0.14
17	13	Skull #1	235	50	0.1	30	10	0.21	0.05	0.16
18	13	Skull #1	235	50	0.1	30	10	0.21	0.11	0.10
19	13	Skull #1	235	50	0.1	30	10	0.23	0.17	0.06
20	13	Skull #1	235	50	0.1	30	10	0.23	0.21	0.02
21	13	Skull #1	235	50	0.1	30	10	0.22	0.17	0.05
22	13	Skull #1	235	50	0.1	30	10	0.24	0.10	0.14

23	13	Skull #1	235	50	0.1	30	10	0.22	0.07	0.15
24	13	Skull #1	235	50	0.1	30	10	0.23	0.24	0.00
25	13	Skull #1	235	50	0.1	30	10	0.23	0.23	0.00
26	13	Skull #1	235	50	0.1	30	10	0.24	0.23	0.01
27	13	Skull #1	235	50	0.1	30	10	0.25	0.22	0.03
28	13	Skull #1	235	50	0.1	30	10	0.24	0.16	0.08
29	13	Skull #1	235	50	0.1	30	10	0.22	0.10	0.11
30	13	Skull #1	235	50	0.1	30	10	0.21	0.06	0.15
31	13	Skull #1	235	50	0.1	30	10	0.23	0.13	0.09
32	13	Skull #1	235	50	0.1	30	10	0.22	0.15	0.07
33	13	Skull #1	235	50	0.1	30	10	0.21	0.05	0.16
34	13	Skull #1	235	50	0.1	30	10	0.21	0.15	0.06
35	13	Skull #1	235	50	0.1	30	10	0.26	0.05	0.21
36	13	Skull #1	235	50	0.1	30	10	0.22	0.11	0.11
37	13	Skull #1	235	50	0.1	30	10	0.26	0.11	0.15
38	13	Skull #1	235	50	0.1	30	10	0.22	0.07	0.15
39	13	Skull #1	235	50	0.1	30	10	0.24	0.05	0.19
40	13	Skull #1	235	50	0.1	30	10	0.27	0.20	0.07
41	13	Skull #1	235	50	0.1	30	10	0.23	0.12	0.11
42	13	Skull #1	235	50	0.1	30	10	0.25	0.13	0.11
43	13	Skull #1	235	50	0.1	30	10	0.24	0.08	0.16
1	14	Skull #1	235	50	1	30	10	0.26	0.13	0.13
2	14	Skull #1	235	50	1	30	10	0.27	0.19	0.07
3	14	Skull #1	235	50	1	30	10	0.24	0.12	0.12
4	14	Skull	235	50	1	30	10	0.26	0.08	0.18

		#1								
5	14	Skull #1	235	50	1	30	10	0.24	0.07	0.17
6	14	Skull #1	235	50	1	30	10	0.21	0.16	0.05
7	14	Skull #1	235	50	1	30	10	0.32	0.11	0.21
8	14	Skull #1	235	50	1	30	10	0.25	0.09	0.16
9	14	Skull #1	235	50	1	30	10	0.28	0.07	0.21
10	14	Skull #1	235	50	1	30	10	0.25	0.18	0.08
11	14	Skull #1	235	50	1	30	10	0.21	0.05	0.16
12	14	Skull #1	235	50	1	30	10	0.28	0.06	0.22
13	14	Skull #1	235	50	1	30	10	0.27	0.06	0.21
14	14	Skull #1	235	50	1	30	10	0.21	0.07	0.14
15	14	Skull #1	235	50	1	30	10	0.24	0.09	0.15
16	14	Skull #1	235	50	1	30	10	0.25	0.11	0.14
17	14	Skull #1	235	50	1	30	10	0.22	0.18	0.04
18	14	Skull #1	235	50	1	30	10	0.22	0.13	0.09
19	14	Skull #1	235	50	1	30	10	0.21	0.15	0.06
20	14	Skull #1	235	50	1	30	10	0.26	0.07	0.19
21	14	Skull #1	235	50	1	30	10	0.26	0.18	0.09
22	14	Skull #1	235	50	1	30	10	0.23	0.16	0.08
23	14	Skull #1	235	50	1	30	10	0.25	0.08	0.17
24	14	Skull #1	235	50	1	30	10	0.23	0.22	0.01
25	14	Skull #1	235	50	1	30	10	0.22	0.10	0.12
26	14	Skull #1	235	50	1	30	10	0.24	0.15	0.09
27	14	Skull #1	235	50	1	30	10	0.21	0.10	0.11
28	14	Skull #1	235	50	1	30	10	0.28	0.05	0.23

29	14	Skull #1	235	50	1	30	10	0.24	0.07	0.17
30	14	Skull #1	235	50	1	30	10	0.25	0.06	0.19
31	14	Skull #1	235	50	1	30	10	0.22	0.14	0.08
32	14	Skull #1	235	50	1	30	10	0.26	0.11	0.15
33	14	Skull #1	235	50	1	30	10	0.24	0.21	0.04
34	14	Skull #1	235	50	1	30	10	0.25	0.05	0.20
35	14	Skull #1	235	50	1	30	10	0.27	0.11	0.16
36	14	Skull #1	235	50	1	30	10	0.22	0.14	0.08
37	14	Skull #1	235	50	1	30	10	0.24	0.07	0.16
38	14	Skull #1	235	50	1	30	10	0.25	0.05	0.19
39	14	Skull #1	235	50	1	30	10	0.22	0.13	0.09
40	14	Skull #1	235	50	1	30	10	0.22	0.10	0.12
1	15	Skull #1	235	50	10	30	10	0.26	0.08	0.19
2	15	Skull #1	235	50	10	30	10	0.24	0.07	0.17
3	15	Skull #1	235	50	10	30	10	0.25	0.13	0.12
4	15	Skull #1	235	50	10	30	10	0.25	0.13	0.12
5	15	Skull #1	235	50	10	30	10	0.24	0.05	0.18
6	15	Skull #1	235	50	10	30	10	0.20	0.06	0.13
7	15	Skull #1	235	50	10	30	10	0.27	0.08	0.19
8	15	Skull #1	235	50	10	30	10	0.29	0.15	0.14
9	15	Skull #1	235	50	10	30	10	0.25	0.05	0.20
10	15	Skull #1	235	50	10	30	10	0.23	0.13	0.09
11	15	Skull #1	235	50	10	30	10	0.25	0.10	0.15
12	15	Skull #1	235	50	10	30	10	0.21	0.10	0.11
13	15	Skull	235	50	10	30	10	0.21	0.07	0.14

		#1								
14	15	Skull #1	235	50	10	30	10	0.25	0.06	0.18
15	15	Skull #1	235	50	10	30	10	0.23	0.05	0.18
16	15	Skull #1	235	50	10	30	10	0.22	0.08	0.14
17	15	Skull #1	235	50	10	30	10	0.22	0.18	0.04
18	15	Skull #1	235	50	10	30	10	0.22	0.21	0.02
19	15	Skull #1	235	50	10	30	10	0.22	0.17	0.05
20	15	Skull #1	235	50	10	30	10	0.21	0.10	0.12
21	15	Skull #1	235	50	10	30	10	0.23	0.19	0.04
22	15	Skull #1	235	50	10	30	10	0.23	0.23	0.00
23	15	Skull #1	235	50	10	30	10	0.28	0.17	0.11
24	15	Skull #1	235	50	10	30	10	0.25	0.22	0.03
25	15	Skull #1	235	50	10	30	10	0.24	0.18	0.06
26	15	Skull #1	235	50	10	30	10	0.23	0.13	0.10
27	15	Skull #1	235	50	10	30	10	0.26	0.15	0.11
28	15	Skull #1	235	50	10	30	10	0.25	0.18	0.07
29	15	Skull #1	235	50	10	30	10	0.21	0.06	0.15
30	15	Skull #1	235	50	10	30	10	0.24	0.14	0.10
31	15	Skull #1	235	50	10	30	10	0.21	0.10	0.10
32	15	Skull #1	235	50	10	30	10	0.24	0.13	0.12
33	15	Skull #1	235	50	10	30	10	0.27	0.14	0.13
34	15	Skull #1	235	50	10	30	10	0.25	0.12	0.13
35	15	Skull #1	235	50	10	30	10	0.27	0.14	0.13
36	15	Skull #1	235	50	10	30	10	0.23	0.13	0.10
37	15	Skull #1	235	50	10	30	10	0.25	0.08	0.17

38	15	Skull #1	235	50	10	30	10	0.25	0.04	0.21
39	15	Skull #1	235	50	10	30	10	0.24	0.09	0.15
40	15	Skull #1	235	50	10	30	10	0.25	0.14	0.11
41	15	Skull #1	235	50	10	30	10	0.27	0.04	0.23
42	15	Skull #1	235	50	10	30	10	0.26	0.05	0.21
1	16	Skull #1	235	50	100	30	10	0.24	0.06	0.18
2	16	Skull #1	235	50	100	30	10	0.23	0.07	0.16
3	16	Skull #1	235	50	100	30	10	0.24	0.05	0.19
4	16	Skull #1	235	50	100	30	10	0.28	0.12	0.17
5	16	Skull #1	235	50	100	30	10	0.27	0.04	0.23
6	16	Skull #1	235	50	100	30	10	0.30	0.06	0.24
7	16	Skull #1	235	50	100	30	10	0.33	0.09	0.24
8	16	Skull #1	235	50	100	30	10	0.28	0.08	0.20
9	16	Skull #1	235	50	100	30	10	0.28	0.05	0.23
10	16	Skull #1	235	50	100	30	10	0.27	0.06	0.21
11	16	Skull #1	235	50	100	30	10	0.25	0.09	0.16
12	16	Skull #1	235	50	100	30	10	0.21	0.06	0.16
13	16	Skull #1	235	50	100	30	10	0.27	0.06	0.22
14	16	Skull #1	235	50	100	30	10	0.24	0.05	0.18
15	16	Skull #1	235	50	100	30	10	0.22	0.09	0.14
16	16	Skull #1	235	50	100	30	10	0.21	0.10	0.11
17	16	Skull #1	235	50	100	30	10	0.22	0.06	0.16
18	16	Skull #1	235	50	100	30	10	0.23	0.11	0.11
19	16	Skull #1	235	50	100	30	10	0.22	0.12	0.11
20	16	Skull	235	50	100	30	10	0.23	0.12	0.11

		#1								
21	16	Skull #1	235	50	100	30	10	0.24	0.06	0.17
22	16	Skull #1	235	50	100	30	10	0.23	0.08	0.14
23	16	Skull #1	235	50	100	30	10	0.22	0.10	0.12
24	16	Skull #1	235	50	100	30	10	0.30	0.21	0.09
25	16	Skull #1	235	50	100	30	10	0.21	0.16	0.05
26	16	Skull #1	235	50	100	30	10	0.24	0.11	0.12
27	16	Skull #1	235	50	100	30	10	0.25	0.13	0.12
28	16	Skull #1	235	50	100	30	10	0.26	0.14	0.12
29	16	Skull #1	235	50	100	30	10	0.28	0.05	0.23
30	16	Skull #1	235	50	100	30	10	0.24	0.16	0.08
31	16	Skull #1	235	50	100	30	10	0.21	0.10	0.11
32	16	Skull #1	235	50	100	30	10	0.21	0.11	0.11
33	16	Skull #1	235	50	100	30	10	0.22	0.13	0.09
34	16	Skull #1	235	50	100	30	10	0.23	0.10	0.12
35	16	Skull #1	235	50	100	30	10	0.26	0.08	0.17
36	16	Skull #1	235	50	100	30	10	0.28	0.10	0.17
37	16	Skull #1	235	50	100	30	10	0.21	0.07	0.13
38	16	Skull #1	235	50	100	30	10	0.24	0.13	0.11
39	16	Skull #1	235	50	100	30	10	0.25	0.08	0.17
40	16	Skull #1	235	50	100	30	10	0.22	0.07	0.15
41	16	Skull #1	235	50	100	30	10	0.21	0.07	0.14
42	16	Skull #1	235	50	100	30	10	0.27	0.16	0.11
43	16	Skull #1	235	50	100	30	10	0.21	0.16	0.05
44	16	Skull #1	235	50	100	30	10	0.23	0.19	0.05

APPENDIX C

OBJECTIVE 3: ACOUSTIC FIELD CHARACTERIZATION

This appendix includes a further explanation of some of the methodological processes and assumptions discussed in Chapter 6.

SPLINE INTERPOLATION AND ACOUSTIC DATA ANALYSIS

Both the 2D and 3D scans were spline interpolated to obtain more complete image information and to enhance the visualization of the acoustic field. These CT scans were spline-interpolated to increase the resolution from 1mm to 0.25mm. When the resolution was then compared to that of the exact function via the actual, high resolution scans, this approximation did not present diminished image quality. An example of this comparison is demonstrated in Figures, C-1, C-2, and C-3.

Figure C-1 shows measurements with 1mm spacing, Figure C-2 shows measurements with 1mm spacing interpolated to 0.25mm spacing, and the Figure C-3 shows measurements with actual 0.25mm measurement spacing. The images are titled accordingly. These successive images illustrate that interpolation is sufficient to achieve better resolution, making the finer measurement spacing redundant and actually producing less noisy data. Thus, an interpolated spacing based on the 1 mm images is an appropriate resolution to select for analysis of the acoustic fields.

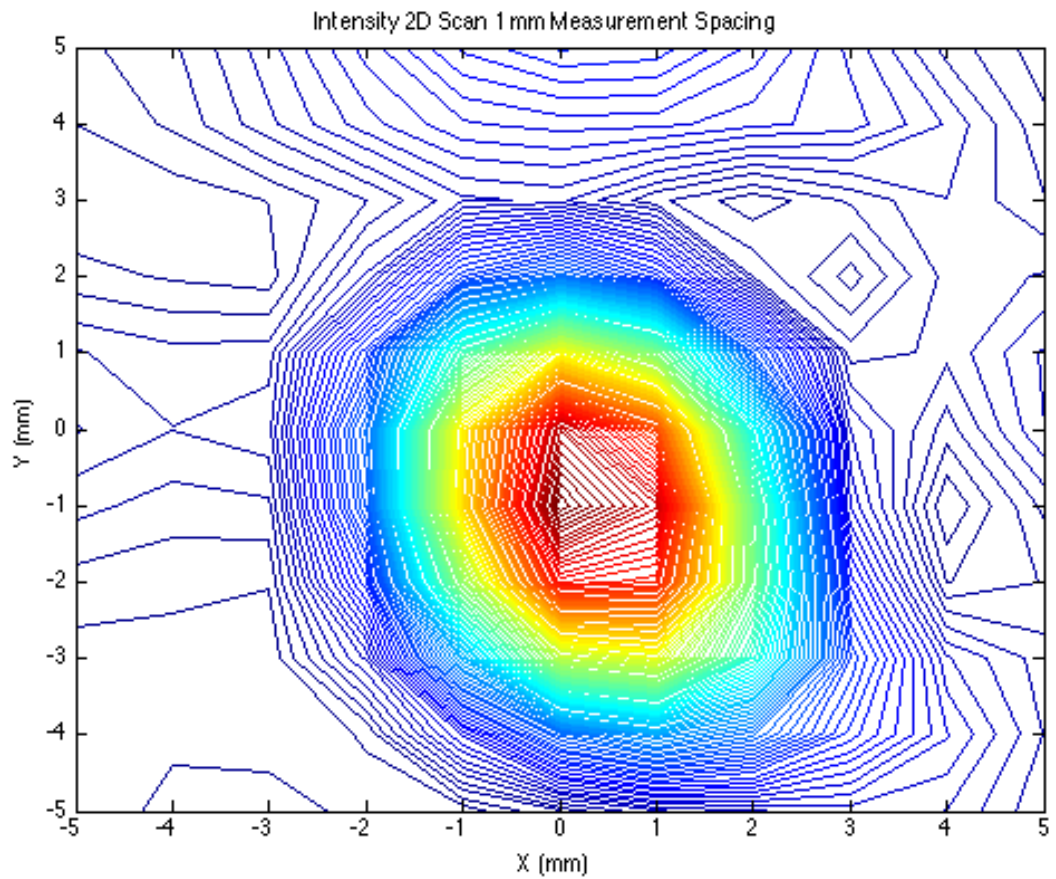


Figure C-1 Acoustic intensity measurements within the focal region made with 1mm spacing.

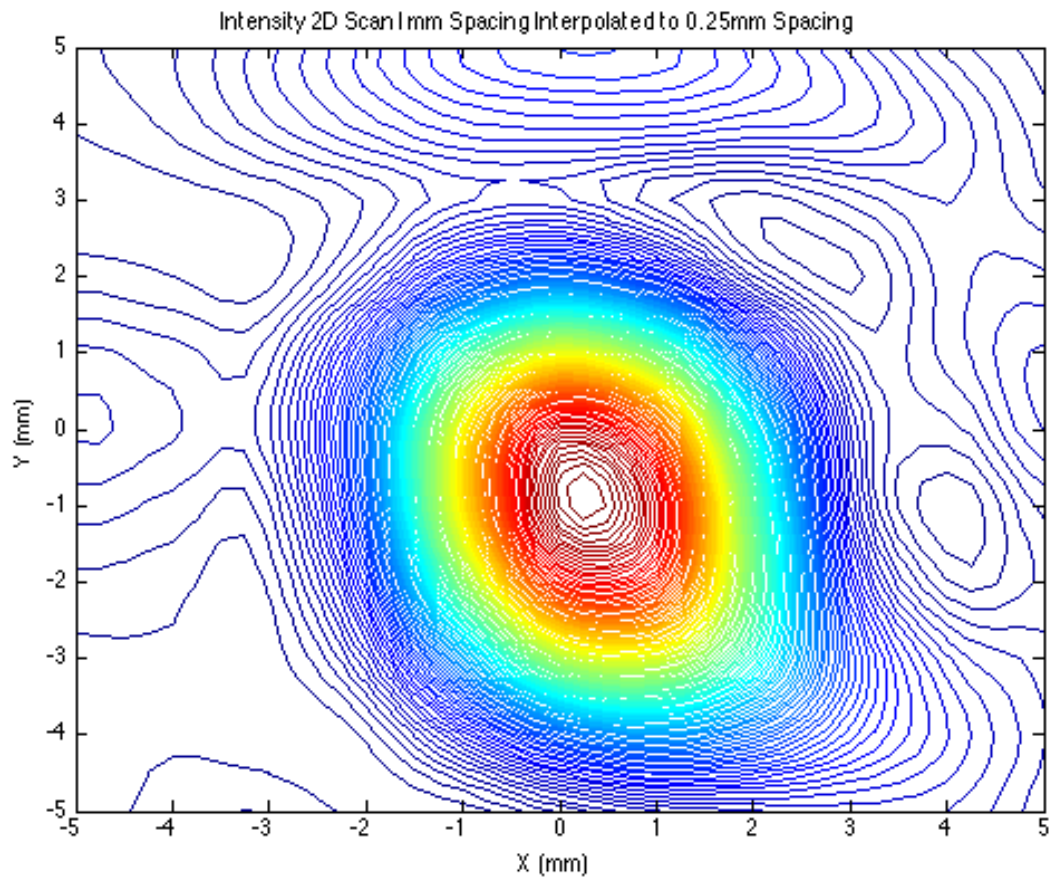


Figure C-2 Acoustic intensity measurements within the focal region made with 1mm spacing interpolated to 0.25mm spacing.

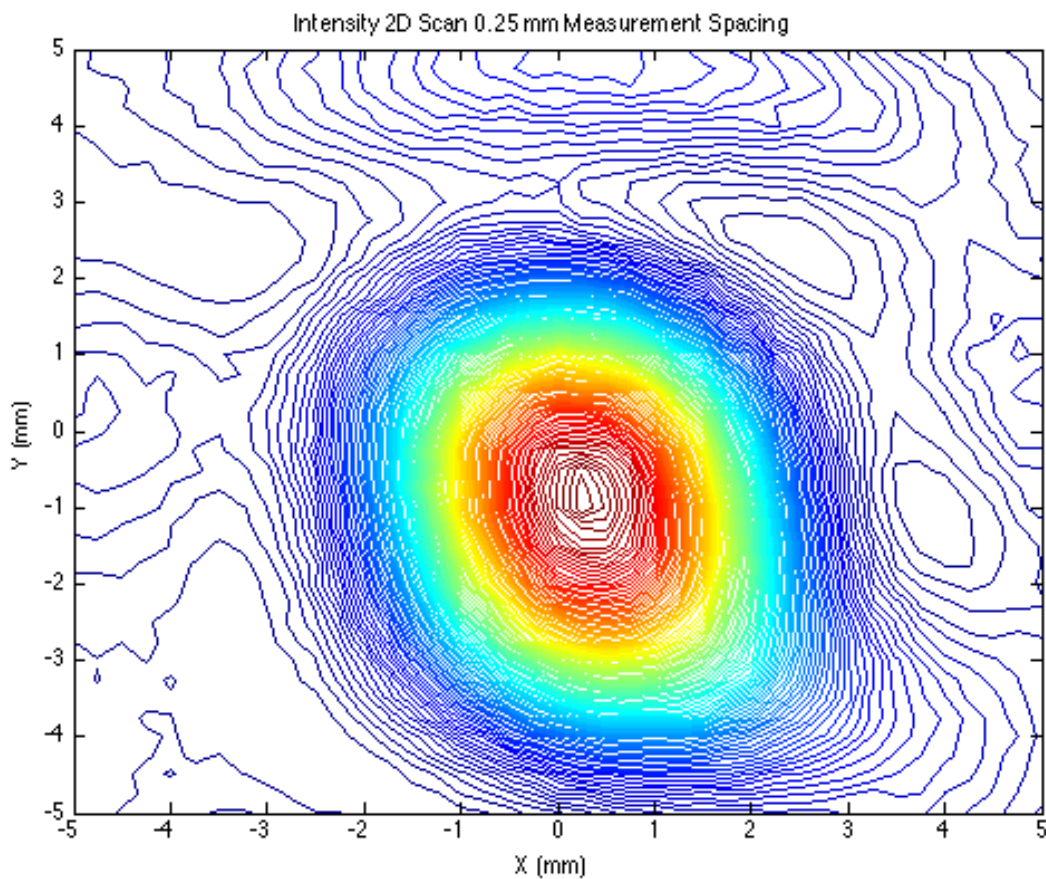


Figure C-3 Acoustic intensity measurements within the focal region made with the exact function, actual 0.25mm measurement spacing.

SKULL THICKNESS AND DENSITY ASSESSMENT

A MATLAB routine that was developed by an expert programmer to create measurement lines, with the length of 150 mm divided into 300 increments of 0.5mm. When the coordinates of the measurement line increments were identified, the CT values in HU in the data volume were spline-interpolated to create radiological density profiles. Figure C-4 and C-5 illustrate a typical measurement profile. The measurement line for the 100th of 973 active FUS transducer elements through skull A was used for the density profiles. This measurement vector for the 100th element traversed a portion of the skull in

the MATLAB data space. The MATLAB function 'interp3' was used by our expert programmer to interpolate the skull density values onto the measurement vector, and this is what is represented in the plot (Figure C-4). In Figure C-5, tilted Density Profile 100 Expanded, the figure focuses in on the Density Profile 100 (Figure C-4) and includes the point positions as well.

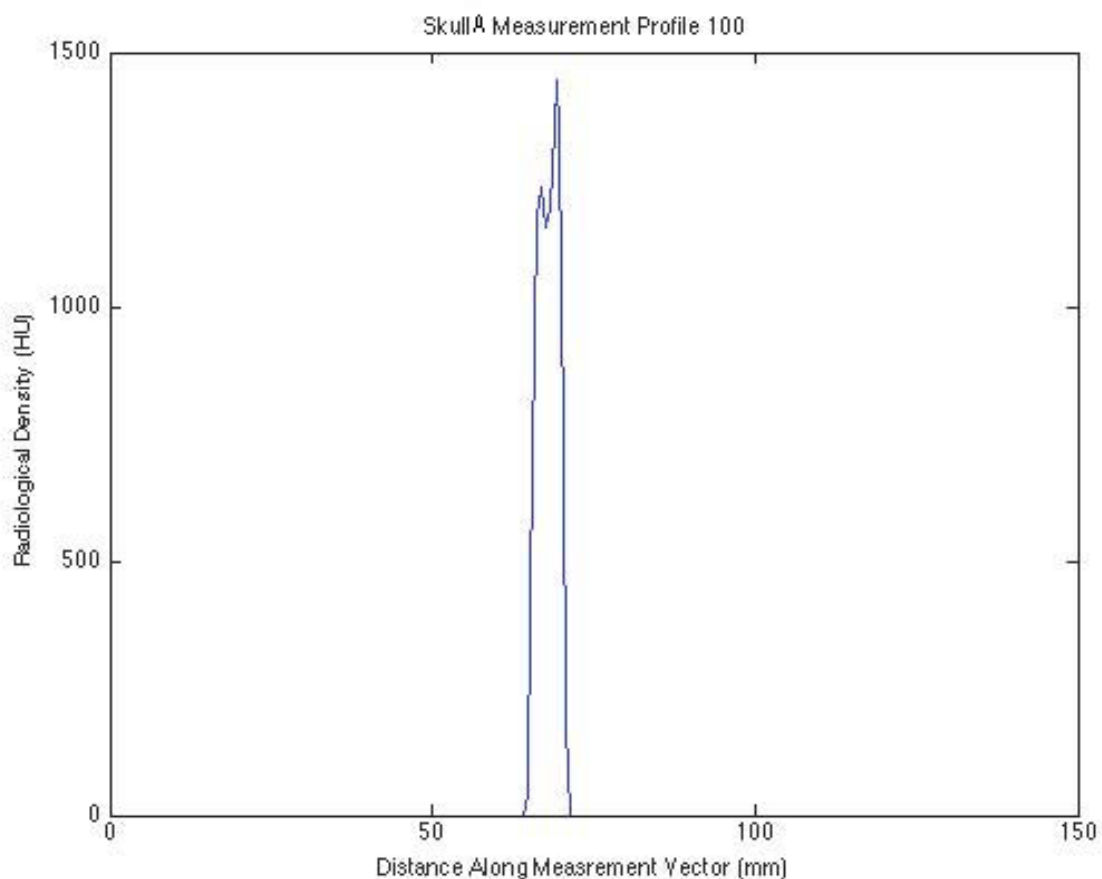


Figure C-4. Skull density values in HU were interpolated onto the measurement vector to create radiological density profiles, as is represented here for the measurement line for the 100th FUS transducer element.

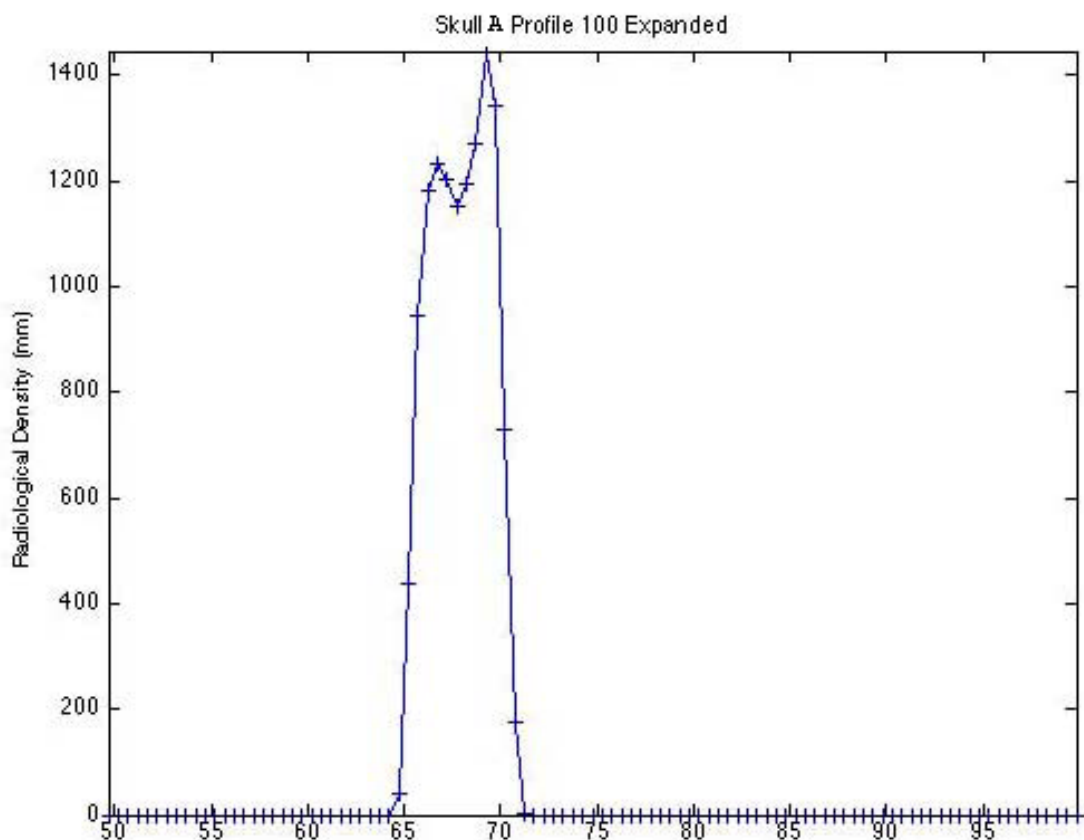


Figure C-5 This is a zoomed-in representation of Figure C-5 where the point position for the density values have been included for the measurement line of the 100th FUS transducer element.

APPENDIX D

OBJECTIVE 4: SONOTHROMBOLYSIS & FRAGMENTATION

This appendix includes additional data in support of Chapter 7.

Efficacy

A total of 561 clots were studied, divided into 9 groups of increasing acoustic output powers. Table D-1—A-9 display the raw data measuring the clot weight loss for each group: 0W, 50W, 100W, 125W, 150W, 200W, 235W, 270W, and 400W.

Table D-1 Raw data on sonothrombolysis efficacy obtained for 0W, used as the control group

Exp #	Skull ID	AP (W)	DC (%)	PW (ms)	ID (sec)	Flow (ml/min)	PreFUS Wt (g)	PostFUS Wt (g)	Wt Loss (g)
1	Skull #1	0	50	100	30	10	0.25	0.23	0.02
2	Skull #1	0	50	100	30	10	0.25	0.25	0.00
3	Skull #1	0	50	100	30	10	0.22	0.22	0.00
4	Skull #1	0	50	100	30	10	0.21	0.20	0.00
5	Skull #1	0	50	100	30	10	0.22	0.22	0.00
6	Skull #1	0	50	100	30	10	0.22	0.22	-0.01
7	Skull #1	0	50	100	30	10	0.23	0.22	0.01
8	Skull #1	0	50	100	30	10	0.22	0.22	0.00
9	Skull #1	0	50	100	30	10	0.21	0.21	0.00
10	Skull #1	0	50	100	30	10	0.22	0.23	-0.01
11	Skull #1	0	50	100	30	10	0.21	0.20	0.00
12	Skull #1	0	50	100	30	10	0.23	0.20	0.03

13	Skull #1	0	50	100	30	10	0.21	0.23	-0.03
14	Skull #1	0	50	100	30	10	0.22	0.20	0.02
15	Skull #1	0	50	100	30	10	0.23	0.22	0.01
16	Skull #1	0	50	100	30	10	0.23	0.23	0.01
17	Skull #1	0	50	100	30	10	0.21	0.21	0.00
18	Skull #1	0	50	100	30	10	0.21	0.21	0.00
19	Skull #1	0	50	100	30	10	0.21	0.21	0.00
20	Skull #1	0	50	100	30	10	0.25	0.24	0.01
21	Skull #1	0	50	100	30	10	0.22	0.22	0.00
22	Skull #1	0	50	100	30	10	0.21	0.22	0.00
23	Skull #1	0	50	100	30	10	0.23	0.23	0.00
24	Skull #1	0	50	100	30	10	0.23	0.23	0.00
25	Skull #1	0	50	100	30	10	0.21	0.21	0.00
26	Skull #1	0	50	100	30	10	0.21	0.21	0.00
27	Skull #1	0	50	100	30	10	0.21	0.20	0.01
28	Skull #1	0	50	100	30	10	0.22	0.20	0.03
29	Skull #1	0	50	100	30	10	0.21	0.20	0.00
30	Skull #1	0	50	100	30	10	0.26	0.25	0.01
31	Skull #1	0	50	100	30	10	0.25	0.25	0.00
32	Skull #1	0	50	100	30	10	0.27	0.27	0.00
33	Skull #1	0	50	100	30	10	0.27	0.26	0.01
34	Skull #1	0	50	100	30	10	0.26	0.24	0.03
35	Skull	0	50	100	30	10	0.25	0.25	0.00

140

	#1								
36	Skull #1	0	50	100	30	10	0.25	0.24	0.01
37	Skull #1	0	50	100	30	10	0.23	0.24	-0.01
38	Skull #1	0	50	100	30	10	0.21	0.20	0.00
39	Skull #1	0	50	100	30	10	0.25	0.25	0.00
40	Skull #1	0	50	100	30	10	0.22	0.22	0.01
41	Skull #1	0	50	100	30	10	0.22	0.24	-0.01
42	Skull #1	0	50	100	30	10	0.24	0.22	0.02
43	Skull #1	0	50	100	30	10	0.21	0.20	0.00
44	Skull #1	0	50	100	30	10	0.23	0.23	0.00
45	Skull #1	0	50	100	30	10	0.24	0.24	0.00
46	Skull #1	0	50	100	30	10	0.23	0.24	0.00
47	Skull #1	0	50	100	30	10	0.21	0.20	0.01
48	Skull #1	0	50	100	30	10	0.23	0.22	0.01
49	Skull #1	0	50	100	30	10	0.26	0.26	0.01
50	Skull #1	0	50	100	30	10	0.24	0.24	0.00
51	Skull #1	0	50	100	30	10	0.28	0.27	0.01
52	Skull #1	0	50	100	30	10	0.27	0.27	0.00
53	Skull #1	0	50	100	30	10	0.23	0.23	0.01
54	Skull #1	0	50	100	30	10	0.26	0.24	0.02
55	Skull #1	0	50	100	30	10	0.26	0.23	0.03
56	Skull #1	0	50	100	30	10	0.28	0.28	0.00
57	Skull #1	0	50	100	30	10	0.27	0.25	0.02

58	Skull #1	0	50	100	30	10	0.23	0.23	0.00
59	Skull #1	0	50	100	30	10	0.23	0.23	0.00
60	Skull #1	0	50	100	30	10	0.25	0.25	0.00

Table D-2 Raw data on sonothrombolysis efficacy obtained using acoustic output power of 50W

Exp #	Skull ID	AP (W)	DC (%)	PW (ms)	ID (sec)	Flow (ml/min)	PreFUS Wt (g)	PostFUS Wt (g)	Wt Loss (g)
1	Skull #1	50	50	100	30	10	0.21	0.21	0.00
2	Skull #1	50	50	100	30	10	0.21	0.21	0.00
3	Skull #1	50	50	100	30	10	0.21	0.21	0.00
4	Skull #1	50	50	100	30	10	0.23	0.22	0.01
5	Skull #1	50	50	100	30	10	0.25	0.23	0.02
6	Skull #1	50	50	100	30	10	0.25	0.23	0.01
7	Skull #1	50	50	100	30	10	0.23	0.23	0.00
8	Skull #1	50	50	100	30	10	0.22	0.22	0.00
9	Skull #1	50	50	100	30	10	0.22	0.22	0.01
10	Skull #1	50	50	100	30	10	0.26	0.24	0.01
11	Skull #1	50	50	100	30	10	0.22	0.22	0.01
12	Skull #1	50	50	100	30	10	0.24	0.24	0.00
13	Skull #1	50	50	100	30	10	0.25	0.25	0.00
14	Skull #1	50	50	100	30	10	0.24	0.23	0.01

15	Skull #1	50	50	100	30	10	0.22	0.21	0.01
16	Skull #1	50	50	100	30	10	0.25	0.24	0.00
17	Skull #1	50	50	100	30	10	0.23	0.22	0.01
18	Skull #1	50	50	100	30	10	0.25	0.23	0.02
19	Skull #1	50	50	100	30	10	0.23	0.23	0.00
20	Skull #1	50	50	100	30	10	0.21	0.21	0.00
21	Skull #1	50	50	100	30	10	0.23	0.20	0.03
22	Skull #1	50	50	100	30	10	0.25	0.22	0.03
23	Skull #1	50	50	100	30	10	0.21	0.20	0.01
24	Skull #1	50	50	100	30	10	0.24	0.21	0.03
25	Skull #1	50	50	100	30	10	0.25	0.25	0.00
26	Skull #1	50	50	100	30	10	0.21	0.19	0.02
27	Skull #1	50	50	100	30	10	0.21	0.20	0.01
28	Skull #1	50	50	100	30	10	0.23	0.19	0.04
29	Skull #1	50	50	100	30	10	0.21	0.21	0.00
30	Skull #1	50	50	100	30	10	0.21	0.21	0.00
31	Skull #1	50	50	100	30	10	0.21	0.21	0.00
32	Skull #1	50	50	100	30	10	0.23	0.21	0.02
33	Skull #1	50	50	100	30	10	0.21	0.20	0.01
34	Skull #1	50	50	100	30	10	0.21	0.21	0.01
35	Skull #1	50	50	100	30	10	0.21	0.20	0.01
36	Skull #1	50	50	100	30	10	0.21	0.20	0.02
37	Skull	50	50	100	30	10	0.21	0.19	0.01

	#1								
38	Skull #1	50	50	100	30	10	0.21	0.20	0.01
39	Skull #1	50	50	100	30	10	0.26	0.25	0.01
40	Skull #1	50	50	100	30	10	0.26	0.25	0.01
41	Skull #1	50	50	100	30	10	0.25	0.24	0.02
42	Skull #1	50	50	100	30	10	0.27	0.25	0.02
43	Skull #1	50	50	100	30	10	0.25	0.24	0.01
44	Skull #1	50	50	100	30	10	0.26	0.24	0.01
45	Skull #1	50	50	100	30	10	0.24	0.23	0.01
46	Skull #1	50	50	100	30	10	0.24	0.24	0.00
47	Skull #1	50	50	100	30	10	0.25	0.25	0.00
48	Skull #1	50	50	100	30	10	0.23	0.22	0.01
49	Skull #1	50	50	100	30	10	0.22	0.21	0.01
50	Skull #1	50	50	100	30	10	0.22	0.22	0.01
51	Skull #1	50	50	100	30	10	0.22	0.21	0.01
52	Skull #1	50	50	100	30	10	0.22	0.21	0.01
53	Skull #1	50	50	100	30	10	0.22	0.20	0.02
54	Skull #1	50	50	100	30	10	0.24	0.24	0.00
55	Skull #1	50	50	100	30	10	0.22	0.21	0.01
56	Skull #1	50	50	100	30	10	0.26	0.26	0.00
57	Skull #1	50	50	100	30	10	0.25	0.22	0.03
58	Skull #1	50	50	100	30	10	0.21	0.21	0.00
59	Skull #1	50	50	100	30	10	0.23	0.17	0.06

60	Skull #1	50	50	100	30	10	0.24	0.23	0.01
61	Skull #1	50	50	100	30	10	0.25	0.24	0.01
62	Skull #1	50	50	100	30	10	0.28	0.28	0.01

Table D-3 Raw data on sonothrombolysis efficacy obtained using acoustic output power of 100W

Exp #	Skull ID	AP (W)	DC (%)	PW (ms)	ID (sec)	Flow (ml/min)	PreFUS Wt (g)	PostFUS Wt (g)	Wt Loss (g)
1	Skull #1	100	50	100	30	10	0.24	0.23	0.01
2	Skull #1	100	50	100	30	10	0.22	0.21	0.01
3	Skull #1	100	50	100	30	10	0.22	0.22	0.01
4	Skull #1	100	50	100	30	10	0.22	0.20	0.02
5	Skull #1	100	50	100	30	10	0.22	0.21	0.01
6	Skull #1	100	50	100	30	10	0.21	0.21	0.01
7	Skull #1	100	50	100	30	10	0.21	0.21	0.00
8	Skull #1	100	50	100	30	10	0.22	0.22	0.00
9	Skull #1	100	50	100	30	10	0.21	0.21	0.00
10	Skull #1	100	50	100	30	10	0.23	0.22	0.01
11	Skull #1	100	50	100	30	10	0.22	0.22	0.00
12	Skull #1	100	50	100	30	10	0.26	0.22	0.03
13	Skull #1	100	50	100	30	10	0.24	0.21	0.03
14	Skull #1	100	50	100	30	10	0.25	0.24	0.00

15	Skull #1	100	50	100	30	10	0.22	0.22	0.00
16	Skull #1	100	50	100	30	10	0.22	0.20	0.01
17	Skull #1	100	50	100	30	10	0.24	0.22	0.02
18	Skull #1	100	50	100	30	10	0.24	0.23	0.01
19	Skull #1	100	50	100	30	10	0.24	0.22	0.01
20	Skull #1	100	50	100	30	10	0.24	0.24	0.01
21	Skull #1	100	50	100	30	10	0.25	0.23	0.02
22	Skull #1	100	50	100	30	10	0.23	0.22	0.02
23	Skull #1	100	50	100	30	10	0.24	0.23	0.02
24	Skull #1	100	50	100	30	10	0.25	0.24	0.01
25	Skull #1	100	50	100	30	10	0.27	0.25	0.01
26	Skull #1	100	50	100	30	10	0.24	0.23	0.01
27	Skull #1	100	50	100	30	10	0.23	0.20	0.02
28	Skull #1	100	50	100	30	10	0.27	0.24	0.02
29	Skull #1	100	50	100	30	10	0.24	0.22	0.02
30	Skull #1	100	50	100	30	10	0.22	0.22	0.01
31	Skull #1	100	50	100	30	10	0.25	0.23	0.02
32	Skull #1	100	50	100	30	10	0.28	0.25	0.03
33	Skull #1	100	50	100	30	10	0.25	0.25	0.01
34	Skull #1	100	50	100	30	10	0.23	0.23	0.00
35	Skull #1	100	50	100	30	10	0.27	0.24	0.02
36	Skull #1	100	50	100	30	10	0.26	0.24	0.02
37	Skull	100	50	100	30	10	0.25	0.24	0.01

	#1								
38	Skull #1	100	50	100	30	10	0.25	0.24	0.01
39	Skull #1	100	50	100	30	10	0.25	0.24	0.01
40	Skull #1	100	50	100	30	10	0.25	0.23	0.02
41	Skull #1	100	50	100	30	10	0.26	0.24	0.02
42	Skull #1	100	50	100	30	10	0.26	0.24	0.01
43	Skull #1	100	50	100	30	10	0.23	0.22	0.01
44	Skull #1	100	50	100	30	10	0.25	0.24	0.01
45	Skull #1	100	50	100	30	10	0.26	0.24	0.02
46	Skull #1	100	50	100	30	10	0.27	0.23	0.03
47	Skull #1	100	50	100	30	10	0.25	0.23	0.01
48	Skull #1	100	50	100	30	10	0.27	0.25	0.02
49	Skull #1	100	50	100	30	10	0.24	0.23	0.01
50	Skull #1	100	50	100	30	10	0.25	0.23	0.02
51	Skull #1	100	50	100	30	10	0.24	0.23	0.01
52	Skull #1	100	50	100	30	10	0.24	0.23	0.01
53	Skull #1	100	50	100	30	10	0.25	0.24	0.01
54	Skull #1	100	50	100	30	10	0.25	0.23	0.02
55	Skull #1	100	50	100	30	10	0.24	0.23	0.01
56	Skull #1	100	50	100	30	10	0.24	0.23	0.01
57	Skull #1	100	50	100	30	10	0.26	0.25	0.02
58	Skull #1	100	50	100	30	10	0.24	0.23	0.01
59	Skull #1	100	50	100	30	10	0.28	0.26	0.02

60	Skull #1	100	50	100	30	10	0.26	0.25	0.01
61	Skull #1	100	50	100	30	10	0.23	0.23	0.01
62	Skull #1	100	50	100	30	10	0.27	0.25	0.02
63	Skull #1	100	50	100	30	10	0.27	0.23	0.04
64	Skull #1	100	50	100	30	10	0.24	0.23	0.02
65	Skull #1	100	50	100	30	10	0.23	0.22	0.01
66	Skull #1	100	50	100	30	10	0.25	0.22	0.03

Table D-4 Raw data on sonothrombolysis efficacy obtained using acoustic output power of 125W

Exp #	Skull ID	AP (W)	DC (%)	PW (ms)	ID (sec)	Flow (ml/min)	PreFUS Wt (g)	PostFUS Wt (g)	Wt Loss (g)
1	Skull #1	125	50	100	30	10	0.25	0.25	0.01
2	Skull #1	125	50	100	30	10	0.25	0.21	0.04
3	Skull #1	125	50	100	30	10	0.23	0.22	0.01
4	Skull #1	125	50	100	30	10	0.21	0.14	0.07
5	Skull #1	125	50	100	30	10	0.25	0.21	0.04
6	Skull #1	125	50	100	30	10	0.23	0.21	0.02
7	Skull #1	125	50	100	30	10	0.24	0.23	0.01
8	Skull #1	125	50	100	30	10	0.25	0.23	0.02
9	Skull #1	125	50	100	30	10	0.25	0.23	0.02
10	Skull #1	125	50	100	30	10	0.23	0.21	0.02

11	Skull #1	125	50	100	30	10	0.23	0.22	0.01
12	Skull #1	125	50	100	30	10	0.24	0.23	0.01
13	Skull #1	125	50	100	30	10	0.24	0.23	0.02
14	Skull #1	125	50	100	30	10	0.24	0.20	0.04
15	Skull #1	125	50	100	30	10	0.24	0.23	0.01
16	Skull #1	125	50	100	30	10	0.21	0.19	0.02
17	Skull #1	125	50	100	30	10	0.21	0.20	0.01
18	Skull #1	125	50	100	30	10	0.23	0.22	0.01
19	Skull #1	125	50	100	30	10	0.27	0.23	0.04
20	Skull #1	125	50	100	30	10	0.25	0.22	0.03
21	Skull #1	125	50	100	30	10	0.22	0.20	0.02
22	Skull #1	125	50	100	30	10	0.23	0.21	0.01
23	Skull #1	125	50	100	30	10	0.25	0.21	0.03
24	Skull #1	125	50	100	30	10	0.23	0.20	0.02
25	Skull #1	125	50	100	30	10	0.24	0.22	0.03
26	Skull #1	125	50	100	30	10	0.23	0.22	0.01
27	Skull #1	125	50	100	30	10	0.23	0.21	0.01
28	Skull #1	125	50	100	30	10	0.23	0.20	0.03
29	Skull #1	125	50	100	30	10	0.24	0.23	0.02
30	Skull #1	125	50	100	30	10	0.24	0.20	0.04
31	Skull #1	125	50	100	30	10	0.24	0.24	0.00
32	Skull #1	125	50	100	30	10	0.23	0.22	0.01
33	Skull	125	50	100	30	10	0.25	0.22	0.03

	#1								
34	Skull #1	125	50	100	30	10	0.23	0.23	0.00
35	Skull #1	125	50	100	30	10	0.23	0.20	0.03
36	Skull #1	125	50	100	30	10	0.21	0.21	0.01
37	Skull #1	125	50	100	30	10	0.21	0.20	0.01
38	Skull #1	125	50	100	30	10	0.21	0.19	0.02
39	Skull #1	125	50	100	30	10	0.21	0.19	0.02
40	Skull #1	125	50	100	30	10	0.25	0.22	0.03
41	Skull #1	125	50	100	30	10	0.26	0.19	0.07
42	Skull #1	125	50	100	30	10	0.27	0.24	0.03
43	Skull #1	125	50	100	30	10	0.26	0.25	0.01
44	Skull #1	125	50	100	30	10	0.27	0.20	0.07
45	Skull #1	125	50	100	30	10	0.25	0.22	0.03
46	Skull #1	125	50	100	30	10	0.26	0.22	0.04
47	Skull #1	125	50	100	30	10	0.24	0.21	0.03
48	Skull #1	125	50	100	30	10	0.23	0.20	0.03
49	Skull #1	125	50	100	30	10	0.23	0.20	0.03
50	Skull #1	125	50	100	30	10	0.25	0.21	0.04
51	Skull #1	125	50	100	30	10	0.24	0.23	0.02
52	Skull #1	125	50	100	30	10	0.23	0.22	0.01
53	Skull #1	125	50	100	30	10	0.21	0.20	0.01
54	Skull #1	125	50	100	30	10	0.25	0.24	0.02
55	Skull #1	125	50	100	30	10	0.21	0.20	0.01

150

56	Skull #1	125	50	100	30	10	0.21	0.20	0.01
57	Skull #1	125	50	100	30	10	0.23	0.23	0.01
58	Skull #1	125	50	100	30	10	0.26	0.24	0.02
59	Skull #1	125	50	100	30	10	0.24	0.21	0.03
60	Skull #1	125	50	100	30	10	0.23	0.23	0.01
61	Skull #1	125	50	100	30	10	0.25	0.24	0.01
62	Skull #1	125	50	100	30	10	0.23	0.22	0.00
63	Skull #1	125	50	100	30	10	0.26	0.25	0.01

Table D-5 Raw data on sonothrombolysis efficacy obtained using acoustic output power of 150W

Exp #	Skull ID	AP (W)	DC (%)	PW (ms)	ID (sec)	Flow (ml/min)	PreFUS Wt (g)	PostFUS Wt (g)	Wt Loss (g)
1	Skull #1	150	50	100	30	10	0.24	0.22	0.03
2	Skull #1	150	50	100	30	10	0.25	0.23	0.02
3	Skull #1	150	50	100	30	10	0.25	0.25	0.00
4	Skull #1	150	50	100	30	10	0.21	0.20	0.01
5	Skull #1	150	50	100	30	10	0.21	0.20	0.01
6	Skull #1	150	50	100	30	10	0.24	0.22	0.02
7	Skull #1	150	50	100	30	10	0.25	0.20	0.05
8	Skull #1	150	50	100	30	10	0.24	0.19	0.04
9	Skull #1	150	50	100	30	10	0.23	0.21	0.02
10	Skull #1	150	50	100	30	10	0.24	0.23	0.02
11	Skull	150	50	100	30	10	0.23	0.19	0.03

	#1								
12	Skull #1	150	50	100	30	10	0.24	0.22	0.02
13	Skull #1	150	50	100	30	10	0.24	0.23	0.01
14	Skull #1	150	50	100	30	10	0.25	0.22	0.03
15	Skull #1	150	50	100	30	10	0.23	0.22	0.02
16	Skull #1	150	50	100	30	10	0.26	0.18	0.08
17	Skull #1	150	50	100	30	10	0.23	0.21	0.02
18	Skull #1	150	50	100	30	10	0.21	0.12	0.09
19	Skull #1	150	50	100	30	10	0.22	0.20	0.02
20	Skull #1	150	50	100	30	10	0.22	0.21	0.01
21	Skull #1	150	50	100	30	10	0.21	0.21	0.00
22	Skull #1	150	50	100	30	10	0.25	0.21	0.04
23	Skull #1	150	50	100	30	10	0.22	0.20	0.02
24	Skull #1	150	50	100	30	10	0.23	0.19	0.04
25	Skull #1	150	50	100	30	10	0.23	0.22	0.01
26	Skull #1	150	50	100	30	10	0.22	0.21	0.01
27	Skull #1	150	50	100	30	10	0.23	0.21	0.02
28	Skull #1	150	50	100	30	10	0.23	0.20	0.03
29	Skull #1	150	50	100	30	10	0.22	0.22	0.01
30	Skull #1	150	50	100	30	10	0.23	0.17	0.07
31	Skull #1	150	50	100	30	10	0.21	0.18	0.03
32	Skull #1	150	50	100	30	10	0.21	0.20	0.02
33	Skull #1	150	50	100	30	10	0.26	0.20	0.06

34	Skull #1	150	50	100	30	10	0.24	0.24	0.01
35	Skull #1	150	50	100	30	10	0.21	0.20	0.01
36	Skull #1	150	50	100	30	10	0.23	0.20	0.03
37	Skull #1	150	50	100	30	10	0.21	0.18	0.03
38	Skull #1	150	50	100	30	10	0.22	0.19	0.03
39	Skull #1	150	50	100	30	10	0.21	0.19	0.02
40	Skull #1	150	50	100	30	10	0.22	0.20	0.02
41	Skull #1	150	50	100	30	10	0.24	0.17	0.07
42	Skull #1	150	50	100	30	10	0.27	0.23	0.04
43	Skull #1	150	50	100	30	10	0.26	0.21	0.05
44	Skull #1	150	50	100	30	10	0.27	0.17	0.10
45	Skull #1	150	50	100	30	10	0.27	0.22	0.05
46	Skull #1	150	50	100	30	10	0.23	0.17	0.06
47	Skull #1	150	50	100	30	10	0.25	0.23	0.02
48	Skull #1	150	50	100	30	10	0.26	0.13	0.13
49	Skull #1	150	50	100	30	10	0.24	0.18	0.06
50	Skull #1	150	50	100	30	10	0.21	0.17	0.04
51	Skull #1	150	50	100	30	10	0.22	0.20	0.03
52	Skull #1	150	50	100	30	10	0.23	0.19	0.04
53	Skull #1	150	50	100	30	10	0.21	0.19	0.02
54	Skull #1	150	50	100	30	10	0.22	0.19	0.03
55	Skull #1	150	50	100	30	10	0.22	0.20	0.02
56	Skull	150	50	100	30	10	0.22	0.21	0.02

	#1								
57	Skull #1	150	50	100	30	10	0.21	0.20	0.00
58	Skull #1	150	50	100	30	10	0.24	0.23	0.01
59	Skull #1	150	50	100	30	10	0.27	0.23	0.04
60	Skull #1	150	50	100	30	10	0.27	0.25	0.02
61	Skull #1	150	50	100	30	10	0.24	0.22	0.02
62	Skull #1	150	50	100	30	10	0.23	0.21	0.02
63	Skull #1	150	50	100	30	10	0.27	0.24	0.03
64	Skull #1	150	50	100	30	10	0.25	0.21	0.05
65	Skull #1	150	50	100	30	10	0.27	0.24	0.03

Table D-6 Raw data on sonothrombolysis efficacy obtained using acoustic output power of 200W

Exp #	Skull ID	AP (W)	DC (%)	PW (ms)	ID (sec)	Flow (ml/min)	PreFUS Wt (g)	PostFUS Wt (g)	Wt Loss (g)
1	Skull #1	200	50	100	30	10	0.26	0.08	0.18
2	Skull #1	200	50	100	30	10	0.26	0.15	0.11
3	Skull #1	200	50	100	30	10	0.27	0.16	0.11
4	Skull #1	200	50	100	30	10	0.28	0.17	0.12
5	Skull #1	200	50	100	30	10	0.23	0.16	0.07
6	Skull #1	200	50	100	30	10	0.21	0.09	0.12
7	Skull #1	200	50	100	30	10	0.23	0.17	0.06
8	Skull #1	200	50	100	30	10	0.22	0.10	0.11
9	Skull #1	200	50	100	30	10	0.22	0.14	0.09

10	Skull #1	200	50	100	30	10	0.23	0.17	0.06
11	Skull #1	200	50	100	30	10	0.24	0.18	0.06
12	Skull #1	200	50	100	30	10	0.23	0.15	0.08
13	Skull #1	200	50	100	30	10	0.27	0.19	0.08
14	Skull #1	200	50	100	30	10	0.25	0.19	0.06
15	Skull #1	200	50	100	30	10	0.21	0.19	0.02
16	Skull #1	200	50	100	30	10	0.24	0.07	0.17
17	Skull #1	200	50	100	30	10	0.21	0.17	0.04
18	Skull #1	200	50	100	30	10	0.24	0.08	0.16
19	Skull #1	200	50	100	30	10	0.22	0.18	0.05
20	Skull #1	200	50	100	30	10	0.23	0.16	0.07
21	Skull #1	200	50	100	30	10	0.24	0.22	0.03
22	Skull #1	200	50	100	30	10	0.28	0.24	0.04
23	Skull #1	200	50	100	30	10	0.24	0.21	0.03
24	Skull #1	200	50	100	30	10	0.24	0.21	0.03
25	Skull #1	200	50	100	30	10	0.26	0.22	0.03
26	Skull #1	200	50	100	30	10	0.24	0.21	0.02
27	Skull #1	200	50	100	30	10	0.27	0.26	0.02
28	Skull #1	200	50	100	30	10	0.23	0.22	0.01
29	Skull #1	200	50	100	30	10	0.27	0.25	0.02
30	Skull #1	200	50	100	30	10	0.26	0.23	0.03
31	Skull #1	200	50	100	30	10	0.25	0.23	0.02
32	Skull	200	50	100	30	10	0.22	0.21	0.01

	#1								
33	Skull #1	200	50	100	30	10	0.27	0.25	0.01
34	Skull #1	200	50	100	30	10	0.22	0.21	0.01
35	Skull #1	200	50	100	30	10	0.27	0.22	0.05
36	Skull #1	200	50	100	30	10	0.26	0.22	0.04
37	Skull #1	200	50	100	30	10	0.23	0.22	0.01
38	Skull #1	200	50	100	30	10	0.29	0.09	0.20
39	Skull #1	200	50	100	30	10	0.25	0.17	0.09
40	Skull #1	200	50	100	30	10	0.29	0.20	0.09
41	Skull #1	200	50	100	30	10	0.24	0.06	0.18
42	Skull #1	200	50	100	30	10	0.25	0.11	0.14
43	Skull #1	200	50	100	30	10	0.27	0.21	0.07
44	Skull #1	200	50	100	30	10	0.25	0.19	0.07
45	Skull #1	200	50	100	30	10	0.24	0.19	0.05
46	Skull #1	200	50	100	30	10	0.27	0.19	0.08
47	Skull #1	200	50	100	30	10	0.27	0.22	0.06
48	Skull #1	200	50	100	30	10	0.25	0.10	0.15
49	Skull #1	200	50	100	30	10	0.28	0.16	0.13
50	Skull #1	200	50	100	30	10	0.26	0.19	0.07
51	Skull #1	200	50	100	30	10	0.26	0.17	0.09
52	Skull #1	200	50	100	30	10	0.23	0.18	0.05
53	Skull #1	200	50	100	30	10	0.24	0.19	0.04
54	Skull #1	200	50	100	30	10	0.23	0.18	0.05

55	Skull #1	200	50	100	30	10	0.23	0.20	0.03
56	Skull #1	200	50	100	30	10	0.23	0.20	0.04
57	Skull #1	200	50	100	30	10	0.24	0.20	0.04
58	Skull #1	200	50	100	30	10	0.25	0.13	0.12
59	Skull #1	200	50	100	30	10	0.24	0.15	0.08
60	Skull #1	200	50	100	30	10	0.25	0.17	0.08
61	Skull #1	200	50	100	30	10	0.24	0.18	0.05

Table D-7 Raw data on sonothrombolysis efficacy obtained using acoustic output power of 235W

Exp #	Skull ID	AP (W)	DC (%)	PW (ms)	ID (sec)	Flow (ml/min)	PreFUS Wt (g)	PostFUS Wt (g)	Wt Loss (g)
1	Skull #1	235	50	100	30	10	0.28	0.07	0.21
2	Skull #1	235	50	100	30	10	0.27	0.11	0.16
3	Skull #1	235	50	100	30	10	0.28	0.11	0.17
4	Skull #1	235	50	100	30	10	0.25	0.12	0.13
5	Skull #1	235	50	100	30	10	0.22	0.09	0.14
6	Skull #1	235	50	100	30	10	0.24	0.15	0.09
7	Skull #1	235	50	100	30	10	0.22	0.16	0.06
8	Skull #1	235	50	100	30	10	0.21	0.14	0.07
9	Skull #1	235	50	100	30	10	0.23	0.14	0.09
10	Skull #1	235	50	100	30	10	0.21	0.13	0.09
11	Skull #1	235	50	100	30	10	0.24	0.11	0.12
12	Skull	235	50	100	30	10	0.26	0.16	0.10

	#1								
13	Skull #1	235	50	100	30	10	0.26	0.21	0.05
14	Skull #1	235	50	100	30	10	0.21	0.10	0.11
15	Skull #1	235	50	100	30	10	0.22	0.20	0.02
16	Skull #1	235	50	100	30	10	0.21	0.15	0.05
17	Skull #1	235	50	100	30	10	0.23	0.12	0.12
18	Skull #1	235	50	100	30	10	0.24	0.18	0.05
19	Skull #1	235	50	100	30	10	0.22	0.20	0.03
20	Skull #1	235	50	100	30	10	0.21	0.18	0.03
21	Skull #1	235	50	100	30	10	0.26	0.18	0.09
22	Skull #1	235	50	100	30	10	0.24	0.18	0.06
23	Skull #1	235	50	100	30	10	0.25	0.15	0.10
24	Skull #1	235	50	100	30	10	0.25	0.18	0.07
25	Skull #1	235	50	100	30	10	0.27	0.16	0.11
26	Skull #1	235	50	100	30	10	0.26	0.19	0.07
27	Skull #1	235	50	100	30	10	0.25	0.21	0.04
28	Skull #1	235	50	100	30	10	0.25	0.07	0.18
29	Skull #1	235	50	100	30	10	0.27	0.10	0.17
30	Skull #1	235	50	100	30	10	0.22	0.17	0.05
31	Skull #1	235	50	100	30	10	0.25	0.19	0.06
32	Skull #1	235	50	100	30	10	0.26	0.22	0.04
33	Skull #1	235	50	100	30	10	0.26	0.12	0.14
34	Skull #1	235	50	100	30	10	0.25	0.08	0.17

35	Skull #1	235	50	100	30	10	0.24	0.17	0.07
36	Skull #1	235	50	100	30	10	0.27	0.18	0.09
37	Skull #1	235	50	100	30	10	0.26	0.19	0.07
38	Skull #1	235	50	100	30	10	0.26	0.18	0.08
39	Skull #1	235	50	100	30	10	0.27	0.18	0.09
40	Skull #1	235	50	100	30	10	0.26	0.13	0.13
41	Skull #1	235	50	100	30	10	0.27	0.20	0.08
42	Skull #1	235	50	100	30	10	0.25	0.07	0.18
43	Skull #1	235	50	100	30	10	0.27	0.06	0.21
44	Skull #1	235	50	100	30	10	0.25	0.07	0.17
45	Skull #1	235	50	100	30	10	0.26	0.18	0.08
46	Skull #1	235	50	100	30	10	0.27	0.22	0.05
47	Skull #1	235	50	100	30	10	0.27	0.05	0.22
48	Skull #1	235	50	100	30	10	0.25	0.17	0.08
49	Skull #1	235	50	100	30	10	0.26	0.07	0.19
50	Skull #1	235	50	100	30	10	0.23	0.18	0.05
51	Skull #1	235	50	100	30	10	0.24	0.14	0.10
52	Skull #1	235	50	100	30	10	0.27	0.07	0.20
53	Skull #1	235	50	100	30	10	0.26	0.11	0.15
54	Skull #1	235	50	100	30	10	0.25	0.08	0.17
55	Skull #1	235	50	100	30	10	0.25	0.22	0.03
56	Skull #1	235	50	100	30	10	0.27	0.10	0.17
57	Skull	235	50	100	30	10	0.25	0.20	0.05

	#1								
58	Skull #1	235	50	100	30	10	0.24	0.09	0.15
59	Skull #1	235	50	100	30	10	0.23	0.11	0.12
60	Skull #1	235	50	100	30	10	0.25	0.21	0.04
61	Skull #1	235	50	100	30	10	0.21	0.14	0.07

Table D-8 Raw data on sonothrombolysis efficacy obtained using acoustic output power of 235W

Exp #	Skull ID	AP (W)	DC (%)	PW (ms)	ID (sec)	Flow (ml/min)	PreFUS Wt (g)	PostFUS Wt (g)	Wt Loss (g)
1	Skull #1	270	50	100	30	10	0.27	0.06	0.21
2	Skull #1	270	50	100	30	10	0.25	0.06	0.20
3	Skull #1	270	50	100	30	10	0.26	0.07	0.19
4	Skull #1	270	50	100	30	10	0.26	0.08	0.18
5	Skull #1	270	50	100	30	10	0.22	0.07	0.16
6	Skull #1	270	50	100	30	10	0.21	0.08	0.13
7	Skull #1	270	50	100	30	10	0.23	0.05	0.18
8	Skull #1	270	50	100	30	10	0.23	0.18	0.05
9	Skull #1	270	50	100	30	10	0.21	0.11	0.11
10	Skull #1	270	50	100	30	10	0.25	0.09	0.16
11	Skull #1	270	50	100	30	10	0.22	0.12	0.10
12	Skull #1	270	50	100	30	10	0.27	0.18	0.09
13	Skull #1	270	50	100	30	10	0.23	0.08	0.15
14	Skull #1	270	50	100	30	10	0.22	0.06	0.16

160										
15	Skull #1	270	50	100	30	10	0.24	0.05	0.19	
16	Skull #1	270	50	100	30	10	0.21	0.13	0.08	
17	Skull #1	270	50	100	30	10	0.24	0.06	0.18	
18	Skull #1	270	50	100	30	10	0.23	0.10	0.14	
19	Skull #1	270	50	100	30	10	0.23	0.06	0.17	
20	Skull #1	270	50	100	30	10	0.22	0.08	0.14	
21	Skull #1	270	50	100	30	10	0.23	0.08	0.15	
22	Skull #1	270	50	100	30	10	0.23	0.06	0.16	
23	Skull #1	270	50	100	30	10	0.24	0.05	0.18	
24	Skull #1	270	50	100	30	10	0.23	0.07	0.16	
25	Skull #1	270	50	100	30	10	0.24	0.08	0.16	
26	Skull #1	270	50	100	30	10	0.25	0.07	0.19	
27	Skull #1	270	50	100	30	10	0.26	0.06	0.20	
28	Skull #1	270	50	100	30	10	0.27	0.07	0.21	
29	Skull #1	270	50	100	30	10	0.23	0.13	0.10	
30	Skull #1	270	50	100	30	10	0.28	0.05	0.24	
31	Skull #1	270	50	100	30	10	0.25	0.06	0.19	
32	Skull #1	270	50	100	30	10	0.23	0.09	0.14	
33	Skull #1	270	50	100	30	10	0.27	0.12	0.15	
34	Skull #1	270	50	100	30	10	0.25	0.14	0.11	
35	Skull #1	270	50	100	30	10	0.29	0.07	0.22	
36	Skull #1	270	50	100	30	10	0.24	0.04	0.20	
37	Skull	270	50	100	30	10	0.23	0.13	0.11	

	#1								
38	Skull #1	270	50	100	30	10	0.28	0.09	0.19
39	Skull #1	270	50	100	30	10	0.27	0.12	0.15
40	Skull #1	270	50	100	30	10	0.27	0.15	0.12
41	Skull #1	270	50	100	30	10	0.26	0.13	0.13
42	Skull #1	270	50	100	30	10	0.29	0.06	0.23
43	Skull #1	270	50	100	30	10	0.27	0.15	0.12
44	Skull #1	270	50	100	30	10	0.26	0.14	0.11
45	Skull #1	270	50	100	30	10	0.26	0.10	0.16
46	Skull #1	270	50	100	30	10	0.25	0.12	0.13
47	Skull #1	270	50	100	30	10	0.25	0.12	0.13
48	Skull #1	270	50	100	30	10	0.24	0.07	0.17
49	Skull #1	270	50	100	30	10	0.26	0.07	0.19
50	Skull #1	270	50	100	30	10	0.28	0.16	0.13
51	Skull #1	270	50	100	30	10	0.24	0.08	0.17
52	Skull #1	270	50	100	30	10	0.24	0.07	0.17
53	Skull #1	270	50	100	30	10	0.27	0.13	0.15
54	Skull #1	270	50	100	30	10	0.25	0.15	0.11
55	Skull #1	270	50	100	30	10	0.24	0.08	0.16
56	Skull #1	270	50	100	30	10	0.27	0.10	0.17
57	Skull #1	270	50	100	30	10	0.25	0.14	0.10
58	Skull #1	270	50	100	30	10	0.24	0.09	0.16
59	Skull #1	270	50	100	30	10	0.25	0.10	0.15

60	Skull #1	270	50	100	30	10	0.24	0.16	0.08
61	Skull #1	270	50	100	30	10	0.25	0.14	0.11
62	Skull #1	270	50	100	30	10	0.25	0.15	0.10

Table D-9 Raw data on sonothrombolysis efficacy obtained using acoustic output power of 400W

Exp #	Skull ID	AP (W)	DC (%)	PW (ms)	ID (sec)	Flow (ml/min)	PreFUS Wt (g)	PostFUS Wt (g)	Wt Loss (g)
1	Skull #1	400	50	100	30	10	0.24	0.11	0.13
2	Skull #1	400	50	100	30	10	0.25	0.05	0.20
3	Skull #1	400	50	100	30	10	0.27	0.05	0.22
4	Skull #1	400	50	100	30	10	0.24	0.05	0.20
5	Skull #1	400	50	100	30	10	0.25	0.05	0.20
6	Skull #1	400	50	100	30	10	0.22	0.06	0.16
7	Skull #1	400	50	100	30	10	0.21	0.13	0.08
8	Skull #1	400	50	100	30	10	0.22	0.06	0.16
9	Skull #1	400	50	100	30	10	0.23	0.10	0.13
10	Skull #1	400	50	100	30	10	0.23	0.05	0.18
11	Skull #1	400	50	100	30	10	0.26	0.08	0.18
12	Skull #1	400	50	100	30	10	0.25	0.11	0.14
13	Skull #1	400	50	100	30	10	0.21	0.05	0.16
14	Skull #1	400	50	100	30	10	0.21	0.07	0.14

15	Skull #1	400	50	100	30	10	0.21	0.05	0.16
16	Skull #1	400	50	100	30	10	0.21	0.04	0.16
17	Skull #1	400	50	100	30	10	0.21	0.09	0.11
18	Skull #1	400	50	100	30	10	0.21	0.05	0.16
19	Skull #1	400	50	100	30	10	0.23	0.06	0.17
20	Skull #1	400	50	100	30	10	0.21	0.04	0.17
21	Skull #1	400	50	100	30	10	0.25	0.05	0.20
22	Skull #1	400	50	100	30	10	0.25	0.07	0.17
23	Skull #1	400	50	100	30	10	0.26	0.05	0.20
24	Skull #1	400	50	100	30	10	0.25	0.05	0.20
25	Skull #1	400	50	100	30	10	0.25	0.06	0.19
26	Skull #1	400	50	100	30	10	0.26	0.08	0.19
27	Skull #1	400	50	100	30	10	0.26	0.06	0.20
28	Skull #1	400	50	100	30	10	0.27	0.04	0.23
29	Skull #1	400	50	100	30	10	0.24	0.08	0.17
30	Skull #1	400	50	100	30	10	0.24	0.05	0.19
31	Skull #1	400	50	100	30	10	0.25	0.04	0.21
32	Skull #1	400	50	100	30	10	0.26	0.05	0.21
33	Skull #1	400	50	100	30	10	0.26	0.06	0.20
34	Skull #1	400	50	100	30	10	0.26	0.05	0.22
35	Skull #1	400	50	100	30	10	0.26	0.04	0.22
36	Skull #1	400	50	100	30	10	0.25	0.14	0.10
37	Skull	400	50	100	30	10	0.25	0.08	0.18

	#1								
38	Skull #1	400	50	100	30	10	0.25	0.08	0.17
39	Skull #1	400	50	100	30	10	0.25	0.07	0.18
40	Skull #1	400	50	100	30	10	0.22	0.07	0.15
41	Skull #1	400	50	100	30	10	0.26	0.05	0.20
42	Skull #1	400	50	100	30	10	0.26	0.05	0.21
43	Skull #1	400	50	100	30	10	0.26	0.09	0.17
44	Skull #1	400	50	100	30	10	0.26	0.05	0.21
45	Skull #1	400	50	100	30	10	0.26	0.04	0.22
46	Skull #1	400	50	100	30	10	0.26	0.05	0.21
47	Skull #1	400	50	100	30	10	0.23	0.05	0.19
48	Skull #1	400	50	100	30	10	0.24	0.05	0.20
49	Skull #1	400	50	100	30	10	0.22	0.08	0.14
50	Skull #1	400	50	100	30	10	0.21	0.04	0.17
51	Skull #1	400	50	100	30	10	0.23	0.04	0.19
52	Skull #1	400	50	100	30	10	0.26	0.04	0.22
53	Skull #1	400	50	100	30	10	0.24	0.04	0.20
54	Skull #1	400	50	100	30	10	0.25	0.04	0.21
55	Skull #1	400	50	100	30	10	0.24	0.04	0.19
56	Skull #1	400	50	100	30	10	0.23	0.04	0.19
57	Skull #1	400	50	100	30	10	0.23	0.05	0.18
58	Skull #1	400	50	100	30	10	0.25	0.05	0.20
59	Skull #1	400	50	100	30	10	0.25	0.05	0.20

60	Skull #1	400	50	100	30	10	0.24	0.04	0.20
61	Skull #1	400	50	100	30	10	0.23	0.05	0.19

Fragmentation

A total of 352 experiments were done to assess clot fragmentation, three filters of different mesh pore sizes (11, 60 and 180 microns). were used to establish if clot fragmentation (post-/pre-filter weight) changed between groups (0W, 50W, 100W, 125W, 150W, 200W, 235W, 270W, 400W) with exposure to increasing acoustic output power for each separate filter size. Table D-10, D-11, and D-12 contain all the data points collected for fragmentation studies, ordered by increasing acoustic output power groups as organized for each filter pore size, 180µm, 60µm, and 11µm, in respective order from largest to smallest (in the serial filtration course placed in the experimental setups).

Table D-10 Clot fragmentation data collected for 180µm sized mesh filters from all acoustic output groups tested

Exp #	Skull ID	AP (W)	DC (%)	PW (ms)	ID (sec)	Flow (ml/min)	180 PreFUS Wt (g)	180 PostFUS Wt (g)	180 Wt Gain (g)
1	Skull #1	0	50	100	30	10	0.046	0.037	-0.009
2	Skull #1	0	50	100	30	10	0.046	0.041	-0.005
3	Skull #1	0	50	100	30	10	0.046	0.038	-0.008
4	Skull #1	0	50	100	30	10	0.046	0.039	-0.007
5	Skull #1	0	50	100	30	10	0.046	0.037	-0.009
6	Skull #1	0	50	100	30	10	0.046	0.039	-0.007
7	Skull #1	0	50	100	30	10	0.046	0.039	-0.007
8	Skull	0	50	100	30	10	0.046	0.041	-0.005

	#1								
9	Skull #1	0	50	100	30	10	0.046	0.039	-0.007
10	Skull #1	0	50	100	30	10	0.046	0.039	-0.007
11	Skull #1	0	50	100	30	10	0.046	0.040	-0.006
12	Skull #1	0	50	100	30	10	0.046	0.043	-0.003
13	Skull #1	0	50	100	30	10	0.046	0.039	-0.007
14	Skull #1	0	50	100	30	10	0.046	0.039	-0.007
15	Skull #1	0	50	100	30	10	0.046	0.039	-0.007
16	Skull #1	0	50	100	30	10	0.046	0.039	-0.007
17	Skull #1	0	50	100	30	10	0.046	0.028	-0.018
18	Skull #1	0	50	100	30	10	0.046	0.040	-0.006
19	Skull #1	0	50	100	30	10	0.046	0.036	-0.010
20	Skull #1	0	50	100	30	10	0.046	0.041	-0.005
21	Skull #1	0	50	100	30	10	0.046	0.038	-0.008
22	Skull #1	0	50	100	30	10	0.046	0.044	-0.002
23	Skull #1	0	50	100	30	10	0.046	0.039	-0.007
24	Skull #1	0	50	100	30	10	0.046	0.043	-0.003
25	Skull #1	0	50	100	30	10	0.046	0.039	-0.007
26	Skull #1	0	50	100	30	10	0.046	0.041	-0.005
27	Skull #1	0	50	100	30	10	0.046	0.036	-0.010
28	Skull #1	0	50	100	30	10	0.046	0.048	0.002
29	Skull #1	0	50	100	30	10	0.046	0.052	0.006
30	Skull #1	0	50	100	30	10	0.046	0.055	0.009

31	Skull #1	0	50	100	30	10	0.046	0.047	0.001
32	Skull #1	0	50	100	30	10	0.046	0.048	0.002
33	Skull #1	0	50	100	30	10	0.046	0.044	-0.002
34	Skull #1	0	50	100	30	10	0.046	0.054	0.008
35	Skull #1	0	50	100	30	10	0.046	0.049	0.003
36	Skull #1	0	50	100	30	10	0.046	0.046	0.000
37	Skull #1	0	50	100	30	10	0.046	0.049	0.003
38	Skull #1	0	50	100	30	10	0.046	0.054	0.008
39	Skull #1	0	50	100	30	10	0.046	0.049	0.003
40	Skull #1	0	50	100	30	10	0.046	0.051	0.005
41	Skull #1	0	50	100	30	10	0.046	0.051	0.005
42	Skull #1	0	50	100	30	10	0.046	0.044	-0.002
43	Skull #1	0	50	100	30	10	0.046	0.053	0.007
44	Skull #1	0	50	100	30	10	0.046	0.048	0.002
45	Skull #1	0	50	100	30	10	0.046	0.051	0.005
46	Skull #1	0	50	100	30	10	0.046	0.043	-0.003
47	Skull #1	0	50	100	30	10	0.046	0.030	-0.016
48	Skull #1	0	50	100	30	10	0.046	0.038	-0.008
49	Skull #1	0	50	100	30	10	0.046	0.034	-0.012
50	Skull #1	0	50	100	30	10	0.046	0.036	-0.010
51	Skull #1	0	50	100	30	10	0.046	0.035	-0.011
52	Skull #1	0	50	100	30	10	0.046	0.040	-0.006
53	Skull	0	50	100	30	10	0.046	0.045	-0.001

	#1								
54	Skull #1	0	50	100	30	10	0.046	0.048	0.002
55	Skull #1	0	50	100	30	10	0.046	0.038	-0.008
56	Skull #1	0	50	100	30	10	0.046	0.046	0.000
57	Skull #1	0	50	100	30	10	0.046	0.043	-0.003
58	Skull #1	0	50	100	30	10	0.046	0.039	-0.007
59	Skull #1	0	50	100	30	10	0.046	0.035	-0.011
60	Skull #1	0	50	100	30	10	0.046	0.042	-0.004
1	Skull #1	50	50	100	30	10	0.046	0.036	-0.010
2	Skull #1	50	50	100	30	10	0.046	0.051	0.005
3	Skull #1	50	50	100	30	10	0.046	0.041	-0.005
4	Skull #1	50	50	100	30	10	0.046	0.046	0.000
5	Skull #1	50	50	100	30	10	0.046	0.050	0.004
6	Skull #1	50	50	100	30	10	0.046	0.044	-0.002
7	Skull #1	50	50	100	30	10	0.046	0.040	-0.006
8	Skull #1	50	50	100	30	10	0.046	0.049	0.003
9	Skull #1	50	50	100	30	10	0.046	0.046	0.000
10	Skull #1	50	50	100	30	10	0.046	0.048	0.002
11	Skull #1	50	50	100	30	10	0.046	0.040	-0.006
12	Skull #1	50	50	100	30	10	0.046	0.037	-0.009
13	Skull #1	50	50	100	30	10	0.046	0.038	-0.008
14	Skull #1	50	50	100	30	10	0.046	0.039	-0.007
15	Skull #1	50	50	100	30	10	0.046	0.037	-0.009

16	Skull #1	50	50	100	30	10	0.046	0.038	-0.008
17	Skull #1	50	50	100	30	10	0.046	0.043	-0.003
18	Skull #1	50	50	100	30	10	0.046	0.045	-0.001
19	Skull #1	50	50	100	30	10	0.046	0.047	0.001
20	Skull #1	50	50	100	30	10	0.046	0.042	-0.004
21	Skull #1	50	50	100	30	10	0.046	0.039	-0.007
22	Skull #1	50	50	100	30	10	0.046	0.045	-0.001
23	Skull #1	50	50	100	30	10	0.046	0.034	-0.012
24	Skull #1	50	50	100	30	10	0.046	0.038	-0.008
25	Skull #1	50	50	100	30	10	0.046	0.049	0.003
26	Skull #1	50	50	100	30	10	0.046	0.038	-0.008
27	Skull #1	50	50	100	30	10	0.046	0.037	-0.009
28	Skull #1	50	50	100	30	10	0.046	0.033	-0.013
29	Skull #1	50	50	100	30	10	0.046	0.040	-0.006
30	Skull #1	50	50	100	30	10	0.046	0.041	-0.005
31	Skull #1	50	50	100	30	10	0.046	0.033	-0.013
32	Skull #1	50	50	100	30	10	0.046	0.039	-0.007
33	Skull #1	50	50	100	30	10	0.046	0.034	-0.012
34	Skull #1	50	50	100	30	10	0.046	0.042	-0.004
35	Skull #1	50	50	100	30	10	0.046	0.057	0.011
36	Skull #1	50	50	100	30	10	0.046	0.045	-0.001
37	Skull #1	50	50	100	30	10	0.046	0.042	-0.004
38	Skull	50	50	100	30	10	0.046	0.039	-0.007

	#1								
39	Skull #1	50	50	100	30	10	0.046	0.053	0.007
40	Skull #1	50	50	100	30	10	0.046	0.053	0.007
41	Skull #1	50	50	100	30	10	0.046	0.048	0.002
42	Skull #1	50	50	100	30	10	0.046	0.053	0.007
43	Skull #1	50	50	100	30	10	0.046	0.062	0.016
44	Skull #1	50	50	100	30	10	0.046	0.047	0.001
45	Skull #1	50	50	100	30	10	0.046	0.050	0.004
46	Skull #1	50	50	100	30	10	0.046	0.045	-0.001
47	Skull #1	50	50	100	30	10	0.046	0.055	0.009
48	Skull #1	50	50	100	30	10	0.046	0.060	0.014
49	Skull #1	50	50	100	30	10	0.046	0.047	0.001
50	Skull #1	50	50	100	30	10	0.046	0.047	0.001
51	Skull #1	50	50	100	30	10	0.046	0.048	0.002
52	Skull #1	50	50	100	30	10	0.046	0.052	0.006
53	Skull #1	50	50	100	30	10	0.046	0.058	0.012
54	Skull #1	50	50	100	30	10	0.046	0.044	-0.002
55	Skull #1	50	50	100	30	10	0.046	0.044	-0.002
56	Skull #1	50	50	100	30	10	0.046	0.046	0.000
57	Skull #1	50	50	100	30	10	0.046	0.038	-0.008
58	Skull #1	50	50	100	30	10	0.046	0.038	-0.008
59	Skull #1	50	50	100	30	10	0.046	0.041	-0.005
60	Skull #1	50	50	100	30	10	0.046	0.036	-0.010

61	Skull #1	50	50	100	30	10	0.046	0.041	-0.005
62	Skull #1	50	50	100	30	10	0.046	0.035	-0.011
1	Skull #1	100	50	100	30	10	0.046	0.039	-0.007
2	Skull #1	100	50	100	30	10	0.046	0.044	-0.002
3	Skull #1	100	50	100	30	10	0.046	0.047	0.001
4	Skull #1	100	50	100	30	10	0.046	0.049	0.003
5	Skull #1	100	50	100	30	10	0.046	0.047	0.001
6	Skull #1	100	50	100	30	10	0.046	0.049	0.003
7	Skull #1	100	50	100	30	10	0.046	0.040	-0.006
8	Skull #1	100	50	100	30	10	0.046	0.051	0.005
9	Skull #1	100	50	100	30	10	0.046	0.042	-0.004
10	Skull #1	100	50	100	30	10	0.046	0.036	-0.010
11	Skull #1	100	50	100	30	10	0.046	0.051	0.005
12	Skull #1	100	50	100	30	10	0.046	0.041	-0.005
13	Skull #1	100	50	100	30	10	0.046	0.050	0.004
14	Skull #1	100	50	100	30	10	0.046	0.046	0.000
15	Skull #1	100	50	100	30	10	0.046	0.047	0.001
16	Skull #1	100	50	100	30	10	0.046	0.039	-0.007
17	Skull #1	100	50	100	30	10	0.046	0.054	0.008
18	Skull #1	100	50	100	30	10	0.046	0.049	0.003
19	Skull #1	100	50	100	30	10	0.046	0.043	-0.003
20	Skull #1	100	50	100	30	10	0.046	0.045	-0.001
1	Skull	125	50	100	30	10	0.046	0.052	0.006

	#1								
2	Skull #1	125	50	100	30	10	0.046	0.047	0.001
3	Skull #1	125	50	100	30	10	0.046	0.052	0.006
4	Skull #1	125	50	100	30	10	0.046	0.042	-0.004
5	Skull #1	125	50	100	30	10	0.046	0.046	0.000
6	Skull #1	125	50	100	30	10	0.046	0.051	0.005
7	Skull #1	125	50	100	30	10	0.046	0.040	-0.006
8	Skull #1	125	50	100	30	10	0.046	0.047	0.001
9	Skull #1	125	50	100	30	10	0.046	0.058	0.012
10	Skull #1	125	50	100	30	10	0.046	0.045	-0.001
11	Skull #1	125	50	100	30	10	0.046	0.042	-0.004
12	Skull #1	125	50	100	30	10	0.046	0.045	-0.001
13	Skull #1	125	50	100	30	10	0.046	0.044	-0.002
14	Skull #1	125	50	100	30	10	0.046	0.047	0.001
15	Skull #1	125	50	100	30	10	0.046	0.039	-0.007
16	Skull #1	125	50	100	30	10	0.046	0.046	0.000
17	Skull #1	125	50	100	30	10	0.046	0.044	-0.002
18	Skull #1	125	50	100	30	10	0.046	0.044	-0.002
19	Skull #1	125	50	100	30	10	0.046	0.049	0.003
20	Skull #1	125	50	100	30	10	0.046	0.048	0.002
21	Skull #1	125	50	100	30	10	0.046	0.048	0.002
22	Skull #1	125	50	100	30	10	0.046	0.037	-0.009
23	Skull #1	125	50	100	30	10	0.046	0.042	-0.004

24	Skull #1	125	50	100	30	10	0.046	0.054	0.008
25	Skull #1	125	50	100	30	10	0.046	0.037	-0.009
26	Skull #1	125	50	100	30	10	0.046	0.031	-0.015
27	Skull #1	125	50	100	30	10	0.046	0.033	-0.013
28	Skull #1	125	50	100	30	10	0.046	0.045	-0.001
29	Skull #1	125	50	100	30	10	0.046	0.046	0.000
30	Skull #1	125	50	100	30	10	0.046	0.040	-0.006
31	Skull #1	125	50	100	30	10	0.046	0.039	-0.007
32	Skull #1	125	50	100	30	10	0.046	0.041	-0.005
33	Skull #1	125	50	100	30	10	0.046	0.039	-0.007
34	Skull #1	125	50	100	30	10	0.046	0.034	-0.012
35	Skull #1	125	50	100	30	10	0.046	0.039	-0.007
36	Skull #1	125	50	100	30	10	0.046	0.043	-0.003
37	Skull #1	125	50	100	30	10	0.046	0.041	-0.005
38	Skull #1	125	50	100	30	10	0.046	0.044	-0.002
39	Skull #1	125	50	100	30	10	0.046	0.042	-0.004
40	Skull #1	125	50	100	30	10	0.046	0.048	0.002
41	Skull #1	125	50	100	30	10	0.046	0.054	0.008
42	Skull #1	125	50	100	30	10	0.046	0.053	0.007
43	Skull #1	125	50	100	30	10	0.046	0.047	0.001
44	Skull #1	125	50	100	30	10	0.046	0.049	0.003
45	Skull #1	125	50	100	30	10	0.046	0.047	0.001
46	Skull	125	50	100	30	10	0.046	0.047	0.001

	#1								
47	Skull #1	125	50	100	30	10	0.046	0.043	-0.003
48	Skull #1	125	50	100	30	10	0.046	0.048	0.002
49	Skull #1	125	50	100	30	10	0.046	0.057	0.011
50	Skull #1	125	50	100	30	10	0.046	0.048	0.002
51	Skull #1	125	50	100	30	10	0.046	0.048	0.002
52	Skull #1	125	50	100	30	10	0.046	0.046	0.000
53	Skull #1	125	50	100	30	10	0.046	0.044	-0.002
54	Skull #1	125	50	100	30	10	0.046	0.061	0.015
55	Skull #1	125	50	100	30	10	0.046	0.055	0.009
56	Skull #1	125	50	100	30	10	0.046	0.047	0.001
57	Skull #1	125	50	100	30	10	0.046	0.041	-0.005
58	Skull #1	125	50	100	30	10	0.046	0.047	0.001
59	Skull #1	125	50	100	30	10	0.046	0.036	-0.010
60	Skull #1	125	50	100	30	10	0.046	0.035	-0.011
61	Skull #1	125	50	100	30	10	0.046	0.040	-0.006
62	Skull #1	125	50	100	30	10	0.046	0.040	-0.006
63	Skull #1	125	50	100	30	10	0.046	0.039	-0.007
1	Skull #1	150	50	100	30	10	0.046	0.049	0.003
2	Skull #1	150	50	100	30	10	0.046	0.047	0.001
3	Skull #1	150	50	100	30	10	0.046	0.052	0.006
4	Skull #1	150	50	100	30	10	0.046	0.052	0.006
5	Skull #1	150	50	100	30	10	0.046	0.057	0.011

6	Skull #1	150	50	100	30	10	0.046	0.048	0.002
7	Skull #1	150	50	100	30	10	0.046	0.045	-0.001
8	Skull #1	150	50	100	30	10	0.046	0.041	-0.005
9	Skull #1	150	50	100	30	10	0.046	0.047	0.001
10	Skull #1	150	50	100	30	10	0.046	0.044	-0.002
11	Skull #1	150	50	100	30	10	0.046	0.046	0.000
12	Skull #1	150	50	100	30	10	0.046	0.045	-0.001
13	Skull #1	150	50	100	30	10	0.046	0.047	0.001
14	Skull #1	150	50	100	30	10	0.046	0.047	0.001
15	Skull #1	150	50	100	30	10	0.046	0.042	-0.004
16	Skull #1	150	50	100	30	10	0.046	0.049	0.003
17	Skull #1	150	50	100	30	10	0.046	0.046	0.000
18	Skull #1	150	50	100	30	10	0.046	0.055	0.009
19	Skull #1	150	50	100	30	10	0.046	0.045	-0.001
20	Skull #1	150	50	100	30	10	0.046	0.045	-0.001
21	Skull #1	150	50	100	30	10	0.046	0.043	-0.003
22	Skull #1	150	50	100	30	10	0.046	0.039	-0.007
23	Skull #1	150	50	100	30	10	0.046	0.034	-0.012
24	Skull #1	150	50	100	30	10	0.046	0.040	-0.006
25	Skull #1	150	50	100	30	10	0.046	0.038	-0.008
26	Skull #1	150	50	100	30	10	0.046	0.047	0.001
27	Skull #1	150	50	100	30	10	0.046	0.040	-0.006
28	Skull	150	50	100	30	10	0.046	0.038	-0.008

	#1								
29	Skull #1	150	50	100	30	10	0.046	0.039	-0.007
30	Skull #1	150	50	100	30	10	0.046	0.043	-0.003
31	Skull #1	150	50	100	30	10	0.046	0.043	-0.003
32	Skull #1	150	50	100	30	10	0.046	0.037	-0.009
33	Skull #1	150	50	100	30	10	0.046	0.040	-0.006
34	Skull #1	150	50	100	30	10	0.046	0.042	-0.004
35	Skull #1	150	50	100	30	10	0.046	0.042	-0.004
36	Skull #1	150	50	100	30	10	0.046	0.056	0.010
37	Skull #1	150	50	100	30	10	0.046	0.040	-0.006
38	Skull #1	150	50	100	30	10	0.046	0.043	-0.003
39	Skull #1	150	50	100	30	10	0.046	0.043	-0.003
40	Skull #1	150	50	100	30	10	0.046	0.042	-0.004
41	Skull #1	150	50	100	30	10	0.046	0.053	0.007
42	Skull #1	150	50	100	30	10	0.046	0.046	0.000
43	Skull #1	150	50	100	30	10	0.046	0.048	0.002
44	Skull #1	150	50	100	30	10	0.046	0.047	0.001
45	Skull #1	150	50	100	30	10	0.046	0.056	0.010
46	Skull #1	150	50	100	30	10	0.046	0.041	-0.005
47	Skull #1	150	50	100	30	10	0.046	0.047	0.001
48	Skull #1	150	50	100	30	10	0.046	0.053	0.007
49	Skull #1	150	50	100	30	10	0.046	0.050	0.004
50	Skull #1	150	50	100	30	10	0.046	0.049	0.003

51	Skull #1	150	50	100	30	10	0.046	0.051	0.005
52	Skull #1	150	50	100	30	10	0.046	0.050	0.004
53	Skull #1	150	50	100	30	10	0.046	0.056	0.010
54	Skull #1	150	50	100	30	10	0.046	0.044	-0.002
55	Skull #1	150	50	100	30	10	0.046	0.048	0.002
56	Skull #1	150	50	100	30	10	0.046	0.046	0.000
57	Skull #1	150	50	100	30	10	0.046	0.044	-0.002
58	Skull #1	150	50	100	30	10	0.046	0.048	0.002
59	Skull #1	150	50	100	30	10	0.046	0.044	-0.002
60	Skull #1	150	50	100	30	10	0.046	0.041	-0.005
61	Skull #1	150	50	100	30	10	0.046	0.035	-0.011
62	Skull #1	150	50	100	30	10	0.046	0.038	-0.008
63	Skull #1	150	50	100	30	10	0.046	0.049	0.003
64	Skull #1	150	50	100	30	10	0.046	0.040	-0.006
65	Skull #1	150	50	100	30	10	0.046	0.039	-0.007
1	Skull #1	200	50	100	30	10	0.046	0.056	0.010
2	Skull #1	200	50	100	30	10	0.046	0.044	-0.002
3	Skull #1	200	50	100	30	10	0.046	0.036	-0.010
4	Skull #1	200	50	100	30	10	0.046	0.039	-0.007
5	Skull #1	200	50	100	30	10	0.046	0.038	-0.008
6	Skull #1	200	50	100	30	10	0.046	0.040	-0.006
7	Skull #1	200	50	100	30	10	0.046	0.047	0.001
8	Skull	200	50	100	30	10	0.046	0.038	-0.008

	#1								
9	Skull #1	200	50	100	30	10	0.046	0.039	-0.007
10	Skull #1	200	50	100	30	10	0.046	0.034	-0.012
11	Skull #1	200	50	100	30	10	0.046	0.052	0.006
12	Skull #1	200	50	100	30	10	0.046	0.480	0.434
13	Skull #1	200	50	100	30	10	0.046	0.044	-0.002
14	Skull #1	200	50	100	30	10	0.046	0.043	-0.003
15	Skull #1	200	50	100	30	10	0.046	0.050	0.004
16	Skull #1	200	50	100	30	10	0.046	0.052	0.006
17	Skull #1	200	50	100	30	10	0.046	0.046	0.000
18	Skull #1	200	50	100	30	10	0.046	0.029	-0.017
19	Skull #1	200	50	100	30	10	0.046	0.045	-0.001
20	Skull #1	200	50	100	30	10	0.046	0.043	-0.003
1	Skull #1	235	50	100	30	10	0.046	0.053	0.007
2	Skull #1	235	50	100	30	10	0.046	0.046	0.000
3	Skull #1	235	50	100	30	10	0.046	0.041	-0.005
4	Skull #1	235	50	100	30	10	0.046	0.040	-0.006
5	Skull #1	235	50	100	30	10	0.046	0.041	-0.005
6	Skull #1	235	50	100	30	10	0.046	0.047	0.001
7	Skull #1	235	50	100	30	10	0.046	0.045	-0.001
8	Skull #1	235	50	100	30	10	0.046	0.036	-0.010
9	Skull #1	235	50	100	30	10	0.046	0.036	-0.010
10	Skull #1	235	50	100	30	10	0.046	0.046	0.000

11	Skull #1	235	50	100	30	10	0.046	0.051	0.005
12	Skull #1	235	50	100	30	10	0.046	0.048	0.002
13	Skull #1	235	50	100	30	10	0.046	0.043	-0.003
14	Skull #1	235	50	100	30	10	0.046	0.041	-0.005
15	Skull #1	235	50	100	30	10	0.046	0.043	-0.003
16	Skull #1	235	50	100	30	10	0.046	0.045	-0.001
17	Skull #1	235	50	100	30	10	0.046	0.048	0.002
18	Skull #1	235	50	100	30	10	0.046	0.039	-0.007
19	Skull #1	235	50	100	30	10	0.046	0.042	-0.004
20	Skull #1	235	50	100	30	10	0.046	0.042	-0.004
1	Skull #1	270	50	100	30	10	0.046	0.045	-0.001
2	Skull #1	270	50	100	30	10	0.046	0.047	0.001
3	Skull #1	270	50	100	30	10	0.046	0.041	-0.005
4	Skull #1	270	50	100	30	10	0.046	0.039	-0.007
5	Skull #1	270	50	100	30	10	0.046	0.041	-0.005
6	Skull #1	270	50	100	30	10	0.046	0.040	-0.006
7	Skull #1	270	50	100	30	10	0.046	0.044	-0.002
8	Skull #1	270	50	100	30	10	0.046	0.045	-0.001
9	Skull #1	270	50	100	30	10	0.046	0.035	-0.011
10	Skull #1	270	50	100	30	10	0.046	0.039	-0.007
11	Skull #1	270	50	100	30	10	0.046	0.049	0.003
12	Skull #1	270	50	100	30	10	0.046	0.046	0.000
13	Skull	270	50	100	30	10	0.046	0.053	0.007

180

	#1								
14	Skull #1	270	50	100	30	10	0.046	0.055	0.009
15	Skull #1	270	50	100	30	10	0.046	0.047	0.001
16	Skull #1	270	50	100	30	10	0.046	0.041	-0.005
17	Skull #1	270	50	100	30	10	0.046	0.045	-0.001
18	Skull #1	270	50	100	30	10	0.046	0.048	0.002
19	Skull #1	270	50	100	30	10	0.046	0.062	0.016
20	Skull #1	270	50	100	30	10	0.046	0.034	-0.012
21	Skull #1	270	50	100	30	10	0.046	0.043	-0.003
22	Skull #1	270	50	100	30	10	0.046	0.055	0.009
1	Skull #1	400	50	100	30	10	0.046	0.044	-0.002
2	Skull #1	400	50	100	30	10	0.046	0.052	0.006
3	Skull #1	400	50	100	30	10	0.046	0.061	0.015
4	Skull #1	400	50	100	30	10	0.046	0.049	0.003
5	Skull #1	400	50	100	30	10	0.046	0.043	-0.003
6	Skull #1	400	50	100	30	10	0.046	0.045	-0.001
7	Skull #1	400	50	100	30	10	0.046	0.053	0.007
8	Skull #1	400	50	100	30	10	0.046	0.044	-0.002
9	Skull #1	400	50	100	30	10	0.046	0.039	-0.007
10	Skull #1	400	50	100	30	10	0.046	0.046	0.000
11	Skull #1	400	50	100	30	10	0.046	0.044	-0.002
12	Skull #1	400	50	100	30	10	0.046	0.048	0.002
13	Skull #1	400	50	100	30	10	0.046	0.052	0.006

14	Skull #1	400	50	100	30	10	0.046	0.055	0.009
15	Skull #1	400	50	100	30	10	0.046	0.042	-0.004
16	Skull #1	400	50	100	30	10	0.046	0.065	0.019
17	Skull #1	400	50	100	30	10	0.046	0.039	-0.007
18	Skull #1	400	50	100	30	10	0.046	0.049	0.003
19	Skull #1	400	50	100	30	10	0.046	0.054	0.008
20	Skull #1	400	50	100	30	10	0.046	0.046	0.000

Table D-11 Clot fragmentation data collected for 60µm sized mesh filters from all acoustic output groups tested

Exp #	Skull ID	AP (W)	DC (%)	PW (ms)	ID (sec)	Flow (ml/min)	60 PreFUS Wt (g)	60 PostFUS Wt (g)	60 Wt Gain (g)
1	Skull #1	0	50	100	30	10	0.019	0.021	0.002
2	Skull #1	0	50	100	30	10	0.019	0.024	0.005
3	Skull #1	0	50	100	30	10	0.019	0.021	0.002
4	Skull #1	0	50	100	30	10	0.019	0.021	0.002
5	Skull #1	0	50	100	30	10	0.019	0.018	-0.001
6	Skull #1	0	50	100	30	10	0.019	0.021	0.002
7	Skull #1	0	50	100	30	10	0.019	0.019	0.000
8	Skull #1	0	50	100	30	10	0.019	0.021	0.002
9	Skull #1	0	50	100	30	10	0.019	0.020	0.001
10	Skull #1	0	50	100	30	10	0.019	0.020	0.001
11	Skull #1	0	50	100	30	10	0.019	0.021	0.002
12	Skull	0	50	100	30	10	0.019	0.022	0.003

	#1								
13	Skull #1	0	50	100	30	10	0.019	0.026	0.007
14	Skull #1	0	50	100	30	10	0.019	0.023	0.004
15	Skull #1	0	50	100	30	10	0.019	0.018	-0.001
16	Skull #1	0	50	100	30	10	0.019	0.020	0.001
17	Skull #1	0	50	100	30	10	0.019	0.021	0.002
18	Skull #1	0	50	100	30	10	0.019	0.022	0.003
19	Skull #1	0	50	100	30	10	0.019	0.022	0.003
20	Skull #1	0	50	100	30	10	0.019	0.019	0.000
21	Skull #1	0	50	100	30	10	0.019	0.021	0.002
22	Skull #1	0	50	100	30	10	0.019	0.022	0.003
23	Skull #1	0	50	100	30	10	0.019	0.021	0.002
24	Skull #1	0	50	100	30	10	0.019	0.021	0.002
25	Skull #1	0	50	100	30	10	0.019	0.021	0.002
26	Skull #1	0	50	100	30	10	0.019	0.019	0.000
27	Skull #1	0	50	100	30	10	0.019	0.021	0.002
28	Skull #1	0	50	100	30	10	0.019	0.020	0.001
29	Skull #1	0	50	100	30	10	0.019	0.021	0.002
30	Skull #1	0	50	100	30	10	0.019	0.021	0.002
31	Skull #1	0	50	100	30	10	0.019	0.026	0.007
32	Skull #1	0	50	100	30	10	0.019	0.024	0.005
33	Skull #1	0	50	100	30	10	0.019	0.023	0.004
34	Skull #1	0	50	100	30	10	0.019	0.041	0.022

35	Skull #1	0	50	100	30	10	0.019	0.026	0.007
36	Skull #1	0	50	100	30	10	0.019	0.026	0.007
37	Skull #1	0	50	100	30	10	0.019	0.021	0.002
38	Skull #1	0	50	100	30	10	0.019	0.024	0.005
39	Skull #1	0	50	100	30	10	0.019	0.025	0.006
40	Skull #1	0	50	100	30	10	0.019	0.027	0.008
41	Skull #1	0	50	100	30	10	0.019	0.024	0.005
42	Skull #1	0	50	100	30	10	0.019	0.022	0.003
43	Skull #1	0	50	100	30	10	0.019	0.024	0.005
44	Skull #1	0	50	100	30	10	0.019	0.025	0.006
45	Skull #1	0	50	100	30	10	0.019	0.028	0.009
46	Skull #1	0	50	100	30	10	0.019	0.027	0.008
47	Skull #1	0	50	100	30	10	0.019	0.022	0.003
48	Skull #1	0	50	100	30	10	0.019	0.024	0.005
49	Skull #1	0	50	100	30	10	0.019	0.020	0.001
50	Skull #1	0	50	100	30	10	0.019	0.024	0.005
51	Skull #1	0	50	100	30	10	0.019	0.024	0.005
52	Skull #1	0	50	100	30	10	0.019	0.020	0.001
53	Skull #1	0	50	100	30	10	0.019	0.026	0.007
54	Skull #1	0	50	100	30	10	0.019	0.022	0.003
55	Skull #1	0	50	100	30	10	0.019	0.025	0.006
56	Skull #1	0	50	100	30	10	0.019	0.023	0.004
57	Skull	0	50	100	30	10	0.019	0.023	0.004

	#1								
58	Skull #1	0	50	100	30	10	0.019	0.025	0.006
59	Skull #1	0	50	100	30	10	0.019	0.028	0.009
60	Skull #1	0	50	100	30	10	0.019	0.023	0.004
1	Skull #1	50	50	100	30	10	0.019	0.020	0.001
2	Skull #1	50	50	100	30	10	0.019	0.020	0.001
3	Skull #1	50	50	100	30	10	0.019	0.022	0.003
4	Skull #1	50	50	100	30	10	0.019	0.021	0.002
5	Skull #1	50	50	100	30	10	0.019	0.023	0.004
6	Skull #1	50	50	100	30	10	0.019	0.021	0.002
7	Skull #1	50	50	100	30	10	0.019	0.027	0.008
8	Skull #1	50	50	100	30	10	0.019	0.021	0.002
9	Skull #1	50	50	100	30	10	0.019	0.021	0.002
10	Skull #1	50	50	100	30	10	0.019	0.021	0.002
11	Skull #1	50	50	100	30	10	0.019	0.020	0.001
12	Skull #1	50	50	100	30	10	0.019	0.027	0.008
13	Skull #1	50	50	100	30	10	0.019	0.023	0.004
14	Skull #1	50	50	100	30	10	0.019	0.021	0.002
15	Skull #1	50	50	100	30	10	0.019	0.021	0.002
16	Skull #1	50	50	100	30	10	0.019	0.020	0.001
17	Skull #1	50	50	100	30	10	0.019	0.022	0.003
18	Skull #1	50	50	100	30	10	0.019	0.023	0.004
19	Skull #1	50	50	100	30	10	0.019	0.020	0.001

20	Skull #1	50	50	100	30	10	0.019	0.020	0.001
21	Skull #1	50	50	100	30	10	0.019	0.020	0.001
22	Skull #1	50	50	100	30	10	0.019	0.025	0.006
23	Skull #1	50	50	100	30	10	0.019	0.022	0.003
24	Skull #1	50	50	100	30	10	0.019	0.030	0.011
25	Skull #1	50	50	100	30	10	0.019	0.024	0.005
26	Skull #1	50	50	100	30	10	0.019	0.026	0.007
27	Skull #1	50	50	100	30	10	0.019	0.018	-0.001
28	Skull #1	50	50	100	30	10	0.019	0.020	0.001
29	Skull #1	50	50	100	30	10	0.019	0.018	-0.001
30	Skull #1	50	50	100	30	10	0.019	0.021	0.002
31	Skull #1	50	50	100	30	10	0.019	0.019	0.000
32	Skull #1	50	50	100	30	10	0.019	0.024	0.005
33	Skull #1	50	50	100	30	10	0.019	0.021	0.002
34	Skull #1	50	50	100	30	10	0.019	0.022	0.003
35	Skull #1	50	50	100	30	10	0.019	0.022	0.003
36	Skull #1	50	50	100	30	10	0.019	0.019	0.000
37	Skull #1	50	50	100	30	10	0.019	0.025	0.006
38	Skull #1	50	50	100	30	10	0.019	0.021	0.002
39	Skull #1	50	50	100	30	10	0.019	0.021	0.002
40	Skull #1	50	50	100	30	10	0.019	0.021	0.002
41	Skull #1	50	50	100	30	10	0.019	0.026	0.007
42	Skull	50	50	100	30	10	0.019	0.029	0.010

	#1								
43	Skull #1	50	50	100	30	10	0.019	0.025	0.006
44	Skull #1	50	50	100	30	10	0.019	0.027	0.008
45	Skull #1	50	50	100	30	10	0.019	0.021	0.002
46	Skull #1	50	50	100	30	10	0.019	0.020	0.001
47	Skull #1	50	50	100	30	10	0.019	0.025	0.006
48	Skull #1	50	50	100	30	10	0.019	0.024	0.005
49	Skull #1	50	50	100	30	10	0.019	0.022	0.003
50	Skull #1	50	50	100	30	10	0.019	0.028	0.009
51	Skull #1	50	50	100	30	10	0.019	0.027	0.008
52	Skull #1	50	50	100	30	10	0.019	0.028	0.009
53	Skull #1	50	50	100	30	10	0.019	0.029	0.010
54	Skull #1	50	50	100	30	10	0.019	0.027	0.008
55	Skull #1	50	50	100	30	10	0.019	0.020	0.001
56	Skull #1	50	50	100	30	10	0.019	0.020	0.001
57	Skull #1	50	50	100	30	10	0.019	0.023	0.004
58	Skull #1	50	50	100	30	10	0.019	0.019	0.000
59	Skull #1	50	50	100	30	10	0.019	0.020	0.001
60	Skull #1	50	50	100	30	10	0.019	0.024	0.005
61	Skull #1	50	50	100	30	10	0.019	0.027	0.008
62	Skull #1	50	50	100	30	10	0.019	0.020	0.001
1	Skull #1	100	50	100	30	10	0.019	0.023	0.004
2	Skull #1	100	50	100	30	10	0.019	0.021	0.002

3	Skull #1	100	50	100	30	10	0.019	0.022	0.003
4	Skull #1	100	50	100	30	10	0.019	0.200	0.181
5	Skull #1	100	50	100	30	10	0.019	0.021	0.002
6	Skull #1	100	50	100	30	10	0.019	0.031	0.012
7	Skull #1	100	50	100	30	10	0.019	0.023	0.004
8	Skull #1	100	50	100	30	10	0.019	0.028	0.009
9	Skull #1	100	50	100	30	10	0.019	0.022	0.003
10	Skull #1	100	50	100	30	10	0.019	0.022	0.003
11	Skull #1	100	50	100	30	10	0.019	0.023	0.004
12	Skull #1	100	50	100	30	10	0.019	0.022	0.003
13	Skull #1	100	50	100	30	10	0.019	0.025	0.006
14	Skull #1	100	50	100	30	10	0.019	0.021	0.002
15	Skull #1	100	50	100	30	10	0.019	0.023	0.004
16	Skull #1	100	50	100	30	10	0.019	0.021	0.002
17	Skull #1	100	50	100	30	10	0.019	0.025	0.006
18	Skull #1	100	50	100	30	10	0.019	0.023	0.004
19	Skull #1	100	50	100	30	10	0.019	0.021	0.002
20	Skull #1	100	50	100	30	10	0.019	0.026	0.007
1	Skull #1	125	50	100	30	10	0.019	0.022	0.003
2	Skull #1	125	50	100	30	10	0.019	0.024	0.005
3	Skull #1	125	50	100	30	10	0.019	0.022	0.003
4	Skull #1	125	50	100	30	10	0.019	0.015	-0.004
5	Skull	125	50	100	30	10	0.019	0.022	0.003

	#1								
6	Skull #1	125	50	100	30	10	0.019	0.023	0.004
7	Skull #1	125	50	100	30	10	0.019	0.024	0.005
8	Skull #1	125	50	100	30	10	0.019	0.023	0.004
9	Skull #1	125	50	100	30	10	0.019	0.022	0.003
10	Skull #1	125	50	100	30	10	0.019	0.020	0.001
11	Skull #1	125	50	100	30	10	0.019	0.020	0.001
12	Skull #1	125	50	100	30	10	0.019	0.023	0.004
13	Skull #1	125	50	100	30	10	0.019	0.022	0.003
14	Skull #1	125	50	100	30	10	0.019	0.023	0.004
15	Skull #1	125	50	100	30	10	0.019	0.023	0.004
16	Skull #1	125	50	100	30	10	0.019	0.024	0.005
17	Skull #1	125	50	100	30	10	0.019	0.024	0.005
18	Skull #1	125	50	100	30	10	0.019	0.021	0.002
19	Skull #1	125	50	100	30	10	0.019	0.022	0.003
20	Skull #1	125	50	100	30	10	0.019	0.027	0.008
21	Skull #1	125	50	100	30	10	0.019	0.021	0.002
22	Skull #1	125	50	100	30	10	0.019	0.020	0.001
23	Skull #1	125	50	100	30	10	0.019	0.022	0.003
24	Skull #1	125	50	100	30	10	0.019	0.021	0.002
25	Skull #1	125	50	100	30	10	0.019	0.021	0.002
26	Skull #1	125	50	100	30	10	0.019	0.018	-0.001
27	Skull #1	125	50	100	30	10	0.019	0.019	0.000

28	Skull #1	125	50	100	30	10	0.019	0.019	0.000
29	Skull #1	125	50	100	30	10	0.019	0.022	0.003
30	Skull #1	125	50	100	30	10	0.019	0.019	0.000
31	Skull #1	125	50	100	30	10	0.019	0.025	0.006
32	Skull #1	125	50	100	30	10	0.019	0.020	0.001
33	Skull #1	125	50	100	30	10	0.019	0.024	0.005
34	Skull #1	125	50	100	30	10	0.019	0.024	0.005
35	Skull #1	125	50	100	30	10	0.019	0.021	0.002
36	Skull #1	125	50	100	30	10	0.019	0.023	0.004
37	Skull #1	125	50	100	30	10	0.019	0.019	0.000
38	Skull #1	125	50	100	30	10	0.019	0.021	0.002
39	Skull #1	125	50	100	30	10	0.019	0.020	0.001
40	Skull #1	125	50	100	30	10	0.019	0.022	0.003
41	Skull #1	125	50	100	30	10	0.019	0.025	0.006
42	Skull #1	125	50	100	30	10	0.019	0.027	0.008
43	Skull #1	125	50	100	30	10	0.019	0.028	0.009
44	Skull #1	125	50	100	30	10	0.019	0.025	0.006
45	Skull #1	125	50	100	30	10	0.019	0.027	0.008
46	Skull #1	125	50	100	30	10	0.019	0.022	0.003
47	Skull #1	125	50	100	30	10	0.019	0.024	0.005
48	Skull #1	125	50	100	30	10	0.019	0.025	0.006
49	Skull #1	125	50	100	30	10	0.019	0.026	0.007
50	Skull	125	50	100	30	10	0.019	0.026	0.007

	#1								
51	Skull #1	125	50	100	30	10	0.019	0.027	0.008
52	Skull #1	125	50	100	30	10	0.019	0.019	0.000
53	Skull #1	125	50	100	30	10	0.019	0.026	0.007
54	Skull #1	125	50	100	30	10	0.019	0.020	0.001
55	Skull #1	125	50	100	30	10	0.019	0.031	0.012
56	Skull #1	125	50	100	30	10	0.019	0.020	0.001
57	Skull #1	125	50	100	30	10	0.019	0.023	0.004
58	Skull #1	125	50	100	30	10	0.019	0.020	0.001
59	Skull #1	125	50	100	30	10	0.019	0.023	0.004
60	Skull #1	125	50	100	30	10	0.019	0.021	0.002
61	Skull #1	125	50	100	30	10	0.019	0.022	0.003
62	Skull #1	125	50	100	30	10	0.019	0.021	0.002
63	Skull #1	125	50	100	30	10	0.019	0.018	-0.001
1	Skull #1	150	50	100	30	10	0.019	0.007	-0.012
2	Skull #1	150	50	100	30	10	0.019	0.023	0.004
3	Skull #1	150	50	100	30	10	0.019	0.022	0.003
4	Skull #1	150	50	100	30	10	0.019	0.020	0.001
5	Skull #1	150	50	100	30	10	0.019	0.026	0.007
6	Skull #1	150	50	100	30	10	0.019	0.023	0.004
7	Skull #1	150	50	100	30	10	0.019	0.022	0.003
8	Skull #1	150	50	100	30	10	0.019	0.020	0.001
9	Skull #1	150	50	100	30	10	0.019	0.023	0.004

10	Skull #1	150	50	100	30	10	0.019	0.027	0.008
11	Skull #1	150	50	100	30	10	0.019	0.020	0.001
12	Skull #1	150	50	100	30	10	0.019	0.020	0.001
13	Skull #1	150	50	100	30	10	0.019	0.021	0.002
14	Skull #1	150	50	100	30	10	0.019	0.026	0.007
15	Skull #1	150	50	100	30	10	0.019	0.021	0.002
16	Skull #1	150	50	100	30	10	0.019	0.025	0.006
17	Skull #1	150	50	100	30	10	0.019	0.022	0.003
18	Skull #1	150	50	100	30	10	0.019	0.021	0.002
19	Skull #1	150	50	100	30	10	0.019	0.021	0.002
20	Skull #1	150	50	100	30	10	0.019	0.022	0.003
21	Skull #1	150	50	100	30	10	0.019	0.020	0.001
22	Skull #1	150	50	100	30	10	0.019	0.016	-0.003
23	Skull #1	150	50	100	30	10	0.019	0.021	0.002
24	Skull #1	150	50	100	30	10	0.019	0.021	0.002
25	Skull #1	150	50	100	30	10	0.019	0.020	0.001
26	Skull #1	150	50	100	30	10	0.019	0.024	0.005
27	Skull #1	150	50	100	30	10	0.019	0.025	0.006
28	Skull #1	150	50	100	30	10	0.019	0.022	0.003
29	Skull #1	150	50	100	30	10	0.019	0.021	0.002
30	Skull #1	150	50	100	30	10	0.019	0.021	0.002
31	Skull #1	150	50	100	30	10	0.019	0.024	0.005
32	Skull	150	50	100	30	10	0.019	0.021	0.002

	#1								
33	Skull #1	150	50	100	30	10	0.019	0.021	0.002
34	Skull #1	150	50	100	30	10	0.019	0.022	0.003
35	Skull #1	150	50	100	30	10	0.019	0.022	0.003
36	Skull #1	150	50	100	30	10	0.019	0.020	0.001
37	Skull #1	150	50	100	30	10	0.019	0.020	0.001
38	Skull #1	150	50	100	30	10	0.019	0.021	0.002
39	Skull #1	150	50	100	30	10	0.019	0.020	0.001
40	Skull #1	150	50	100	30	10	0.019	0.020	0.001
41	Skull #1	150	50	100	30	10	0.019	0.022	0.003
42	Skull #1	150	50	100	30	10	0.019	0.025	0.006
43	Skull #1	150	50	100	30	10	0.019	0.030	0.011
44	Skull #1	150	50	100	30	10	0.019	0.025	0.006
45	Skull #1	150	50	100	30	10	0.019	0.022	0.003
46	Skull #1	150	50	100	30	10	0.019	0.025	0.006
47	Skull #1	150	50	100	30	10	0.019	0.019	0.000
48	Skull #1	150	50	100	30	10	0.019	0.024	0.005
49	Skull #1	150	50	100	30	10	0.019	0.021	0.002
50	Skull #1	150	50	100	30	10	0.019	0.035	0.016
51	Skull #1	150	50	100	30	10	0.019	0.023	0.004
52	Skull #1	150	50	100	30	10	0.019	0.020	0.001
53	Skull #1	150	50	100	30	10	0.019	0.027	0.008
54	Skull #1	150	50	100	30	10	0.019	0.030	0.011

55	Skull #1	150	50	100	30	10	0.019	0.023	0.004
56	Skull #1	150	50	100	30	10	0.019	0.027	0.008
57	Skull #1	150	50	100	30	10	0.019	0.020	0.001
58	Skull #1	150	50	100	30	10	0.019	0.022	0.003
59	Skull #1	150	50	100	30	10	0.019	0.026	0.007
60	Skull #1	150	50	100	30	10	0.019	0.026	0.007
61	Skull #1	150	50	100	30	10	0.019	0.021	0.002
62	Skull #1	150	50	100	30	10	0.019	0.024	0.005
63	Skull #1	150	50	100	30	10	0.019	0.018	-0.001
64	Skull #1	150	50	100	30	10	0.019	0.020	0.001
65	Skull #1	150	50	100	30	10	0.019	0.022	0.003
1	Skull #1	200	50	100	30	10	0.019	0.024	0.005
2	Skull #1	200	50	100	30	10	0.019	0.210	0.191
3	Skull #1	200	50	100	30	10	0.019	0.023	0.004
4	Skull #1	200	50	100	30	10	0.019	0.022	0.003
5	Skull #1	200	50	100	30	10	0.019	0.023	0.004
6	Skull #1	200	50	100	30	10	0.019	0.019	0.000
7	Skull #1	200	50	100	30	10	0.019	0.023	0.004
8	Skull #1	200	50	100	30	10	0.019	0.021	0.002
9	Skull #1	200	50	100	30	10	0.019	0.022	0.003
10	Skull #1	200	50	100	30	10	0.019	0.021	0.002
11	Skull #1	200	50	100	30	10	0.019	0.021	0.002
12	Skull	200	50	100	30	10	0.019	0.023	0.004

	#1								
13	Skull #1	200	50	100	30	10	0.019	0.021	0.002
14	Skull #1	200	50	100	30	10	0.019	0.200	0.181
15	Skull #1	200	50	100	30	10	0.019	0.025	0.006
16	Skull #1	200	50	100	30	10	0.019	0.025	0.006
17	Skull #1	200	50	100	30	10	0.019	0.022	0.003
18	Skull #1	200	50	100	30	10	0.019	0.022	0.003
19	Skull #1	200	50	100	30	10	0.019	0.023	0.004
20	Skull #1	200	50	100	30	10	0.019	0.017	-0.002
1	Skull #1	235	50	100	30	10	0.019	0.023	0.004
2	Skull #1	235	50	100	30	10	0.019	0.019	0.000
3	Skull #1	235	50	100	30	10	0.019	0.018	-0.001
4	Skull #1	235	50	100	30	10	0.019	0.021	0.002
5	Skull #1	235	50	100	30	10	0.019	0.021	0.002
6	Skull #1	235	50	100	30	10	0.019	0.021	0.002
7	Skull #1	235	50	100	30	10	0.019	0.026	0.007
8	Skull #1	235	50	100	30	10	0.019	0.020	0.001
9	Skull #1	235	50	100	30	10	0.019	0.017	-0.002
10	Skull #1	235	50	100	30	10	0.019	0.025	0.006
11	Skull #1	235	50	100	30	10	0.019	0.026	0.007
12	Skull #1	235	50	100	30	10	0.019	0.020	0.001
13	Skull #1	235	50	100	30	10	0.019	0.019	0.000
14	Skull #1	235	50	100	30	10	0.019	0.019	0.000

15	Skull #1	235	50	100	30	10	0.019	0.026	0.007
16	Skull #1	235	50	100	30	10	0.019	0.020	0.001
17	Skull #1	235	50	100	30	10	0.019	0.022	0.003
18	Skull #1	235	50	100	30	10	0.019	0.024	0.005
19	Skull #1	235	50	100	30	10	0.019	0.024	0.005
20	Skull #1	235	50	100	30	10	0.019	0.023	0.004
1	Skull #1	270	50	100	30	10	0.019	0.023	0.004
2	Skull #1	270	50	100	30	10	0.019	0.019	0.000
3	Skull #1	270	50	100	30	10	0.019	0.017	-0.002
4	Skull #1	270	50	100	30	10	0.019	0.018	-0.001
5	Skull #1	270	50	100	30	10	0.019	0.026	0.007
6	Skull #1	270	50	100	30	10	0.019	0.024	0.005
7	Skull #1	270	50	100	30	10	0.019	0.023	0.004
8	Skull #1	270	50	100	30	10	0.019	0.200	0.181
9	Skull #1	270	50	100	30	10	0.019	0.020	0.001
10	Skull #1	270	50	100	30	10	0.019	0.021	0.002
11	Skull #1	270	50	100	30	10	0.019	0.026	0.007
12	Skull #1	270	50	100	30	10	0.019	0.021	0.002
13	Skull #1	270	50	100	30	10	0.019	0.018	-0.001
14	Skull #1	270	50	100	30	10	0.019	0.021	0.002
15	Skull #1	270	50	100	30	10	0.019	0.023	0.004
16	Skull #1	270	50	100	30	10	0.019	0.013	-0.006
17	Skull	270	50	100	30	10	0.019	0.027	0.008

	#1								
18	Skull #1	270	50	100	30	10	0.019	0.025	0.006
19	Skull #1	270	50	100	30	10	0.019	0.022	0.003
20	Skull #1	270	50	100	30	10	0.019	0.024	0.005
21	Skull #1	270	50	100	30	10	0.019	0.017	-0.002
22	Skull #1	270	50	100	30	10	0.019	0.025	0.006
1	Skull #1	400	50	100	30	10	0.019	0.022	0.003
2	Skull #1	400	50	100	30	10	0.019	0.020	0.001
3	Skull #1	400	50	100	30	10	0.019	0.023	0.004
4	Skull #1	400	50	100	30	10	0.019	0.021	0.002
5	Skull #1	400	50	100	30	10	0.019	0.023	0.004
6	Skull #1	400	50	100	30	10	0.019	0.022	0.003
7	Skull #1	400	50	100	30	10	0.019	0.024	0.005
8	Skull #1	400	50	100	30	10	0.019	0.210	0.191
9	Skull #1	400	50	100	30	10	0.019	0.026	0.007
10	Skull #1	400	50	100	30	10	0.019	0.023	0.004
11	Skull #1	400	50	100	30	10	0.019	0.023	0.004
12	Skull #1	400	50	100	30	10	0.019	0.022	0.003
13	Skull #1	400	50	100	30	10	0.019	0.027	0.008
14	Skull #1	400	50	100	30	10	0.019	0.018	-0.001
15	Skull #1	400	50	100	30	10	0.019	0.026	0.007
16	Skull #1	400	50	100	30	10	0.019	0.024	0.005
17	Skull #1	400	50	100	30	10	0.019	0.027	0.008

18	Skull #1	400	50	100	30	10	0.019	0.023	0.004
19	Skull #1	400	50	100	30	10	0.019	0.022	0.003
20	Skull #1	400	50	100	30	10	0.019	0.024	0.005

Table D-12 Clot fragmentation data collected for 11µm sized mesh filters from all acoustic output groups tested

Exp #	Skull ID	AP (W)	DC (%)	PW (ms)	ID (sec)	Flow (ml/min)	11 PreFUS Wt (g)	11 PostFUS Wt (g)	11 Wt Gain (g)
1	Skull #1	0	50	100	30	10	0.029	0.026	-0.003
2	Skull #1	0	50	100	30	10	0.029	0.027	-0.002
3	Skull #1	0	50	100	30	10	0.029	0.028	-0.001
4	Skull #1	0	50	100	30	10	0.029	0.025	-0.004
5	Skull #1	0	50	100	30	10	0.029	0.029	0.000
6	Skull #1	0	50	100	30	10	0.029	0.029	0.000
7	Skull #1	0	50	100	30	10	0.029	0.030	0.001
8	Skull #1	0	50	100	30	10	0.029	0.030	0.001
9	Skull #1	0	50	100	30	10	0.029	0.030	0.001
10	Skull #1	0	50	100	30	10	0.029	0.030	0.001
11	Skull #1	0	50	100	30	10	0.029	0.031	0.002
12	Skull #1	0	50	100	30	10	0.029	0.030	0.001
13	Skull #1	0	50	100	30	10	0.029	0.030	0.001
14	Skull #1	0	50	100	30	10	0.029	0.030	0.001
15	Skull #1	0	50	100	30	10	0.029	0.032	0.003
16	Skull	0	50	100	30	10	0.029	0.027	-0.002

	#1								
17	Skull #1	0	50	100	30	10	0.029	0.027	-0.002
18	Skull #1	0	50	100	30	10	0.029	0.029	0.000
19	Skull #1	0	50	100	30	10	0.029	0.033	0.004
20	Skull #1	0	50	100	30	10	0.029	0.027	-0.002
21	Skull #1	0	50	100	30	10	0.029	0.028	-0.001
22	Skull #1	0	50	100	30	10	0.029	0.029	0.000
23	Skull #1	0	50	100	30	10	0.029	0.032	0.003
24	Skull #1	0	50	100	30	10	0.029	0.031	0.002
25	Skull #1	0	50	100	30	10	0.029	0.031	0.002
26	Skull #1	0	50	100	30	10	0.029	0.031	0.002
27	Skull #1	0	50	100	30	10	0.029	0.031	0.002
28	Skull #1	0	50	100	30	10	0.029	0.037	0.008
29	Skull #1	0	50	100	30	10	0.029	0.035	0.006
30	Skull #1	0	50	100	30	10	0.029	0.038	0.009
31	Skull #1	0	50	100	30	10	0.029	0.035	0.006
32	Skull #1	0	50	100	30	10	0.029	0.034	0.005
33	Skull #1	0	50	100	30	10	0.029	0.041	0.012
34	Skull #1	0	50	100	30	10	0.029	0.036	0.007
35	Skull #1	0	50	100	30	10	0.029	0.033	0.004
36	Skull #1	0	50	100	30	10	0.029	0.037	0.008
37	Skull #1	0	50	100	30	10	0.029	0.032	0.003
38	Skull #1	0	50	100	30	10	0.029	0.035	0.006

39	Skull #1	0	50	100	30	10	0.029	0.039	0.010
40	Skull #1	0	50	100	30	10	0.029	0.036	0.007
41	Skull #1	0	50	100	30	10	0.029	0.035	0.006
42	Skull #1	0	50	100	30	10	0.029	0.037	0.008
43	Skull #1	0	50	100	30	10	0.029	0.034	0.005
44	Skull #1	0	50	100	30	10	0.029	0.036	0.007
45	Skull #1	0	50	100	30	10	0.029	0.033	0.004
46	Skull #1	0	50	100	30	10	0.029	0.030	0.001
47	Skull #1	0	50	100	30	10	0.029	0.032	0.003
48	Skull #1	0	50	100	30	10	0.029	0.029	0.000
49	Skull #1	0	50	100	30	10	0.029	0.034	0.005
50	Skull #1	0	50	100	30	10	0.029	0.031	0.002
51	Skull #1	0	50	100	30	10	0.029	0.028	-0.001
52	Skull #1	0	50	100	30	10	0.029	0.030	0.001
53	Skull #1	0	50	100	30	10	0.029	0.032	0.003
54	Skull #1	0	50	100	30	10	0.029	0.034	0.005
55	Skull #1	0	50	100	30	10	0.029	0.031	0.002
56	Skull #1	0	50	100	30	10	0.029	0.040	0.011
57	Skull #1	0	50	100	30	10	0.029	0.028	-0.001
58	Skull #1	0	50	100	30	10	0.029	0.029	0.000
59	Skull #1	0	50	100	30	10	0.029	0.021	-0.008
60	Skull #1	0	50	100	30	10	0.029	0.031	0.002
1	Skull	50	50	100	30	10	0.029	0.033	0.004

200

	#1								
2	Skull #1	50	50	100	30	10	0.029	0.027	-0.002
3	Skull #1	50	50	100	30	10	0.029	0.029	0.000
4	Skull #1	50	50	100	30	10	0.029	0.033	0.004
5	Skull #1	50	50	100	30	10	0.029	0.033	0.004
6	Skull #1	50	50	100	30	10	0.029	0.032	0.003
7	Skull #1	50	50	100	30	10	0.029	0.036	0.007
8	Skull #1	50	50	100	30	10	0.029	0.032	0.003
9	Skull #1	50	50	100	30	10	0.029	0.032	0.003
10	Skull #1	50	50	100	30	10	0.029	0.032	0.003
11	Skull #1	50	50	100	30	10	0.029	0.049	0.020
12	Skull #1	50	50	100	30	10	0.029	0.035	0.006
13	Skull #1	50	50	100	30	10	0.029	0.031	0.002
14	Skull #1	50	50	100	30	10	0.029	0.032	0.003
15	Skull #1	50	50	100	30	10	0.029	0.031	0.002
16	Skull #1	50	50	100	30	10	0.029	0.026	-0.003
17	Skull #1	50	50	100	30	10	0.029	0.029	0.000
18	Skull #1	50	50	100	30	10	0.029	0.031	0.002
19	Skull #1	50	50	100	30	10	0.029	0.035	0.006
20	Skull #1	50	50	100	30	10	0.029	0.031	0.002
21	Skull #1	50	50	100	30	10	0.029	0.031	0.002
22	Skull #1	50	50	100	30	10	0.029	0.036	0.007
23	Skull #1	50	50	100	30	10	0.029	0.029	0.000

201

24	Skull #1	50	50	100	30	10	0.029	0.021	-0.008
25	Skull #1	50	50	100	30	10	0.029	0.032	0.003
26	Skull #1	50	50	100	30	10	0.029	0.030	0.001
27	Skull #1	50	50	100	30	10	0.029	0.030	0.001
28	Skull #1	50	50	100	30	10	0.029	0.033	0.004
29	Skull #1	50	50	100	30	10	0.029	0.029	0.000
30	Skull #1	50	50	100	30	10	0.029	0.028	-0.001
31	Skull #1	50	50	100	30	10	0.029	0.032	0.003
32	Skull #1	50	50	100	30	10	0.029	0.029	0.000
33	Skull #1	50	50	100	30	10	0.029	0.029	0.000
34	Skull #1	50	50	100	30	10	0.029	0.039	0.010
35	Skull #1	50	50	100	30	10	0.029	0.032	0.003
36	Skull #1	50	50	100	30	10	0.029	0.032	0.003
37	Skull #1	50	50	100	30	10	0.029	0.030	0.001
38	Skull #1	50	50	100	30	10	0.029	0.030	0.001
39	Skull #1	50	50	100	30	10	0.029	0.030	0.001
40	Skull #1	50	50	100	30	10	0.029	0.034	0.005
41	Skull #1	50	50	100	30	10	0.029	0.037	0.008
42	Skull #1	50	50	100	30	10	0.029	0.038	0.009
43	Skull #1	50	50	100	30	10	0.029	0.041	0.012
44	Skull #1	50	50	100	30	10	0.029	0.041	0.012
45	Skull #1	50	50	100	30	10	0.029	0.036	0.007
46	Skull	50	50	100	30	10	0.029	0.031	0.002

	#1								
47	Skull #1	50	50	100	30	10	0.029	0.030	0.001
48	Skull #1	50	50	100	30	10	0.029	0.038	0.009
49	Skull #1	50	50	100	30	10	0.029	0.033	0.004
50	Skull #1	50	50	100	30	10	0.029	0.035	0.006
51	Skull #1	50	50	100	30	10	0.029	0.036	0.007
52	Skull #1	50	50	100	30	10	0.029	0.038	0.009
53	Skull #1	50	50	100	30	10	0.029	0.036	0.007
54	Skull #1	50	50	100	30	10	0.029	0.033	0.004
55	Skull #1	50	50	100	30	10	0.029	0.032	0.003
56	Skull #1	50	50	100	30	10	0.029	0.033	0.004
57	Skull #1	50	50	100	30	10	0.029	0.032	0.003
58	Skull #1	50	50	100	30	10	0.029	0.031	0.002
59	Skull #1	50	50	100	30	10	0.029	0.026	-0.003
60	Skull #1	50	50	100	30	10	0.029	0.034	0.005
61	Skull #1	50	50	100	30	10	0.029	0.031	0.002
62	Skull #1	50	50	100	30	10	0.029	0.031	0.002
1	Skull #1	100	50	100	30	10	0.029	0.029	0.000
2	Skull #1	100	50	100	30	10	0.029	0.030	0.001
3	Skull #1	100	50	100	30	10	0.029	0.030	0.001
4	Skull #1	100	50	100	30	10	0.029	0.340	0.311
5	Skull #1	100	50	100	30	10	0.029	0.027	-0.002
6	Skull #1	100	50	100	30	10	0.029	0.027	-0.002

7	Skull #1	100	50	100	30	10	0.029	0.033	0.004
8	Skull #1	100	50	100	30	10	0.029	0.034	0.005
9	Skull #1	100	50	100	30	10	0.029	0.033	0.004
10	Skull #1	100	50	100	30	10	0.029	0.033	0.004
11	Skull #1	100	50	100	30	10	0.029	0.033	0.004
12	Skull #1	100	50	100	30	10	0.029	0.032	0.003
13	Skull #1	100	50	100	30	10	0.029	0.030	0.001
14	Skull #1	100	50	100	30	10	0.029	0.049	0.020
15	Skull #1	100	50	100	30	10	0.029	0.035	0.006
16	Skull #1	100	50	100	30	10	0.029	0.028	-0.001
17	Skull #1	100	50	100	30	10	0.029	0.036	0.007
18	Skull #1	100	50	100	30	10	0.029	0.031	0.002
19	Skull #1	100	50	100	30	10	0.029	0.030	0.001
20	Skull #1	100	50	100	30	10	0.029	0.035	0.006
1	Skull #1	125	50	100	30	10	0.029	0.023	-0.006
2	Skull #1	125	50	100	30	10	0.029	0.033	0.004
3	Skull #1	125	50	100	30	10	0.029	0.027	-0.002
4	Skull #1	125	50	100	30	10	0.029	0.029	0.000
5	Skull #1	125	50	100	30	10	0.029	0.031	0.002
6	Skull #1	125	50	100	30	10	0.029	0.026	-0.003
7	Skull #1	125	50	100	30	10	0.029	0.029	0.000
8	Skull #1	125	50	100	30	10	0.029	0.030	0.001
9	Skull	125	50	100	30	10	0.029	0.031	0.002

	#1								
10	Skull #1	125	50	100	30	10	0.029	0.033	0.004
11	Skull #1	125	50	100	30	10	0.029	0.026	-0.003
12	Skull #1	125	50	100	30	10	0.029	0.030	0.001
13	Skull #1	125	50	100	30	10	0.029	0.031	0.002
14	Skull #1	125	50	100	30	10	0.029	0.032	0.003
15	Skull #1	125	50	100	30	10	0.029	0.032	0.003
16	Skull #1	125	50	100	30	10	0.029	0.031	0.002
17	Skull #1	125	50	100	30	10	0.029	0.032	0.003
18	Skull #1	125	50	100	30	10	0.029	0.034	0.005
19	Skull #1	125	50	100	30	10	0.029	0.031	0.002
20	Skull #1	125	50	100	30	10	0.029	0.029	0.000
21	Skull #1	125	50	100	30	10	0.029	0.028	-0.001
22	Skull #1	125	50	100	30	10	0.029	0.027	-0.002
23	Skull #1	125	50	100	30	10	0.029	0.028	-0.001
24	Skull #1	125	50	100	30	10	0.029	0.028	-0.001
25	Skull #1	125	50	100	30	10	0.029	0.027	-0.002
26	Skull #1	125	50	100	30	10	0.029	0.028	-0.001
27	Skull #1	125	50	100	30	10	0.029	0.035	0.006
28	Skull #1	125	50	100	30	10	0.029	0.037	0.008
29	Skull #1	125	50	100	30	10	0.029	0.033	0.004
30	Skull #1	125	50	100	30	10	0.029	0.032	0.003
31	Skull #1	125	50	100	30	10	0.029	0.030	0.001

32	Skull #1	125	50	100	30	10	0.029	0.028	-0.001
33	Skull #1	125	50	100	30	10	0.029	0.029	0.000
34	Skull #1	125	50	100	30	10	0.029	0.029	0.000
35	Skull #1	125	50	100	30	10	0.029	0.029	0.000
36	Skull #1	125	50	100	30	10	0.029	0.032	0.003
37	Skull #1	125	50	100	30	10	0.029	0.030	0.001
38	Skull #1	125	50	100	30	10	0.029	0.031	0.002
39	Skull #1	125	50	100	30	10	0.029	0.032	0.003
40	Skull #1	125	50	100	30	10	0.029	0.036	0.007
41	Skull #1	125	50	100	30	10	0.029	0.037	0.008
42	Skull #1	125	50	100	30	10	0.029	0.035	0.006
43	Skull #1	125	50	100	30	10	0.029	0.035	0.006
44	Skull #1	125	50	100	30	10	0.029	0.039	0.010
45	Skull #1	125	50	100	30	10	0.029	0.035	0.006
46	Skull #1	125	50	100	30	10	0.029	0.038	0.009
47	Skull #1	125	50	100	30	10	0.029	0.036	0.007
48	Skull #1	125	50	100	30	10	0.029	0.036	0.007
49	Skull #1	125	50	100	30	10	0.029	0.039	0.010
50	Skull #1	125	50	100	30	10	0.029	0.036	0.007
51	Skull #1	125	50	100	30	10	0.029	0.039	0.010
52	Skull #1	125	50	100	30	10	0.029	0.033	0.004
53	Skull #1	125	50	100	30	10	0.029	0.033	0.004
54	Skull	125	50	100	30	10	0.029	0.033	0.004

	#1								
55	Skull #1	125	50	100	30	10	0.029	0.036	0.007
56	Skull #1	125	50	100	30	10	0.029	0.029	0.000
57	Skull #1	125	50	100	30	10	0.029	0.032	0.003
58	Skull #1	125	50	100	30	10	0.029	0.031	0.002
59	Skull #1	125	50	100	30	10	0.029	0.043	0.014
60	Skull #1	125	50	100	30	10	0.029	0.031	0.002
61	Skull #1	125	50	100	30	10	0.029	0.034	0.005
62	Skull #1	125	50	100	30	10	0.029	0.033	0.004
63	Skull #1	125	50	100	30	10	0.029	0.031	0.002
1	Skull #1	150	50	100	30	10	0.029	0.080	0.051
2	Skull #1	150	50	100	30	10	0.029	0.031	0.002
3	Skull #1	150	50	100	30	10	0.029	0.023	-0.006
4	Skull #1	150	50	100	30	10	0.029	0.040	0.011
5	Skull #1	150	50	100	30	10	0.029	0.029	0.000
6	Skull #1	150	50	100	30	10	0.029	0.029	0.000
7	Skull #1	150	50	100	30	10	0.029	0.026	-0.003
8	Skull #1	150	50	100	30	10	0.029	0.040	0.011
9	Skull #1	150	50	100	30	10	0.029	0.030	0.001
10	Skull #1	150	50	100	30	10	0.029	0.031	0.002
11	Skull #1	150	50	100	30	10	0.029	0.032	0.003
12	Skull #1	150	50	100	30	10	0.029	0.027	-0.002
13	Skull #1	150	50	100	30	10	0.029	0.030	0.001

14	Skull #1	150	50	100	30	10	0.029	0.031	0.002
15	Skull #1	150	50	100	30	10	0.029	0.030	0.001
16	Skull #1	150	50	100	30	10	0.029	0.029	0.000
17	Skull #1	150	50	100	30	10	0.029	0.031	0.002
18	Skull #1	150	50	100	30	10	0.029	0.032	0.003
19	Skull #1	150	50	100	30	10	0.029	0.032	0.003
20	Skull #1	150	50	100	30	10	0.029	0.032	0.003
21	Skull #1	150	50	100	30	10	0.029	0.028	-0.001
22	Skull #1	150	50	100	30	10	0.029	0.032	0.003
23	Skull #1	150	50	100	30	10	0.029	0.030	0.001
24	Skull #1	150	50	100	30	10	0.029	0.050	0.021
25	Skull #1	150	50	100	30	10	0.029	0.030	0.001
26	Skull #1	150	50	100	30	10	0.029	0.029	0.000
27	Skull #1	150	50	100	30	10	0.029	0.031	0.002
28	Skull #1	150	50	100	30	10	0.029	0.031	0.002
29	Skull #1	150	50	100	30	10	0.029	0.031	0.002
30	Skull #1	150	50	100	30	10	0.029	0.032	0.003
31	Skull #1	150	50	100	30	10	0.029	0.029	0.000
32	Skull #1	150	50	100	30	10	0.029	0.031	0.002
33	Skull #1	150	50	100	30	10	0.029	0.033	0.004
34	Skull #1	150	50	100	30	10	0.029	0.030	0.001
35	Skull #1	150	50	100	30	10	0.029	0.031	0.002
36	Skull	150	50	100	30	10	0.029	0.030	0.001

	#1								
37	Skull #1	150	50	100	30	10	0.029	0.028	-0.001
38	Skull #1	150	50	100	30	10	0.029	0.028	-0.001
39	Skull #1	150	50	100	30	10	0.029	0.037	0.008
40	Skull #1	150	50	100	30	10	0.029	0.038	0.009
41	Skull #1	150	50	100	30	10	0.029	0.035	0.006
42	Skull #1	150	50	100	30	10	0.029	0.035	0.006
43	Skull #1	150	50	100	30	10	0.029	0.038	0.009
44	Skull #1	150	50	100	30	10	0.029	0.039	0.010
45	Skull #1	150	50	100	30	10	0.029	0.032	0.003
46	Skull #1	150	50	100	30	10	0.029	0.043	0.014
47	Skull #1	150	50	100	30	10	0.029	0.035	0.006
48	Skull #1	150	50	100	30	10	0.029	0.036	0.007
49	Skull #1	150	50	100	30	10	0.029	0.033	0.004
50	Skull #1	150	50	100	30	10	0.029	0.034	0.005
51	Skull #1	150	50	100	30	10	0.029	0.038	0.009
52	Skull #1	150	50	100	30	10	0.029	0.044	0.015
53	Skull #1	150	50	100	30	10	0.029	0.030	0.001
54	Skull #1	150	50	100	30	10	0.029	0.037	0.008
55	Skull #1	150	50	100	30	10	0.029	0.032	0.003
56	Skull #1	150	50	100	30	10	0.029	0.033	0.004
57	Skull #1	150	50	100	30	10	0.029	0.030	0.001
58	Skull #1	150	50	100	30	10	0.029	0.031	0.002

59	Skull #1	150	50	100	30	10	0.029	0.032	0.003
60	Skull #1	150	50	100	30	10	0.029	0.032	0.003
61	Skull #1	150	50	100	30	10	0.029	0.034	0.005
62	Skull #1	150	50	100	30	10	0.029	0.030	0.001
63	Skull #1	150	50	100	30	10	0.029	0.032	0.003
64	Skull #1	150	50	100	30	10	0.029	0.039	0.010
65	Skull #1	150	50	100	30	10	0.029	0.034	0.005
1	Skull #1	200	50	100	30	10	0.029	0.029	0.000
2	Skull #1	200	50	100	30	10	0.029	0.026	-0.003
3	Skull #1	200	50	100	30	10	0.029	0.031	0.002
4	Skull #1	200	50	100	30	10	0.029	0.028	-0.001
5	Skull #1	200	50	100	30	10	0.029	0.034	0.005
6	Skull #1	200	50	100	30	10	0.029	0.032	0.003
7	Skull #1	200	50	100	30	10	0.029	0.036	0.007
8	Skull #1	200	50	100	30	10	0.029	0.034	0.005
9	Skull #1	200	50	100	30	10	0.029	0.034	0.005
10	Skull #1	200	50	100	30	10	0.029	0.030	0.001
11	Skull #1	200	50	100	30	10	0.029	0.033	0.004
12	Skull #1	200	50	100	30	10	0.029	0.030	0.001
13	Skull #1	200	50	100	30	10	0.029	0.032	0.003
14	Skull #1	200	50	100	30	10	0.029	0.031	0.002
15	Skull #1	200	50	100	30	10	0.029	0.031	0.002
16	Skull	200	50	100	30	10	0.029	0.042	0.013

	#1								
17	Skull #1	200	50	100	30	10	0.029	0.033	0.004
18	Skull #1	200	50	100	30	10	0.029	0.035	0.006
19	Skull #1	200	50	100	30	10	0.029	0.034	0.005
20	Skull #1	200	50	100	30	10	0.029	0.030	0.001
1	Skull #1	235	50	100	30	10	0.029	0.035	0.006
2	Skull #1	235	50	100	30	10	0.029	0.031	0.002
3	Skull #1	235	50	100	30	10	0.029	0.029	0.000
4	Skull #1	235	50	100	30	10	0.029	0.027	-0.002
5	Skull #1	235	50	100	30	10	0.029	0.031	0.002
6	Skull #1	235	50	100	30	10	0.029	0.031	0.002
7	Skull #1	235	50	100	30	10	0.029	0.029	0.000
8	Skull #1	235	50	100	30	10	0.029	0.031	0.002
9	Skull #1	235	50	100	30	10	0.029	0.035	0.006
10	Skull #1	235	50	100	30	10	0.029	0.034	0.005
11	Skull #1	235	50	100	30	10	0.029	0.031	0.002
12	Skull #1	235	50	100	30	10	0.029	0.034	0.005
13	Skull #1	235	50	100	30	10	0.029	0.030	0.001
14	Skull #1	235	50	100	30	10	0.029	0.034	0.005
15	Skull #1	235	50	100	30	10	0.029	0.030	0.001
16	Skull #1	235	50	100	30	10	0.029	0.034	0.005
17	Skull #1	235	50	100	30	10	0.029	0.031	0.002
18	Skull #1	235	50	100	30	10	0.029	0.033	0.004

19	Skull #1	235	50	100	30	10	0.029	0.028	-0.001
20	Skull #1	235	50	100	30	10	0.029	0.031	0.002
1	Skull #1	270	50	100	30	10	0.029	0.032	0.003
2	Skull #1	270	50	100	30	10	0.029	0.033	0.004
3	Skull #1	270	50	100	30	10	0.029	0.038	0.009
4	Skull #1	270	50	100	30	10	0.029	0.029	0.000
5	Skull #1	270	50	100	30	10	0.029	0.026	-0.003
6	Skull #1	270	50	100	30	10	0.029	0.035	0.006
7	Skull #1	270	50	100	30	10	0.029	0.034	0.005
8	Skull #1	270	50	100	30	10	0.029	0.031	0.002
9	Skull #1	270	50	100	30	10	0.029	0.028	-0.001
10	Skull #1	270	50	100	30	10	0.029	0.033	0.004
11	Skull #1	270	50	100	30	10	0.029	0.033	0.004
12	Skull #1	270	50	100	30	10	0.029	0.033	0.004
13	Skull #1	270	50	100	30	10	0.029	0.029	0.000
14	Skull #1	270	50	100	30	10	0.029	0.032	0.003
15	Skull #1	270	50	100	30	10	0.029	0.031	0.002
16	Skull #1	270	50	100	30	10	0.029	0.029	0.000
17	Skull #1	270	50	100	30	10	0.029	0.030	0.001
18	Skull #1	270	50	100	30	10	0.029	0.039	0.010
19	Skull #1	270	50	100	30	10	0.029	0.028	-0.001
20	Skull #1	270	50	100	30	10	0.029	0.029	0.000
21	Skull	270	50	100	30	10	0.029	0.033	0.004

	#1								
22	Skull #1	270	50	100	30	10	0.029	0.027	-0.002
1	Skull #1	400	50	100	30	10	0.029	0.031	0.002
2	Skull #1	400	50	100	30	10	0.029	0.037	0.008
3	Skull #1	400	50	100	30	10	0.029	0.028	-0.001
4	Skull #1	400	50	100	30	10	0.029	0.032	0.003
5	Skull #1	400	50	100	30	10	0.029	0.031	0.002
6	Skull #1	400	50	100	30	10	0.029	0.031	0.002
7	Skull #1	400	50	100	30	10	0.029	0.030	0.001
8	Skull #1	400	50	100	30	10	0.029	0.030	0.001
9	Skull #1	400	50	100	30	10	0.029	0.031	0.002
10	Skull #1	400	50	100	30	10	0.029	0.030	0.001
11	Skull #1	400	50	100	30	10	0.029	0.032	0.003
12	Skull #1	400	50	100	30	10	0.029	0.032	0.003
13	Skull #1	400	50	100	30	10	0.029	0.039	0.010
14	Skull #1	400	50	100	30	10	0.029	0.030	0.001
15	Skull #1	400	50	100	30	10	0.029	0.030	0.001
16	Skull #1	400	50	100	30	10	0.029	0.033	0.004
17	Skull #1	400	50	100	30	10	0.029	0.030	0.001
18	Skull #1	400	50	100	30	10	0.029	0.034	0.005
19	Skull #1	400	50	100	30	10	0.029	0.035	0.006
20	Skull #1	400	50	100	30	10	0.029	0.032	0.003

REFERENCES

- [1] Inc., O., "Acoustic Intensity Measurement System," HTTP://WWW.ONDACORP.COM/IMAGES/BROCHURES/ONDA_AMSIII_DATASHEET.PDF.
- [2] Addo, J., Ayerbe, L., Mohan, K. M., Crichton, S., Sheldenkar, A., Chen, R., Wolfe, C. D., and McKevitt, C., 2012, "Socioeconomic status and stroke: an updated review," *Stroke*, 43(4), pp. 1186-1191.
- [3] Mukherjee, D., and Patil, C. G., "Epidemiology and the global burden of stroke," *World Neurosurg*, 76(6 Suppl), pp. S85-90.
- [4] Zivin, J. A., 2009, "Acute stroke therapy with tissue plasminogen activator (tPA) since it was approved by the U.S. Food and Drug Administration (FDA)," *Ann Neurol*, 66(1), pp. 6-10.
- [5] Murray, V., Norrving, B., Sandercock, P. A., Terént, A., Wardlaw, J. M., and Wester, P., 2010, "The molecular basis of thrombolysis and its clinical application in stroke," *J Intern Med*, 267(2), pp. 191-208.
- [6] Alexandrov, A. V., Mikulik, R., Ribo, M., Sharma, V. K., Lao, A. Y., Tsivgoulis, G., Sugg, R. M., Barreto, A., Sierzenski, P., Malkoff, M. D., and Grotta, J. C., 2008, "A pilot randomized clinical safety study of sonothrombolysis augmentation with ultrasound-activated perflutren-lipid microspheres for acute ischemic stroke," *Stroke*, 39(5), pp. 1464-1469.
- [7] Alonso, A., Dempfle, C. E., Della Martina, A., Stroick, M., Fatar, M., Zohsel, K., Allemann, E., Hennerici, M. G., and Meairs, S., 2009, "In vivo clot lysis of human thrombus

with intravenous abciximab immunobubbles and ultrasound," Thromb Res, 124(1), pp. 70-74.

[8] Daffertshofer, M., and Fatar, M., 2002, "Therapeutic ultrasound in ischemic stroke treatment: experimental evidence," Eur J Ultrasound, 16(1-2), pp. 121-130.

[9] Daffertshofer, M., Huang, Z., Fatar, M., Popolo, M., Schroock, H., Kuschinsky, W., Moskowitz, M. A., and Hennerici, M. G., 2004, "Efficacy of sonothrombolysis in a rat model of embolic ischemic stroke," Neurosci Lett, 361(1-3), pp. 115-119.

[10] Dinia, L., Rubiera, M., Ribo, M., Maisterra, O., Ortega, G., del Sette, M., Alvarez-Sabin, J., and Molina, C. A., 2009, "Reperfusion after stroke sonothrombolysis with microbubbles may predict intracranial bleeding," Neurology, 73(10), pp. 775-780.

[11] Eggers, J., Seidel, G., Koch, B., and Konig, I. R., 2005, "Sonothrombolysis in acute ischemic stroke for patients ineligible for rt-PA," Neurology, 64(6), pp. 1052-1054.

[12] Eggers, J., Konig, I. R., Koch, B., Handler, G., and Seidel, G., 2008, "Sonothrombolysis with transcranial color-coded sonography and recombinant tissue-type plasminogen activator in acute middle cerebral artery main stem occlusion: results from a randomized study," Stroke, 39(5), pp. 1470-1475.

[13] Flores, R., Hennings, L. J., Lowery, J. D., Brown, A. T., and Culp, W. C., "Microbubble-augmented ultrasound sonothrombolysis decreases intracranial hemorrhage in a rabbit model of acute ischemic stroke," Invest Radiol, 46(7), pp. 419-424.

[14] Meairs, S., and Culp, W., 2009, "Microbubbles for thrombolysis of acute ischemic stroke," Cerebrovasc Dis, 27 Suppl 2, pp. 55-65.

- [15] Molina, C. A., Barreto, A. D., Tsivgoulis, G., Sierzenski, P., Malkoff, M. D., Rubiera, M., Gonzales, N., Mikulik, R., Pate, G., Ostrem, J., Singleton, W., Manvelian, G., Unger, E. C., Grotta, J. C., Schellinger, P. D., and Alexandrov, A. V., 2009, "Transcranial ultrasound in clinical sonothrombolysis (TUCSON) trial," *Ann Neurol*, 66(1), pp. 28-38.
- [16] Pfaffenberger, S., Wojta, J., and Gottsauner-Wolf, M., 2005, "High-frequency transtemporal sonothrombolysis," *Stroke*, 36(7), pp. 1356-1357.
- [17] Schlachetzki, F., Herzberg, M., Holscher, T., Ertl, M., Zimmermann, M., Ittner, K. P., Pels, H., Bogdahn, U., and Boy, S., "Transcranial ultrasound from diagnosis to early stroke treatment: part 2: prehospital neurosonography in patients with acute stroke: the Regensburg stroke mobile project," *Cerebrovasc Dis*, 33(3), pp. 262-271.
- [18] Stride, E., 2009, "Physical principles of microbubbles for ultrasound imaging and therapy," *Cerebrovasc Dis*, 27 Suppl 2, pp. 1-13.
- [19] Broussalis, E., Trinka, E., Hitzl, W., Wallner, A., Chroust, V., and Killer-Oberpfalzer, M., "Comparison of Stent-Retriever Devices versus the Merci Retriever for Endovascular Treatment of Acute Stroke," *AJNR Am J Neuroradiol*.
- [20] Noorian, A. R., Gupta, R., and Nogueira, R. G., "Acute stroke: techniques and results with the Merci retriever," *Tech Vasc Interv Radiol*, 15(1), pp. 47-52.
- [21] Dorn, F., Stehle, S., Lockau, H., Zimmer, C., and Liebig, T., "Endovascular Treatment of Acute Intracerebral Artery Occlusions with the Solitaire Stent: Single-Centre Experience with 108 Recanalization Procedures," *Cerebrovasc Dis*, 34(1), pp. 70-77.

- [22] Soize, S., Kadziolka, K., Estrade, L., Serre, I., Bakchine, S., and Pierot, L., "Mechanical Thrombectomy in Acute Stroke: Prospective Pilot Trial of the Solitaire FR Device while Under Conscious Sedation," *AJNR Am J Neuroradiol.*
- [23] Braaten, J. V., Goss, R. A., and Francis, C. W., 1997, "Ultrasound reversibly disaggregates fibrin fibers," *Thromb Haemost*, 78(3), pp. 1063-1068.
- [24] Devcic-Kuhar, B., Pfaffenberger, S., Gherardini, L., Mayer, C., Groschl, M., Kaun, C., Benes, E., Tschachler, E., Huber, K., Maurer, G., Wojta, J., and Gottsauer-Wolf, M., 2004, "Ultrasound affects distribution of plasminogen and tissue-type plasminogen activator in whole blood clots in vitro," *Thromb Haemost*, 92(5), pp. 980-985.
- [25] Datta, S., Ammi A.Y., Coussios C.C., Holland, C.K., 2007, "Monitoring and simulating stable cavitation during ultrasound-enhanced thrombolysis," *Journal of the Acoustic Society of America*, 122(3052).
- [26] Datta, S., Coussios, C. C., McAdory, L. E., Tan, J., Porter, T., De Courten-Myers, G., and Holland, C. K., 2006, "Correlation of cavitation with ultrasound enhancement of thrombolysis," *Ultrasound Med Biol*, 32(8), pp. 1257-1267.
- [27] Prokop, A. F., Soltani, A., and Roy, R. A., 2007, "Cavitational mechanisms in ultrasound-accelerated fibrinolysis," *Ultrasound Med Biol*, 33(6), pp. 924-933.
- [28] Eggers, J., Koch, B., Meyer, K., Konig, I., and Seidel, G., 2003, "Effect of ultrasound on thrombolysis of middle cerebral artery occlusion," *Ann Neurol*, 53(6), pp. 797-800.
- [29] Alexandrov, A. V., 2004, "Ultrasound identification and lysis of clots," *Stroke*, 35(11 Suppl 1), pp. 2722-2725.

- [30] Alexandrov, A. V., Molina, C. A., Grotta, J. C., Garami, Z., Ford, S. R., Alvarez-Sabin, J., Montaner, J., Saqqur, M., Demchuk, A. M., Moye, L. A., Hill, M. D., and Wojner, A. W., 2004, "Ultrasound-enhanced systemic thrombolysis for acute ischemic stroke," *N Engl J Med*, 351(21), pp. 2170-2178.
- [31] Collet, J. P., Montalescot, G., Lesty, C., and Weisel, J. W., 2002, "A structural and dynamic investigation of the facilitating effect of glycoprotein IIb/IIIa inhibitors in dissolving platelet-rich clots," *Circ Res*, 90(4), pp. 428-434.
- [32] Weisel, J. W., and Litvinov, R. I., 2008, "The biochemical and physical process of fibrinolysis and effects of clot structure and stability on the lysis rate," *Cardiovasc Hematol Agents Med Chem*, 6(3), pp. 161-180.
- [33] Meunier, J. M., Holland, C. K., Lindsell, C. J., and Shaw, G. J., 2007, "Duty cycle dependence of ultrasound enhanced thrombolysis in a human clot model," *Ultrasound Med Biol*, 33(4), pp. 576-583.
- [34] Porter, T. R., LeVeen, R. F., Fox, R., Kricsfeld, A., and Xie, F., 1996, "Thrombolytic enhancement with perfluorocarbon-exposed sonicated dextrose albumin microbubbles," *Am Heart J*, 132(5), pp. 964-968.
- [35] Pieters, M., Hekkenberg, R. T., Barrett-Bergshoeff, M., and Rijken, D. C., 2004, "The effect of 40 kHz ultrasound on tissue plasminogen activator-induced clot lysis in three in vitro models," *Ultrasound Med Biol*, 30(11), pp. 1545-1552.
- [36] White, D. N., 1967, "The limitations of echo-encephalography," *Ultrasonics*, 5, pp. 88-90.

- [37] Ballantine, H. T., Jr., Bolt, R. H., Hueter, T. F., and Ludwig, G. D., 1950, "On the detection of intracranial pathology by ultrasound," *Science*, 112(2914), pp. 525-528.
- [38] Ludwig, G. D., Bolt, R. H., Heuter, T. F., and Ballantine, H. T., Jr., 1950, "Factors influencing the use of ultrasound as a diagnostic aid," *Trans Am Neurol Assoc*, 51, pp. 225-228.
- [39] Martin, E., Jeanmonod, D., Morel, A., Zadicario, E., and Werner, B., 2009, "High-intensity focused ultrasound for noninvasive functional neurosurgery," *Ann Neurol*, 66(6), pp. 858-861.
- [40] Damianou, C., Ioannides, K., Hadjisavvas, V., Mylonas, N., Couppis, A., and Iosif, D., 2009, "In vitro and in vivo brain ablation created by high-intensity focused ultrasound and monitored by MRI," *IEEE Trans Ultrason Ferroelectr Freq Control*, 56(6), pp. 1189-1198.
- [41] ter Haar, G. R., 2001, "High intensity focused ultrasound for the treatment of tumors," *Echocardiography*, 18(4), pp. 317-322.
- [42] Jolesz, F. A., and McDannold, N., 2008, "Current status and future potential of MRI-guided focused ultrasound surgery," *J Magn Reson Imaging*, 27(2), pp. 391-399.
- [43] White, D. N., Clark, J. M., White, D. A., Campbell, J. K., Bahuleyan, K., Kraus, A. S., and Brinker, R. A., 1969, "The deformation of the ultrasonic field in passage across the living and cadaver head," *Med Biol Eng*, 7(6), pp. 607-618.
- [44] Hynynen, K., Darkazanli, A., Damianou, C. A., Unger, E., and Schenck, J. F., 1993, "Tissue thermometry during ultrasound exposure," *Eur Urol*, 23 Suppl 1, pp. 12-16.

- [45] Hynynen, K., Vykhodtseva, N. I., Chung, A. H., Sorrentino, V., Colucci, V., and Jolesz, F. A., 1997, "Thermal effects of focused ultrasound on the brain: determination with MR imaging," *Radiology*, 204(1), pp. 247-253.
- [46] Marder, V. J., Chute, D. J., Starkman, S., Abolian, A. M., Kidwell, C., Liebeskind, D., Ovbiagele, B., Vinuela, F., Duckwiler, G., Jahan, R., Vespa, P. M., Selco, S., Rajajee, V., Kim, D., Sanossian, N., and Saver, J. L., 2006, "Analysis of thrombi retrieved from cerebral arteries of patients with acute ischemic stroke," *Stroke*, 37(8), pp. 2086-2093.
- [47] Edwards, M. T., Murphy, M. M., Geraghty, J. J., Wulf, J. A., and Konzen, J. P., 1999, "Intra-arterial cerebral thrombolysis for acute ischemic stroke in a community hospital," *AJNR Am J Neuroradiol*, 20(9), pp. 1682-1687.
- [48] Saver, J. L., 2006, "Time is brain--quantified," *Stroke*, 37(1), pp. 263-266.
- [49] Alexandrov, A. V., 2002, "Ultrasound-enhanced thrombolysis for stroke: clinical significance," *Eur J Ultrasound*, 16(1-2), pp. 131-140.
- [50] Alexandrov, A. V., Demchuk, A. M., Burgin, W. S., Robinson, D. J., and Grotta, J. C., 2004, "Ultrasound-enhanced thrombolysis for acute ischemic stroke: phase I. Findings of the CLOTBUST trial," *J Neuroimaging*, 14(2), pp. 113-117.
- [51] Daffertshofer, M., Gass, A., Ringleb, P., Sitzer, M., Sliwka, U., Els, T., Sedlaczek, O., Koroshetz, W. J., and Hennerici, M. G., 2005, "Transcranial low-frequency ultrasound-mediated thrombolysis in brain ischemia: increased risk of hemorrhage with combined ultrasound and tissue plasminogen activator: results of a phase II clinical trial," *Stroke*, 36(7), pp. 1441-1446.

- [52] Maxwell, A. D., Cain, C. A., Duryea, A. P., Yuan, L., Gurm, H. S., and Xu, Z., 2009, "Noninvasive thrombolysis using pulsed ultrasound cavitation therapy - histotripsy," *Ultrasound Med Biol*, 35(12), pp. 1982-1994.
- [53] Lynn, J. G., Zwemer, R. L., Chick, A. J., and Miller, A. E., 1942, "A New Method for the Generation and Use of Focused Ultrasound in Experimental Biology," *J Gen Physiol*, 26(2), pp. 179-193.
- [54] Lele, P. P., 1962, "A simple method for production of trackless focal lesions with focused ultrasound: physical factors," *J Physiol*, 160, pp. 494-512.
- [55] Fry, F. J., Kossoff, G., Eggleton, R. C., and Dunn, F., 1970, "Threshold ultrasonic dosages for structural changes in the mammalian brain," *J Acoust Soc Am*, 48(6), p. Suppl 2:1413+.
- [56] Fry, W. J., Barnard, J. W., Fry, E. J., Krumins, R. F., and Brennan, J. F., 1955, "Ultrasonic lesions in the mammalian central nervous system," *Science*, 122(3168), pp. 517-518.
- [57] Fry, W. J., Barnard, J. W., Fry, F. J., and Brennan, J. F., 1955, "Ultrasonically produced localized selective lesions in the central nervous system," *Am J Phys Med*, 34(3), pp. 413-423.
- [58] Bakay, L., Ballantine, H. T., Jr., Hueter, T. F., and Sosa, D., 1956, "Ultrasonically produced changes in the blood-brain barrier," *AMA Arch Neurol Psychiatry*, 76(5), pp. 457-467.
- [59] Fry, W. J., and Fry, F. J., 1960, "Fundamental neurological research and human neurosurgery using intense ultrasound," *IRE Trans Med Electron*, ME-7, pp. 166-181.

- [60] Fry, F. J., and Goss, S. A., 1980, "Further studies of the transskull transmission of an intense focused ultrasonic beam: lesion production at 500 kHz," *Ultrasound Med Biol*, 6(1), pp. 33-38.
- [61] Hynynen, K., and Jolesz, F. A., 1998, "Demonstration of potential noninvasive ultrasound brain therapy through an intact skull," *Ultrasound Med Biol*, 24(2), pp. 275-283.
- [62] Clement, G. T., White, P. J., King, R. L., McDannold, N., and Hynynen, K., 2005, "A magnetic resonance imaging-compatible, large-scale array for trans-skull ultrasound surgery and therapy," *J Ultrasound Med*, 24(8), pp. 1117-1125.
- [63] Hynynen, K., Darkazanli, A., Unger, E., and Schenck, J. F., 1993, "MRI-guided noninvasive ultrasound surgery," *Med Phys*, 20(1), pp. 107-115.
- [64] Darkazanli, A., Hynynen, K., Unger, E. C., and Schenck, J. F., 1993, "On-line monitoring of ultrasonic surgery with MR imaging," *J Magn Reson Imaging*, 3(3), pp. 509-514.
- [65] Hynynen, K., McDannold, N., Clement, G., Jolesz, F. A., Zadicario, E., Killiany, R., Moore, T., and Rosen, D., 2006, "Pre-clinical testing of a phased array ultrasound system for MRI-guided noninvasive surgery of the brain--a primate study," *Eur J Radiol*, 59(2), pp. 149-156.
- [66] Frenkel, V., Oberoi, J., Stone, M. J., Park, M., Deng, C., Wood, B. J., Neeman, Z., Horne, M., 3rd, and Li, K. C., 2006, "Pulsed high-intensity focused ultrasound enhances thrombolysis in an in vitro model," *Radiology*, 239(1), pp. 86-93.

- [67] Stone, M. J., Frenkel, V., Dromi, S., Thomas, P., Lewis, R. P., Li, K. C., Horne, M., 3rd, and Wood, B. J., 2007, "Pulsed-high intensity focused ultrasound enhanced tPA mediated thrombolysis in a novel in vivo clot model, a pilot study," *Thromb Res*, 121(2), pp. 193-202.
- [68] Rosenschein, U., Furman, V., Kerner, E., Fabian, I., Bernheim, J., and Eshel, Y., 2000, "Ultrasound imaging-guided noninvasive ultrasound thrombolysis: preclinical results," *Circulation*, 102(2), pp. 238-245.
- [69] Hitchcock, K. E., Ivancevich, N. M., Haworth, K. J., Caudell Stamper, D. N., Vela, D. C., Sutton, J. T., Pyne-Geithman, G. J., and Holland, C. K., "Ultrasound-enhanced rt-PA thrombolysis in an ex vivo porcine carotid artery model," *Ultrasound Med Biol*, 37(8), pp. 1240-1251.
- [70] Greenberg, R. K., Ouriel, K., Srivastava, S., Shortell, C., Ivancev, K., Waldman, D., Illig, K., and Green, R., 2000, "Mechanical versus chemical thrombolysis: an in vitro differentiation of thromolytic mechanisms," *J Vasc Interv Radiol*, 11(2 Pt 1), pp. 199-205.
- [71] Hartnell, G. G., Saxton, J. M., Friedl, S. E., Abela, G. S., and Rosenschein, U., 1993, "Ultrasonic thrombus ablation: in vitro assessment of a novel device for intracoronary use," *J Interv Cardiol*, 6(1), pp. 69-76.
- [72] Wright, C., Hynynen, K., and Goertz, D., "In Vitro and In Vivo High-Intensity Focused Ultrasound Thrombolysis," *Invest Radiol*.
- [73] Watura, R., Cobley, M., and Taylor, J., 2004, "Multislice CT in imaging of trauma of the spine, pelvis and complex foot injuries," *Br J Radiol*, 77 Spec No 1, pp. S46-63.

- [74] Fry, F. J., and Barger, J. E., 1978, "Acoustical properties of the human skull," *J Acoust Soc Am*, 63(5), pp. 1576-1590.
- [75] Nahirnyak, V. M., Yoon, S. W., and Holland, C. K., 2006, "Acousto-mechanical and thermal properties of clotted blood," *J Acoust Soc Am*, 119(6), pp. 3766-3772.
- [76] Nahirnyak, V., Mast, T. D., and Holland, C. K., 2007, "Ultrasound-induced thermal elevation in clotted blood and cranial bone," *Ultrasound Med Biol*, 33(8), pp. 1285-1295.
- [77] Sakharov, D. V., and Rijken, D. C., 2000, "The effect of flow on lysis of plasma clots in 1
- [79] Hynynen, K., Clement, G. T., McDannold, N., Vykhodtseva, N., King, R., White, P. J., Vitek, S., and Jolesz, F. A., 2004, "500-element ultrasound phased array system for noninvasive focal surgery of the brain: a preliminary rabbit study with ex vivo human skulls," *Magn Reson Med*, 52(1), pp. 100-107.
- [80] White, J., Clement, G. T., and Hynynen, K., 2005, "Transcranial ultrasound focus reconstruction with phase and amplitude correction," *IEEE Trans Ultrason Ferroelectr Freq Control*, 52(9), pp. 1518-1522.
- [81] Aarnio, J., Clement, G. T., and Hynynen, K., 2005, "A new ultrasound method for determining the acoustic phase shifts caused by the skull bone," *Ultrasound Med Biol*, 31(6), pp. 771-780.
- [82] White, P. J., Clement, G. T., and Hynynen, K., 2006, "Longitudinal and shear mode ultrasound propagation in human skull bone," *Ultrasound Med Biol*, 32(7), pp. 1085-1096.

- [83] Aubry, J. F., Tanter, M., Pernot, M., Thomas, J. L., and Fink, M., 2003, "Experimental demonstration of noninvasive transskull adaptive focusing based on prior computed tomography scans," *J Acoust Soc Am*, 113(1), pp. 84-93.
- [84] Zanelli, C. I., and Howard, S. M., 2006, "Schlieren metrology for high frequency medical ultrasound," *Ultrasonics*, 44 Suppl 1, pp. e105-107.
- [85] Kleppner, D., and Kolenkow, R. J., 2010, <>An>> introduction to mechanics, Cambridge University Press, Cambridge.
- [86] Litvin, F. L., and Fuentes, A., 2004, Gear geometry and applied theory, Cambridge University Press, Cambridge.
- [87] Roy, R., 2013, "Zooming Digital Images using Interpolation Techniques," M. Maharishi Markandeshwar University, India, ed. International Journal of Application or Innovation in Engineering & Management, pp. 34-45.
- [88] Hangartner, T. N., and Short, D. F., 2007, "Accurate quantification of width and density of bone structures by computed tomography," *Med Phys*, 34(10), pp. 3777-3784.
- [89] Ward, K. A., Adams, J. E., and Hangartner, T. N., 2005, "Recommendations for thresholds for cortical bone geometry and density measurement by peripheral quantitative computed tomography," *Calcif Tissue Int*, 77(5), pp. 275-280.
- [90] Clement, G. T., and Hynynen, K., 2002, "A non-invasive method for focusing ultrasound through the human skull," *Phys Med Biol*, 47(8), pp. 1219-1236.

- [91] Pernot, M., Aubry, J. F., Tanter, M., Marquet, F., Montaldo, G., Boch, A. L., Kujas, M., Seilhean, D., and Fink, M., 2007, "High power phased array prototype for clinical high intensity focused ultrasound : applications to transcostal and transcranial therapy," Conf Proc IEEE Eng Med Biol Soc, 2007, pp. 234-237.
- [92] Pichardo, S., Sin, V. W., and Hynynen, K., "Multi-frequency characterization of the speed of sound and attenuation coefficient for longitudinal transmission of freshly excised human skulls," Phys Med Biol, 56(1), pp. 219-250.
- [93] Larrat, B., Pernot, M., Aubry, J. F., Dervishi, E., Sinkus, R., Seilhean, D., Marie, Y., Boch, A. L., Fink, M., and Tanter, M., 2010, "MR-guided transcranial brain HIFU in small animal models," Phys Med Biol, 55(2), pp. 365-388.
- [94] Pernot, M., Aubry, J. F., Tanter, M., Thomas, J. L., and Fink, M., 2003, "High power transcranial beam steering for ultrasonic brain therapy," Phys Med Biol, 48(16), pp. 2577-2589.
- [95] Canney, M. S., Bailey, M. R., Crum, L. A., Khokhlova, V. A., and Sapozhnikov, O. A., 2008, "Acoustic characterization of high intensity focused ultrasound fields: a combined measurement and modeling approach," J Acoust Soc Am, 124(4), pp. 2406-2420.
- [96] Cheeke, J. D. N., 2012, "Fundamentals and applications of ultrasonic waves," CRC Press,, Boca Raton, FL, p. 1 online resource.
- [97] Clement, G. T., White, P. J., and Hynynen, K., 2004, "Enhanced ultrasound transmission through the human skull using shear mode conversion," J Acoust Soc Am, 115(3), pp. 1356-1364.

- [98] White, P. J., Clement, G. T., and Hynynen, K., 2006, "Local frequency dependence in transcranial ultrasound transmission," *Phys Med Biol*, 51(9), pp. 2293-2305.
- [99] Clement, G. T., Sun, J., and Hynynen, K., 2001, "The role of internal reflection in transskull phase distortion," *Ultrasonics*, 39(2), pp. 109-113.
- [100] Clement, G. T., and Hynynen, K., 2002, "Correlation of ultrasound phase with physical skull properties," *Ultrasound Med Biol*, 28(5), pp. 617-624.
- [101] Connor, C. W., and Hynynen, K., 2004, "Patterns of thermal deposition in the skull during transcranial focused ultrasound surgery," *IEEE Trans Biomed Eng*, 51(10), pp. 1693-1706.
- [102] Pichardo, S., Sin, V. W., and Hynynen, K., 2011, "Multi-frequency characterization of the speed of sound and attenuation coefficient for longitudinal transmission of freshly excised human skulls," *Phys Med Biol*, 56(1), pp. 219-250.
- [103] Pulkkinen, A., Huang, Y., Song, J., and Hynynen, K., 2011, "Simulations and measurements of transcranial low-frequency ultrasound therapy: skull-base heating and effective area of treatment," *Phys Med Biol*, 56(15), pp. 4661-4683.
- [104] Jones, G., Hunter, F., Hancock, H. A., Kapoor, A., Stone, M. J., Wood, B. J., Xie, J., Dreher, M. R., and Frenkel, V., "In vitro investigations into enhancement of tPA bioavailability in whole blood clots using pulsed-high intensity focused ultrasound exposures," *IEEE Trans Biomed Eng*, 57(1), pp. 33-36.

[105] Wright, C. C., Hynynen, K., and Goertz, D. E., 2012, "Pulsed focused ultrasound-induced displacements in confined in vitro blood clots," IEEE Trans Biomed Eng, 59(3), pp. 842-851.

[106] Kennedy, J. E., Ter Haar, G. R., and Cranston, D., 2003, "High intensity focused ultrasound: surgery of the future?," Br J Radiol, 76(909), pp. 590-599.

ABSTRACT

USE OF FOCUSED ULTRASOUND FOR TRANSCRANIAL SONOTHROMBOLYSIS

by

GOLNAZ AHADI

August 2013

Advisor: Dr. Michele Jeanette Grimm

Co-Advisor: Dr. Thilo Hoelscher

Major: Biomedical Engineering

Degree: Doctor of Philosophy

Worldwide, stroke is the second most common cause of death. Ischemic stroke remains accountable for the majority of the 20 million devastating stroke events occurring globally each year. Use of transcranial focused ultrasound (FUS) for sonothrombolysis is a new research field for ischemic stroke treatment. If shown to be effective, FUS sonothrombolysis could become a widely available treatment option for the majority of the stroke sufferers that do not qualify or do not have access to current thrombolytic treatment options, such as tPA or neurointerventional methods.

The current study was an *in vitro* transcranial FUS headsystenm investigation for the potential treatment of stroke. It was segmented and approached as four progressively building, specific objectives that were developed to collectively answer the investigational question: is focused ultrasound effective for transcranial sonothrombolysis in stroke?

- (1) Determine the technique feasibility of a FUS system for transcranial sonothrombolysis
- (2) Perform a parameter optimization for the FUS system for effective sonothrombolysis by varying duty cycle and pulse width settings
- (3) Characterize the acoustic field produced by the transcranial FUS and determine how it is affected by the skull
- (4) Determine how sonothrombolysis efficacy and potential clot fragmentation are impacted by varying the FUS intensity

The observed, novel *in vitro* experiences using this new technology are very encouraging. From the four sets of experiments, we have learned that: 1) FUS sonothrombolysis is feasible in an *in vitro* transcranial flow model; 2) FUS operating parameters such as duty cycle and pulse width can be varied for optimized clot lysis efficacy; 3) transcranial sonothrombolysis efficacy is also dependent on individual skull bone characteristics; and 4) clot lysis depends on the acoustic output power of the FUS system as it relates to effective clot breakdown and potential clot fragments.

AUTOBIOGRAPHICAL STATEMENT

Education

Wayne State University **2013**

Ph.D., Biomedical Engineering

Use of Focused Ultrasound for Transcranial Sonothrombolysis

Wayne State University **2007**

M.S., Biomedical Engineering

Graduate School Masters Scholarship Award Winner

University of Michigan **2004**

B.S., Biology & Psychology

Experience

Department of Radiology, Brain Ultrasound Research Laboratory, UCSD

Graduate Research Associate, Ph.D. Candidate, San Diego, CA 2009 – 2013

Department of Surgery, Division Of Trauma And Burn, UCSD

Graduate Research Associate, Assistant Investigator, San Diego, CA 2009 - 2010

Department of Emergency Medicine Basic Research Laboratory, WSU

Graduate Research Associate, Assistant Investigator, Detroit, MI 2006 – 2007

Certification

Technology Business Creation,

Jacobs School of Engineering, University of California San Diego

Research Commercialization Technology Business Creation,

National Council of Entrepreneurial Tech Transfer